

**Fossils, Fruits, and Phylogeny: An Integrative Approach to Understanding
the Evolutionary History of Palms (Arecaceae)**

by

Kelly Matsunaga

A dissertation submitted in partial fulfillment
of the requirements for the degree of
Doctor of Philosophy
(Earth and Environmental Sciences)
in The University of Michigan
2019

Doctoral Committee:

Assistant Professor Selena Y. Smith, Chair
Professor Catherine Badgley
Professor Emerita Robyn J. Burnham
Associate Professor Matthew Friedman
Professor Nathan D. Sheldon

Kelly Matsunaga
matsuke@umich.edu
ORCID iD: 0000-0002-9533-2934

© Kelly Matsunaga 2019

DEDICATION

This dissertation is dedicated with love and gratitude to Doris, Peter, Joel, and Yasuko.

ACKNOWLEDGEMENTS

This dissertation was generously funded by the department of Earth and Environmental Sciences Turner fund, the Rackham Graduate School, and the United States National Science Foundation (DDIG 1701645). The research in chapter 2 was performed in collaboration with Drs. Steven R. Manchester, Dashrath Kapgate, Rashmi Srivastava, and Selena Y. Smith. µCT datasets were processed with the help of undergraduate research assistants Mireille Farjo, Serena Safawi, and Jasimine Ash. James Saulsbury provided patient assistance with programming and figure construction in R. Much of this work would also not have been possible without the natural history collections that provided access to specimens. I thank Harry Smith and Dr. William Baker of the Royal Botanic Gardens, Kew, Dr. Brett Jestrow of Fairchild Tropical Botanic Garden, Drs. Anna Stalter and Kevin Nixon of L.H. Bailey Hortorium Herbarium, Drs. Steven Manchester and Hongshan Wang of Florida Museum of Natural History, and Drs. S.D. Bonde and P.G. Gamre of the Agharkar Research Institute. I also thank my committee members for their guidance and constructive feedback, which greatly improved this dissertation. My success in completing this dissertation would not have been possible without my family, friends, and the paleobotany community. I extend a special thanks to Dr. Alexandru Tomescu, who showed me I could be a scientist, and to James Saulsbury and Alessio Capobianco for challenging me intellectually and inspiring me to expand my horizons. Finally, I am grateful to my adviser, Dr. Selena Y. Smith, for her unwavering support and commitment, for always finding my typos, and for being a positive role model as an accomplished woman in science.

TABLE OF CONTENTS

DEDICATION	ii
ACKOWLEDGEMENTS	iii
LIST OF TABLES	vi
LIST OF FIGURES	vii
LIST OF APPENDICES	x
ABSTRACT	xi
CHAPTER	
1. Introduction	1
2. Fossil Palm Fruits from India Indicate a Cretaceous Origin of Tribe Borasseae (Areceae)	20
Abstract	20
Introduction	21
Methods	23
Results	29
Discussion	42
Conclusions	58
References	59

3. Fossil Palm Reading: The Utility of Fruits for Understanding the Evolution and	
Fossil Record of Palms	64
Abstract	64
Introduction	65
Methods	68
Results	73
Discussion	98
Conclusions	109
References	111
4. New Insights into the Diversification of Palms (Arecaceae) from an Expanded	
Fossil Record of Fruits	115
Abstract	115
Introduction	116
Methods	118
Results	128
Discussion	137
Conclusions	143
References	145
5. Conclusions	152

LIST OF TABLES

TABLES

2.1 Comparison of described species and new specimens included in synonymy as <i>Hyphaeneocarpon indicum</i>	45
3.1 Palm fruit fossils suitable as node calibrations	110
4.1 Stem and crown ages for subfamilies and tribes obtained using lognormal and uniform priors	131
F.1 MEDUSA summary for analysis shown in Fig. F.1	234
F.2 MEDUSA summary for analysis shown in Fig. F.2	235
F.3 MEDUSA summary for analysis shown in Fig. F.3	236
F.4 MEDUSA summary for analysis shown in Fig. F.6	239

LIST OF FIGURES

FIGURES

1.1 Phylogenetic relationships of subfamilies and tribes of Arecaceae	6
2.1 Deccan Intertrappean Bed localities in which <i>Hyphaeneocarpon indicum</i> fossils occur	24
2.2 Fruit and pericarp structure of <i>Hyphaeneocarpon indicum</i>	34
2.3 Seed structure of <i>Hyphaeneocarpon indicum</i>	36
2.4 Abortive carpels of <i>Hyphaeneocarpon indicum</i>	38
2.5 Germination pores of <i>Hyphaeneocarpon indicum</i>	39
2.6 Phylogenetic relationships of <i>Hyphaeneocarpon indicum</i>	41
3.1 Calamoideae	77
3.2 <i>Nypa fruticans</i> (Nypoideae)	79
3.3 Coryphoideae, syncarpous clade	82
3.4 Coryphoideae, apocarpous clade	84
3.5 Ceroxyloideae	86
3.6 Arecoideae	90
3.7 Morphospace plots based on fruit characters from morphological matrix	92
3.8 Phylogenetic relationships of six fossils from total-evidence maximum-likelihood analysis	97
4.1 Chronogram based on node-dating analysis using lognormal priors	130

4.2 Lineage through time (LTT) plots based on trees generated using different priors and calibrations	135
4.3 Diptych plots comparing distributions of joint priors and posteriors for each calibrated node in the tree	136
B1 Scree plot of percent variance along ordination axes from principal coordinate analysis	186
D.1 Maximum likelihood total evidence tree with all six fossils	226
D.2 Constrained analysis with all fossils except the Mahurzari palm	227
D.3 Constrained analysis with all fossils except <i>Friedemannia messelensis</i>	228
E.1 Chronogram from node-dating analysis using lognormal priors	230
E.2 Chronogram from node-dating analysis using uniform priors	231
E.3 Chronogram from node-dating analysis using calibrations on only the Areceaceae crown and stem nodes	232
F.1 MEDUSA output using birth-death model and critical threshold value of 6	234
F.2 MEDUSA output using both birth-death and Yule models, with critical threshold value of 6	235
F.3 MEDUSA output using Yule model and critical threshold value of 6	236
F.4 Net diversification rates from BAMM mapped on chronogram	237
F.5 Rates of extinction (top) and speciation (bottom) from BAMM, mapped onto chronogram	238

F.6 MEDUSA output using species-level tree of Faurby et al. 2016	239
F.7 Rates of net diversification from BAMM mapped onto species-level tree of Faurby et al. 2016	240
F.8 Rates of extinction (top) and speciation (bottom) from BAMM, mapped onto species-level tree of Faurby et al. 2016	241

LIST OF APPENDICES

APPENDIX

A. GenBank accession numbers and taxon sampling from chapter 2	164
B. Character definitions, morphological matrix, PCoA scree plot, and list of eigenvalues from chapter 3	178
C. GenBank accession numbers and taxon sampling from chapters 3 and 4	192
D. RAxML trees from chapter 3	225
E. BEAST2 trees from chapter 4	229
F. MEDUSA and BAMM results from chapter 4	233

ABSTRACT

Reconstructing evolutionary radiations is essential for understanding the processes that have generated the extraordinary biodiversity of modern ecosystems. Fossils are an empirical record of the presence, morphology, and geographic distribution of organisms through time, making them critical for understanding evolutionary history. Integrating data from fossils and living biota can therefore reveal important insights into the history of life and Earth systems. In this dissertation I focused on the palm family (Arecaceae), a diverse and widespread lineage of tropical flowering plants, and used their extensive fossil record to understand their early diversification. In chapter 2, I described new fossil fruits from the Late Cretaceous–early Paleocene Deccan Intertrappean Beds of India and used phylogenetic analyses to understand their relationships with modern palms.

Chapter 3 focused on advancing knowledge of basic palm biology and establishing a foundation for future studies of the fossil record. I performed a genus-level survey of palm fruit anatomy using X-ray micro-computed tomography (μ CT) and scanned over 200 species representing nearly all extant genera. Using these scans, I created a morphological dataset, which I combined with DNA sequence data to analyze the evolutionary relationships of six fossil fruits. The results of these analyses

provided important insights into the origins of major palm lineages, including tribes Borasseae, Trachycarpeae, Cocoseae, and Areceae. Additionally, the production of this new comparative morphological dataset, and recognition of key character suites for major clades, will aid in future identification of fossil fruits.

Chapter 4 integrated data from chapters 2 and 3 to investigate the diversification history of palms. I performed molecular dating and diversification-rate analyses using fruit fossils as new age calibrations. The results of these three chapters pushed back age estimates for some groups by over 40 million years, and revealed that palms underwent an extensive Late Cretaceous diversification that coincided with their initial geographic expansion. The radiation of most modern tribes occurred during the warm and wet intervals of the Paleogene, coeval with the expansion of angiosperm-dominated megathermal rainforest environments. Finally, the age of tribe Areceae and a shift towards higher speciation rates associated with the tribe suggest that geologic activity and avian radiations in the Indo-Pacific region may have had an important role in the history of Areceae and other species-rich lineages. This dissertation contributes new data and insights into the timing and environmental context of palm diversification, with broader relevance to fundamental questions in evolutionary biology and Earth sciences.

CHAPTER 1

Introduction

The evolutionary radiation of angiosperms transformed terrestrial ecosystems and generated extraordinary diversity of plant form (McElwain, Willis, & Lupia, 2005; Boyce & Lee, 2010; Friis, Crane, & Pedersen, 2011). The time scale over which this diversification took place and the contributions of ecological and climatic factors remain a central problem and an area of active research in plant evolutionary biology and the Earth sciences. Owing to the relatively young age of angiosperms and diversity of early fossils, Charles Darwin famously reflected on the apparently sudden origin and rapid diversification of angiosperms as an “abominable mystery” (Friedman, 2009; Friis, Pedersen, & Crane, 2010). Over the last ~150 years considerable progress has been made in solving Darwin’s “abominable mystery,” a phrase now used to signify the numerous gaps in our knowledge of angiosperm evolution (Soltis, Folk, & Soltis, 2019). New paleontological discoveries, data syntheses, and methodological advances have refined our understanding of the temporal origins of major clades, the sequence of character acquisition among early angiosperms, and the phylogenetic relationships of major lineages (e.g. Friis *et al.*, 2010; Doyle, 2015; APG IV, 2016; Coiro, Doyle, & Hilton, 2019). However, details of the fossil record and evolutionary history of many angiosperm families and orders remain poorly known, limiting our knowledge of the nuances of this radiation and our broader knowledge of changes in terrestrial environments during the Cretaceous and Cenozoic. In this dissertation, I focus on improving our understanding of the evolution of Arecaceae, the palm

family, which is a widespread, ecologically important, and morphologically diverse group of tropical monocot angiosperms with an extensive but poorly understood fossil record.

The rise of angiosperms

Modern flowering plants comprise six major groups: monocots, eudicots, eumagnoliids, Chloranthales, Ceratophyllales, and the early-diverging ANA grade lineages — *Amborella* Baill., Nymphaeales (water lilies), and Austrobaileyales (APG IV, 2016). The Cretaceous Period (~145–66 million years ago [Ma]) was a critical interval in the evolution of angiosperms because it encompasses their origin in the fossil record and initial evolutionary, geographic, and ecological radiation. The earliest fossil evidence of angiosperms comes from pollen grains. Monosulcate pollen from the Valanginian–Hauterivian boundary (~132.9 Ma), which are characterized by a single elongate aperture in the spore wall, so far represent the oldest records of angiosperm pollen (Brenner, 1996; Coiro *et al.*, 2019). However, the affinities of these monosulcate grains with extant lineages or angiosperm stem groups is not known (Brenner, 1996; see Coiro *et al.*, 2019). Unequivocal evidence for the presence of crown angiosperms comes from tricolporate pollen, which is known from multiple localities near the end of the Barremian (~125 Ma; Magallón *et al.*, 2015; Herendeen *et al.*, 2017; Coiro *et al.*, 2019). Tricolporate pollen grains are today found only in eudicots (Magallón *et al.*, 2015; Herendeen *et al.*, 2017; Coiro *et al.*, 2019).

Although there are some macrofossil occurrences as early as the Barremian (131–126 Ma; Sun *et al.*, 2002; Sun, Dilcher, & Zheng, 2008; Gomez *et al.*, 2015), the macrofossil record of angiosperms is sparse until around the Aptian–Albian (~125–100 Ma) when records surface of ANA grade angiosperms, Chloranthales, eumagnoliids, and eudicots (Herendeen *et al.*, 2017), as

well as the earliest monocot pollen (Doyle & Hickey, 1976; Iles *et al.*, 2015). By the Late Cretaceous all major groups of angiosperms are represented in the macrofossil record. The abundance, geographic distribution, and sequence of appearance of lineages in the fossil record indicate two main phases in angiosperm diversification. Angiosperms first undergo a rapid ecological radiation and taxonomic diversification during the Aptian through the Cenomanian (~125–94 Ma), during which time angiosperms expanded into new environments and established many major lineages (Lidgard & Crane, 1990; McElwain *et al.*, 2005). This initial diversification was followed by a rise to floristic dominance during the Late Cretaceous, in which angiosperms became abundant and sometimes dominant within terrestrial floras (Lidgard & Crane, 1990; McElwain *et al.*, 2005). Today angiosperms are the most diverse clade of extant and land plants representing nearly 90% of known species (Christenhusz & Byng, 2016).

Monocot evolution and the fossil record

Monocots comprise an estimated 20–25% of modern angiosperm species (Christenhusz & Byng, 2016; Givnish *et al.*, 2018). They first appear in the fossil record during the Aptian (Early Cretaceous; ~113–125 Ma) and undergo an initial radiation, by the end of the Cretaceous generating most of the major lineages including Alismatales, Pandanales, Liliales, Asparagales, and commelinid monocots (e.g. Zingiberales, Poales, Arecales; Smith, 2013; Givnish *et al.*, 2018). However, occurrences of most families are absent until the Cenozoic and the fossil record of monocots as a whole is spotty, with many fossils having unknown or contentious affinities (Smith, 2013; Iles *et al.*, 2015; Matsunaga *et al.*, 2018). Their relatively poor fossil record probably results from a combination of low preservation potential and other taphonomic or investigator biases (Gandolfo, Nixon, & Crepet, 2000; Smith, 2013). Most monocots are

herbaceous, low-growing, non-deciduous, and insect pollinated, and thus produce less biomass than other groups. These qualities reduce the probability of both entering the sedimentary record and being preserved as fossils. It can also be difficult to identify many monocot fossils owing to a paucity of comparative data on modern taxa, which stymies our ability to apply the fossil record to understanding monocot diversification (Smith, 2013).

An exception is the palm family (Arecaceae), which has arguably the most extensive fossil record among monocots. Palms have relatively high potential for preservation and fossil recovery owing in part to the arborescent habit of many species, highly fibrous nature of their tissues, and distinctive morphology and anatomy that make them easy to identify. Palms are one of the first recognizable monocot families in the Cretaceous. Throughout the Cretaceous and Cenozoic occurrences of fossil palms are numerous, geographically extensive, and temporally continuous (Gee, 2001; Harley, 2006; Pan *et al.*, 2006; Dransfield *et al.*, 2008). They therefore represent an excellent study system for using fossil data to understand evolutionary tempo within a major monocot lineage during the Cretaceous angiosperm radiation.

Palms — the princes among plants

Arecaceae are ubiquitous components of modern tropical and subtropical ecosystems, found in numerous environments such as rainforests, freshwater swamps, dry forests, and arid desert oases (Dransfield *et al.*, 2008). Palms comprise over 2,500 species in five subfamilies, 29 tribes (Fig. 1.1), and 181 genera that fill numerous ecological niches and provide important ecosystem services throughout their range (Tomlinson, 2006; Baker & Dransfield, 2016). Formerly placed in the order Principes — the “princes among plants,” from a passage in Carl Linnaeus’ *Systema Naturae* — palms have fascinated naturalists for centuries and are avidly

sought by horticulturists for their beauty and wide range of forms (Reynolds, 1997; Tomlinson, 2006; Balslev, Bernal, & Fay, 2016; Dowe & Maroske, 2016). Palms exhibit high diversity in morphology and growth habit, ranging from small understory herbs to tall canopy trees and with foliage spanning colors from silvery white to deep red (Dransfield *et al.*, 2008). Many species are heavily armed with spines and prickles, and some climbing palms in subfamily Calamoideae (rattans) are myrmecophytic, hosting ant colonies that actively defend the plants from predators (Mattes *et al.*, 1998; Dransfield *et al.*, 2008). Palms hold several botanical records as plants with the tallest (*Ceroxylon quindiuense* (H.Karst.) H.Wendl.) and widest stems lacking wood (*Jubaea chilensis* (Molina) Baill.), the longest self-supporting leaves (25 m, *Raphia regalis* Becc.), largest seeds (25 kg, *Lodoicea maldivica* (J.F.Gmel.) Pers.) and largest inflorescences (20 m tall, est. 23.9 million flowers; *Corypha umbraculifera* L.) (Tomlinson, 2006).

Palms are restricted to frost-free regions of the world because of anatomical and physiological constraints of their vascular system, which is unable to withstand cavitation and embolism caused by freezing (Tomlinson, 1979, 2006), although a few “cold-hardy” species are adapted to cooler temperate climates or high elevations (Francko, 2003; Dransfield *et al.*, 2008). Consequently, fossil palms also serve as a proxy for frost-free environments and inform global climate trends through time (Reichgelt, West, & Greenwood, 2018). For example, palm pollen and macrofossils provide one line of evidence for high-latitude warmth during the Eocene, during which time palms had global distributions that extended into polar latitudes of both hemispheres (Sluijs *et al.*, 2009; Pross *et al.*, 2012). Moreover, approximately 90% of modern species are restricted to the tropical rainforest biome and therefore palms also represent an important study system for understanding the assembly of modern tropical rainforests in deep time (Couvreur, Forest, & Baker, 2011).

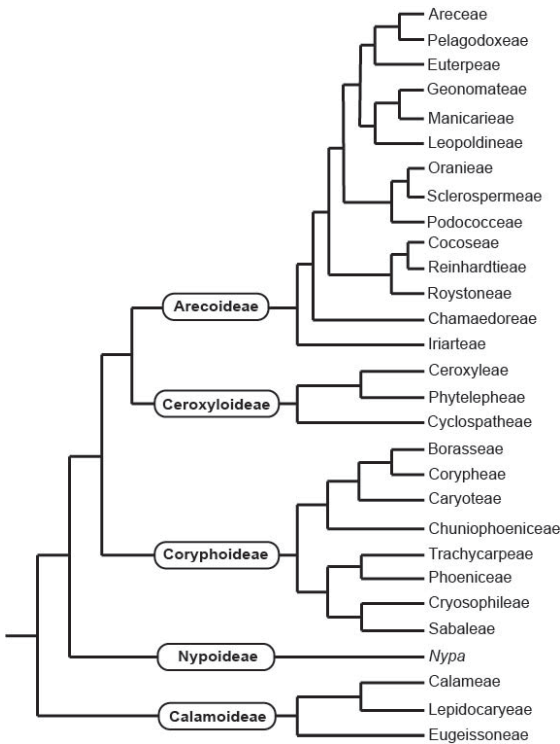


Figure 1.1 Phylogenetic relationships among subfamilies and tribes of Arecaceae. Relationships based on the strict consensus tree of Baker *et al.* (2009). Subfamilies are labeled on corresponding stem branches.

Palm evolution from the ground up — what does the fossil record tell us?

Fossil palms are ubiquitous in latest Cretaceous and Cenozoic floras. The earliest reported occurrences are permineralized (anatomically preserved) stems potentially from the Turonian (93.9–89.9 Ma; Crié, 1892), but the precise age of these fossils is unclear and needs to be verified. Otherwise, the oldest unequivocal records include leaf compressions and permineralized stem material from the late Coniacian–Santonian of North America (~86.3–83.6 Ma; Berry, 1905, 1914, 1916). By the Maastrichtian (~72–66 Ma), palm pollen and macrofossils are known from localities in the United States, Canada, Mexico, Argentina, Cameroon, Somalia, India, Egypt, Austria, France, and Japan (Crié, 1892; Ôyama & Matsuo, 1964; Delevoryas, 1964;

Schrank, 1994; Ancibor, 1995; Cevallos-Ferriz & Ricalde-Moreno, 1995; Harley, 2006; Ottone, 2007; Bonde, 2008; Dransfield *et al.*, 2008; Manchester, Lehman, & Wheeler, 2010; El-Soughier *et al.*, 2011; Estrada-Ruiz *et al.*, 2012). This pattern in the fossil record is indicative of a major geographic expansion of palms, which started during the Cretaceous and continued into the Cenozoic, when palms moved into polar latitudes in response to the warm and equable climatic conditions of the early Eocene (Eldrett *et al.*, 2009; Pross *et al.*, 2012; Greenwood & West, 2017; Reichgelt *et al.*, 2018).

This extensive fossil record provides insights into the geographic expansion of palms and range shifts associated with climatic changes. What is less clear is whether the geographic radiation and taxonomic diversification of palms were concomitant processes. Was the worldwide expansion of palms during the Late Cretaceous occurring primarily among extinct or stem lineages, which later produced the modern subfamilies and tribes? Or, alternatively, were palms undergoing a major diversification of modern clades as they expanded into new environments? The fossil record as we currently understand it does not provide a straightforward answer. Palm fossils, especially leaves and stems, are easy to recognize and difficult to mistake for other families. However, they can also be difficult to assign to lower taxonomic ranks (Read & Hickey, 1972), which hinders our ability to answer questions about taxonomic and ecological diversification within the family.

Leaf characters are important in field taxonomy and for identifying modern palms, but the large size of leaves precludes complete recovery of many fossil specimens, and important features like leaf splitting and folding can be obscured by taphonomic compression. For fossil stems (mostly assigned to the form genus *Palmoxylon* Schenk), recent comparative work on modern stem anatomy has made identification of stem specimens below the family level much

more feasible, and is a crucial step forward in understanding the taxonomy of *Palmoxylon* (Bouchaud, Thomas, & Tengberg, 2011; Tomlinson, Horn, & Fisher, 2011; Thomas & De Franceschi, 2012, 2013; Thomas & Boura, 2015; Nour-El-Deen, Thomas, & El-Saadawi, 2017). However, anatomical variation in subfamily Arecoideae is still not well understood, and hundreds of *Palmoxylon* occurrences are yet to be re-examined in light of these new comparative data. Additionally, some stem anatomical traits (like the single wide metaxylem vessels of most members of Arecoideae) are functional traits that probably evolved as adaptations to tropical rainforest environments during the Cenozoic (Thomas & Boura, 2015). Therefore, using stem anatomy to resolve phylogenetic relationships of fossils may prove difficult if the fossils have ancestral anatomical characters that (1) reflect drier Cretaceous climates, and (2) are not present in modern representatives of the group. Pollen records add some resolution, especially for identifying lineages with clear apomorphies, but many palms have simple, tectate, monosulcate pollen also seen in other angiosperms (e.g. Magnoliales, monocots; Zavada, 1983; Harley & Baker, 2001; Sampson, 2002). Unequivocal palm pollen does not appear in the fossil record until the Maastrichtian, long after the earliest macrofossil occurrences (Harley, 2006).

Currently, the fossil record indicates that the divergence of modern subfamilies likely occurred by the Cretaceous–Paleogene boundary. The earliest palm fossils are palmate and costapalmate leaf impressions indicative of Coryphoideae (Berry, 1905, 1914; Kvaček & Herman, 2004), although the very earliest Coniacian–Santonian fossils could arguably represent stem lineages (see Chapter 4). However, other Late Cretaceous through early Danian records include pollen belonging to Calamoideae (Schrank, 1994), widespread fossils closely resembling *Nypa* (Gee, 2001), leaves and seeds of Coryphoideae (Kvaček & Herman, 2004; Manchester *et al.*, 2010), and at least one unequivocal record of tribe Cocoseae (Arecoideae; Manchester *et al.*,

2016). Fossils that are placed within modern tribes, subtribes, or genera are not common until the Eocene or later, when fossilized reproductive structures such as fruits, seeds, and flowers become common in Lagerstätten such as the London Clay Formation or Messel oil shales (Reid & Chandler, 1933; Collinson, Manchester, & Wilde, 2012). Divergence time estimates based on molecular clocks are broadly consistent with the pattern observed in the fossil record. Such analyses consistently place the origin of the Arecaceae crown group in the middle Cretaceous, divergence of subfamilies in the Late Cretaceous, and diversification within subfamilies in the Cenozoic, with most modern genera originating during the Oligocene to Miocene (Couvreur *et al.*, 2011; Baker & Couvreur, 2013a,b).

Data from the palm fossil record and molecular dating analyses currently converge on a Cenozoic palm diversification, implying that most of their taxonomic diversification occurred after their initial geographic expansion. However, several observations suggest that this might not represent the full story. First, the hypothesis of a Cenozoic palm diversification is informed primarily by the fossil record of leaves and pollen, which are notoriously difficult to assign to groups within palms. Information content in the early fossil record is therefore low, with respect to taxonomic diversity. Second, the fossils that provide early evidence for divergence tribes, subtribes, and genera are fruits and seeds. These include Maastrichtian fruits of *Nypa* Steck (Chitaley & Nambudiri, 1969; Gee, 2001), Campanian *Sabal*-like seeds (Manchester *et al.*, 2010), Maastrichtian–Danian fruits of subtribe Attaleinae (Manchester *et al.*, 2016), and numerous seeds from the early Eocene London Clay Formation (Reid & Chandler, 1933). These highly informative fossils indicate that, as in many other angiosperm groups, reproductive structures are highly taxonomically informative and contain valuable data for understanding evolutionary history. However, none of these fossils have been used in phylogenetic or

molecular dating analyses to inform evolutionary hypotheses for the Arecaceae. This raises the question of whether our picture of palm diversification might change when the fossil record of fruits is given full consideration, and localities with palm fossils are revisited with fruits and other reproductive structures in mind.

Palm fossils from localities of the Maastrichtian–Danian (~66 Ma) Deccan Intertrappean Beds of India are particularly promising for understanding the early diversification of palms. These floras contain abundant palm fossils including those of stems, leaves, fruits, seeds, and flowers preserved three-dimensionally and with high anatomical fidelity in chert deposits located throughout central India (Bonde, 2008; Kapgate, 2009). However, some of these fossils are unpublished, documented only in gray literature, or are published in Indian journals that can be difficult to access. As a result, many of the Indian fossils have been overlooked in the literature summarizing the fossil record of palms or treated as unverified owing to difficulties in evaluating taxonomic determinations. Nevertheless, approximately 35 species based on fruit specimens have been described from the Deccan cherts (Bonde, 2008; Kapgate, 2009). These fossils, and the fossil record of palm fruits more generally, represent an important source of data for understanding which palm lineages were present by the end of the Cretaceous.

The problem with fruits

Studying palm fruit fossils — understanding their morphology, determining systematic relationships, and evaluating the existing fossil record — presents numerous challenges. For previously described fossils, reasonable caution should be taken in accepting taxonomic determinations at face value, particularly those described from historical collections and placed in extant genera (e.g. Berry, 1926, 1927; Hollick, 1928; Reid & Chandler, 1933). A long

tradition in angiosperm paleobotany encouraged placement of fossils in modern genera, and sometimes affinities with extinct or stem lineages were not considered. Moreover, many fossils have been described based on limited comparative material or now outdated evolutionary hypotheses for palms and need to be revisited considering new data.

Although the phylogenetic relationships among major palm lineages are now well understood and mostly stable, comparative data on palm fruit and seed structure are still relatively sparse. *Genera Palmarum* (Dransfield *et al.*, 2008) is an important resource and covers all modern genera, but information on fruit structure is limited. Baker *et al.* (2009) assembled a genus-level morphological matrix that included some fruit and gynoecial characters. This dataset is useful for visualizing character distributions but does not include many pericarp and seed characters, which are often preserved in fossils. A series of papers by Essig and colleagues documents fruit anatomy in several groups of Arecoideae, but comparable data for many other groups are so far lacking (Essig, 1977, 2002; Essig, Manka, & Bussard, 1999; Essig, Bussard, & Hernandez, 2001; Chapin, Essig, & Pintaud, 2001; Essig & Hernandez, 2002). Finally, fruit structure of several genera have been documented in depth by Russian botanists (Romanov *et al.*, 2011; Bobrov, Romanov, & Romanova, 2012b; Bobrov *et al.*, 2012a), but the original manuscripts on some taxa are difficult or impossible to obtain, although some of the information is summarized by Bobrov *et al.* (2012a). Overall, while there is considerable data on palm fruit structure, the information is spread out in the literature, taxonomic sampling is spotty, and significant gaps remain. For instance, relatively little information on pericarp structure is available, particularly the distribution and arrangement of vascular and sclerenchymatous tissues in the pericarp. Such pericarp features are often preserved in fossils and may provide useful characters for understanding systematic relationships.

Even with adequate comparative data, however, palms exhibit considerable morphological diversity and convergence of characters and therefore objectively evaluating systematic relationships based on fruit morphology can be difficult. This morphological diversity adds to the challenges of describing new fossils. Phylogenetic analyses can be used to understand evolutionary relationships between fossils and living species, and are particularly useful when dealing with large numbers of characters and complex character distributions among species. However, performing phylogenetic analyses with fossil palm fruits requires both detailed morpho-anatomical data on modern fruits and taxon sampling that adequately captures the diversity and distributions of characters. Therefore, despite fossil fruits being a promising source of information on the diversification of palms in deep time, leveraging this record is currently not feasible. Doing so will first require assembling comparative morphological data on extant fruit structure, critically evaluating the fossil record, describing new fruit specimens, and synthesizing these data in a phylogenetic framework. This is the problem I address in this dissertation.

Fossils, fruits, and phylogeny: an integrative approach to understanding the evolutionary history of palms

The overarching goal of this dissertation is to understand the evolution and diversification of Arecaceae using the fossil record of fruits. How does our understanding of palm evolutionary history change when we integrate fruit fossils? What can including fossils tell us about the factors underlying the diversification of a diverse and widespread tropical family? And, more generally, how can palms help refine our understanding of evolutionary tempo of the Cretaceous angiosperm radiation? To answer these questions, I use an integrative approach that combines paleontology, comparative anatomy, 3D digital morphology (X-ray micro-computed

tomography), phylogenetics, molecular dating, and diversification rate analyses. I consider the Late Cretaceous and Paleogene fossil record of fruits, emphasizing fossils from the Maastrichtian–Danian Deccan Intertrappean Beds.

In Chapter 2, I describe the morphology of several new fossil specimens from the Deccan Intertrappean Beds of India and revise the taxonomy of five previously described fossil species. I include these fossils in a phylogenetic analysis of the family using a slightly modified version of the Baker *et al.* (2009) matrix. These analyses represent a proof of concept for the phylogenetic utility of fruit characters and the potential impact of a single new fossil on inferences of evolutionary tempo in palms. Chapter 3 surveys fruit morphology and anatomy of nearly all palm genera using literature review and µCT scans of over 200 extant species. I developed a dataset of fruit characters and used it to test the phylogenetic relationships of six fossil palm fruits. Finally, in Chapter 4 I synthesize data from the first two chapters to investigate evolutionary tempo in palm diversification using the fossil record of fruits. I performed node dating and diversification analyses, using a new set of fossil calibrations based on review of the palm fossil record and the phylogenetic relationships of fossil fruits inferred in Chapters 2 and 3. In the concluding chapter, I summarize the contributions of this dissertation and discuss its significance in the context of broader questions about palm evolution, changes in terrestrial ecosystems and climate through the Cretaceous and Cenozoic, and the importance of palms for understanding fundamental questions in evolutionary biology and the Earth sciences.

References

- Ancibor E.** 1995. Palmeras fosiles del Cretacico Tardio de la Patagonia Argentina (Bajo de Santa Rosa, Rio Negro). *Ameghiniana* **32**: 287–299.
- APG IV.** 2016. An update of the Angiosperm Phylogeny Group classification for the orders and families of flowering plants: APG IV. *Botanical Journal of the Linnean Society* **161**: 105–121.
- Baker WJ & Couvreur TLP.** 2013a. Global biogeography and diversification of palms sheds light on the evolution of tropical lineages. II. Diversification history and origin of regional assemblages. *Journal of Biogeography* **40**: 286–298.
- Baker WJ & Couvreur TLP.** 2013b. Global biogeography and diversification of palms sheds light on the evolution of tropical lineages. I. Historical biogeography. *Journal of Biogeography* **40**: 274–285.
- Baker WJ & Dransfield J.** 2016. Beyond Genera Palmarum: progress and prospects in palm systematics. *Botanical Journal of the Linnean Society* **182**: 207–233.
- Baker WJ, Savolainen V, Asmussen-Lange CB, et al.** 2009. Complete generic-level phylogenetic analyses of palms (Arecaceae) with comparisons of supertree and supermatrix approaches. *Systematic Biology* **58**: 240–256.
- Balslev H, Bernal R & Fay MF.** 2016. Palms – emblems of tropical forests. *Botanical Journal of the Linnean Society*: 195–200.
- Berry EW.** 1905. A palm from the mid-Cretaceous. *Torreya* **5**: 30–33.
- Berry EW.** 1914. The Upper Cretaceous and Eocene floras of South Carolina and Georgia. *US Geological Survey, Professional Paper* **84**: 1–200.
- Berry EW.** 1916. A petrified palm from the Cretaceous of New Jersey. *American Journal of Science* **41**: 193–197.
- Berry EW.** 1926. *Cocos* and *Phymatocaryon* in the Pliocene of New Zealand. *American Journal of Science* **7**: 181–184.
- Berry EW.** 1927. Petrified fruits and seeds from Oligocene of Peru. *Pan-American Geologist* **47**: 121–133.
- Bobrov AVFC, Lorence DH, Romanov MS, et al.** 2012a. Fruit Development and Pericarp Structure in *Nypa fruticans* Wurmb (Arecaceae): A Comparison with Other Palms. *International Journal of Plant Sciences* **173**: 751–766.
- Bobrov A, Romanov MS & Romanova ES.** 2012b. Gynoecium and fruit histology and development in *Eugeissona* (Calamoideae: Arecaceae). *Botanical Journal of the Linnean Society* **168**: 377–394.

- Bonde SD.** 2008. Indian fossil monocotyledons; current status, recent developments and future directions. *The Palaeobotanist* **57**: 141–164.
- Bouchaud C, Thomas R & Tengberg M.** 2011. The multipurpose date palm “tree”: anatomical identification of modern palm stems and practical application in the archaeological site of Madâ’in Sâlih (Saudi Arabia). *SAGVNTVM Extra* **11**: 47–48.
- Boyce CK & Lee JE.** 2010. An exceptional role for flowering plant physiology in the expansion of tropical rainforests and biodiversity. *Proceedings. Biological sciences / The Royal Society* **277**: 3437–3443.
- Brenner GJ.** 1996. Evidence for the earliest stage of angiosperm pollen evolution: a paleoequatorial section from Israel. In: Taylor DW, Hickey LJ, eds. *Flowering plant origin, evolution and phylogeny*. New York: Chapman & Hall, 91–115.
- Cevallos-Ferriz SRS & Ricalde-Moreno OS.** 1995. Palmeras fosiles del norte de mexico. *Anales Inst. Biol. Univ. Nac. Auton. Mexico* **66**: 37–106.
- Chapin MH, Essig FB & Pintaud JC.** 2001. The morphology and histology of the fruits of Pelagodoxa (Arecaceae): taxonomic and biogeographical Implications. *Systematic Botany* **26**: 779–785.
- Chitaley SD & Nambudiri EMV.** 1969. Anatomical studies of Nypa fruits from the Deccan intertrappean beds of India I. In: *Recent Advances in the Anatomy of Tropical Seed Plants*. Hindustan Publishing Company, 235–258.
- Christenhusz MJM & Byng JW.** 2016. The number of known plants species in the world and its annual increase. *Phytotaxa* **261**: 201–217.
- Coiro M, Doyle JA & Hilton J.** 2019. How deep is the conflict between molecular and fossil evidence on the age of angiosperms? *New Phytologist*.
- Collinson ME, Manchester SR & Wilde V.** 2012. Fossil fruits and seeds of the Middle Eocene Messel biota, Germany. *Abh. Senckenberg Ges. Naturforsch.* **570**: 1–251.
- Couvreur T, Forest F & Baker WJ.** 2011. Origin and global diversification patterns of tropical rain forests: inferences from a complete genus-level phylogeny of palms. *BMC Biology* **9**: 44.
- Crié L.** 1892. Recherches sur les Palmiers silicifiés des terrains Crétacés de l’Anjou. *Bulletin de la Société d’Études Sci-entifiques d’Angers* **21**: 97–103.
- Delevoryas T.** 1964. Two Petrified Angiosperms from the Upper Cretaceous of South Dakota. *Journal of Paleontology* **38**: 584–586.
- Dowe JL & Maroske S.** 2016. ‘These Princely Plants’: Ferdinand Mueller and the Naming of Australasian Palms. *Historical Records of Australian Science* **27**: 13.
- Doyle J a.** 2015. Recognising angiosperm clades in the Early Cretaceous fossil record. *Historical*

Biology **27**: 414–429.

Doyle JA & Hickey LJ. 1976. Pollen and leaves from the mid-Cretaceous Potomac Group and their bearing on early angiosperm evolution. In: Beck CB, ed. *Origin and early evolution of angiosperms*. New York: Columbia University Press, 139–206.

Dransfield J, Uhl NW, Asmussen CB, et al. 2008. *Genera Palmarum: the evolution and classification of palms*. Richmond, Surrey, UK: Kew Publishing.

El-Soughier MI, Mehrotra RC, Zhou ZY, et al. 2011. *Nypa* fruits and seeds from the Maastrichtian-Danian sediments of Bir Abu Minqar, South Western Desert, Egypt. *Palaeoworld* **20**: 75–83.

Eldrett JS, Greenwood DR, Harding IC, et al. 2009. Increased seasonality through the Eocene to Oligocene transition in northern high latitudes. *Nature* **459**: 969–973.

Essig FB. 1977. A systematic histological study of palm fruits. I. The Ptychosperma alliance. *Systematic Botany* **2**: 151–168.

Essig FB. 2002. A systematic histological study of palm fruits. VI. Subtribe Linospadicinae (Arecaceae). *Brittonia* **54**: 196–201.

Essig FB, Bussard L & Hernandez N. 2001. A systematic histological study of palm fruits. IV. Subtribe Oncospermatinae (Arecaceae). *Brittonia* **53**: 466–471.

Essig FB & Hernandez N. 2002. A systematic histological study of palm fruits. V. Subtribe Archontophoenicinae (Arecaceae). *Brittonia* **54**: 65–71.

Essig FB, Manka TJ & Bussard L. 1999. A systematic histological study of palm fruits. III. Subtribe Iguanurinae (Arecaceae). *Brittonia* **51**: 307–325.

Estrada-Ruiz E, Upchurch GR, Wheeler EA, et al. 2012. Late Cretaceous Angiosperm Woods from the Crevasse Canyon and McRae Formations, South-Central New Mexico, USA: Part 1. *International Journal of Plant Sciences* **173**: 412–428.

Francko DA. 2003. *Palms won't grow here and other myths*. Timber Press.

Friedman WE. 2009. The meaning of Darwin's 'abominable mystery'. *American Journal of Botany* **96**: 5–21.

Friis EM, Crane PR & Pedersen KR. 2011. *Early Flowers and Angiosperm Evolution*. Cambridge: Cambridge University Press.

Friis EM, Pedersen KR & Crane PR. 2010. Diversity in obscurity: fossil flowers and the early history of angiosperms. *Philosophical transactions of the Royal Society of London. Series B, Biological sciences* **365**: 369–82.

Gandolfo MA, Nixon KC & Crepet WL. 2000. Monocotyledons: a review of their Early

Cretaceous record. In: *Monocots: Systematics and Evolution.*, 44–51.

Gee CT. 2001. The mangrove palm *Nypa* in the geologic past of the new world. *Wetlands Ecology and Management* **9**: 181–194.

Givnish TJ, Zuluaga A, Spalink D, et al. 2018. Monocot plastid phylogenomics, timeline, net rates of species diversification, the power of multi-gene analyses, and a functional model for the origin of monocots. *American Journal of Botany* **105**: 1888–1910.

Gomez B, Daviero-Gomez V, Coiffard C, et al. 2015. Montsechia , an ancient aquatic angiosperm . *Proceedings of the National Academy of Sciences* **112**: 10985–10988.

Greenwood DR & West CK. 2017. A fossil coryphoid palm from the Paleocene of western Canada. *Review of Palaeobotany and Palynology* **239**: 55–65.

Harley MM. 2006. A summary of fossil records for Arecaceae. *Botanical Journal of the Linnean Society* **151**: 39–67.

Harley MM & Baker WJ. 2001. *Pollen aperture morphology in Arecaceae: Application within phylogenetic analyses, and a summary of record of palm-like pollen the fossil.*

Herendeen PS, Friis EM, Pedersen KR, et al. 2017. Palaeobotanical redux : revisiting the age of the angiosperms. *Nature Publishing Group* **3**: 1–8.

Hollick A. 1928. *Paleobotany of Porto Rico*. New York: New York Academy of Sciences.

Iles WJDD, Smith SY, Gandolfo MA, et al. 2015. Monocot fossils suitable for molecular dating analyses. *Botanical Journal of the Linnean Society* **178**: 346–374.

Kapgate DK. 2009. *Palaeovegetation, palaeophytogeography and palaeoenvironmental study of Central India*. J.M. Patel College of Arts, Commerce & Science.

Kvaček J & Herman AB. 2004. Monocotyledons from the Early Campanian (Cretaceous) of Grünbach, Lower Austria. *Review of Palaeobotany and Palynology* **128**: 323–353.

Lidgard S & Crane PR. 1990. Angiosperm Diversification and Cretaceous Floristic Trends: A Comparison of Palynofloras and Leaf Macrofloras. *Paleobiology* **16**: 77–93.

Magallón S, Gómez-Acevedo S, Sánchez-Reyes LL, et al. 2015. A metacalibrated time-tree documents the early rise of flowering plant phylogenetic diversity. *New Phytologist* **207**: 437–453.

Manchester SR, Bonde SD, Nipunage DS, et al. 2016. Trilocular Palm Fruits from the Deccan Intertrappean Beds of India. *International Journal of Plant Sciences* **177**: 633–641.

Manchester SR, Lehman TM & Wheeler EA. 2010. Fossil Palms (Arecaceae, Coryphoideae) Associated with Juvenile Herbivorous Dinosaurs in the Upper Cretaceous Aguja Formation, Big Bend National Park, Texas. *International Journal of Plant Sciences* **171**: 679–689.

Matsunaga KKS, Smith SY, Manchester SR, et al. 2018. Reinvestigating an enigmatic Late Cretaceous monocot: morphology, taxonomy, and biogeography of *Viracarpon*. *PeerJ* **6**:e4580: 1–32.

Mattes M, Moog J, Werner B, et al. 1998. The rattan palm *Korthalsia robusta* Bl. and its ant and aphid partners: studies on a myrmecophytic association in Kinabalu Park. *Sabah Parks Nature Journal* **1**: 47–60.

McElwain JC, Willis KJ & Lupia R. 2005. Cretaceous CO₂ decline and the radiation and diversification of angiosperms. *A History of Atmospheric CO₂ and its Effects on Plants, Animals and Ecosystems*: 133–165.

Nour-El-Deen S, Thomas R & El-Saadawi W. 2017. First record of fossil Trachycarpeae in Africa: three new species of *Palmoxylon* from the Oligocene (Rupelian) Gebel Qatrani Formation, Fayum, Egypt. *Journal of Systematic Palaeontology* **16**: 741–766.

Ottone EG. 2007. A new palm trunk from the Upper Cretaceous of Argentina. *Ameghiniana* **44**: 719–725.

Ôyama T & Matsuo H. 1964. Notes on palmaean leaf from the Ôarai Flora (Upper Cretaceous), Ôarai Machi, Ibaraki Prefecture, Japan. *Transactions and Proceedings of the Paleontological Society of Japan* **55**: 241–246.

Pan AD, Pan AD, Jacobs BF, et al. 2006. The fossil history of palms (Arecaceae) in Africa and new records from the Late Oligocene (28–27 Mya) of north-western Ethiopia. *Botanical Journal of the Linnean Society* **151**: 69–81.

Pross J, Contreras L, Bijl PK, et al. 2012. Persistent near-tropical warmth on the Antarctic continent during the early Eocene epoch. *Nature* **488**: 73–7.

Read RW & Hickey LJ. 1972. A Revised Classification of Fossil Palm and Palm-like Leaves. *International Association for Plant Taxonomy* **21**: 129–137.

Reichgelt T, West CK & Greenwood DR. 2018. The relation between global palm distribution and climate. *Scientific Reports* **8**: 2–12.

Reid EM & Chandler MEJ. 1933. *The London Clay Flora*. London: British Museum (Natural History).

Reynolds J. 1997. ‘Palm tree shivering in Surrey shrubbery’ - a history of subtropical gardening. *Principes* **41**: 74–83.

Romanov MS, Bobrov AVFC, Wijsundara DSA, et al. 2011. Pericarp development and fruit structure in borassoid palms (Arecaceae-Coryphoideae-Borasseae). *Annals of Botany* **108**: 1489–1502.

Sampson FB. 2002. Pollen Diversity in Some Modern Magnoliids. *International Journal of Plant Sciences* **161**: S193–S210.

- Schrank E.** 1994. Palynology of the Yesomma Formation in Northern Somalia: a study of pollen, spores and associated phytoplankton from the Late Cretaceous Palmae Province. *Palaeontographica Abteilung B* **231**: 63–112.
- Sluijs A, Schouten S, Donders TH, et al.** 2009. Warm and wet conditions in the Arctic region during Eocene Thermal Maximum 2. *Nature Geoscience* **2**: 777–780.
- Smith SY.** 2013. The fossil record of noncommelinid monocots. In: Wilkin P, Mayo S, eds. *Early Events in Monocot Evolution*. New York: Cambridge University Press, 29–59.
- Soltis PS, Folk RA & Soltis DE.** 2019. Darwin review: angiosperm phylogeny and evolutionary radiations. *Proceedings of the Royal Society B: Biological Sciences* **286**: 20190099.
- Sun G, Dilcher DL & Zheng SL.** 2008. A review of recent advances in the study of early angiosperms from northeastern China. *Palaeoworld* **17**: 166–171.
- Sun G, Ji Q, Dilcher DL, et al.** 2002. Archaefructaceae, a new basal angiosperm family. *Science* **296**: 899–904.
- Thomas R & Boura A.** 2015. Palm stem anatomy: phylogenetic or climatic signal? *Botanical Journal of the Linnean Society* **178**: 467–488.
- Thomas R & De Franceschi D.** 2012. First evidence of fossil Cryosophileae (Arecaceae) outside the Americas (early Oligocene and late Miocene of France): Anatomy, palaeobiogeography and evolutionary implications. *Review of Palaeobotany and Palynology* **171**: 27–39.
- Thomas R & De Franceschi D.** 2013. Palm stem anatomy and computer-aided identification: The Coryphoideae (Arecaceae). *American Journal of Botany* **100**: 289–313.
- Tomlinson PB.** 1979. Systematics and Ecology of the Palmae. *Annual Review of Ecology and Systematics* **10**: 85–107.
- Tomlinson PB.** 2006. The uniqueness of palms. *Botanical Journal of the Linnean Society* **151**: 5–14.
- Tomlinson PB, Horn JW & Fisher JB.** 2011. *The Anatomy of Palms: Arecaceae - Palmae*. OUP Oxford.
- Zavada MS.** 1983. Comparative Morphology of Monocot Pollen and Wall Structures. *The Botanical Review* **49**: 331–379.

CHAPTER 2

Fossil Palm Fruits from India Indicate a Cretaceous Origin of Tribe Borasseae (Arecaceae)¹

Abstract

The fossil record of palms (Arecaceae) is essential for understanding the deep evolutionary and geographic history of the family. We studied palm fruit fossils from the ~67–64 million-year-old Deccan Intertrappean Beds of India to infer the systematic relationships of the fossils and their relevance to palm evolution. Using X-ray micro-computed tomography (μ CT), physical sectioning techniques, and a total-evidence phylogenetic analysis, we show that these fossils represent a crown group member of subtribe Hyphaeninae (tribe Borasseae, subfamily Coryphoideae) allied with the extant genera *Satranala* and *Bismarckia*, which are now endemic to Madagascar. These fossils, synonymized here as *Hyphaeneocarpus indicum*, provide evidence for the existence of crown group Hyphaeninae during the late Maastrichtian–early Danian. This predates prior age estimates for the Hyphaeninae crown node by nearly 40 million years and implies an earlier divergence of tribe Borasseae. The presence of *Hyphaeneocarpus* in India shows that Borasseae has persisted in the Indian Ocean region for more than 64 million years. This study illustrates the utility of palm fruit characters for placing fossils in a phylogenetic

¹ Matsunaga KKS, Manchester SR, Srivastava R, Kapgate D, Smith SY. 2019. Fossil palm fruits from India indicate a Cretaceous origin of Arecaceae tribe Borasseae. *Botanical Journal of the Linnean Society* 190: 260–280.

context and has important implications for understanding the evolution and diversification of Borasseae and the paleobiogeography of palms.

Introduction

Palms (Arecaceae) are found today throughout tropical regions worldwide occupying a variety of environments ranging from arid deserts to tropical rainforests (Dransfield *et al.*, 2008). Currently, palms comprise approximately 2,600 species classified into 5 subfamilies and 181 genera (Baker & Dransfield, 2016). They additionally have a rich fossil record extending back to the Late Cretaceous; unequivocal palm fossils first appear during the Turonian (~94–90 Ma) and are geographically widespread by the Maastrichtian (~72–66 Ma; Gee, 2001; Harley, 2006; Dransfield *et al.*, 2008). Subsequently, they achieved global distribution, extending into high latitude regions such as Alaska and Antarctica during the warm and equable climatic conditions of the Eocene (Sluijs *et al.*, 2009; Pross *et al.*, 2012; Suan *et al.*, 2017). The fossil record of palms thus represents an important source of data for understanding both the deep evolutionary history of the family, and terrestrial environments of the geologic past.

The Maastrichtian–Danian (~67–64 Ma) Deccan Intertrappean Beds of India host plant fossil assemblages with numerous palm macrofossils (Bonde, 2008; Kapgate, 2009; Srivastava, 2011). Located primarily in central India, these localities preserve the remains of palm stems, leaves, roots, pollen, inflorescences, and fruits, indicating that palms were an important component of the vegetation of central India during the Late Cretaceous and Paleocene, during which time India was geographically isolated from other major landmasses (Ali & Aitchison, 2008; Chatterjee, Goswami, & Scotes, 2013). Today palms do not comprise a significant component of the vegetation of central India. Although the flora of India includes about 96

species in 20 genera (Kulkarni & Mulani, 2004), India's modern palms are thought to descend from relatively recent colonizations rather than an ancient flora (Baker & Couvreur, 2013). However, little is known about the taxonomic composition of historical palm assemblages and the role of India in the evolutionary and biogeographic history of Arecaceae.

Over the course of nearly a century of study on the Deccan flora, approximately 168 fossil species have been assigned to Arecaceae, including 85 species based on stem specimens, 37 fruits, 28 from leaves, roots, and inflorescence axes, and 18 palynomorphs (Bonde, 2008; Kapgate, 2009). These diverse assemblages could be essential for understanding evolutionary tempo in palm diversification, historical biogeography of palm lineages, and transitions in India's terrestrial vegetation through time. For example, recent re-examination of *Palmocarpon drypeteoides* revealed morphological characters diagnostic of subtribe Attaleinae, a group that is most diverse in South America today and has no representatives in India or Asia (Manchester *et al.*, 2016). However, the systematic affinities of most of the palm fossils in the Deccan Intertrappean beds are poorly understood, as is the extent to which the number of described palms accurately represents the true species richness in these fossil assemblages. Morphological studies and taxonomic revisions are therefore essential for understanding the Deccan floras and applying them to broader questions on palm evolution.

In this study we re-examined five previously described fossil palm species, in light of new specimens recovered from the Deccan Intertrappean Beds at Dhangaon, Keria, and Mohgaonkalan: *Hyphaeneocarpon indicum* Bande, Prakash, & Ambwani, *Palmocarpon arecoides* Mehrotra, *Arecoidocarpon kulkarnii* Bonde, *Arecoidocarpon palasundarensis* Bonde, and *Pandanusocarpon umariense* Bonde (Bande, Prakash, & Ambwani, 1982; Mehrotra, 1987; Bonde, 1990a,b, 1995). We used comparative anatomy to investigate the taxonomic affinities of

the new fruit specimens and evaluate conspecificity of the previously described fossils, which exhibit some shared features. To understand their systematic relationships and significance in an evolutionary and biogeographic context, we included the fossils in a total-evidence phylogenetic analysis of extant palms. Palms exhibit significant diversity and convergence in fruit structure and other features. It can therefore be difficult or unwieldy to evaluate objectively whether some combinations of characters are unique to clades, have evolved multiple times, or are possibly plesiomorphic. Phylogenetic analyses can also help to frame more precise systematic hypotheses, such as placement of fossils in the stem or crown of a group and alliances with particular extant taxa. This information can facilitate inferences of historical biogeography, character evolution, and inform node calibrations in future dating analyses, providing valuable information on the diversification of palms in deep time.

Material and methods

Locality and age

The Deccan Volcanic Province (DVP) comprises a sequence of continental flood basalts (traps) formed during the late Maastrichtian to early Danian (~67–64 Ma, chron 30N-29N; (Hooper, Widdowson, & Kelley, 2010; Schoene *et al.*, 2015; Renne *et al.*, 2015), exposed across central and western peninsular India. Intertrappean sedimentary layers, which occur between some basalt flows and represent quiescent intervals between volcanic episodes, frequently contain permineralized plants preserved three-dimensionally in chert deposits. Over 50 plant fossil-bearing localities have been discovered over the last century, most of which are concentrated in central India in the states of Maharashtra and Madhya Pradesh, and occur primarily in the northeastern portion of the Deccan Main Plateau or in the Mandla subprovince

(Fig. 2.1; Kapgate, 2009; Smith *et al.*, 2015). Where magnetostratigraphic data are available, many of these localities fall within Chron 29R, which straddles the Cretaceous-Paleogene (K-Pg) boundary (Mike Widdowson pers. comm. 2018). Although more precise ages of most macrofossil localities are poorly constrained, many are considered either late Maastrichtian or early Danian depending on their location within the DVP, stratigraphic continuity with dated outcrops, and palynomorph content (Samant & Mohabey, 2009). Specifically, the localities exposed in the northeastern Deccan Main Plateau and southwestern portion of the Mandla subprovince are currently considered late Maastrichtian, while those in the eastern region of the Mandla subprovince are probably all early Danian (Shrivastava, Duncan, & Kashyap, 2015; Smith *et al.*, 2015).

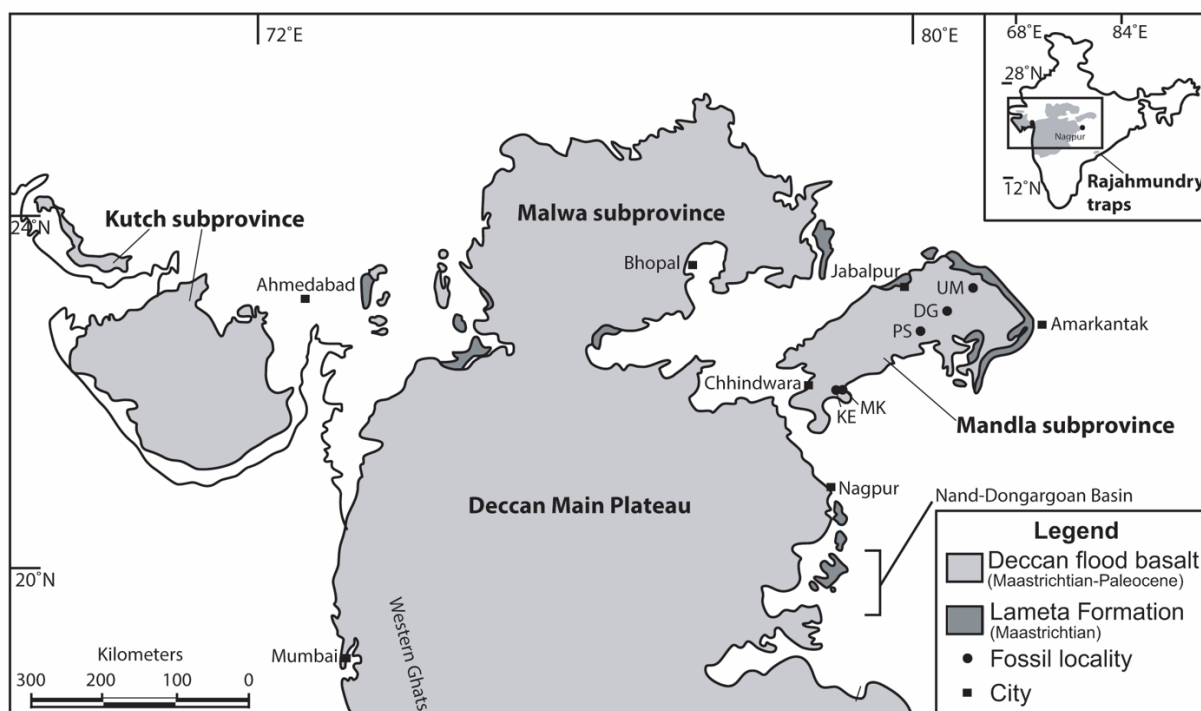


Figure 2.1. Deccan Intertrappean Bed localities in which *Hyphaeneocarpon indicum* fossils occur. Note that all the localities are in the Mandla subprovince of the Deccan Volcanic Province. The Shahpura locality was not included in the map, as its precise location is not certain, but at the map scale shown it would most likely overlap the dot for the Umaria locality. KE = Keria, MK = Mohgaonkalan, PS = Palasundar, DG = Dhangaon, UM = Umaria.

Specimens studied

Specimens were examined from existing and new collections. Fossils come from six localities within the DVP: Mohgaonkalan, Keria, Dhangaon, Palasundar, Umaria, and Shahpura. The new macrofossil specimens (UF19415-69208, UF19415-62614, UF19438-68879, UF19329-62153) originate from the Keria, Mohgaonkalan, and Dhangaon localities of the Deccan Intertrappean Beds of India. Keria (coordinates: 21.9984, 79.173633) and Mohgaonkalan (coordinates: 22.023583, 79.186733) are located in the southwestern edge of the Mandla subprovince of the DVP, in the state of Maharashtra, while Dhangaon (coordinates: 22.84083333, 80.44333333) is further east within Mandla subprovince in the state of Madhya Pradesh. The specimens are curated in the paleobotanical collections of the Florida Museum of Natural History in Gainesville, Florida, USA (UF). Other specimens examined by us and revised here represent previously described species from several other localities. These include specimens curated at the Agarkhar Research Institute (ARI) in Pune, India, of *Arecoidocarpon kulkarnii* (Bonde, 1990a; Mohgaonkalan locality, ARI5285), *Arecoidocarpon palasundarensis* (Bonde, 1995; Palasundar, ARI5288), and *Pandanusocarpon umariense* (Bonde, 1990b; Umaria, ARI5284), and *Hyphaeneocarpon indicum* (Bande *et al.* 1982; Shahpura) from the Birbal Sahni Institute of Palaeosciences (BSIP) in Lucknow, India (BSIP 35408, slide 6182). The distribution of these localities within the Mandla subprovince indicates varying ages: Keria and Mohgaonkalan, which are considered part of the same intertrappean bed, are most likely Maastrichtian, while the other localities located further east in the Mandla subprovince and all probably early Danian. The precise location within the Mandla district (Madhya Pradesh) of the Shahpura locality from which the *Hyphaeneocarpon indicum* holotype was described was not

specified (Bande *et al.* 1982), but it is likely in the vicinity of the Umaria locality, near the town of Shahpura, and is thus probably Danian as well.

Extant comparative material included fruit specimens of approximately 80 species representing most genera sampled in the phylogenetic analysis, including all genera of Borasseae. Specimens were obtained either on loan or examined in the herbarium collections at the Royal Botanic Gardens, Kew (K), L.H. Bailey Hortorium Herbarium (BH), and Fairchild Tropical Botanic Garden (FTG), or collected on the grounds at Fairchild Tropical Botanic Garden. Specimens of *Bismarckia nobilis* Hildebr. & H.Wendl., *Satranala decussilvae* Beentje & J.Dransf., *Medemia argun* (Mart.) Württemb. ex H.Wendl., *Borassus flabellifer* L., *Borassodendron machadonis* (Ridl.) Becc., and *Hyphaene thebaica* (L.) Mart. were further studied using X-ray micro-computed tomography (μ CT; see below) to better understand their anatomical similarities with *Hyphaeneocarpion* and to identify potential synapomorphies.

The fossil fruits from Keria, Mohgaonkalan, and Dhangaon were studied using a combination of serial peels (cellulose acetate or butyl acetate) mounted on microscope slides for documenting anatomy, and μ CT to observe three-dimensional structure. μ CT scans were performed at the University of Michigan CTEES facility using a Nikon XT H 225ST industrial μ CT system with a Perkin Elmer 1620 X-ray detector panel and a tungsten reflection target. Depending on the specimen, scans were set at 68–130 kV, 130–175 μ A, and used 0–0.5 mm of copper filter, which reduces strong artifacts in reconstructed images by suppressing lower energy X-rays. Pixel size varied from ca. 12–16.5 μ m. μ CT scans of figured extant species, *Bismarckia nobilis* and *Satranala decussilvae* (K000300252; Fig. 2.4C, 2.6D-E), were scanned on the same system using 58–60 kV and 155–175 μ A, with 27–31 μ m pixel size resolution. Scans were acquired using Inspect-X and reconstructed using CT Pro 3D (Nikon Metrology, USA), which

uses a FDK (Feldkamp-Davis-Kress) type algorithm. The reconstruction software takes the 2D projection images acquired by the X-ray detector and generates a 3D image represented by gray values distributed in a volumetric space. Reconstructed datasets were analyzed with Avizo 9 Lite 3D software (FEI, Hillsboro, Oregon, USA). We refer to sections obtained from the reconstructed μ CT data as digital sections. Videos based on μ CT scans, raw scan data (image stacks), and associated metadata are archived and freely accessible at MorphoSource (www.morphosource.org) under project number 634.

Phylogenetic analysis

A genus-level morphological and molecular dataset focused on Coryphoideae was assembled to test the systematic relationships of the fossil within the subfamily, while considering possible affinities with other groups. The taxon sampling was based on the dataset of Baker *et al.* (2009) and included exemplar species of each genus in subfamilies Coryphoideae, Nypoideae, and Calamoideae, as well as a single species representing each tribe of subfamilies Ceroxyloideae and Arecoideae. The species *Dasypogon bromeliifolius* R.Br., Prodr. Fl. Nov. Holland. and *Kingia australis* R.Br. (Dasypogonaceae) were also included as outgroups in the molecular partitions, for a total of 85 sampled taxa. The molecular dataset included 5 plastid (*matK*, *rbcL*, *rps16*, *trnL-trnF*) and 2 nuclear (*PRK*, *RPB2*) markers, all obtained from GenBank (Appendix A). Coding sequences (*rbcL*, *matK*, *ndhF*) were aligned using MUSCLE (v.3.8) and adjusted minimally by hand in AliView (v1.25). Non-coding sequences (*rps16*, *trnL-trnF*, *PRK*, *RPB2*) were aligned initially using MAFFT and refined with PRANK, if necessary; for these sequences, this procedure produced better alignments than manually adjusting MUSCLE results.

The morphological matrix used to incorporate the fossil into the phylogenetic analysis contained 110 characters scored for 83 taxa (*Dasypogon* and *Kingia* were not included as there is

insufficient published fruit data and we could not obtain specimens). This matrix was modified from Baker *et al.* (2009) to reflect the taxon sampling of this study and updated generic concepts within palms. The original Baker *et al.* (2009) dataset contained 105 vegetative and reproductive characters, to which we added five additional fruit characters; the original character coding and scoring were left unmodified. The new characters were added primarily to elucidate placement of the fossils within Borasseae. Preliminary analyses using the unmodified Baker *et al.* (2009) matrix showed strong support for placement of the fossil with subtribe Hyphaeninae, but with relationships otherwise unresolved. The new characters include: seed number per fruit (one, up to three, or more than three), endocarp origin within the pericarp (from the inner zone [e.g. locular epidermis], or middle zone of pericarp), germination structure shape (circular, slit/elongate), germination structure type (pore, valve [e.g. *Satranala*], or operculum), and basal intrusion of endocarp into the seed (absent, present). Scoring of the five added characters was based on descriptions in the literature and observations of herbarium material. The fossil species was scored for 20 characters. Although the fossil could not be scored for some morphological characters, all the morphological characters were retained in the analysis to aid in placing extant genera for which DNA sequence data are sparse. In most cases, morphological characters and all DNA sequences were sampled from the same species. However, some sequences were not available for all focal species and were instead taken from closely related, congeneric taxa (Appendix A). The morphological matrix and aligned DNA sequences were concatenated using SequenceMatrix (v1.8), with all external gaps coded as question marks.

Phylogenetic analysis of the combined dataset was performed using Markov chain Monte Carlo (MCMC) methods in MrBayes (v.3.2.6) on the CIPRES Science Gateway (Miller, Pfeiffer, & Schwartz, 2010). We used PartitionFinder2 with AICc model selection (Akaike Information

Criterion, correcting for sample size) and the ‘greedy’ search function to estimate the optimal partitioning scheme for the DNA sequence data limited to the models available in MrBayes (Guindon *et al.*, 2010; Lanfear *et al.*, 2012, 2016). For comparison, we also ran PartitionFinder2 including all substitution models and found that for some partitions, substitution models not available in MrBayes yielded the highest AICc scores. In most cases these models had comparable AICc scores ($\Delta\text{AIC} < 2$), but for two partitions (*matK* position 1 and 2) the ΔAIC between the best fit and available models were as high as 5. Since the objective of the analysis was to place the fossil within a phylogenetic context, we accepted these higher ΔAIC scores because the difference in substitution models was probably inconsequential relative to our goals. The morphological data were analyzed with the MKv model. Across all partitions, the rate prior was set to ‘variable’ to allow for different relative transition rates (ratepr = variable) and the following model parameters were unlinked: transition/transversion ratio (tratio), substitution rates of the GTR model (revmat), character state frequencies (statefreq), gamma shape parameter (shape), proportion of invariable sites (pinvar). We used the default settings in MrBayes for all other parameters. Tree searches comprised two independent MCMC runs with four chains each (three hot, one cold), running for 20 million generations and sampling every 100 generations, with burnin left at the default 25%. Standard deviation of split frequencies was <0.02 when runs terminated and convergence of MCMC runs was confirmed using Tracer (v1.6).

Results

Systematic paleobotany

Division — Magnoliophyta

Class — Liliopsida

Family — Arecaceae

Subfamily — Coryphoideae

Tribe — Borasseae

Subtribe — Hyphaeninae

Genus — *Hyphaeneocarpon* Bande, Prakash, & Ambwani, emend. Matsunaga, S.Y.Sm., Manch., Srivastava, & Kapgate

Emended generic diagnosis — Fruits globose to slightly oblong, single-seeded, with two abortive carpels basally. Abortive ovules/seeds basally attached in locules. Pericarp with three zones — inner zone parenchymatous, absent at maturity; middle zone of interwoven fiber bundles forming endocarp; outer zone parenchymatous with radially oriented fiber bundles from endocarp. Epicarp thin, smooth. Endocarp enclosing fertile and locules of abortive carpels separately, forming pyrenes; elongate apical germination pore above fertile locule. Seeds with intact seed coat surrounded by the locular epidermis, with prominent basal groove from intrusion of the endocarp. Endosperm homogeneous. Embryo apical. Stigmatic remains basal, near locules of abortive carpels.

Type: *Hyphaeneocarpon indicum* Bande, Prakash, & Ambwani emend. Matsunaga, S.Y.Sm., Manch., Srivastava, & Kapgate.

Basionym: *Hyphaeneocarpon indicum* Bande, Prakash, & Ambwani, The Palaeobotanist 30: 307. 1982.

Synonymy: *Arecoidocarpon kulkarnii* Bonde, Palaeobotanist 38: 213, 1990, *Arecoidocarpon palasundarensis* Bonde, Birbal Sahni Centenary Vol.: 67, 1995, *Pandanusocarpon umariense* Bonde, Proceedings 3IOP Conference, Melbourne 1988: 60, 1990, *Palmocarpon arecoides* Mehrotra, Geophytology 17: 205. 1987.

Holotype: BSIP 35408 (Fig. 2.2D&E), Bande, Prakash, & Ambwani, 1982: Figs. 2.1–2.7

Other specimens studied: UF19415-69208 (Figs. 2.2B, 2.5G–I), UF19415-62614 (Figs. 2.2A&C, 3D&E, 2.5C&D), UF19438-68879 (Figs. 2.3B, 2.4A, 2.4B&F, 2.5A&B, 2.5E&F), UF19329-62153 (Fig. 2.2F).

Type locality, stratigraphy, and age: Shahpura, Mandla District, Madhya Pradesh — Deccan Intertrappean Beds, India, late Maastrichtian–early Danian.

Other occurrences: Dhangaon, Keria, Mohgaonkalan, Palasundar, Umaria — Deccan Intertrappean Beds, India, late Maastrichtian–early Danian.

Emended specific diagnosis — As for genus. Fruits 1.5–4.0 cm long, 1.5–3.0 cm wide. Pericarp up to 9.0 mm thick, thinner at maturity. Inner pericarp zone up to 4.0 mm thick or absent at maturity. Endocarp 0.5–1.5 mm thick, composed of fiber bundles 75–200 μm in diameter; fiber bundles extending into outer pericarp of similar diameter. Individual fibers approximately 8.0–12.0 μm in diameter. Parenchyma cells of outer pericarp zone isodiametric to elongate, up to 50 μm wide and 100 μm long. Seeds approximately 9.0–11.0 mm in diameter.

Description

Size and shape: The fruits are globose to subglobose and range from about 1.5–2.5 cm in diameter (Fig. 2.2A–D). Fruits collected from the Mohgaonkalan and Keria localities tend to be smaller, around 1.5 cm wide, whereas those from other localities tend to be larger. Fruit sizes for new material and published specimens are summarized in Table 2.1.

Pericarp structure: The pericarp ranges in thickness from about 2.0–9.0 mm. The large variation results from a combination of the size of the fruits, developmental stage, and taphonomic factors

such as dehydration or compression. The pericarp can be divided into three zones that most likely correspond to the mesocarp, although developmental stages needed for determining exact homology are not preserved. We recognize an ephemeral inner parenchymatous zone, a sclerenchymatous middle zone, and an outer zone of radial fiber bundles and parenchyma (Fig. 2.2E–H). Additionally, to the inside of the pericarp there is a thin layer associated with the seed coat that is probably the locular epidermis. To the outside sometimes a thin epicarp is preserved.

Inner zone: The inner zone is variable in thickness (up to 4.0 mm) and consists of thin-walled parenchyma cells (Fig. 2.2E). This tissue is only clearly visible in one specimen, but remnants of it are present in most other well-preserved specimens between the middle pericarp layer and the locular epidermis. It probably represents a tissue present only in immature fruits, a feature common in some groups of palms (see discussion section “Taxonomic affinities inferred from fruit morphology”; Romanov *et al.*, 2011). Note that the fruit with the thickest documented pericarp (9.0 mm at the widest point) is preserved at a developmental stage in which this inner layer is still prominent; this fruit is also probably somewhat compressed, and possibly somewhat obliquely sectioned, likely exaggerating thickness on some axes.

Middle zone: The middle zone is composed of densely interwoven bundles of fibers that form a thick, sclerenchymatous layer (Fig. 2.2C–F, 2.3D&G). Conventionally, most of the literature on palms refers to any hard inner layer of the fruit as an endocarp. We follow this convention here, noting that the developmental origin of the endocarp is variable within the family and can be derived from the locular epidermis, various regions of the mesocarp, or both (Murray, 1973; Bobrov *et al.*, 2012b). In these fossils the functional “endocarp” originates from the mesocarp; evidence of this is based on a thick zone of parenchyma to the inside of the sclerenchymatous “endocarp” in some stages of development (the “inner zone” described above). Individual fibers

of the endocarp are approximately 8.0–12.0 μm in diameter, with very narrow lumina, and form thick bundles around 50–100 μm wide (Fig. 2.2F). Small lacunae are sometimes present in between some of the fiber bundles of the endocarp, which may have been occupied by parenchyma cells as documented by Bonde (1995). To the outside of the endocarp is a single ring of large fibrovascular bundles, which run longitudinally from the base of the fruit to the apex (Fig. 2.2D&G). These fibrovascular bundles directly abut the endocarp and sometimes appear partially embedded in it. In specimens for which the outer layer of the pericarp is not preserved, these bundles can be clearly seen on the surface of the endocarp (Fig. 2.2B).

Outer zone: Some fiber bundles of the endocarp extend radially into the outer zone of the pericarp, oriented perpendicular to the outer surface of the fruit (Fig. 2.2C&D, 2.3D). This outer zone is otherwise parenchymatous, consisting of thin-walled cells that are elongate to nearly isodiametric, up to 50 μm wide and 100 μm long (Fig. 2.2H). The epicarp is thin, membranous, and typically poorly preserved.

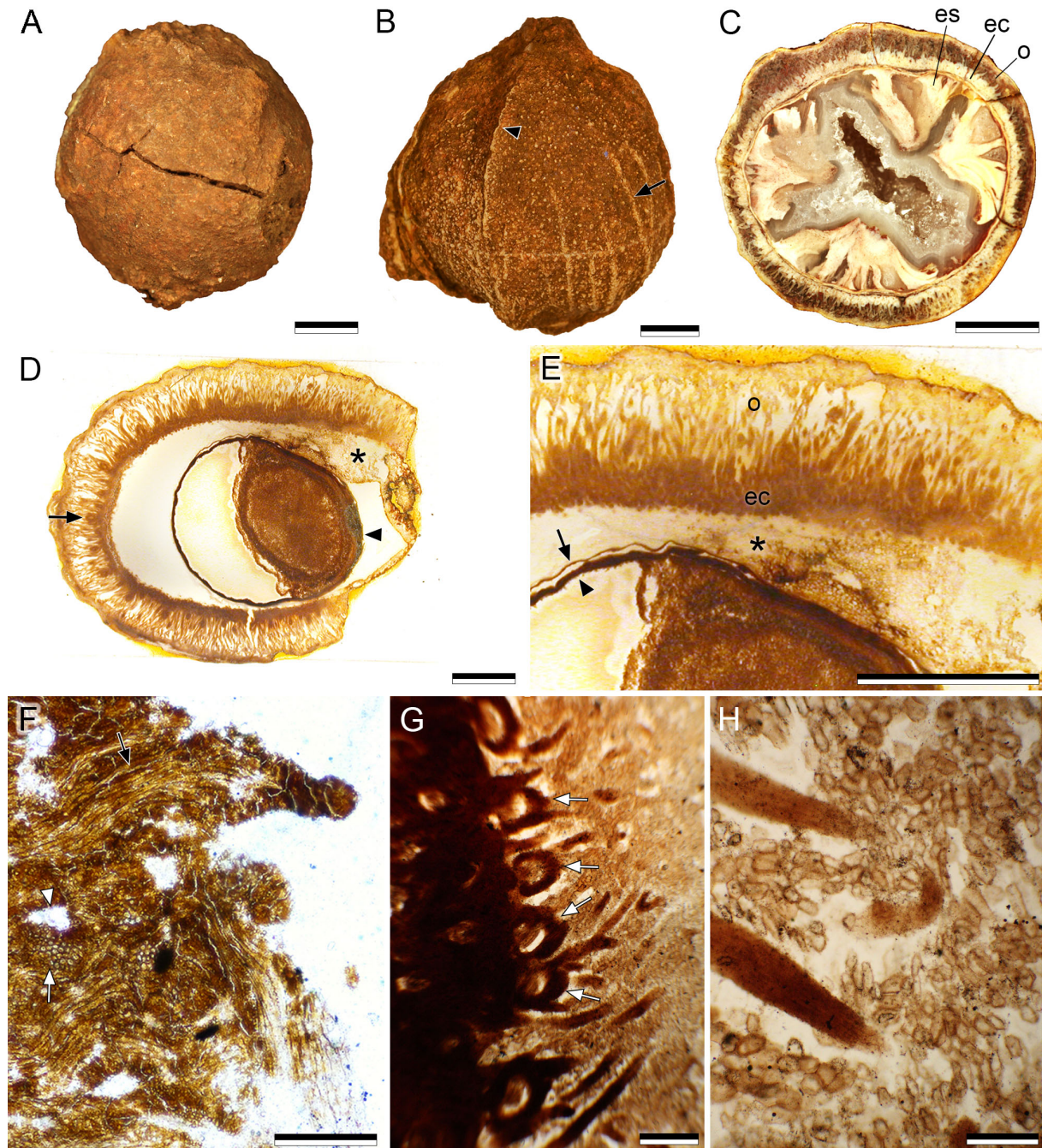


Figure 2.2 Fruit and pericarp structure of *Hyphaeneocarpon indicum*. (A–B) External view of fruits isolated from matrix. The specimen shown in (B) is missing outermost pericarp, exposing large longitudinal fibrovascular bundles on endocarp surface (arrow). Note ridge formed by germination pore on upper half of fruit (arrowhead). Specimens UF19415-62614(A) and UF 19415-69208 (B). Scale = 5 mm. (C) Polished transverse surface section of specimen shown in A. Note endosperm of seed is partially preserved. Specimen UF19415-62614. Scale = 5 mm. (D) Transverse section through holotype of *Hyphaeneocarpon indicum*. Note parenchymatous inner zone of pericarp (asterisk) preserved between the seed (arrowhead) and endocarp, large longitudinal fibrovascular bundles to outside of endocarp (arrow), and relatively large size of specimen. Specimen BSIP 35408 (peel). Scale = 5 mm. (E) Detail of three pericarp layers shown in (D). Note that layer interpreted as the locular epidermis (arrow) is positioned between inner pericarp and seed coat (arrowhead). Scale = 5 mm. (F) Light micrograph showing endocarp anatomy consisting of interwoven bundles of fiber,

visible in longitudinal (black arrow) and transverse sections (white arrow). Note lacunae dispersed throughout this tissue (arrowhead), which may have been filled with parenchyma. Specimen UF19329-62153 (peel). Scale = 100 μ m. (G) Light micrograph focused on large longitudinal fibrovascular bundles to outside of endocarp (arrows). Note large size of these bundles relative to endocarp fiber bundles. Specimen ARI 5288 (thin section; *Arecoidocarpon palasundarensis*). Scale = 200 μ m. (H) Light micrograph from thin section. Detail of outer pericarp zone showing parenchyma cells and fiber bundles. Specimen ARI 5288 (thin section; *Arecoidocarpon palasundarensis*). Scale 200 μ m. es = endosperm, ec = endocarp, o = outer pericarp zone.

Seed structure: Seeds are globose, 9.0–11.0 mm in diameter, with a basal indentation corresponding with an inward protrusion of the endocarp (Fig. 2.3A–C). Several large fibro-vascular bundles run vertically through this protrusion to vascularize the seed, indicating that seeds are basally attached within fruits (Fig. 2.3B&C). Note that in many palms, ovule placentation within the ovary may differ from the seed attachment observed in mature fruits and thus seed attachment should not be used to infer ovule placentation (Dransfield *et al.*, 2008). The densely interwoven fibers of the endocarp form part of this protrusion. At the periphery of each seed two membranous layers are seen: the inner one constituting the seed coat itself and the outer representing the locular epidermis of the fruit (Fig. 2.3D&E). Both the seed coat and locular epidermis are thin and too poorly preserved to resolve anatomical details. The endosperm is homogeneous (non-ruminate) – lacking deep invaginations of the seed coat seen in some palms (Fig. 2.3F). Embryos, when preserved, are positioned apically within the seed (Fig. 2.3G). Anatomical preservation of embryos is insufficient to resolve additional details.

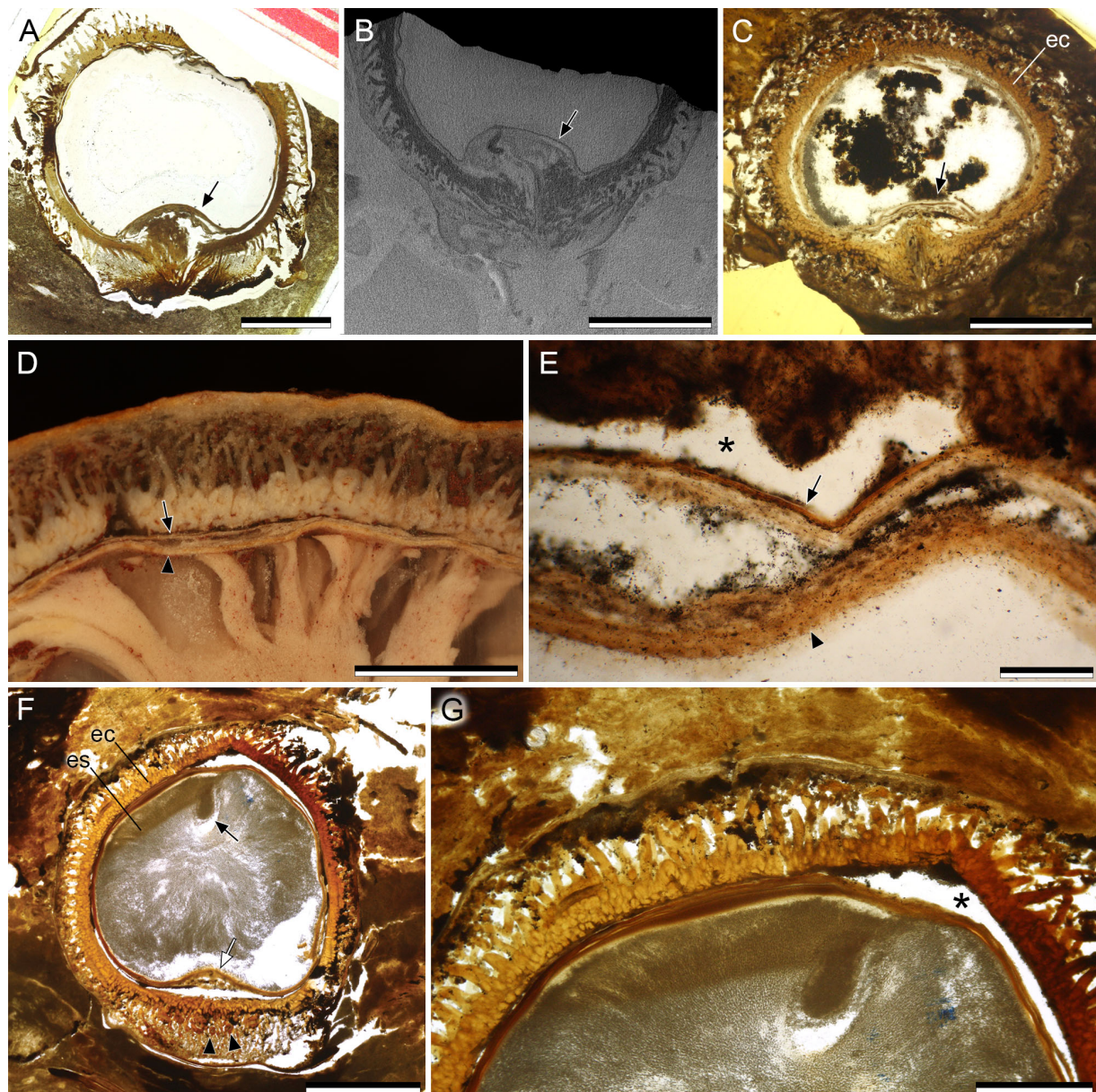


Figure 2.3 Seed structure of *Hyphaeneocarpus indicum*. (A–C) Longitudinal sections showing basal intrusion of pericarp into seed (arrows). Specimen in (B) is a digital longitudinal section from a μ CT scan, (A) and (C) are light micrographs of thin sections. Specimens ARI 5288 (thin section; *Arecoidocarpus palasundarensis*) (A), UF19438-68879 (B), ARI 5285 (thin section; *Arecoidocarpus kulkarnii*) (C). Scale = 5 mm. (D) Detail of fruit in Fig. 2.2C in which pericarp and part of seed are preserved. Note two layers surrounding endosperm: outer, locular epidermis (arrow), inner, seed coat (arrowhead). Specimen UF19415-62614. Scale = 2 mm. (E) Detail of locular epidermis (arrow) and seed coat (arrowhead). Preservation of this specimen is not sufficient to determine anatomical composition of these tissues. Note that the locular epidermis and seed coat are pulled away from the endocarp in (E&G), leaving a gap (asterisk). ARI 5288 (thin section; *Arecoidocarpus palasundarensis*). Scale = 250 μ m. (F&G) Fruit with entire seed preserved, including endosperm and embryo (black arrow). Edge of basal protrusion is captured in plane of section (white arrow) and several longitudinal vascular bundles are seen in transverse section (arrowheads). Specimen ARI 5285 (thin section; *Arecoidocarpus kulkarnii*). Scale = 5 mm. es = endosperm, ec = endocarp.

Abortive carpels: µCT scanning revealed that each fruit has two abortive carpels represented by small locules at the extreme base, just above the remnants of the perianth (Fig. 2.4). In one specimen the locules contain ovules or abortive seeds, which appear to be attached basally (Fig. 2.4A&B). Each locule is surrounded by a layer of small, interwoven fiber bundles, with some fiber bundles radiating outwards in a pattern identical to the fertile locule (Fig. 2.4C&D). This feature indicates that the endocarp encloses each seed separately (forming multiple pyrenes) rather than forming a continuous tissue around all locules. Although each locule has a separate endocarp, the outer parenchymatous zone is continuous between the fertile and abortive locules. Together these features indicate that the fruits developed from flowers with three fused carpels at maturity and were not apocarpous or pseudomonomerous like some modern palms.

Stigmatic remains: Although superficial remnants of the stigma are not clearly visible on the external surface of fruits, serial digital sections were used to detect remnants of locular canals and infer the position of stigmatic remains. In digital transverse sections of the specimen with well-preserved abortive carpels, we observed thin channels connecting the locules of the aborted carpels to the external surface of the fruit; these channels converge just below the epidermis (Fig. 2.4E). Similar channels can be seen in fruits of many extant species connecting the locules to the stigmatic remains (Matsunaga pers. obs.). The position of these channels indicates that the fruits have basal stigmatic remains.

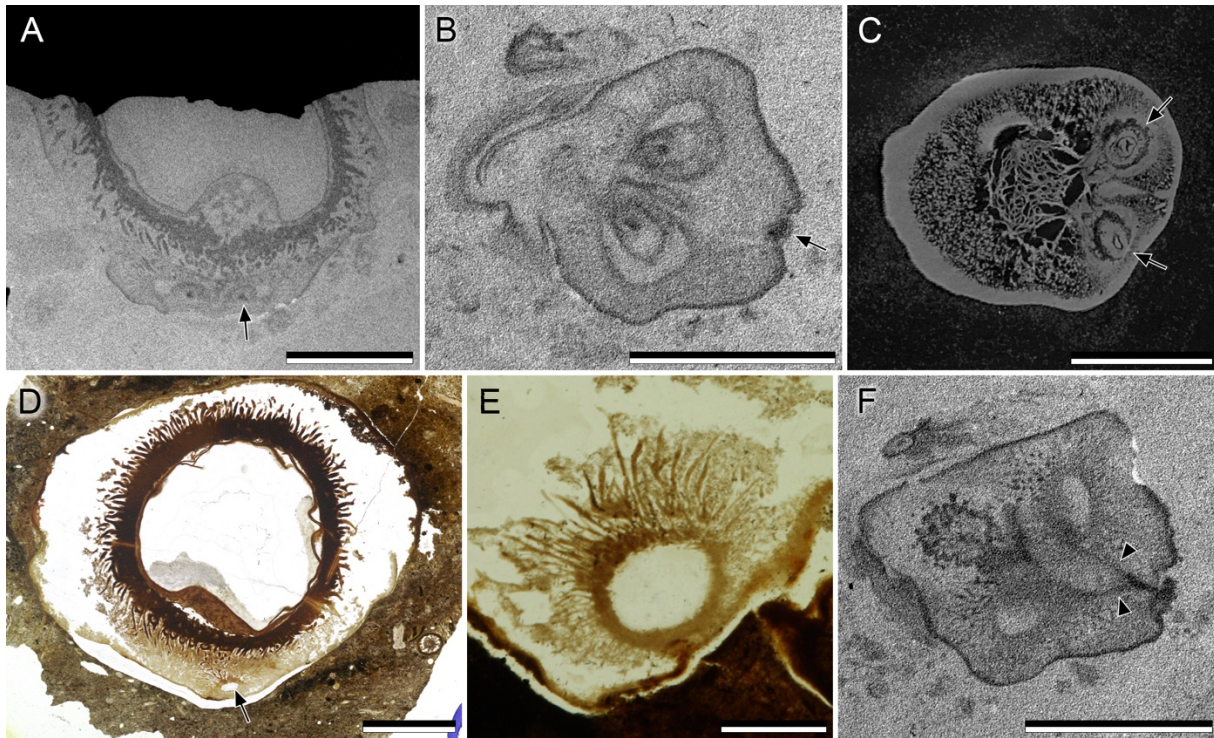


Figure 2.4 Abortive carpels of *Hyphaeneocarpus indicum*. (A) Digital longitudinal section of fruit showing two locules of aborted carpels below fertile locule (arrow). Each locule contains an ovule or abortive seed. Specimen UF 68879. Scale = 5 mm. (B) Digital transverse section through locules of abortive carpels in fruit shown in (A). Note indentation on edge of fruit (arrow) corresponding to stigmatic remains seen more clearly in (F). Specimen UF 68879. Scale = 5 mm. (C) Digital transverse section through the base of an extant *Bismarckia nobilis* fruit with two abortive carpels (arrows), for comparison with *Hyphaeneocarpus*. Note presence of thin endocarp around each locule. Scale = 5 mm. (D) Light micrograph of thin section in which the locule of an abortive carpel is visible at the base of the fruit, below the fertile locule (arrow). Specimen ARI 5288 (thin section; *Arecoidocarpus palasundarensis*). Scale = 5 mm. (E) Detail of abortive locule seen in (D) from another section in same series. Note endocarp structure, from which thin fiber bundles radiate, which is identical to that of fertile locules. Specimen ARI 5288 (thin section; *Arecoidocarpus palasundarensis*). Scale = 5 mm. (F) Digital longitudinal section through base of fruit shown in (A) and (B). Plane of section passes through two locular canals extending to surface of fruit (arrowheads), indicating position of stigmatic remains. Specimen UF 68879. Scale = 5 mm.

Germination: At the apical end of each fruit the endocarp forms a long ridge with a narrow gap at the apex that spans approximately one third of the fruit's circumference (Fig. 2.5A–F). This structure is consistently observed in the fruits and its position relative to the embryo suggests it is an apical germination pore. One specimen with an attached seedling preserved confirms this (Fig. 2.5G–I). The specimen consists of an isolated fruit with part of the pericarp missing on one side, exposing the endocarp. The center of the seed is hollow and only the seed coat is preserved.

Digital longitudinal sections reveal a structure protruding from the top of the fruit, through the aperture in the endocarp. The structure is laterally flattened (Fig. 2.5I), conforming to the elongate shape of the germination pore, and contains longitudinal strands probably representing vascular tissues or fibers. Although the seed is poorly preserved, tissues of the seedling can be traced to the inside of the seed coat. Mode of germination, whether remote tubular, remote ligular, or adjacent ligular, could not be determined.

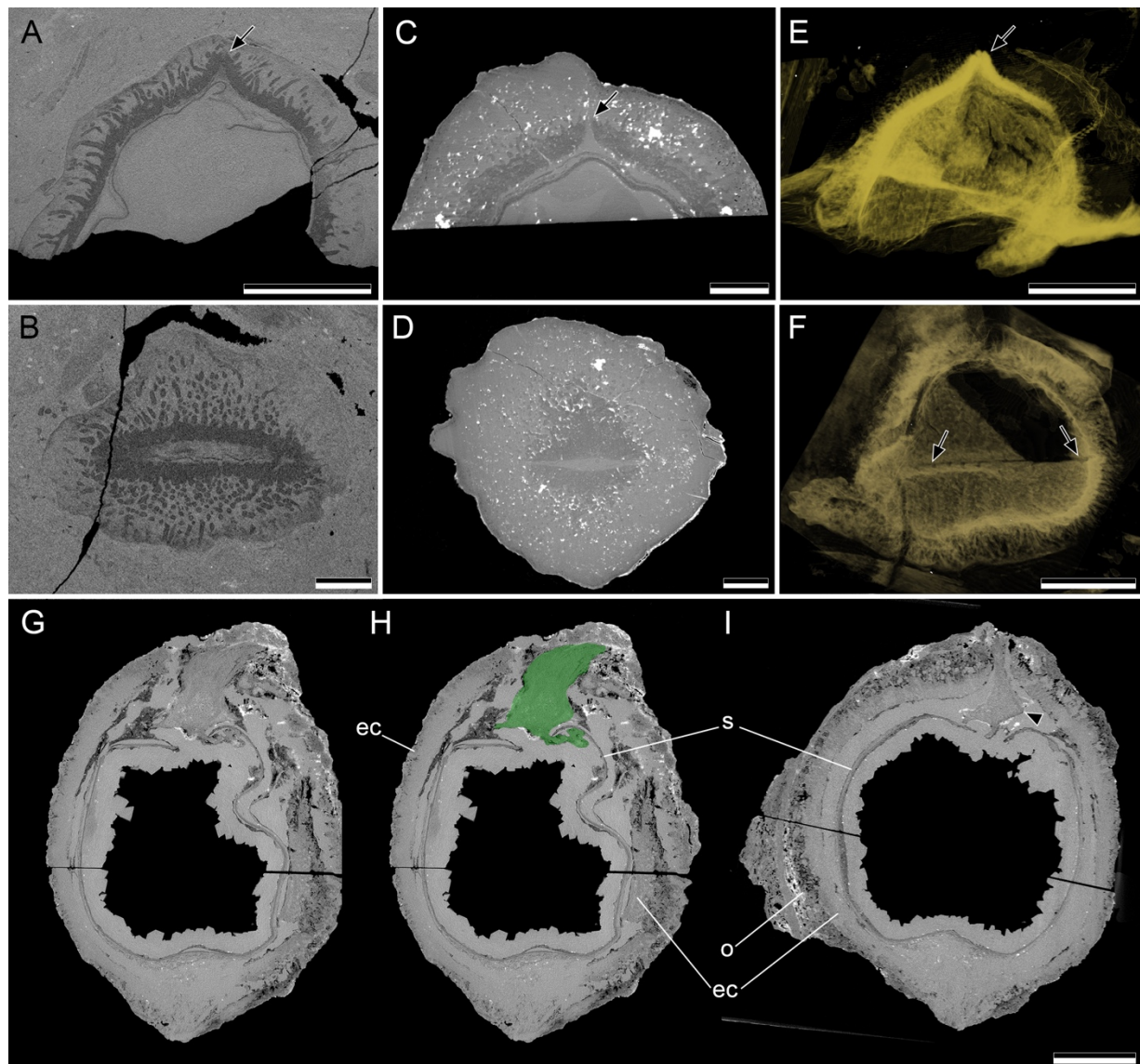


Figure 2.5 Germination pores of *Hyphaeneocarpon indicum*. (A–F) Endocarp germination pores (arrows) seen in digital longitudinal (A&C) and corresponding transverse sections (B&D), as well as from lateral and

apical perspectives of volume rendered specimen (E&F). Note narrow, elongate shape of pore seen in transverse section (B&D), prominent ridge it forms (E), and length of pore revealed by volume rendering, showing pore extending nearly half of fruit circumference (F). (G&H) Digital longitudinal section through fruit shown in Fig. 2.2A, revealing preserved seedling highlighted in green in (H). Tissues of seedling can be traced to inside seed coat (arrow). Note that much of outer pericarp is not preserved and that part of endocarp is broken on the right-hand side of the section. Specimen UF 19415-69208. (I) Longitudinal section of specimen shown in (G) and (H), rotated 90 degrees to show germination pore through which seedling (arrowhead) protrudes. Scale = 5 mm. ec = endocarp, s = seed coat, o = outer pericarp zone.

Phylogenetic analysis

The 50% majority rule consensus tree summarizing the posterior distribution of our analysis is well-resolved and generally conforms to previously published trees, with some differences (see discussion). Borasseae resolves as monophyletic (posterior = 1), with *Hyphaeneocarpon* nested in subtribe Hyphaeninae with very high support (posterior = 0.99). Within Hyphaeninae, *Hyphaeneocarpon* forms a clade with the extant genera *Bismarckia* Hildebr. & H.Wendl. and *Satranala* J.Dransf. & Beentje (posterior = 0.93) that is sister to *Hyphaene* Gaertn. and *Medemia* Württemb. ex H.Wendl. In this tree, *Hyphaeneocarpon* is most closely related to *Satranala*, support for which is low compared to other nodes but moderate for a relationship based solely on morphological characters (posterior = 0.53).

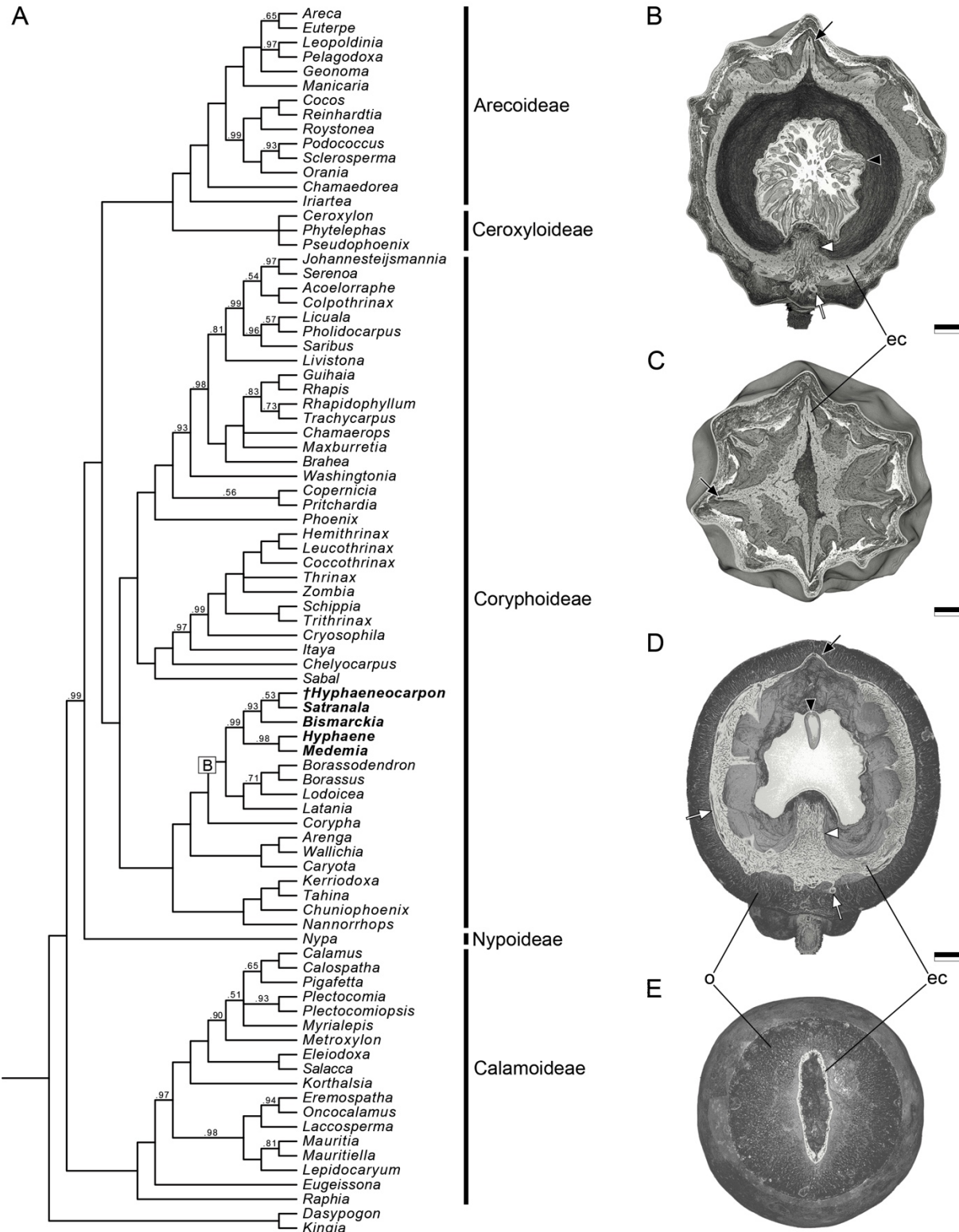


Figure 2.6 Phylogenetic relationships of *Hyphaeneocarpus indicum*. (A) Majority rule consensus tree drawn as a cladogram. Node labels are posterior probabilities, and all unlabeled nodes have a posterior probability of 1. Borasseae stem labeled “B”, genera of subtribe Hyphaeninae indicated with bold text. (B–E) Volume rendering of µCT scans of extant species *Satranala decussilvae* (B&C) and *Bismarckia nobilis* (D&E),

digitally sliced to show internal structure. (B) Lateral view of *S. decussilvae* fruit cut in longitudinal section showing the apical germination pore (black arrow), basal intrusion of endocarp into seed (white arrowhead), and large longitudinal vascular bundles cut in transverse section (white arrow). Note that seed (black arrowhead) is dry and shriveled up inside the endocarp. (C) Apical view of *S. decussilvae* fruit cut in transverse section along ridge formed by germination pore, showing its elongate shape. Note large longitudinal vascular bundles that run along apex of each endocarp ridge (arrow). Specimen K000300252. (D) Lateral view of *B. nobilis* fruit cut in longitudinal section showing apical germination pore (black arrow), basal intrusion of endocarp into seed (white arrowhead), and large longitudinal vascular bundles intercepted in transverse and oblique longitudinal section (white arrows). The seed is dry and shriveled up inside endocarp, but embryo is still visible (black arrowhead). Note structure of outer pericarp zone, with numerous fine radial fiber bundles, and two basal bulges corresponding to abortive carpels. (E) Apical view of *B. nobilis* fruit cut in transverse section along ridge formed by germination pore, showing its elongate shape. Note similarities with comparable sections from *Hyphaeneocarpus indicum* in Fig. 2.5. All scale bars = 5 mm. ec = endocarp, o = outer pericarp zone.

Discussion

Justification for synonymy of species

Several characters shared by the new specimens and the five previously described fossil species indicate they most likely represent occurrences of a single species (Table 2.1). These characters include: (1) endocarp consisting of interwoven fiber bundles, (2) a single layer of large longitudinal fibro-vascular bundles to the outside of the endocarp, (3) fiber bundles that radiate from the endocarp into the outer, parenchymatous zone of the mesocarp, (4) a prominent basal protrusion of the pericarp into the seed, and (5) a thin seed coat attached or appressed to locular epidermis (sometimes described as a two-layered seed coat). Other characters that are important but not documented in all specimens include the apical embryo, apical germination pores, seedlings, abortive carpels, and the inner zone of parenchyma in the pericarp. The variability in observation of these features is due to differences in development, preservation quality, or the methods used to study specimens. With respect to the latter, some characters may be present in the previously described species, particularly the abortive carpels, germination pore, and large longitudinal bundles, but are not documented because visualizing them requires

specific planes of section that are easy to acquire with μ CT data but generally not feasible using physical sectioning techniques.

The five diagnostic characters listed above are all present in the recently collected Keria and Dhangaon specimens, as well as in the previously published specimens attributed to *Arecoidocarpon kulkarnii* (Bonde, 1990a; Fig. 2.3C, 2.3F&G), *Arecoidocarpon palasundarensis* (Bonde, 1995; Fig. 2.2G&H, 2.3A&E, 2.4D&E), and *Pandanusocarpon umariense* (Bonde, 1990b). In addition, we observed abortive carpels and germination pores in specimens of *Arecoidocarpon palasundarensis* not shown in the original published images. *Hyphaeneocarpon indicum* was described from a single specimen, from which one transverse section was taken (Bande *et al.* 1982; Fig. 2.2 D&E). All of the key characters were documented, except the basal protrusion of the pericarp (the physical section did not pass through the base of the fruit). *Palmocarpon arecoides* (Mehrotra, 1987) is also described from a single specimen and is the least thoroughly described example. The features that indicate *Palmocarpon arecoides* is likely conspecific with the aforementioned taxa are similarities in the size of the fruits, the presence of a basal protrusion of the pericarp into the seed, and the overall structure of the pericarp consisting of an inner sclerified layer and an outer parenchymatous layer containing fiber and fibrovascular bundles. The orientation of the fiber bundles in the outer layer is not clear from the published descriptions and images and overall preservation of the fruits is poor, and we were unable to examine or obtain new images of the original specimens. Despite this, we include *Palmocarpon arecoides* in synonymy with the other species owing to the presence of the basal protrusion and the general structure of the pericarp.

Based on these morpho-anatomical similarities and considerations described above, we treat *Arecoidocarpon kulkarnii*, *Arecoidocarpon palasundarensis*, *Hyphaeneocarpon indicum*,

Palmocarpon arecoides, *Pandanusocarpon umariense*, and the new specimens from Dhangaon and Keria as conspecific. We have included them here in the synonymy presented for *Hyphaeneocarpon indicum* Bande, Prakash, & Ambwani emend. Matsunaga, S.Y.Sm., Manch., Srivastava, & Kapgate, based on the first name to be validly published. Another species, *Palmocarpon insigne* from Mohgaonkalan (Mahabale, 1950), looks very similar to *Hyphaeneocarpon indicum* and is also likely conspecific. However, it lacks nomenclatural priority because it was never validly published, and we do not include it in synonymy with the other species because the illustration and description lack sufficient detail to identify it unequivocally as *Hyphaeneocarpon*, and we were unable to locate the original specimen.

Table 2.1 Comparison of described species and new specimens included in synonymy as *Hyphaenocarpus indicum*. Important features for recognizing synonymy and for systematic placement are listed, including pericarp structure, embryo position, and germination pores. Fruit size is also included to show the range of fruit sizes observed in the different specimens. For some specimens exact height and width was difficult to determine, as the outer pericarp is frequently missing or partially preserved (indicated by \geq). The symbol “+” denotes a feature that was observed in published descriptions, figures, or in the actual specimen. “-“ indicates a character either not preserved or not observed in the available preparations of the specimen (e.g. only one or a few sections made). “?” was used in situations where a feature could not be observed due to insufficient detail in published descriptions and/or relevant material not being available for study.

Species	Locality	Size (cm; length x width)	Endocarp: interwoven fiber bundles	Pericarp: longitudinal vascular bundles	Pericarp: radial fiber bundles	Embryo or seedling	Abortive locules	Basal intrusion of endocarp	Evidence of germination pore
<i>Arecoidocarpus kulkarnii</i> Bonde 1990a	Mohgaonkalan	1.6 x 1.4	+	+	+	+	-	+	+
<i>Arecoidocarpus palasundarensis</i> Bonde 1995	Palasundar	2.0 x 2.2	+	+	+	-	+	+	+
<i>Hyphaeneocarpus indicum</i> Bande et al. 1982	Shahpura	4.0 x 2.3– 3.2	+	+	+	-	-	-	-
<i>Palmocarpus arecoides</i> Mehrotra 1987	Samnapur	\geq 2.0 x 2.2– 2.3	?	?	?	-	-	+	-
<i>Pandanuscocarpus umariense</i> Bonde 1990b	Umaria	2.1–2.5 x 1.8–2.0	+	+	+	-	-	+	+
New specimen	Keria	\geq 1.0 x \geq 1.3	+	+	+	-	-	+	+
New specimens	Dhangaoon	1.7–2.3 x 1.5– \geq 2.0	+	+	+	+	?	+	+
New specimen	Mohgaonkalan	\sim 2.0 x 1.4	+	+	+	-	+	+	+

Variation in fruit size

Fruits exhibit considerable variation in size between the different localities (Table 2.1). The smallest specimens are from the Keria and Mohgaonkalan localities (ca. 1.5 cm), while the largest is the *Hyphaeneocarpon indicum* type specimen from Shahpura. The latter was described as approximately 4.0 cm long and 3.2 cm in diameter at the widest point, but the fruits are somewhat compressed, which may exaggerate the size measurements. Most fruits are approximately 2.0–2.5 cm in diameter. We do not consider the size variation to be grounds for recognizing two different species because there is no strong bimodal pattern in fruit size, and we have not found any characters that distinguish the smaller specimens from Keria and Mohgaonkalan from the others. In modern palms fruit size does sometimes vary between species, but it can also vary within and between individuals. Moreover, disparity in fruit size of the fossils may reflect developmental, preservational, or local environmental differences. Among palms, fruit size tends to increase as the seed matures and the endosperm transitions from a free-nuclear to a cellular phase (DeMason, Sekhar, & Harris, 2006), and therefore some of the size variation could reflect fruit maturity. However, this does not fully explain the range in observed fruit size because some of the smaller specimens appear to have mature seeds (Fig. 2.3F), while the largest specimen is probably slightly immature (Fig. 2.2D; see discussion below). Temporal differences could also account for this variation, as the Mohgaonkalan and Keria localities are part of the Deccan Main Plateau and currently considered late Maastrichtian, whereas the other localities are all in the eastern Mandla subprovince and are most likely early Danian; so far, *Hyphaeneocarpon* is the only plant species known to occur at localities in both regions. It is

therefore possible that the smaller size of some fruits is related to environmental or other biotic changes that occurred over the K-Pg boundary in India, but this would need to be tested further.

Taxonomic affinities inferred from fruit morphology

Owing to significant morphological diversity among palm fruits, there are few clear characters with which palm fruits can be universally recognized. However, the following characters of the fossils strongly indicate relationships with Arecaceae: fruits indehiscent, single-seeded, derived from three fused uni-ovulate carpels (one of which forms the mature fruit), presence of albuminous seeds containing small conical embryos, and pericarp with a sclerenchymatous endocarp and longitudinal fibrovascular bundles (Dransfield *et al.*, 2008; Matsunaga pers. obs.). Several additional key characters are present that constrain the likely affinities of the fossil taxon to subfamily Coryphoideae, tribe Borasseae, subtribe Hyphaeninae: (1) syncarpous gynoecium with three carpels, (2) fruit, single-seeded, derived from one of the carpels, (3) pericarp with a thick zone of parenchyma to the inside of the endocarp in some developmental stages, (4) endocarp composed of interwoven fiber bundles that radiate into outer parenchymatous zone of pericarp, (5) embryo apical, (6) apical germination pore in endocarp, and (7) basal stigmatic remains (Dransfield *et al.*, 2008; Romanov *et al.*, 2011).

Gynoecium structure and development is variable among modern palms, but the most prevalent and likely ancestral condition is for the gynoecium to be syncarpous and trimerous at anthesis (Moore & Uhl, 1982; Dransfield *et al.*, 2008). However, some palms consistently produce more than three carpels (e.g. Phytelepheae), several genera of coryphoid palms have only a single carpel (most Cryosophileae), and many members of Arecoideae are pseudomonomerous, with two of the carpels aborting usually early in floral development (e.g.

tribes Areceae and Euterpeae). In most genera that have three carpels at anthesis only one of the seeds matures; in some of these taxa the abortive carpels are obvious in mature fruits, forming basal bulges or protuberances (e.g. *Hyphaene*, *Bismarckia*). Therefore, despite the basic condition being trimery of the gynoecium, palm fruits are most commonly single-seeded (Moore & Uhl, 1982; Dransfield *et al.*, 2008).

The fossils of *Hyphaeneocarpon* have a gynoecium of three carpels, two of which are abortive but easily seen at the base of mature fruits. This indicates that *Hyphaeneocarpon* is unlikely to belong to a group of palms that are either pseudomonomerous or unicarpellate. The inner layer of parenchyma between the endocarp and seed (Fig. 2.2D&E) helps to further refine potential affinities. This tissue is found in fruits of many modern members of Coryphoideae, as well as *Nypa* (Nypoideae) and *Eugeissona* Griff. (Calamoideae; Romanov *et al.*, 2011; Bobrov *et al.*, 2012b,a). In such fruits, this inner layer is initially thick but compresses as the seed matures during the final phases of fruit development; on reaching maturity the seed completely displaces the parenchyma and fills the entire space within the endocarp. This inner parenchyma is, furthermore, not present in other taxa with thick endocarps like the Cocoseae, in which the endocarp develops from the innermost layers of the pericarp (Dransfield *et al.*, 2008; Bobrov *et al.*, 2012b). The ephemeral nature of this tissue helps to explain why we did not observe it in most specimens (e.g. Fig. 2.2C, 2.3F) and why the locular epidermis is often pulled away from the endocarp in mature fruits (Fig. 2.3E&G). Among palms that exhibit this inner parenchyma, affinities with Coryphoideae are the most likely. Fruits of *Nypa* and *Eugeissona* are highly distinctive and inconsistent with the morphology of the *Hyphaeneocarpon* fossils. *Nypa* fruits are derived from an apocarpous gynoecium and have an obovate, angular shape related to their dense aggregation in globose heads (Bobrov *et al.*, 2012b). *Eugeissona* and all modern Calamoideae

have an epicarp composed of helically arranged imbricate scales, a character not present in these fossils (Dransfield *et al.*, 2008; Bobrov *et al.*, 2012a). Other features including gynoecium morphology and the positions of stigmatic remains, embryo, and germination pore make affinities with *Eugeissona* or *Nypa* highly unlikely.

Subfamily Coryphoideae comprise two clades—the “syncarpous clade” a second group containing *Sabal* Adans., *Phoenix* L., and tribes Cryosophileae and Trachycarpeae, all of which are apocarpous except for *Sabal* (Fig. 2.6A; Dransfield *et al.*, 2008; Baker *et al.*, 2009; Faurby *et al.*, 2016). The syncarpous condition of *Hyphaeneocarpon* is consistent with the syncarpous clade, which includes 16 genera in four tribes: Caryoteae, Chuniophoeniceae, Corypheae, and Borasseae. Among these tribes, only Borasseae have thick endocarps composed of interwoven fiber bundles, apical embryos, and apical germination pores consisting of very thin zones of the endocarp (Dransfield *et al.*, 2008; Romanov *et al.*, 2011). Tribe Borasseae includes eight genera in two subtribes: Hyphaeninae (*Hyphaene*, *Bismarckia*, *Medemia*, and *Satranala*) and Lataninae (*Latania* Comm. ex Juss., *Lodoicea* Comm. ex DC., *Borassus* L., and *Borassodendron* Becc.). Members of subtribe Lataninae produce three-seeded fruits, although seed number in *Lodoicea* is variable, with each seed surrounded by a separate endocarp, forming pyrenes. Stigmatic remains are consistently apical. In contrast, fruits of Hyphaeninae are typically single-seeded, with the abortive carpels forming bulges at the base of the fruit (Fig. 2.6D); sometimes, more than one seed develops producing a deeply lobed fruit resembling two smaller ones conjoined at the base. Stigmatic remains are basal in Hyphaeninae. Fossils of *Hyphaeneocarpon*, which are single-seeded with basal stigmatic remains, are therefore much more similar to Hyphaeninae than to Lataninae.

Several other characters of *Hyphaeneocarpon* are also seen in Hyphaeninae: (1) the pericarp of both *Bismarckia* and *Hyphaene* have fiber bundles that extend radially from the endocarp into a predominantly parenchymatous zone of the pericarp (Fig. 2.6D). (2) In *Bismarckia* and *Satranala* fruits, the endocarp protrudes into the base of the seed (Fig. 2.6B–E). (3) The germination pores of *Bismarckia* and *Satranala* are elongate and form a ridge, rather than circular as in other members of Borasseae (note: germination pores in *Medemia* also appear to be very slightly elongate, but do not form a ridge; Fig. 2.6 B–E). This ridge is much shallower and broader in *Bismarckia* than in *Satranala* or *Hyphaeneocarpon*. In *Satranala* the ridge runs around much of the circumference of the fruit, and instead of germinating through the pore, the endocarp splits to release the entire seed; among palms this germination mode is unique to *Satranala* (Dransfield *et al.*, 2008). (4) In *Bismarckia* and *Satranala* there is a single layer of large longitudinal fibrovascular bundles in the outermost zone of the endocarp. In *Bismarckia* these bundles are visible in longitudinal and transverse sections through the endocarp (Fig. 2.6D), while in *Satranala* the bundles form the crests of the longitudinal ridges of the endocarp, as seen in transverse section (Fig. 2.6C). Based on these features, *Hyphaeneocarpon* is much more similar to *Satranala* and *Bismarckia* than it is to *Hyphaene* and *Medemia*. However, one notable difference is the absence of sculpturing in *Hyphaeneocarpon* endocarps; the endocarp is smooth, lacking the deep ridges formed externally in *Satranala*, or protruding internally into the seed as in *Bismarckia* (Fig. 2.6B&D). Overall, all the characters described above strongly indicate that the *Hyphaeneocarpon* fossils have close affinities with subtribe Hyphaeninae in tribe Borasseae of subfamily Coryphoideae. This is congruent with the conclusions of Bande *et al.* (1982) who, in their original description of *Hyphaeneocarpon indicum*, placed it in subtribe Hyphaeninae based on similarities in pericarp anatomy, notably the presence of parenchyma to

the inside of the endocarp. Although Bande *et al.* (1982) thought it more closely resembled *Hyphaene*, our comparisons based on additional specimens and several new characters suggest greater similarity with *Bismarckia* and *Satranala*, the latter of which was not discovered until 1995 (Dransfield & Beentje, 1995).

Phylogenetic analysis

We conducted a phylogenetic analysis to test the systematic relationships of *Hyphaeneocarpon* within palms, and to obtain complementary information about its phylogenetic position. In our analysis *Hyphaeneocarpon* is positioned within subtribe Hyphaeninae, forming a well-supported clade with the extant genera *Satranala* and *Bismarckia*. This clade is united by the following morphological synapomorphies, the first two of which were scored in the morphological matrix: (1) Presence of an elongate germination pore or valve that usually forms a ridge, (2) endocarp that protrudes into the seed basally, forming a distinctive groove, and (3) a single layer of large longitudinal fibrovascular bundles embedded in the endocarp. Further, *Hyphaeneocarpon* resolves as sister to *Satranala* with moderate support given the limited morphological characters scored (posterior = 0.53). However, we consider this relationship highly uncertain, as the *Hyphaeneocarpon-Satranala-Bismarckia* group collapsed into a polytomy in some iterations of our analysis. Moreover, the vegetative morphology of *Hyphaeocarpon* is currently unknown and therefore it is possible its phylogenetic position could change with the addition of more characters such as those of the stems and leaves. Nevertheless, we consider *Hyphaeneocarpon* to be a reliable fossil for calibrating the crown group of subtribe Hyphaeninae in future dating analyses. Although *Hyphaeneocarpon* might be used to calibrate divergence of *Satranala* and *Bismarckia*, we feel there is too much uncertainty in the

relationships between the three genera to justify using *Hyphaeneocarpion* as a calibration for that node. In contrast, there is very little uncertainty in the position of *Hyphaeneocarpion* within the crown group of Hyphaeninae and we feel it would be appropriate as a crown node calibration for the subtribe, with an age of 67–64 Ma.

The overall topology recovered in our analysis is consistent with those of previously published phylogenetic trees with respect to subfamily and tribe-level relationships among palms, and conforms to current genus-level classifications within those larger clades. Moreover, our analysis corroborates some relationships for which conflicting results have been obtained in other studies and recovers similar areas of uncertainty. For instance, the relationships between genera of Hyphaeninae agree with those of some previous analyses, wherein *Bismarckia* and *Satranala* form a clade sister to one comprising *Hyphaene* and *Medemia* (Asmussen *et al.*, 2006; Baker *et al.*, 2009; Faurby *et al.*, 2016). Our analysis shows strong support for these relationships, with *Hyphaeneocarpion* part of the *Bismarckia-Satranala* group. In contrast, relationships within tribe Trachycarpeae and subfamily Calamoideae are poorly supported, consistent with uncertainties observed in previous studies (e.g. Asmussen *et al.*, 2006; Baker *et al.*, 2009; Bacon, Baker, & Simmons, 2012; Barrett *et al.*, 2016; Faurby *et al.*, 2016). The lack of resolution within these groups may be related to the paucity of DNA sequence data available to us on GenBank for some genera in Calamoideae and Trachycarpeae and may generally reflect the need for more data in resolving intergeneric relationships of palms (Faurby *et al.*, 2016). Therefore, despite fairly high support in our analysis for some nodes within these groups, we treat our results for Calamoideae and Trachycarpeae cautiously. However, these uncertainties do not change our confidence in the affinities of *Hyphaeneocarpion* with subtribe Hyphaeninae.

Other occurrences of Borasseae in the Deccan Intertrappean Beds

Several other fossils from the Deccan Intertrappean Beds have been assigned to or compared with Borasseae, some of which originate from the same localities in which *Hyphaeneocarpon* occur. They include leaves of *Sabalites dindoriensis* R. Srivastava, G. Srivastava, & D. L. Dilcher and *Amensoneuron borassoides* Bonde, petioles of *Palmocaulon hyphaeneoides* Shete & Kulkarni, and stems of *Palmoxylon hyphaeneoides* Rao & Shete (Shete & Kulkarni, 1980; Bonde, 1986; Rao & Shete, 1989; Srivastava, Srivastava, & Dilcher, 2014). Vegetative structures alone, particularly leaves, are generally insufficient for confident systematic placement within palms (Read & Hickey, 1972), but some of these fossils potentially represent Borasseae.

Fossils of *Sabalites dindoriensis* consist of impressions of costapalmate leaves with unarmed petioles and an associated inflorescence (Srivastava *et al.*, 2014). Strongly costapalmate leaves lacking spines are found in a number coryphoid genera (Dransfield *et al.*, 2008), and while the robust unbranched inflorescence associated with *S. dindoriensis* resembles those of Borasseae, possible affinities with other groups cannot be ruled out entirely. These fossils originate from the Ghughua locality, which is near the Umaria locality in which *Hyphaeneocarpon* occurs. *Amensoneuron borassoides* is a palmate or costapalmate leaf impression with some vein structure preserved, originating from the Mohgaonkalan locality where some fruits of *Hyphaeneocarpon* occur (Bonde, 1986). However, the specimen consists of a single lamina fragment and lacks additional features helpful for identification. *Palmocaulon hyphaeneoides* is a permineralized palm petiole exhibiting anatomical similarities with Borasseae (Shete & Kulkarni, 1980). Taxonomic affinities with other groups of palms are possible, but the

anatomical similarities documented by the original authors do indicate potential relationships with Borasseae.

Palmoxylon hyphaeneoides was described from a basal stem segment bearing numerous roots, and based on comparisons with modern palms was considered by Rao & Shete (1989) to resemble *Hyphaene*. We applied the original description of *Palmoxylon hyphaeneoides* to the dataset of anatomical descriptors of palm stem anatomy compiled by Thomas & De Franceschi (2013). Using the relevant anatomical characters documented by Rao & Shete (1989), *Palmoxylon hyphaeneoides* exhibits stem anatomy consistent with several groups of coryphoid palms including Borasseae, *Sabal*, Trachycarpeae, and Chuniophoeniceae, as well as *Nypa*, and thus its placement in Borasseae is equivocal.

Implications for divergence time estimates – Late Cretaceous diversification of crown Coryphoideae?

Placement of *Hyphaeneocarpion* in subtribe Hyphaeninae of tribe Borasseae has implications for elucidating evolutionary tempo and historical biogeography of Coryphoideae, and palms more generally. Currently the oldest macrofossil assigned to Borasseae, *Hyphaene kappelmanni* A.D. Pan, B.F. Jacobs, J. Dransf. & W. J. Baker (Pan *et al.*, 2006), is late Oligocene (28–27 Ma) — significantly younger than *Hyphaeneocarpion*, which is late Maastrichtian–early Danian (67–64 Ma). With *H. kappelmannii* employed as a calibration for stem Hyphaeninae, molecular dating analyses have estimated the age of the Borasseae stem node between 49–29 Ma and the Hyphaeninae crown node between 26–13 Ma (Baker & Couvreur, 2013). The position of *Hyphaeneocarpion* within crown Hyphaeninae indicates a much earlier origin of Borasseae and Hyphaeninae than analyses using the *H. kappelmannii* calibration have so far predicted, indicating

an origin of the Hyphaeninae crown group by 67–64 Ma, approximately 40 million years earlier than current estimates. This implies an even earlier origin of tribe Borasseae, likely within the Late Cretaceous.

The age of *Hyphaeneocarpon* is interesting in the context of the fossil record of palms. The earliest palm macrofossils and much of the Late Cretaceous fossil record consist of costapalmate leaf fossils assigned to the form genus *Sabalites* G. Saporta (Berry, 1914; Harley, 2006). While these provide compelling evidence for Coryphoideae in the Cretaceous (costapalmate leaves are today restricted to Coryphoideae), leaf and stem fossils generally cannot be assigned below the subfamily level and are often placed in form genera (Read & Hickey, 1972). Reproductive structures, which potentially can provide strong evidence for divergence of crown lineages, are not seen in abundance until around the Eocene (Harley, 2006; Dransfield *et al.*, 2008 and references therein) and many earlier occurrences of palm fruits are, in our opinion, unreliable records for major groups within Arecaceae owing to the absence of clear diagnostic characters in the fossils. Moreover, most molecular dating studies, for which relatively few reliable fossil calibrations are available, place much of the diversification of Coryphoideae in the Cenozoic (Couvreur, Forest, & Baker, 2011; Bacon *et al.*, 2012; Baker & Couvreur, 2013). An exception to this paucity of reproductive organs in the early fossil record are seeds of *Sabal bigbendense* Manch., Wheeler, & Lehman and *Sabal bracknellense* (Chandler) Mai from the Campanian of Texas (Manchester, Lehman, & Wheeler, 2010). These are indistinguishable from modern *Sabal* seeds and were found in association with costapalmate leaf compressions. The *Sabal* fossils, along with the *Hyphaeneocarpon* fossils from India, together suggest that there was a much more extensive Late Cretaceous diversification of crown Coryphoideae than indicated by both molecular dating analyses and the fossil record of vegetative organs. This

could extend to other subfamilies as more of the Deccan palms are described and revised; a recent study of fossils now assigned to *Palmocarpus drypeteoides* indicates subtribe Attaleinae (tribe Cocoseae, subfamily Arecoideae) had diverged by the Maastrichtian–Danian (Manchester *et al.*, 2016). Further analyses are needed to determine the precise influence of these fossils on divergence time estimates, but *Hyphaeneocarpus* will serve as a very reliable and probably highly informative calibration.

Biogeographic implications

Today members of Borasseae are found throughout the Indian Ocean region, from Africa into Southeast Asia (Dransfield *et al.*, 2008). Most genera are geographically restricted. *Bismarckia* and *Satranala* are endemic to Madagascar, *Medemia* is found only the deserts of Southern Egypt and Northern Sudan, *Lodoicea* is endemic to the Seychelles and *Latania* to the Mascarene Islands, and *Borassodendron* is distributed in parts of Southeast Asia. The exceptions are *Borassus*, which is one of the most widespread palm genera, stretching from Africa to Southeast Asia, and *Hyphaene*, found throughout Africa, Madagascar, the Middle East, and India (Bayton, Obunyali, & Ranaivojaona, 2003; Dransfield *et al.*, 2008). The fossil record of Borasseae contains only a few occurrences, all from within its modern distribution. In addition to *Hyphaene kappelmannii* from Ethiopia, there is *Borassus*-type pollen from Kenya (late Oligocene to early Miocene; Vincens, Tiercelin, & Buchet, 2006) and two fruit fossils assigned to the group: *Hyphaene coriacea* Gaertn. from Uganda (late Miocene; Dechamps, Senut, & Pickford, 1992), and *Hyphaeneocarpus aegypticum* Vaudois-Miéja & Lejal-Nicol from Egypt (Aptian; Vaudois-Miéja & Lejal-Nicol, 1987). However, the specimens of *H. aegypticum* are of uncertain affinity (Pan *et al.*, 2006) and are questionably palms, and until they can be reexamined

do not represent a reliable record for the group. The fossils of *Hyphaeneocarpon indicum* from the Maastrichtian–Danian of India are thus the oldest reliable record of Borasseae.

The close affinities of *Hyphaeneocarpon* with two genera endemic to Madagascar are curious from a biogeographic perspective, since India and Madagascar were joined as a single continent throughout the Early Cretaceous after the breakup of Gondwana (Ali & Aitchison, 2008; Chatterjee, Goswami, & Scotese, 2013). The syncarpous clade of Coryphoideae, to which Borasseae belongs, is hypothesized as having a Laurasian origin, with subsequent spread of Borasseae stem lineages into the Indian Ocean where the diversification of the tribe subsequently occurred (Dransfield *et al.*, 2008; Baker & Couvreur, 2013). If this hypothesis is correct, the ancestor of *Hyphaeneocarpon* could have entered India either via dispersal from Madagascar, or during the separation of Madagascar and India around the Turonian (~90 Ma). Alternatively, the *Hyphaeneocarpon-Bismarckia-Satranala* clade or its ancestors may have been more widespread in the past, persisting to modern times only in Madagascar. Regarding dispersal vectors, modern representatives of Borasseae have large, typically animal-dispersed fruits (mammals, large birds; Zona & Henderson, 1989) and are considered poor dispersers (Baker & Couvreur, 2013). The Indian fossils, while smaller than fruits of most modern Borasseae, are structurally very similar to those of extant members and lack features suggesting different dispersal adaptations. These considerations raise intriguing and unanswered questions about the role of dispersal versus vicariance in the biogeographic history of Borasseae, as well as the identity of fruit dispersers, since these events predate the evolution of modern mammalian and avian vectors.

Conclusions

We document the morphology and anatomy of several new palm fruit specimens from the Deccan Intertrappean Beds of India, and revise the taxonomy of five previously described species, placed here in synonymy as *Hyphaeneocarpus indicum*. X-ray µCT scans revealed several key characters essential for systematic placement of the fossils within subtribe Hyphaeninae of tribe Borasseae, including the presence of abortive carpels and germination pores with seedlings. Phylogenetic analysis further indicated affinities with the extant genera *Bismarckia* and *Satranala* within Hyphaeninae, which are today endemic to Madagascar. This is the oldest reliable occurrence of Borasseae in the fossil record. Our results indicate that divergence of subtribe Hyphaeninae occurred by the late Maastrichtian–early Danian and tribe Borasseae has persisted in the Indian Ocean region since the end of the Cretaceous. Inclusion of this fossil in dating analyses will be necessary to determine the influence of these fossils on the predicted ages of other phylogenetic nodes, but they nevertheless suggest a more extensive Late Cretaceous diversification of palms than was previously known. This highlights the importance of the Deccan palms, and fruit fossils more generally, in elucidating the deep evolutionary history of Arecaceae.

References

- Ali JR & Aitchison JC.** 2008. Gondwana to Asia: Plate tectonics, paleogeography and the biological connectivity of the Indian sub-continent from the Middle Jurassic through latest Eocene (166–35 Ma). *Earth-Science Reviews* **88**: 145–166.
- Asmussen CB, Dransfield J, Deickmann V, et al.** 2006. A new subfamily classification of the palm family (Arecaceae): Evidence from plastid DNA phylogeny. *Botanical Journal of the Linnean Society* **151**: 15–38.
- Bacon CD, Baker WJ & Simmons MP.** 2012. Miocene dispersal drives island radiations in the palm tribe trachycarpeae (Arecaceae). *Systematic Biology* **61**: 426–442.
- Baker WJ & Dransfield J.** 2016. Beyond Genera Palmarum: progress and prospects in palm systematics. *Botanical Journal of the Linnean Society* **182**: 207–233.
- Baker WJ & Couvreur TLP.** 2013. Global biogeography and diversification of palms sheds light on the evolution of tropical lineages. I. Historical biogeography. *Journal of Biogeography* **40**: 274–285.
- Baker WJ, Savolainen V, Asmussen-Lange CB, et al.** 2009. Complete generic-level phylogenetic analyses of palms (Arecaceae) with comparisons of supertree and supermatrix approaches. *Systematic Biology* **58**: 240–256.
- Bande MB, Prakash U & Ambwani K.** 1982. A fossil palm fruit *Hyphaeneocarpus indicum* gen. et sp. nov. from the Deccan Intertrappean Beds, India. *The Palaeobotanist* **30**: 303–309.
- Barrett CF, Baker WJ, Comer JR, et al.** 2016. Plastid genomes reveal support for deep phylogenetic relationships and extensive rate variation among palms and other commelinid monocots. : 855–870.
- Bayton RP, Obunyali C & Ranaivojaona R.** 2003. A Re-examination of *Borassus* in Madagascar. *Palms* **47**: 206–219.
- Berry EW.** 1914. The Upper Cretaceous and Eocene floras of South Carolina and Georgia. *US Geological Survey, Professional Paper* **84**: 1–200.
- Bobrov AVFC, Dransfield J, Romanov MS, et al.** 2012a. Gynoecium and fruit histology and development in *Eugeissona* (Calamoideae: Arecaceae). *Botanical Journal of the Linnean Society* **168**: 377–394.
- Bobrov AVFC, Lorence DH, Romanov MS, et al.** 2012b. Fruit Development and Pericarp Structure in *Nypa fruticans* Wurmb (Arecaceae): A Comparison with Other Palms. *International Journal of Plant Sciences* **173**: 751–766.
- Bonde SD.** 1986. *Amesoneuron borassoides* sp. nov. A borassoid palm leaf from the Deccan Intertrappean bed at Mohgaonkalan, India. *Biovigyanam* **12**: 89–91.

- Bonde SD. 1990a.** *Arecoidocarpon kulkarnii* gen. et sp. nov., an arecoid palm fruit from Mohgaon Kalan, Madhya Pradesh. *The Palaeobotanist* **38**: 212–216.
- Bonde SD. 1990b.** A new palm peduncle *Palmostroboxylon umariense* (Arecaceae) and a fruit *Pandanusocarpon umariense* (Pandanaceae) from the Deccan Intertrappean Beds of India. In: JG D, DC C, eds. *Proceedings of the 3rd International Organization of Palaeobotany Conference, Melbourne 1988*. A-Z Printers, Melbourne, 59–65.
- Bonde SD. 1995.** A palm peduncle and fruit from the Deccan Intertrappean Beds of India. In: Pant D, ed. *Proceedings of the Birbal Sahni Birth Centenary International Conference: Symposium on Global Environment and Diversification of Plants through Geological Time: Birbal Sahni Centenary Volume*. Allahabad, 63–69.
- Bonde SD. 2008.** Indian fossil monocotyledons: Current Status, Recent Developments and Future Directions. *The Palaeobotanist* **57**: 141–164.
- Chatterjee S, Goswami A & Scotese CR. 2013.** The longest voyage : Tectonic , magmatic , and paleoclimatic evolution of the Indian plate during its northward flight from Gondwana to Asia. *Gondwana Research* **23**: 238–267.
- Couvreur T, Forest F & Baker WJ. 2011.** Origin and global diversification patterns of tropical rain forests: inferences from a complete genus-level phylogeny of palms. *BMC Biology* **9**: 44.
- Dechamps R, Senut B & Pickford M. 1992.** Fruits fossiles pliocènes et pléistocènes du Rift Occidental ougandais. Signification paléoenvironnementale. *Comptes Rendus de l'Académie des Sciences Paris, Série II* **314**: 325–331.
- DeMason DA, Sekhar KC & Harris M. 1989.** Endosperm Development in the Date Palm (*Phoenix dactylifera*) (Arecaceae). *American Journal of Botany* **76**: 1255–1265.
- Dransfield J & Beentje HJ. 1995.** *Satranala* (Coryphoideae : Borasseae : Hyphaeninae), a New Palm Genus from Madagascar. *Kew Bulletin* **50**: 85–92.
- Dransfield J, Uhl NW, Asmussen CB, et al. 2008.** *Genera Palmarum: the evolution and classification of palms*. Richmond, Surrey, UK: Kew Publishing.
- Faurby S, Eiserhardt WL, Baker WJ, et al. 2016.** An all-evidence species-level supertree for the palms (Arecaceae). *Molecular Phylogenetics and Evolution* **100**: 57–69.
- Gee CT. 2001.** The mangrove palm *Nypa* in the geologic past of the new world. *Wetlands Ecology and Management* **9**: 181–194.
- Govaerts R, Dransfield J, Zona S, et al. 2018.** World Checklist of Arecaceae. *Royal Botanic Gardens, Kew*. Published on the Internet; <http://wcsp.science.kew.org/> Retrieved 4 November 2018.

Guindon S, Dufayard JF, Lefort V, et al. 2010. New algorithms and methods to estimate maximum-likelihood phylogenies: Assessing the performance of PhyML 3.0. *Systematic Biology* **59**: 307–321.

Harley MM. 2006. A summary of fossil records for Arecaceae. *Botanical Journal of the Linnean Society* **151**: 39–67.

Hooper P, Widdowson M & Kelley S. 2010. Tectonic setting and timing of the final Deccan flood basalt eruptions. *Geology* **38**: 839–842.

Kapgate DK. 2009. *Palaeovegetation, palaeophytogeography and palaeoenvironmental study of Central India*. J.M. Patel College of Arts, Commerce & Science.

Kulkarni AR & Mulani RM. 2004. Indigenous palms of India. *Current Science* **86**: 1598–1603.

Lanfear R, Calcott B, Ho SYW, et al. 2012. PartitionFinder: Combined selection of partitioning schemes and substitution models for phylogenetic analyses. *Molecular Biology and Evolution* **29**: 1695–1701.

Lanfear R, Frandsen PB, Wright AM, et al. 2016. PartitionFinder 2 : New Methods for Selecting Partitioned Models of Evolution for Molecular and Morphological Phylogenetic Analyses. *34*: 772–773.

Mahabale TS. 1950. Palaeobotany in India VII. Some new fossil plants from the Deccan Intertrappeans. *Journal of the Indian Botanical Society* **29**: 31–33.

Manchester SR, Bonde SD, Nipunage DS, et al. 2016. Trilocular Palm Fruits from the Deccan Intertrappean Beds of India. *International Journal of Plant Sciences* **177**: 633–641.

Manchester SR, Lehman TM & Wheeler EA. 2010. Fossil Palms (Arecaceae, Coryphoideae) Associated with Juvenile Herbivorous Dinosaurs in the Upper Cretaceous Aguja Formation, Big Bend National Park, Texas. *International Journal of Plant Sciences* **171**: 679–689.

Mehrotra RC. 1987. Some new palm fruits from the Deccan Intertrappean Beds of Mandla District, Madhya Pradesh. *Geophytology* **17**: 204–208.

Miller MA, Pfeiffer W & Schwartz T. 2010. Creating the CIPRES Science Gateway for inference of large phylogenetic trees. *2010 Gateway Computing Environments Workshop, GCE 2010*.

Moore HE & Uhl NW. 1982. Major trends of evolution in palms. *The Botanical Review* **48**: 1–69.

Murray SG. 1973. The formation of endocarp in palm fruits. *Principes* **17**: 91–102.

Pan AD, Pan AD, Jacobs BF, et al. 2006. The fossil history of palms (Arecaceae) in Africa and new records from the Late Oligocene (28–27 Mya) of north-western Ethiopia. *Botanical Journal of the Linnean Society* **151**: 69–81.

Pross J, Contreras L, Bijl PK, et al. 2012. Persistent near-tropical warmth on the Antarctic continent during the early Eocene epoch. *Nature* **488**: 73–7.

Rao G V & Shete RH. 1989. *Palmoxylon hyphaeneoides* sp. nov. from the Deccan Intertrappean beds of Wardha District Maharashtra, India. *Proceedings of the Special Indian Geophytological Conference, Pune, 1986* **1**: 123–128.

Read RW & Hickey LJ. 1972. A Revised Classification of Fossil Palm and Palm-like Leaves. *International Association for Plant Taxonomy* **21**: 129–137.

Renne PR, Sprain CJ, Richards MA, et al. 2015. State shift in Deccan volcanism at the Cretaceous-Paleogene boundary, possibly induced by impact. *Science* **350**: 76–78.

Romanov MS, Bobrov AVFC, Wijesundara DSA, et al. 2011. Pericarp development and fruit structure in borassoid palms (Arecaceae-Coryphoideae-Borasseae). *Annals of Botany* **108**: 1489–1502.

Samant B & Mohabey DM. 2009. Palynoflora from deccan volcano-sedimentary sequence (Cretaceous-Palaeogene transition) of central India: Implications for spatio-temporal correlation. *Journal of Biosciences* **34**: 811–823.

Schoene B, Samperton KM, Eddy MP, et al. 2015. U-Pb geochronology of the Deccan Traps and relation to the end-Cretaceous mass extinction. *Science* **347**: 182–184.

Shete RH & Kulkarni AR. 1980. *Palmocaulon hyphaeneoides* sp. nov. from the Deccan Intertrappean beds of Wardha District, Maharashtra, India. *Palaeontographica Abteilung B* **172**: 117–124.

Shrivastava JP, Duncan RA & Kashyap M. 2015. Post-K/PB younger ^{40}Ar - ^{39}Ar ages of the Mandla lavas: Implications for the duration of the Deccan volcanism. *Lithos* **224–225**: 214–224.

Sluijs A, Schouten S, Donders TH, et al. 2009. Warm and wet conditions in the Arctic region during Eocene Thermal Maximum 2. *Nature Geoscience* **2**: 777–780.

Smith S, Manchester SR, Samant B, et al. 2015. Integrating paleobotanical, paleosol, and stratigraphic data to study critical transitions: A case study from the Late Cretaceous-Paleocene of India. *Earth-Life Transitions: Paleobiology in the Context of Earth System Evolution* **21**: 137–166.

Srivastava R. 2011. Indian Upper Cretaceous-Tertiary Flora before Collision of Indian Plate : A Reappraisal of Central and Western Indian Flora. *Memoir of the Geological Society of India* **77**: 281–292.

Srivastava R, Srivastava G & Dilcher DL. 2014. Coryphoid Palm Leaf Fossils from the Maastrichtian – Danian of Central India with Remarks on Phytogeography of the Coryphoideae (Arecaceae). *PLoS ONE* **9**: e111738.

Suan G, Popescu SM, Suc J pierre P, et al. 2017. Subtropical climate conditions and mangrove growth in Arctic Siberia during the early Eocene. *Geology* **45**: 539–542.

Thomas R & De Franceschi D. 2013. Palm stem anatomy and computer-aided identification: The Coryphoideae (Arecaceae). *American Journal of Botany* **100**: 289–313.

Vaudois-Miéja N & Lejal-Nicol A. 1987. Paléocarpologie africaine: apparition dès l’Aptien en Égypte d’un palmier (*Hyphaeneocarpon aegyptiacum* n. sp.). *Comptes Rendus de l’Académie des Sciences Paris Série II* **304**: 233–238.

Vincens A, Tiercelin J jacques J & Buchet G. 2006. New Oligocene-early Miocene microflora from the southwestern Turkana Basin. Palaeoenvironmental implications in the northern Kenya Rift. *Palaeogeography, Palaeoclimatology, Palaeoecology* **239**: 470–486.

Zona S & Henderson A. 1989. A review of animal-mediated seed dispersal of palms. *Selbyana* **11**: 6–21.

CHAPTER 3

Fossil Palm Reading: The Utility of Fruits for Understanding the Evolution and Fossil Record of Palms

Abstract

The fossil record has the potential to contribute valuable data for understanding the evolutionary history and early diversification of palms (family Arecaceae). However, few fossils can be assigned confidently below the family level, due in part to limited availability of comparative data on modern palm structure, and to a paucity of taxonomically informative characters in many fossilized organs, such as leaves. As a result, only a handful of fossils have been used to infer the spatial and temporal distributions of major lineages of Arecaceae through time. In this chapter I surveyed the structure of palm fruits using X-ray micro-computed tomography (μ CT) and developed a morphological dataset to test whether the fossil record of fruits can improve our understanding of palm macroevolution. By including six fossil palm fruits in phylogenetic analyses at the genus level, I show that even a limited number of fruit characters can be informative for reconstructing systematic relationships of fossils at the tribe and subtribe level. This study provides 3D μ CT data for nearly every palm genus, a morphological dataset of fruit characters to which other fossils can be added, and four new reliable fossil calibrations. My results suggest that palms underwent a more extensive diversification in the Late Cretaceous than previously known. This research is an important contribution to our knowledge of fruit structure

in palms, lays a foundation for applying the fruit fossil record to palm macroevolution, and provides new insights into the deep evolutionary history and early diversification of Arecaceae.

Introduction

Arecaceae (palms) are a widespread tropical angiosperm family comprising approximately 2,500 species organized into five subfamilies (Arecoideae, Ceroxyloideae, Coryphoideae, Nypoideae, and Calamoideae), 28 tribes, and 27 subtribes (Baker & Dransfield, 2016). They exhibit broad morphological and ecological diversity. Ranging in habit from acaulescent understory herbs to gracile canopy trees and heavily armed lianas, palms occupy nearly all terrestrial environments of the tropics from rainforests to arid deserts. In these environments, they are important both ecologically and economically, sometimes functioning as keystone species capable of shaping forest community composition (Peters *et al.*, 2004; Roncal, Zona, & Lewis, 2008), and providing numerous ecosystem services to humans (Fadini *et al.*, 2009). Palms have been prominent components of terrestrial environments for the last ~85 million years, during the Late Cretaceous and Cenozoic. Macrofossils first appear during the Coniacian of the Late Cretaceous and become widespread by the Maastrichtian, demonstrated by occurrences of mangrove palms (subfamily Nypoideae) in localities throughout the Americas, Africa, India, and Asia (Gee, 2001; Harley, 2006; Dransfield *et al.*, 2008). Moreover, palms were ubiquitous in many Late Cretaceous and Cenozoic floras around the world and exhibited broad geographic ranges that extended into high latitudes during warm and equable climatic intervals like the Eocene (Eldrett *et al.*, 2009; Pross *et al.*, 2012; Greenwood & West, 2017).

Most of the macrofossil record of palms consists of vegetative organs, particularly leaves and stems. Although readily recognized as palms owing to their distinctive morphology and anatomy, most leaf and stem specimens cannot be placed beyond the family or subfamily level and are frequently assigned to broad artificial groups (morphogenera) comprised of potentially unrelated taxa that share a suite of general characters (Read & Hickey, 1972). Common palm morphogenera include *Sabalites* G. Saporta (costapalmate leaves), *Phoenicites* A. Brongniart (pinnate leaves), and *Palmoxylon* (stems). Morphogenera are useful for documenting the presence and abundance of palms in a fossil flora and, while taxonomic information may be limited, such fossils provide important information about the geographic distribution of the family through time, the composition of regional floras, and environmental conditions (e.g. Greenwood & West, 2017; Reichgelt, West, & Greenwood, 2018). However, these fossils tell us little about the deep evolutionary history of palms, including past taxonomic diversity, the tempo of diversification, and the biogeographic history of major lineages. Consequently, much of our understanding of their diversification is based on studies of extant species, which may not accurately reflect the true diversity and distributions of palms through time.

Fossils of reproductive structures such as flowers and fruits are rare in the geologic record, but can possess informative morphological characters essential for systematic placement below the family or subfamily level (Manchester *et al.*, 2016; Matsunaga *et al.*, 2019). For palms, fossil fruits and flowers may be essential for understanding when and where major lineages originated, establishing the tempo of evolution within the family, and refining details of diversification. However, interpreting the fossil record of palm reproductive structures and describing new specimens present significant challenges, and thus existing records have rarely been applied to understanding broader questions of palm evolution. Sometimes important

morphological and anatomical characters are simply not preserved in the fossils. However, other difficulties include the high number of species and genera comprising Arecaceae, substantial morphological diversity and convergence of traits within palms, and a lack of accessible and detailed comparative data on reproductive morphology. The latter is particularly true of features, such as internal anatomy, that are not relevant to field taxonomy but are useful for studying fossils. These factors converge to make morphological comparisons unwieldy and the potential for taxonomic misidentification high. Phylogenetic analyses can help resolve some of these issues but performing them requires thorough documentation of morpho-anatomical characters across the family.

To address this gap in our knowledge of palm fruit structure and character distributions across Arecaceae, I performed a genus-level survey of modern fruit morphology using X-ray micro-computed tomography (μ CT) and compiled information from the literature, including the *Genera Palmarum* and anatomical studies of individual clades (Essig, 1977, 2002; Essig, Manka, & Bussard, 1999; Essig, Bussard, & Hernandez, 2001; Chapin, Essig, & Pintaud, 2001; Essig & Hernandez, 2002; Dransfield *et al.*, 2008; Baker *et al.*, 2009; Romanov *et al.*, 2011; Bobrov, Romanov, & Romanova, 2012b; Bobrov *et al.*, 2012a). I summarize the data here to serve as a resource for describing new fossils, placing fossils in phylogenies, and understanding morphological evolution among palms. To test the utility and limitations of fruit characters for understanding the phylogenetic placement of fossil palms, I included new and previously described fossils in genus-level phylogenetic analyses of Arecaceae. Diagnostic character suites of the family, subfamilies, and tribes are discussed, and patterns of morphospace occupation are examined. Finally, I provide recommendations for recognizing fossil palm fruits and assigning them to extant lineages.

Material and Methods

I performed a μ CT survey of palm fruit structure at the genus level to understand character distributions and variation among living genera, and to develop a morphological character matrix. This morphological matrix was used in both morphospace and phylogenetic analyses to visualize the morphological diversity of palm fruits and understand the evolutionary relationships of fossils.

X-ray μ CT survey

Specimens of extant palm fruits were obtained on loan from herbarium collections at the Fairchild Tropical Botanic Garden (FTG), Royal Botanic Gardens, Kew (K), and L.H. Bailey Hortorium Herbarium (BH), and Florida Museum of Natural History (UF). Some specimens were collected from the living collection on the grounds of FTG and subsequently dried prior to μ CT scanning. Scans were performed at the University of Michigan Earth and Environmental Sciences μ CT facility (UM CTEES) on a Nikon XTH 225ST industrial CT system. Whole fruits were scanned using 40–105 kV and 100–210 μ A of X-ray power. The strategy was to maximize resolution while keeping the entire specimen in the field of view, and thus effective pixel size ranged from around 4 μ m in the smallest specimen (*Hemithrinax ekmaniana* Burret.) to 119 μ m in the largest (*Cocos nucifera* L.). Exposure was set to 1–2.83 s, depending on the specimen, averaging two frames per projection. Scan parameters for each specimen are available with the raw scan data on MorphoSource (project P776). Approximately 220 species, representing nearly all currently accepted genera, were scanned. Specimens of *Tectiphiala* H.E.Moore, *Masoala* Jum., *Laccospadix* H.Wendl. & Drude., *Ammandra* O.F.Cook, *Guishaia* J.Dransf., S.K.Lee &

F.N.Wei, and *Wendlandiella* Dammer could not be obtained and some characters were scored based on descriptions in the literature. Genera erected since the publication of *Genera Palmarum* in 2008 (*Lanonia* A.J.Hend. & C.D.Bacon, *Saribus* Blume, *Sabinaria* R.Bernal & Galeano, *Jailoloa* Heatubun & W.J.Baker, *Manjekia* W.J.Baker & Heatubun, and *Wallaceodoxa* Heatubun & W.J.Baker) were also excluded, as neither specimens nor adequate morphological descriptions could be obtained. Fossil seeds of *Sabal bigbendense* Manch., Wheeler, & Lehman were also µCT scanned to determine if they could be included in phylogenetic analyses, using similar settings as for extant palm fruits.

Morphological dataset

The morphological dataset of fruits was modified from the matrix of Baker et al. (2009). This allowed inclusion of some fruit and gynoecial characters that I was unable to observe, and left open the possibility of including other vegetative and reproductive characters from the original matrix in future analyses. When possible the same species as in the original dataset were used to document fruit morphology, but in some cases another species of the same genus was substituted. Multiple species of some genera were studied in the survey, which revealed that many fruit characters scored did not typically vary between congeneric species. Characters were scored based on observations made from µCT scans, drawings and descriptions from *Genera Palmarum* (Dransfield et al., 2008), and anatomical descriptions and illustrations from the literature (Essig, 1977, 2002, Essig et al., 1999, 2001; Chapin et al., 2001; Essig & Hernandez, 2002; Baker et al., 2009; Romanov et al., 2011; Bobrov et al., 2012b,a; Manchester et al., 2016). Some of the original characters of Baker et al. (2009) were recoded or rescored to match my character definitions and hierarchy. The final matrix used in the phylogenetic and morphospace

analyses contained 45 fruit and gynoecial characters, 13 of which originated from the Baker *et al.* (2009) matrix (Appendix B).

Morphospace analysis

Morphospace analyses were performed to visualize similarity among major lineages of palms based on my dataset of fruit characters. I first computed a distance matrix from the morphological character matrix, using the Maximum Observable Rescaled Distance (MORD; Lloyd, 2016) as the distance metric. The MORD distance metric scales distances from 0 to 1, with 1 as the maximum possible distance based on the observed characters. I also applied a correction for hierarchical characters, introduced by Hopkins and John (2018), which proportionally weights primary characters by their secondary characters using a tuning parameter (here set to 0.5), rather than treating inapplicable characters as missing data. This distance matrix was then used in a principle coordinate ordination to visualize similarity in a two-dimensional space, using the Cailliez procedure to correct for negative eigenvalues (Cailliez, 1983). The results were plotted using the first two principle coordinate axes, which were the axes capturing the highest amount of variance in the data, with convex hulls delimiting subfamilies and tribes. All analyses were performed in R (v. 3.5.2) using the packages 'Claddis' (v. 0.3.0; Lloyd, 2016) and 'ape' (v. 5.3; Paradis & Schliep, 2019)

Phylogenetic placement of fossils

Fossil fruits were scored in the morphological matrix based on descriptions from the literature, direct examination of specimens, or both. Fossils that could confidently be assigned to palms, represented older occurrences in the fossil record (Eocene or older), and that preserved

sufficient scorable morphological characters were selected. Older fossils were prioritized because of their greater potential for refining divergence-time estimates within Arecaceae, as node-dating analyses use the oldest occurrences of lineages. These fossils were *Hyphaeneocarpus indicum* Bande, Prakash, & Ambwani emend. Matsunaga, S.Y.Sm., Manch., Srivastava, & Kapgate (Matsunaga *et al.*, 2019), *Palmocarpus drypeteoides* (Mehrotra, Prakash & Bande) Manchester, Bonde, Nipunage, Srivastava, Mehrotra & Smith (Manchester *et al.*, 2016), and the “Mahurzari palm” (which has not yet been formally described) from the Maastrichtian-Danian Deccan Intertrappean Beds of India (67–64 Ma), *Coryphoides poulseni* Koch from the Danian Agatdal Formation of Greenland (64–62 Ma; Koch, 1972), *Friedemannia messelensis* Collinson Manch. & Wilde from the middle Eocene Messel oil shales of Germany (~47 Ma; Collinson, Manchester, & Wilde, 2012), and *Nypa burtini* Brongniart from the Eocene London Clay Formation (~47 Ma; Reid & Chandler, 1933). I made direct observations of *Hyphaeneocarpus indicum*, *Palmocarpus drypeteoides*, and the Mahurzari palm, but *Friedemannia messelensis*, *Coryphoides poulseni*, and *Nypa burtini* were scored from their original publications.

The phylogenetic placement of fossils was inferred with maximum likelihood in the program RAxML (Stamatakis, 2014) and posterior non-parametric bootstrapping using the majority rule stopping criterion to determine convergence of bootstrap replicates (the “autoMRE” option in RAxML; Pattengale *et al.*, 2009). The initial analyses included all six fossils and a matrix containing both molecular and morphological characters. The molecular dataset included 10 genes obtained from GenBank: *18S*, *atpB*, *matK*, *ndhF*, *PRK*, *rbcL*, *RPB2*, *rps16*, *trnL-trnF* intragenic spacer, and *trnQ-rps16* intergenic spacer (Appendix C). Each gene was initially aligned using MAFFT (Katoh & Standley, 2013) and refined with PRANK

(Löytynoja, 2014). No manual adjustments were made except to trim alignment edges. All partitions were concatenated using SequenceMatrix (v1.8; Vaidya, Lohman, & Meier, 2011). The molecular data were separated into ten partitions, one for each gene, with each analyzed using a general time-reversible model of rate substitution with gamma-distributed rate variation among sites. The morphological characters were analyzed using the Mkv model. These analyses yielded tree topologies consistent with published genus-level trees, but bootstrap values were generally low, even for clades that are usually well-supported in analyses of the molecular data alone (Appendix D). I attribute the low bootstrap support of these initial analyses to two main sources of uncertainty. First, simultaneously analyzing the phylogenetic position of multiple fossils may introduce greater uncertainty across the tree, particularly if the affinities of some fossils are much more poorly resolved than others. In other words, low support may be generated by one or a few fossils moving around the tree during bootstrap runs. Second, genus-level relationships within several tribes, such as Areceae and Trachycarpeae, are poorly resolved in most molecular phylogenetic analyses. Therefore, low support in some parts of the tree could instead result from the molecular data being uninformative for resolving some genus-level relationships and sensitive to bootstrap resampling. Several of the fossils included in the initial analysis had affinities with these groups, making it difficult to determine whether low support resulted from uncertainties in the molecular data or the placement of fossils (i.e. the morphological data).

To disentangle these two sources of uncertainty, I first performed an analysis containing all fossil species using a backbone topological constraint, and then did separate constrained analyses for each fossil with 100 bootstrap replicates (Appendix D). The backbone constraint

limits the tree search to topologies that conform to the supplied tree; because the fossils are not included as tips in the constraint tree, they can move freely and their placement is determined by the distribution of morphological characters. The topological constraint removed uncertainties associated with the molecular data, while analyzing each fossil independently enabled me to evaluate their placement in the tree without the influence of other fossils. The tree used as a topological constraint was constructed using the same dataset and parameters as the total-evidence analysis (described above), but with the fossils and morphological data removed. Affinities for each fossil were determined based on the shallowest subtending node for which support was very high in the constrained analysis (~ 95% bootstrap support). In other words, starting from the fossil tip, I moved down the tree until I encountered a node for which bootstrap support was 95% or higher, indicating strong support for monophyly of the group with the fossil included. Other factors were also considered and are discussed for each fossil below (see Discussion).

Results

Morphological diversity of palm fruits

Palms exhibit tremendous diversity in fruit morphology (Figs. 3.1–3.7). Fruit size varies from a few millimeters (*Geonoma* Willd.) to ~50 cm in length (*Lodoicea maldivica* (J.F.Gmel.) Pers.) (Dransfield *et al.*, 2008). Pericarp structure ranges from completely fleshy and parenchymatous (e.g. Fig. 3.3A–C), to highly sclerenchymatous and fibrous (e.g. Fig. 3.2, 3.3D–L); the exocarp can be smooth, bumpy, prickly, corky (Fig. 3.4D, 3.5A, & 6F), or scaly (Fig. 3.1A). Palm fruits also occupy a broad spectrum of overall shape from spherical to fusiform (Fig. 3.6H) to highly irregular and deeply lobed (Fig. 3.3K&L). The endosperm can be homogeneous

or ruminant (e.g. Fig. 3.3A), a character that is often labile even within species. Embryo position within seeds can be basal (Fig. 3.6J), variously lateral (Fig. 3.1B, 3.4A&B), and apical (Fig. 3.3D&F). The gynoecia from which fruits develop are equally varied; they range from completely apocarpous to fully syncarpous and are comprised of one (Fig. 3.6J–N), three (Fig. 3.3B&J), or sometimes more than three carpels (Fig. 3.5A). Moreover, many palms are pseudomonomerous with two carpels aborting early in floral development, but often retaining traces in the form of trilobed stigmas and vestigial locules. Consequently, although most palm fruits have a single seed at maturity, many species produce up to three and sometimes more than three seeds. Ovules can be anatropous, hemianatropous, campylotropous, or orthotropous with placentation apical, variously lateral, or basal.

Development also plays a role in this diversity of fruit structure. Endocarp, used hereafter for the hard inner tissue of the pericarp that surrounds the seed, can develop from different regions of the pericarp: the locular epidermis, inner zone of the pericarp, or from the middle zone of the pericarp (Murray, 1973; Romanov *et al.*, 2011; Bobrov *et al.*, 2012a). Further, several characters appear to be related to where growth is concentrated within the gynoecium during fruit and seed development, although the specific processes responsible for producing these features are not clear and have not been studied in detail. These characters include: (1) The position of stigmatic remains in mature fruits, (2) the position of ovule and seed attachment, and (3) whether fruits with more than one seed are deeply lobed versus unlobed. Stigmatic remains can be located almost anywhere on the fruit, and their position may also depend on whether more than one carpel produces a mature seed. Further, the location of ovule placentation within the gynoecium and seed attachment in mature fruits often differs; this occurs in 61 genera in Arecoideae, five genera of Ceroxyloideae, and eight genera of Coryphoideae. For this reason,

seed attachment cannot be used to infer ovule placentation, and vice versa. Finally, multi-seeded fruits derived from syncarpous gynoecia can be either multilocular or deeply lobed, the latter resembling two smaller fruits conjoined at the base (Fig. 3.3).

All this variation makes it difficult to circumscribe a set of characters by which all palm fruits are defined and can be universally recognized, making identification of fossil palm fruits especially challenging. Nevertheless, all palm fruits share the following traits: they develop from uniovulate carpels with a superior ovary, seeds are albuminous at maturity (contain endosperm), and embryos are small, conical to cylindrical, straight, and occupy a relatively small fraction of mature seed volume (Dransfield *et al.*, 2008). Although there are almost certainly other characters shared among fruits of all palms, this survey revealed few common characters for which there are no major exceptions. It is more useful, therefore, to focus on the features that characterize major groups within Arecaceae, such as subfamilies, tribes, and subtribes. I highlight some of these below, with the caveat that there are often exceptions within these groups.

Calamoideae

Subfamily Calamoideae comprises 17 genera grouped into three tribes and nine subtribes, and is consistently resolved as sister to all other palms (Baker & Dransfield, 2016). Some genera are acaulescent or arborescent (e.g. *Raphia* P.Beauv., *Metroxylon* Rottb.) but most are lianas — the rattan palms. Within inflorescences, flowers are typically borne in dyads. However, a few genera bear solitary flowers and *Oncocalamus* (G.Mann & H.Wendl.) H.Wendl. produces floral clusters consisting of a central pistillate flower and two lateral cincinni containing both staminate and pistillate flowers, a character not seen in any other palms (Dransfield *et al.*, 2008). Flowers

are unisexual in most species, but a few genera have bisexual flowers or both. Fruits of Calamoideae can be readily distinguished from those of other palms by their distinctive epicarp composed of basally-oriented, imbricate scales (Fig. 3.1). These scales develop basipetally from outgrowths of the ovary surface, a process that begins early in gynoecial development (Bobrov *et al.*, 2012b). At maturity the scales contain tissues of both the epicarp and the mesocarp. Stigmatic remains are always apical (Fig. 3.1B&D).

In most genera, the mesocarp is fleshy with no endocarp surrounding the seed (Fig. 3.1B–F). The exception is *Eugeissona* Griff., which has a pericarp containing numerous longitudinal fibrovascular bundles and a prominent endocarp derived from the central zone of the mesocarp (Bobrov *et al.*, 2012b). Seed number ranges from one to three, and multi-seeded fruits are multilocular (not deeply lobed). Embryos are either basal or lateral (Fig. 3.1B) and seeds are always attached basally. In many genera, the seed coat is either unevenly thickened on one side or has a thick, fleshy sarcotesta to attract seed dispersers (Fig. 3.1D–F). In *Oncocalamus*, the inner part of the seed coat forms a deep lateral intrusion into the endosperm (Fig. 3.1C), sometimes referred to as a postament, similar to that of some members of Coryphoideae.

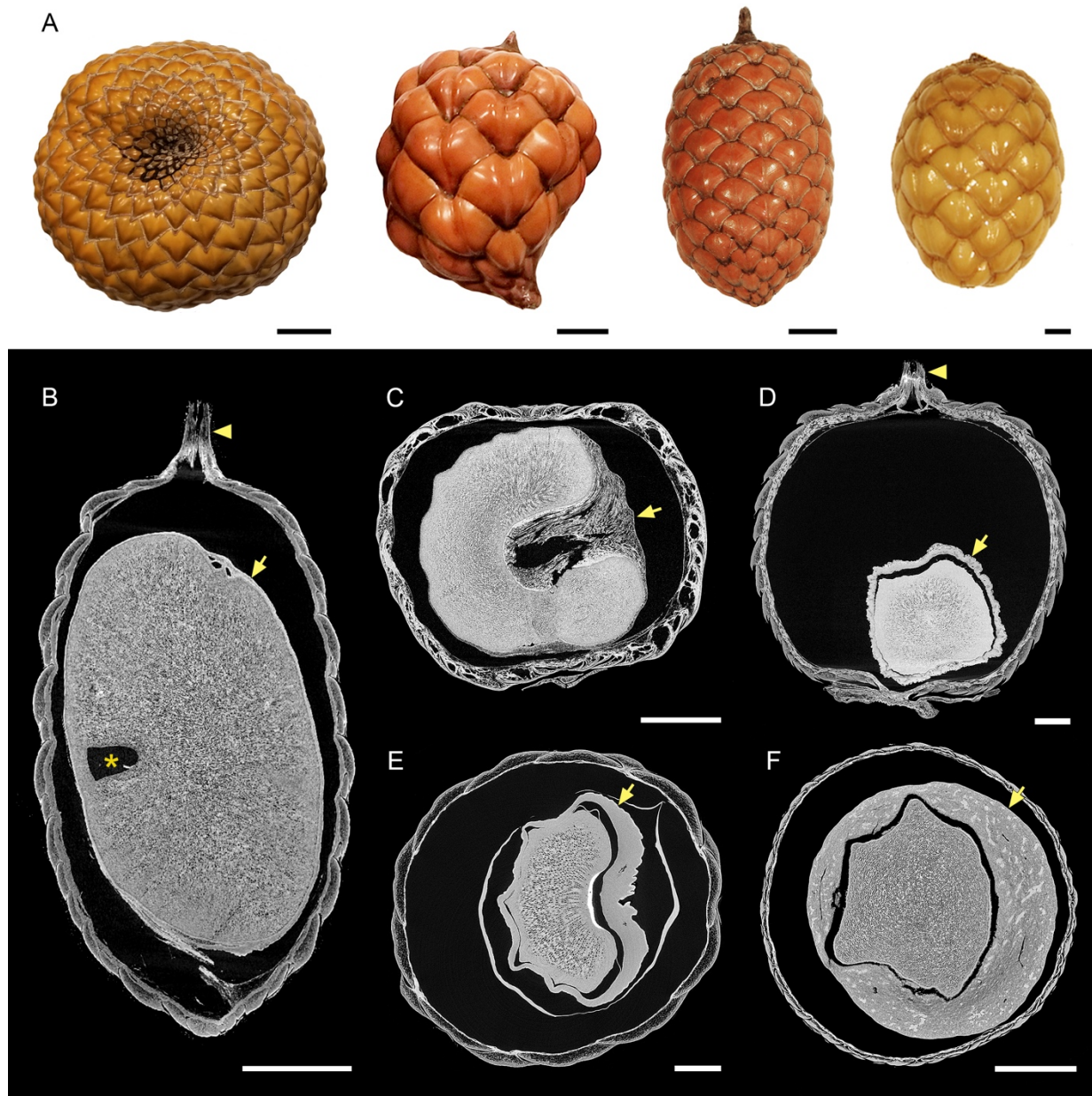


Figure 3.1 Calamoideae. Images B–F from μ CT scans. (A) External view of fruits showing basally-oriented pericarp scales. From left to right: *Metroxylon salmonense* (20 mm; K000754987), *Raphia farinifera* (10 mm; FTG76039), *Lepidocaryum tenue* (5 mm; FTG136527), and *Pigafetta filaris* (1 mm; FTG88176). (B) Longitudinal section (LS) of *Lepidocaryum tenue* (tribe Lepidocaryeae) showing apical stigmatic remains (arrowhead), lateral embryo (asterisk), and uniformly thin seed coat (arrow). Note lack of endocarp or fiber bundles in pericarp. Scale = 5 mm. FTG136527. (C) LS of *Oncocalamus mannii* (tribe Calameae). Seed with lateral postament (arrow). Scale = 5 mm. BH000104592. (D) LS of *Mauritiella armata* (tribe Lepidocaryeae). Seed is shrunken but shows remnants of thick, fleshy sarcotesta of seed coat (arrow). Note apical stigmatic remains (arrowhead). Scale = 2 mm. FTG117555. (E) Transverse section (TS) of *Pigafetta filaris* (tribe Calameae) with thickened sarcotesta (arrow). Scale = 1 mm. FTG88176. (F) TS of *Plectocomia mulleri* (tribe Calameae). Seed with thickened sarcotesta (arrow). Scale = 5 mm. BH000154523.

Nypoideae

Nypoideae is monotypic and contains only the extant species *Nypa fruticans* Wurmb, the mangrove palm. *Nypa* fruits are large and borne in dense globose heads, resulting in individual fruits that are roughly obovate, often laterally compressed, and angular in transverse section with longitudinal ridges (Fig. 3.2). Stigmatic remains form a prominent apical nub, sometimes referred to as an umbo (Fig. 3.2A&B). Fruit anatomy and development has been described in detail by Bobrov *et al.* (2012a). The endocarp is thick (Fig. 3.2B&D), derived from the middle zone of the pericarp (Bobrov *et al.*, 2012a), and has a round basal germination pore (Fig. 3.2B&E). It also has a thin longitudinal ridge that protrudes into the seed (Fig. 3.2D). Fruits are water dispersed and the pericarp is dry at maturity, containing numerous longitudinal fiber and fibrovascular bundles (Fig. 3.2B&D).

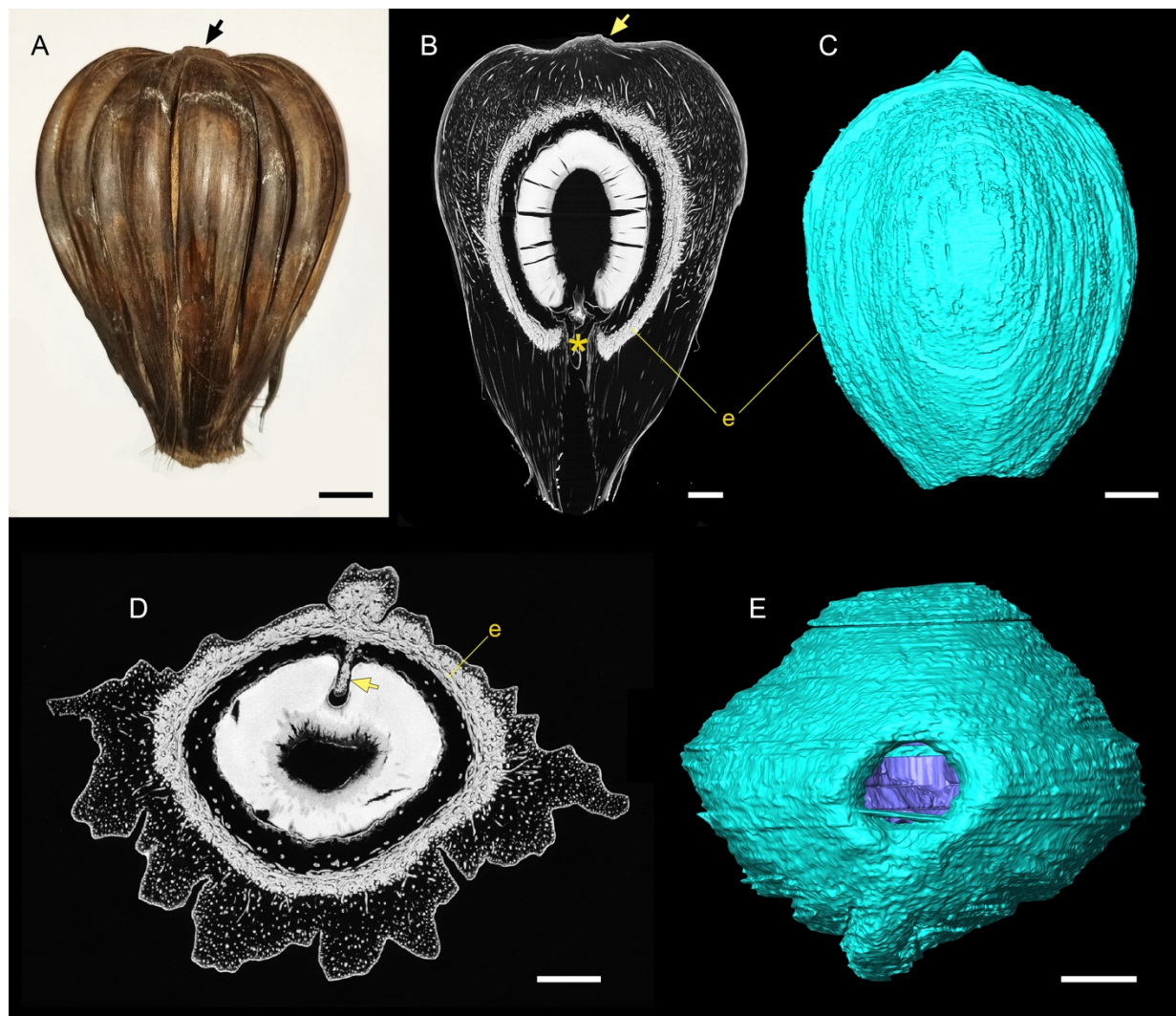


Figure 3.2 *Nypa fruticans* (Nypoideae). Images B–E from µCT scans. (A) External view of fruit showing obovate shape and deep longitudinal grooves. Note apical stigmatic remains forming structure referred to as an "umbo" (arrow). Scale = 20 mm. (B) Longitudinal section of fruit shown in (A). Pericarp with numerous longitudinal fiber and fibrovascular bundles to outside of thick endocarp ("e"). Note basal germination pore of endocarp (asterisk). Scale = 10 mm. (C) 3D model of endocarp seen laterally, segmented from µCT scan shown in (B). Scale = 10 mm. (D) Transverse section of fruit from A–C. Endocarp ("e") forms longitudinal ridge intruding into seed (arrow). Note numerous fiber and fibrovascular bundles of pericarp in transverse section (white dots). Scale = 10 mm. (E) Basal view of endocarp model from C, showing circular germination pore of endocarp. Scale = 10 mm. FTG84164.

Coryphoideae

Subfamily Coryphoideae includes 47 genera in eight tribes (Baker & Dransfield, 2016).

All extant genera have palmate or costapalmate leaves, except for *Phoenix* L. (date palm),

Caryota L., and *Arenga* Labill. ex DC., which have pinnate leaves. Floral morphology varies, but

nearly all Coryphoideae have gynoecia with prominent styles elevating the stigma (Dransfield *et al.*, 2008), a character that is uncommon in other groups. Coryphoideae have considerable variation in fruit morphology and can be separated into two major clades based in part on gynoecial structure: a syncarpous clade comprising tribes Borasseae, Caryoteae, Chuniophoeniceae, and Corypheae (*Corypha* L.), and an apocarpous clade containing tribes Trachycarpeae, Cryosophileae, and Phoeniceae (*Phoenix*) and Sabaleae (*Sabal* Adans.). Members of this “apocarpous clade” are either completely apocarpous or synstylos with free ovaries; the exception is *Sabal*, which is syncarpous.

Within the syncarpous clade Corypheae, Chuniophoeniceae, and Caryoteae have fleshy fruits lacking both a prominent endocarp and fibrovascular bundles within the pericarp (Fig. 3.3A–C). *Corypha* and Chuniophoeniceae (Fig. 3.3A) produce single-seeded fruits, whereas all the other tribes have up to three seeds (Fig. 3.3B–L). Multi-seeded fruits can either be multilocular (Caryoteae, Borasseae – subtribe Lataninae; Fig. 3.3B&J) or deeply lobed (Borasseae – subtribe Hyphaeninae; Fig. 3.3K&L). Tribe Borasseae has highly distinctive fruits that are typically fibrous and relatively large (Fig. 3.3D–L). Most notably, *Lodoicea maldivica* produces the largest fruits among palms and the largest seeds of all extant plants. All genera have thick endocarps that originate from the middle zone of the pericarp (like *Nypa* and *Eugeissona*), form pyrenes around each seed (e.g. Fig. 3.3J), and have apical germination pores consisting of holes or very thin regions of the endocarp above the embryo. In *Satranala* J.Dransf. & Beentje (Fig. 3.3E&L), instead of the seedling germinating through the pore the endocarp splits into two valves to release the seed, a germination mode not documented in any other palms (Dransfield *et al.*, 2008).

Most genera in the apocarpous clade have simple, fleshy, single-seeded fruits, and several members of tribe Cryosophileae are unicarpellate (Uhl & Moore, 1971; Fig. 3.4). Stigmatic remains are apical in all genera, except for *Sabal*. Many have a thin endocarp derived from the middle zone of the pericarp, and lack germination pores. In most genera, the seed coat either forms a deep, broad intrusion in the endosperm (postament; Fig. 3.4A,D,&F) or is irregularly thickened along one side (Fig. 3.4B&E). Embryos are usually lateral within the seed, although a few genera have embryos that are apically or basally attached (Fig. 3.4).

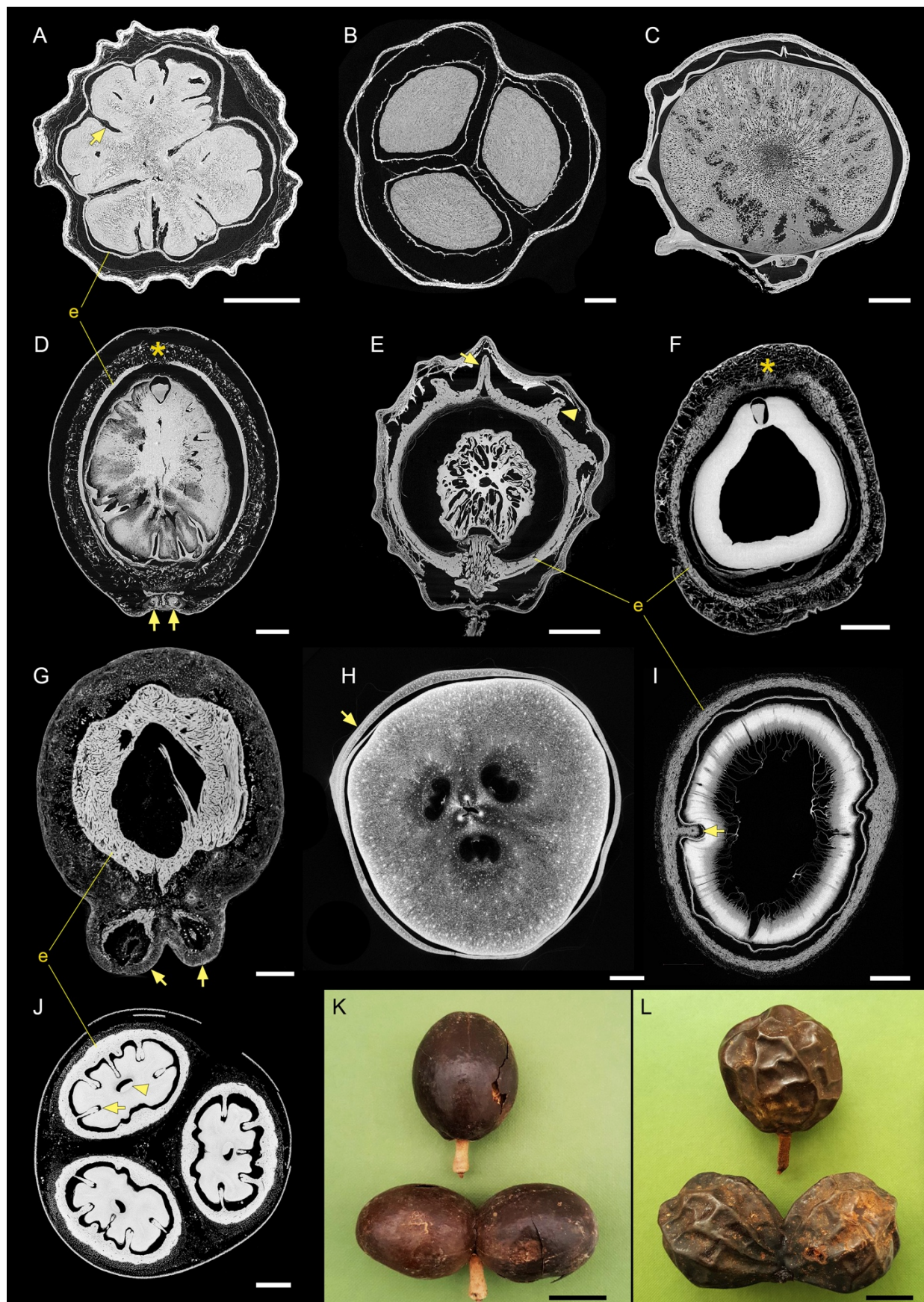


Figure 3.3 Coryphoideae, syncarpous clade. Images A–J from µCT scans. (A) Transverse section (TS) of *Tahina spectabilis* (tribe Chuniophoeniceae). Note thin endocarp ("e") and deeply ruminant endosperm forming radial furrows in seed (arrow). Scale = 5 mm. K000525955 (holotype). (B) TS of *Arenga engleri* (tribe Caryoteae). Fruit is trilocular with three seeds. Note lack of prominent endocarp and fibrovascular bundles in pericarp. Scale = 2 mm. FTG10076. (C) Longitudinal section (LS) of *Caryota mitis* (tribe Caryoteae). Note lack of prominent endocarp and remnants of fleshy pericarp, shrunken around seed. Scale = 2 mm. FTG89-34 A. (D) LS of *Medemia argun* (tribe Borasseae). Fruit with prominent endocarp ("e") and apical germination pore consisting of gap in endocarp above the embryo (below asterisk). Note deeply ruminant endosperm and two abortive carpels basally (arrows). Scale = 5 mm. K000208672. (E) LS of *Satranala decussilvae* (tribe Borasseae). Endocarp thick, externally sculptured with prominent ridges (arrowhead). Apical ridge (arrow) functions as germination valve. Seed is shrunken, forming pockets around endosperm ruminations. Scale = 10 mm. K000525955. (F) LS of *Hyphaene thebaica* (tribe Borasseae). Note apical germination pore (below asterisk), consisting of thinner zone of endocarp with sparser fiber bundles. Scale = 10 mm. FTG136617. (G) Off-median LS of *Bismarckia nobilis* (tribe Borasseae), showing two abortive carpels forming basal bulges (arrows). Endocarp ("e") is thick, composed of interwoven fiber bundles. Scale = 5 mm. FTG76031. (H) TS of immature fruit of *Borassus madagascariensis* (tribe Borasseae). Specimen fresh collected and scanned prior to drying. Section taken near base, passing through three empty locules. Note perianth remnants surrounding fruit (arrow). (I) TS of *Borassus flabellifer* pyrene (seed + endocarp). Endocarp ("e") is thick, forming a ridge that intrudes laterally into seed (arrow). Scale = 10 mm. FTG10156. (J) TS of *Borassodendron machadonis* (tribe Borasseae). Fruit is trilocular, with three pyrenes. Endocarp forms multiple longitudinal ridges that intrude into seed (arrow). Note embryo in transverse section (arrowhead). Scale = 10 mm. FTG68387B. (K&L) One- and two-seeded fruits of *Medemia argun* (K) and *Satranala decussilvae* (L). Fruits are deeply lobed when more than one carpel matures, appearing as two fruits fused at base. Scale = 20 mm. K000208672 (K), K000525955 (L).

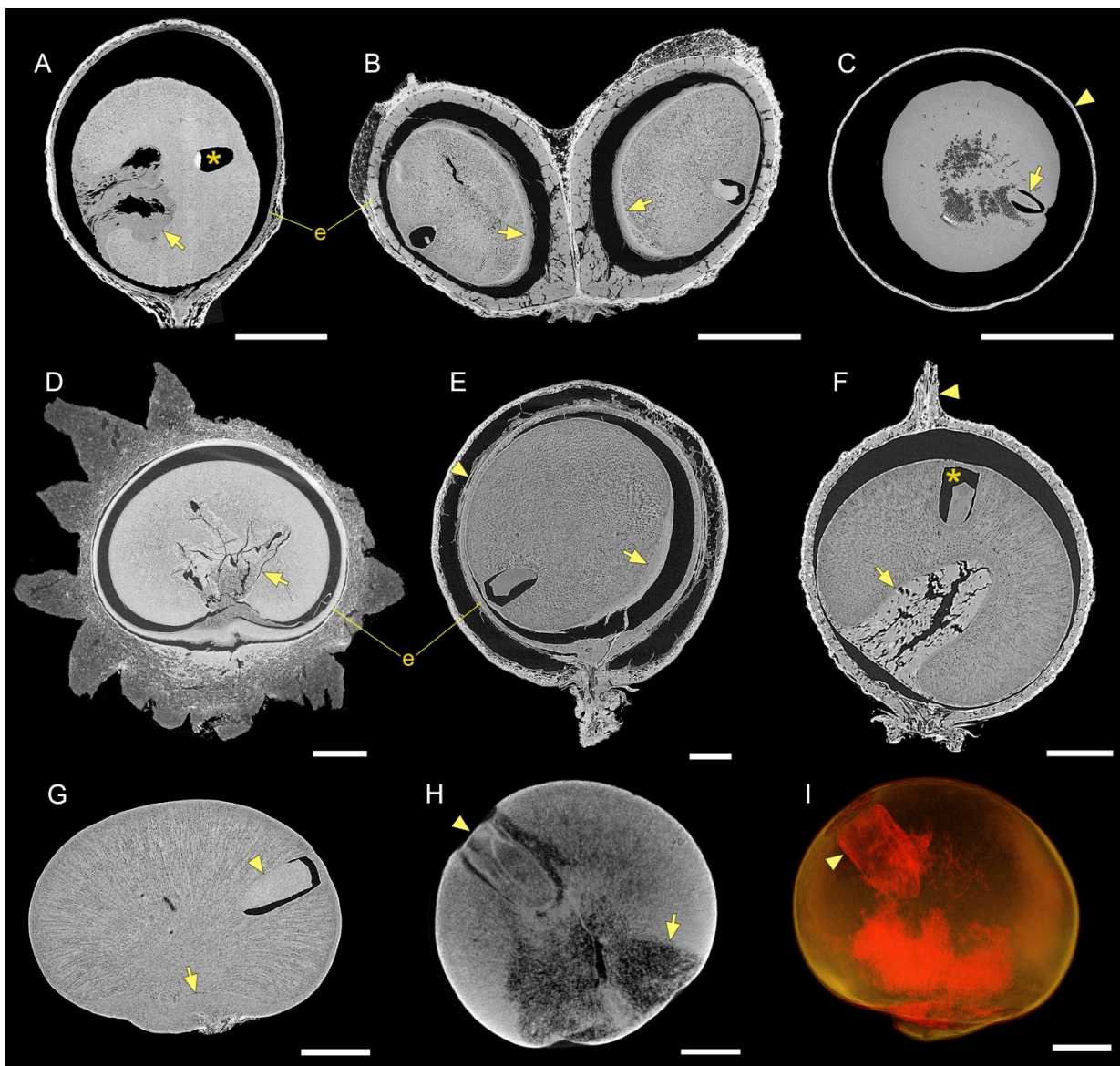


Figure 3.4 Coryphoideae, apocarpous clade. All images from μ CT scans. (A) Longitudinal section (LS) of *Livistona benthamii* (tribe Livistoninae). Seed with prominent lateral postament (seed coat intrusion; arrow), lateral embryo (asterisk in embryo cavity), and thin endocarp ("e"). Scale = 2.5 mm. FTG2001-0637B. (B) LS of *Rhipidophyllum hystrix* (tribe Trachycarpeae). Fruit formed from two out of three unfused carpels, connected at base near perianth remnants. Note that pericarp is not fused, and seed coat thickened on one side (arrows), opposite embryo. Scale = 5 mm. FTG16959. (C) Transverse section (TS) of *Schippia concolor* (tribe Cryosophileae). Note embryo in seed (arrow), lack of endocarp, and fleshy pericarp shrunken into thin layer (arrowhead). Scale = 10 mm. FTG2002-0575B. (D) LS of *Johannesteijsmannia altifrons* (tribe Livistoninae). Endocarp ("e") prominent, thickened basally. Seed with basal postament (arrow). Note corky pericarp with irregular, warty protrusions. Scale = 5 mm. K000933830. (E) LS of *Acoelorraphe wrightii* (tribe Livistoninae). Note prominent endocarp ("e"), thickened region of seed coat (arrow), and longitudinal fibrovascular bundles adjacent endocarp, seen in grazing section (arrowhead). Scale = 1 mm. FTG10066. (F) LS of *Leucothrinax morrisii* (tribe Cryosophileae). Seed has prominent lateral postament (arrow) and lateral embryo (asterisk). Note that seed is loose within dried fruit and has rotated from original position. Apical stigmatic remains at arrowhead. Scale = 1 mm. FTG10528. (G) LS of *Sabal palmetto* (tribe Sabaleae) seed for comparison with

Sabal bigbendense fossil (H&I). Note thickened seed coat basally (arrow) and lateral embryo (arrowhead). Scale = 2 mm. UF1158. (H) LS of *Sabal bigbendense* fossil seed. Note darker area in seed (arrow), which is the thickened zone of seed coat, and lateral embryo (arrowhead). Scale = 3 mm. UF402-53789. (I) Translucent volume rendering of specimen in (H), with embryo indicated by arrowhead. Scale = 3 mm. UF402-53789.

Ceroxyloideae

Ceroxyloideae includes eight genera in three tribes: Cyclospatheae (*Pseudophoenix* H.Wendl. ex Sarg.), Ceroxyleae (*Ceroxylon* Bonpl. ex DC., *Juania* Drude, *Oraniopsis* (Becc.) J.Dransf., and *Ravenea* H.Wendl. ex C.D.Bouché), and Phytelepheae (*Ammandra* O.F.Cook, *Aphandra* Barfod, and *Phytelephas* Ruiz & Pav.). Most genera have a prominent endocarp at maturity, which lacks a germination pore. Among species for which fruit anatomy has been studied in detail, the endocarp is composed of a single layer of palisade sclereids derived from the locular epidermis, and sometimes additional layers of sclerenchyma from the inner pericarp (Bobrov *et al.*, 2012a). Seed number varies within the subfamily. *Pseudophoenix* fruits have up to three seeds and are deeply lobed when multi-seeded, Ceroxyleae produce a single seed, and Phytelepheae have multilocular fruits with up to ten seeds (Fig. 3.5). The pericarp of Phytelepheae is dry, composed of numerous pointed warts formed by clusters of large radial fiber bundles (Fig. 3.5A). In contrast, the pericarp of Ceroxyleae and *Pseudophoenix* is mostly fleshy, lacking significant fiber and fibrovascular bundles (Fig. 3.5B–D). In some genera the endocarp is discontinuous at the point of seed attachment, forming a “hilar seam” (Fig. 3.5B). I documented this trait only in *Pseudophoenix* but it could be present in other genera with prominent endocarps that I was not able to observe (e.g. *Phytelephas*).

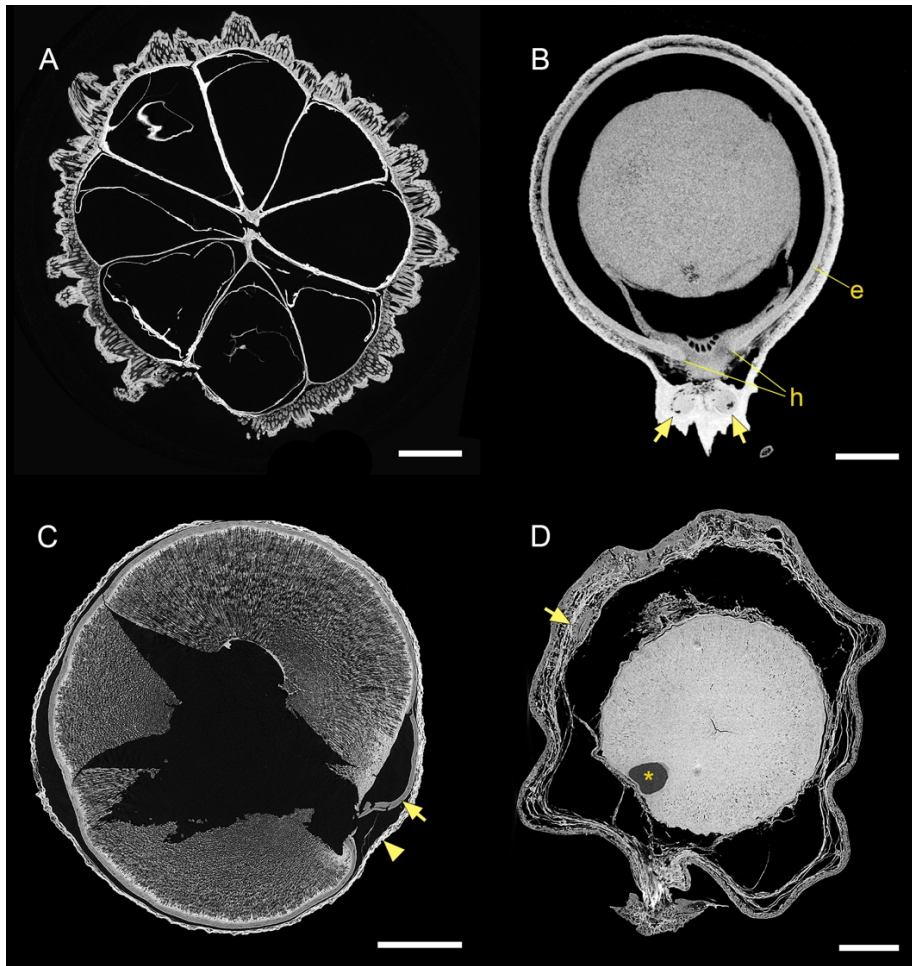


Figure 3.5 Cercoxyloideae. All images from μ CT scans. (A) Transverse section (TS) of *Ammandra decasperma* (tribe Phytelepheae). Fruit is immature, all eight locules lacking seeds. Pericarp comprised of corky warts formed by numerous radial fiber bundles like in *Pelagodoxa henryana* (see Fig. 3.6F). Scale = 1 cm. FTG60393. (B) Longitudinal section (LS) of *Pseudophoenix vinifera* (tribe Cyclospatheae). Note two abortive carpels basally (arrows) and thin endocarp (“e”), which is discontinuous at point of seed attachment, forming hilar seam (“h”). FTG814015. (C) TS of *Oraniopsis appendiculata* (tribe Cercoxyleae). Note thin, shrunken pericarp (arrowhead) to the outside of the seed coat (arrow), and absence of prominent endocarp. Scale = 5 mm. BH000154548. (D) LS of *Juania australis* (tribe Cercoxyleae). There is at least one large fibrovascular bundle in the pericarp (arrow), which was otherwise mostly fleshy. Note lack of prominent endocarp and embryo cavity in endosperm (asterisk). Scale = 2 mm. Moore 9368 (Kew).

Arecoideae

The Arecoideae form the largest subfamily, comprising 108 genera, 14 tribes, and currently ten unplaced genera; the largest tribe, Areceae, includes 11 subtribes. Flowers are organized into cincinni consisting of a central pistillate and two lateral staminate flowers, which are frequently modified within inflorescences to form regions containing only staminate flowers.

Floral triads are found only in Arecoideae and tribe Caryoteae (subfamily Coryphoideae). Fruits develop from syncarpous gynoecia comprised of three carpels and many species are pseudomonomerous. Pericarp structure is highly variable within the subfamily, ranging from fleshy with no endocarp to fibrous with very thick endocarp (Fig. 3.6). However, many species have multiple layers of prominent longitudinal fiber and fibrovascular bundles in the pericarp (Fig. 3.6K). Like Cercoxyloideae, most genera with well-developed endocarp have an innermost layer of palisade sclereids derived from the locular epidermis (Essig, 1977, 2002; Essig & Young, 1979; Essig *et al.*, 1999, 2001; Chapin *et al.*, 2001; Essig & Hernandez, 2002; Fig. 3.6), although this character has not been investigated in all groups. Endocarp opercula are common throughout Arecoideae and were not documented in any other subfamilies (Fig. 3.6). Germination pores lacking opercula were also observed in several genera.

Several tribes of Arecoideae occupy non-overlapping regions of morphospace, indicating that there are suites of fruit characters that distinguish major groups (Fig. 3.7). Tribes that do overlap are in some cases closely related (e.g. Areceae and Euterpeae) and all the monotypic tribes are variously distributed throughout the morphospace, sometimes positioned distantly from sister lineages (e.g. *Sclerosperma* G.Mann & H.Wendl.). Despite segregation of many tribes in these analyses, character suites are difficult to circumscribe for some groups. I focus here on clades that are more easily recognizable and for which there are documented fossil occurrences.

Tribe Cocoseae includes 17 genera in three tribes: Attaleinae, Bactridinae, and Elaeidinae (Fig. 2.6A–C). All cocosoid palms have thick endocarps, derived from the locular epidermis and inner zones of the pericarp, with three circular germination pores (although some teratological specimens have more than three; pers. obs.). In many genera the germination pores contain opercula (Fig. 3.6A&C); it is not clear whether the presence of opercula is variable or related to

developmental stage, but they were not present in all specimens studied. These germination pores are diagnostic of Cocoseae and their position can be informative for subtribe classification. Basal or subbasal germination pores are found only among Attaleinae (Fig. 3.6C), while subapical pores occur only in Bactridinae and Elaeidinae. Lateral germination pores are found in both subtribes (Fig. 3.6A). Subapical and subbasal pores are defined here as those occurring in the upper or lower thirds of the endocarp, respectively; lateral germination pores are positioned within the middle third of the endocarp, usually at the midline. In some cases, lateral pores are just above or below the midline, consistent with the presence of subapical or subbasal pores in their respective subtribes. Seed number is variable, with some genera consistently producing one seed (e.g. *Cocos*) and others up to three (e.g. *Butia* (Becc.) Becc., *Attalea* Kunth). When fruits have more than one seed they form locules within the endocarp (Fig. 3.6C), as opposed to pyrenes (e.g. Lataninae) or deeply lobed fruits (e.g. Hyphaeninae, *Podococcus* G.Mann & H.Wendl.). One-seeded fruits have clear aborted locules with germination pores, adjacent to the fertile locules. The pericarp usually has several layers of longitudinal fiber and fibrovascular bundles that are either relatively uniform in size or exhibit a subtle size gradient (Fig. 3.6A&B).

Tribe Areceae (Fig. 3.6J–N) are the largest tribe among palms but have a number of distinctive characters that make them potentially recognizable in the fossil record. All members are pseudomonomerous and thus fruits are single seeded, lacking any traces of abortive carpels. Although not defining features of the tribe, fruits tend to be relatively elliptical in shape, retain remnants of the perianth at maturity, and have apical stigmatic remains that, together with the pericarp, form a beak at the apical end of fruits above the seed. Longitudinal fiber and fibrovascular bundles of the pericarp exhibit either a relatively narrow size gradient, or they consist of smaller bundles intermixed with larger ones with massive fibrous sheaths (Fig. 3.6K).

The presence of these very large longitudinal fibrovascular bundles is restricted to Areceae and Geonomeae. Most genera have a prominent but relatively thin endocarp consisting of a single layer of palisade sclereids derived from the locular epidermis and sometimes the innermost cells of the pericarp (Fig. 3.6J–N). The endocarp often forms an operculum (Fig. 3.6J&M), as well as a hilar seam (Fig. 3.6N). A few genera have apically attached seeds, a character that is absent in all other palm tribes.

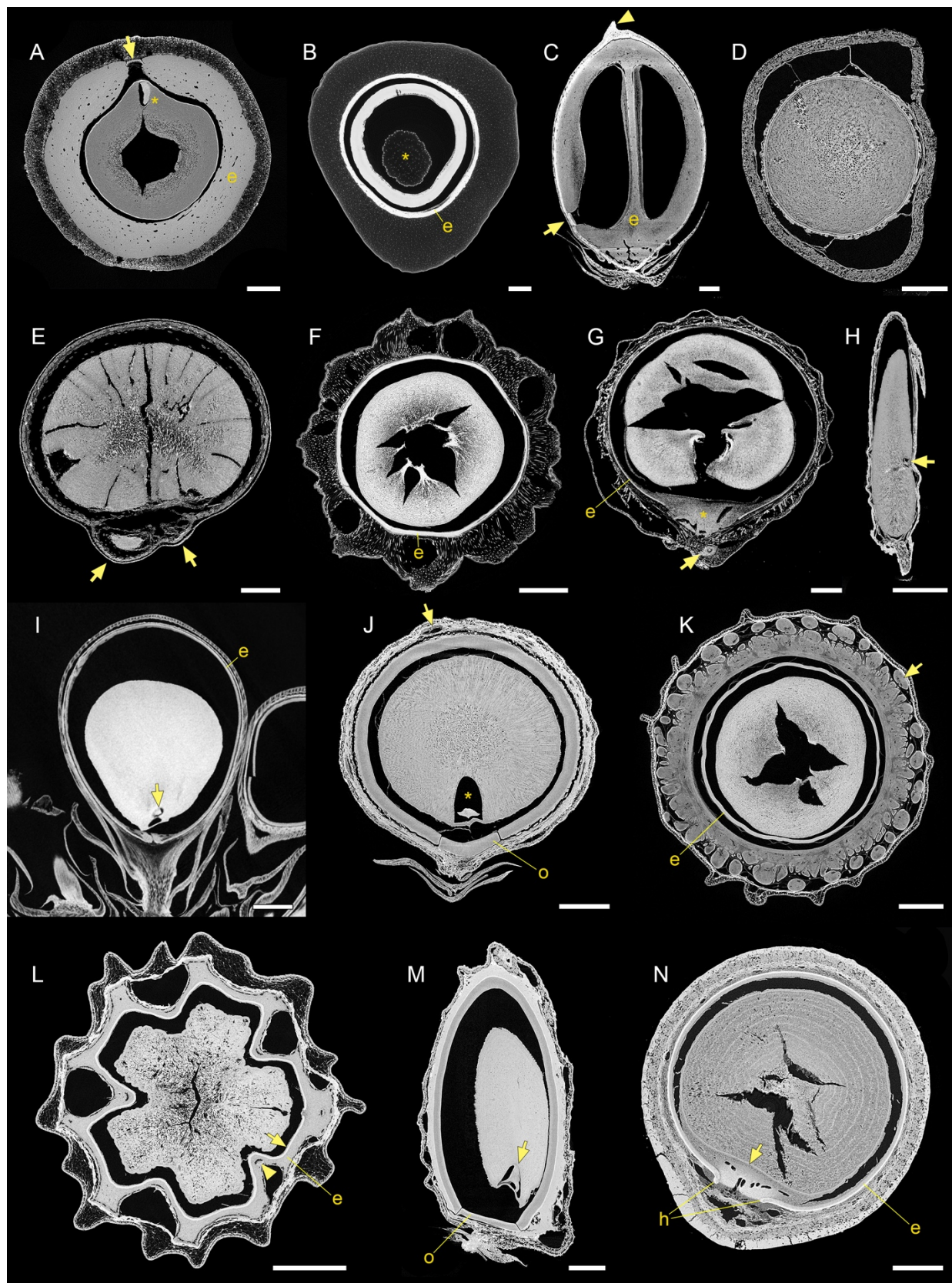


Figure 3.6 Arecoideae. All images from µCT scans. (A–C) Tribe Cocoseae. (A) Median transverse section (TS) of *Jubaeopsis caffra*, passing through lateral germination pore of endocarp. Note small scattered vascular bundles in pericarp, embryo to the inside of the germination pore (left of asterisk), hollow cavity in seed endosperm, and thin operculum in germination pore (arrow). Scale = 5 mm. K001083912. (B) TS of *Cocos nucifera*. Endosperm is hollow, with the seedling haustorium in the center (asterisk). Note numerous small longitudinal fiber and fibrovascular bundles in the pericarp to the outside of the endocarp. Scale = 2 cm. BH000199147. (C) Longitudinal section (LS) of *Butia capitata* with two locules. Note subbasal germination pore with operculum (arrow), and apical stigmatic remains (arrowhead). Scale = 2 mm. FTG76645. (D) TS through *Iriartella setigera* (tribe Iriarteeae). Note absence of prominent endocarp and longitudinal fibrovascular bundles. Scale = 2 mm. K0001244565. (E) LS of *Euterpe oleracea* (tribe Euterpeae) with two abortive carpels basally (arrows). Note endosperm ruminations, corresponding to the deep radial cracks in the seed. Scale = 2 mm. FTG72880. (F) TS of *Pelagodoxa henryana* (tribe Pelagodoxeae). Note pericarp of numerous large corky warts composed of radial fiber bundles and thin but prominent endocarp. BH000154524 (G) LS of *Orania lauterbauchiana* (tribe Oranieae). Fruit has a very thin endocarp and a thickened region of the seed coat at the hilum (asterisk). Note abortive carpel basally (arrow). Scale = 5 mm. K000114185. (H) LS of *Podococcus barteri* (tribe Podococceae). Note slender, elongate shape and small lateral embryo (arrow). Scale = 5 mm. K000114526. (I) LS of *Sclerosperma profiziana* (tribe Sclerospermeae). Note basal embryo (arrow) and thin endocarp. Scale = 5 mm. Profizi 841 (Kew). (J) LS of *Cyphokentia (Moratia) cerifera* (tribe Areceae). Endocarp is thick with a prominent basal operculum beneath embryo (asterisk), which is shrunken. Note large flattened fibrovascular bundle seen apically (arrow). Scale = 2 mm. BH000154527. (K) TS of *Wodyetia bifurcata* (tribe Areceae). Note prominent endocarp to the inside of thick zone of compacted longitudinal fiber and fibrovascular bundles with massive sheaths (arrow). Scale = 5 mm. FTG140799. (L) TS of *Ptychococcus paradoxus* (tribe Areceae). Endocarp comprised of locular epidermis (thin white layer at arrow) and sclerenchymatous inner zone of pericarp in which large longitudinal fibrovascular bundles are embedded (arrowhead). Scale = 5 mm. FTG82784. (M) LS of *Brongniartikentia lanuginosa* (tribe Areceae). Note basal embryo (arrow) and prominent operculum in endocarp. Scale = 2 mm. BH000154515. (N) TS of *Acanthophoenix rubra* (tribe Areceae). Endocarp is discontinuous at region of seed attachment, forming a hilar seam (“h”). Note thickening of seed coat at hilum (arrow). Scale = 2 mm. Vaughan 851 (Kew). Labels: e = endocarp, o = operculum.

Morphospace analyses

The morphospace plots based on the first two principal coordinate axes, which together capture 17.52% of the variation in extant fruit structure (11.17% and 6.35%, respectively), show substantial overlap between the subfamilies (Fig. 3.7). This is particularly true of Coryphoideae, Calamoideae, and Ceroxyloideae. Within subfamilies, however, many tribes occupy distinct and sometimes non-overlapping regions of morphospace. The tribes that do converge in morphospace are often closely related, such as tribes Trachycarpeae and Cryosophileae in subfamily Coryphoideae. See Appendix B for scree plot showing percent variance along all principal coordinate axes and table of eigenvalues.

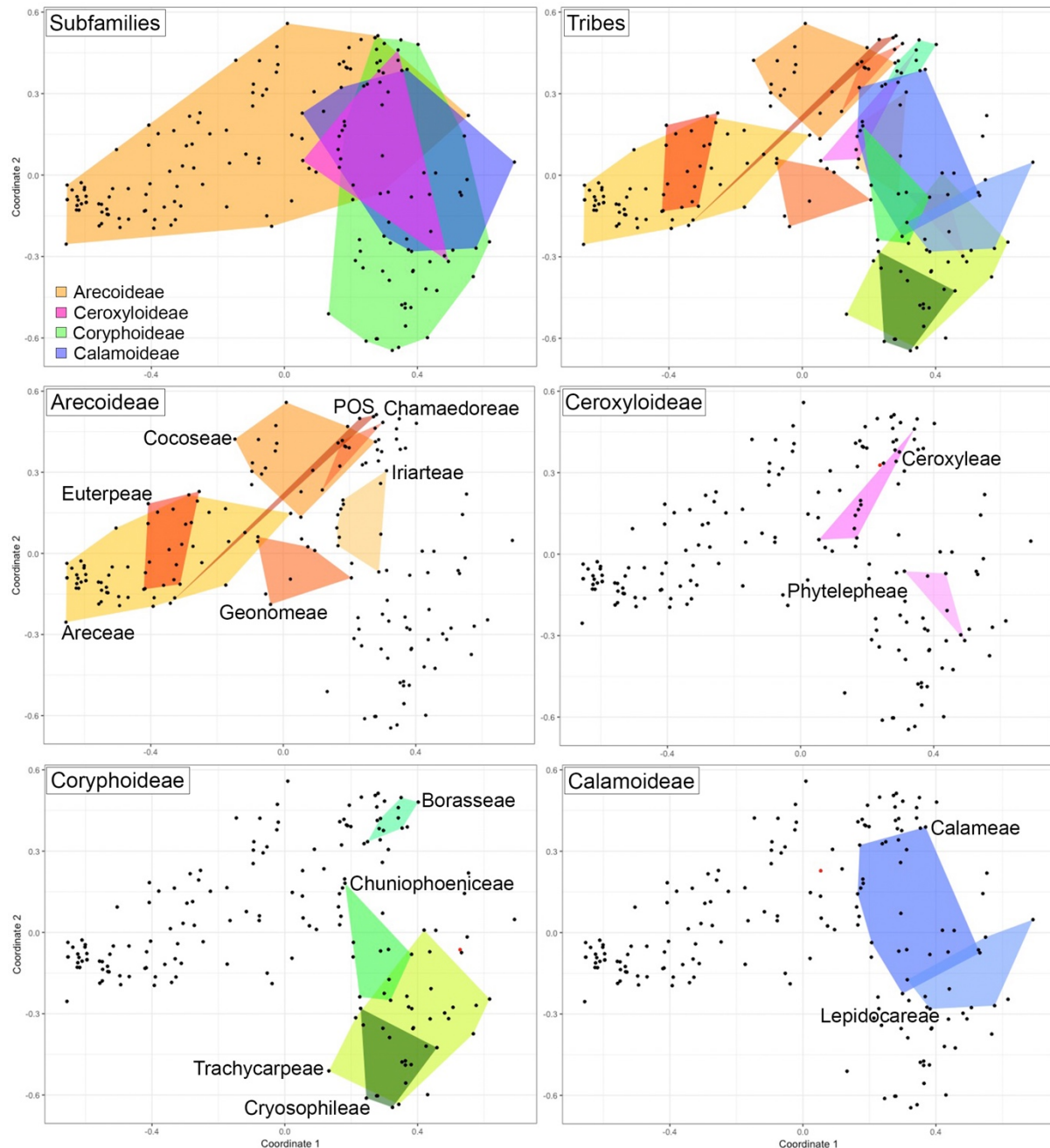


Figure 3.7 Morphospace plots based on fruit characters from morphological matrix. First (x-axis, 11.17%) and second (y-axis, 6.35%) principal coordinate axes are shown. Convex hulls delimit subfamilies and tribes. For tribes, only those with more than three genera are shown with convex hulls. Note that for Arecoideae POS corresponds to the clade formed by the monogeneric tribes Podococceae, Oranieae, and Sclerospermeae.

Phylogenetic placement of fossil palm fruits

Nypa burtini

Nypa burtini from the Eocene London Clay Formation preserves details of pericarp structure, including the basal germination pore and lateral internal ridge of the endocarp (Reid & Chandler, 1933). Unlike modern *Nypa*, the endocarp ridge does not extend the full length of the seed and is only present in the basal half. The constrained analysis placed *Nypa burtini* sister to extant *Nypa fruticans* (Fig. 3.8), which is the only extant species in subfamily Nypoideae (96% bootstrap support).

Hyphaeneocarpon indicum

Hyphaeneocarpon indicum was described from the Deccan Intertrappean Beds of India and is late Maastrichtian–early Danian (~67–64 Ma) in age (Matsunaga et al., 2019). Results of the phylogenetic analyses were consistent with those obtained by Matsunaga et al. (2019), who used a more limited morphological dataset. In the total-evidence analysis, bootstrap support for placement of *Hyphaeneocarpon* in the Hyphaeninae crown group, allied with *Bismarckia* and *Satranala*, is high (99%; Fig. 3.8). In contrast to the results of Matsunaga et al. (2019), in which *Hyphaeneocarpon* is sister to *Satranala* (posterior probability 0.53), *Hyphaeneocarpon* is here resolved as sister to *Bismarckia* with fairly high bootstrap support (89%).

Coryphoides poulseni

Coryphoides poulseni originates from the Danian (64–62 Ma) Agatdal Formation of Nuussuaq, West Greenland, and was described from both seed and fruit specimens (Koch, 1972). Koch (1972) documented several informative characters including some aspects of pericarp

anatomy, the presence of a prominent intrusion of the seed coat into the endosperm (postament), elongate raphe, basal seed attachment, and lateral embryo position. The total-evidence analysis places *Coryphoides poulseni* in subtribe Trachycarpeae, with 100% bootstrap support for monophyly of the tribe with *Coryphoides* included (Fig. 3.8). *Coryphoides* is positioned sister to *Licuala* Wurmb in subtribe Livistoninae, but node support for relationships within the tribe is generally low. Using a backbone constraint, support for placement in Livistoninae (94%) within crown Trachycarpeae (Livistoninae + Raphidinae) is high (99%).

Palmocarpon drypeteoides

Fruits of *Palmocarpon drypeteoides* from the Deccan Intertrappean Beds of India are trilocular and three-seeded, with a thick endocarp bearing three subbasal germination pores, a layer of palisade sclereids lining each locule, and pericarp with longitudinal fibrovascular bundles (Manchester *et al.*, 2016). the total-evidence analysis indicates moderate support for the monophyly of Attaleinae with *Palmocarpon drypeteoides* included (86%). Placement within the crown group, allied with genera exhibiting subbasal germination pores, receives strong support when the molecular topology is constrained (99%; Fig. 3.8).

Mahurzari palm

The Mahurzari palm includes flowers and a single fruit specimen from the Mahurzari locality of the Deccan Intertrappean Beds of India. Owing to morphological and anatomical similarities between the fruits and the floral gynoecium, which are indistinguishable except for the presence of a seed, and their co-occurrence within the same chert block, I consider them to be developmental stages of the same species. The fruits preserve the relative size and organization

of fibrovascular bundles in the pericarp, details of the endocarp, seed structure, and embryo position. The flowers indicate that the gynoecium contained a single locule, lacked a style, and had three low, round stigmas, one of which sits above a canal continuous with the locule. The total-evidence analysis places the Mahurzari palm in tribe Areceae of subfamily Arecoideae (91%; (Fig. 3.8), although node support throughout the core arecoid clade (Manicarieae, Geonomeae, Leopoldineae, Euterpeae, and Areceae) is low overall (Appendix D). Constrained analyses place the Mahurzari palm in tribe Areceae (100% bootstrap support) but with low support for internal nodes within the tribe, indicating that the position of the Mahurzari palm changes substantially between bootstrap runs.

Friedemannia messelensis

Friedemannia messelensis is represented by compressed fruits and seeds from the Messel oil shale of Germany (Collinson *et al.*, 2012). Fruits are elliptical, with persistent perianth at the base and apical stigmatic remains. Despite their preservation as lignitized compressions, which precludes observation of many fruit and seed characters, Collinson *et al.* (2012) documented several additional features that enabled their inclusion in the phylogenetic analyses. These characters include the presence of several layers of longitudinal fiber or fibrovascular bundles in the pericarp and, by dissection of seeds from fruit specimens, apically attached seeds with an apical hilum and elongate raphe. Apical seed attachment is rare in palms and is only found in some members of tribe Areceae. A total-evidence analysis, with the other fossil species excluded, recovered strong support for inclusion of *Friedemannia* in Areceae (91%; Fig. 3.8). Analyses employing a backbone constraint indicated high bootstrap support for inclusion of *Friedemannia* in Areceae (100%), in the western Pacific clade (Ptychospermatinae,

Archontophoenicinae, Basseliniinae, Carpoxylinae, *Dransfieldia* W.J.Baker & Zona, and *Heterospathe* Scheff.; 94%), with low support for affinities with subtribe Ptychospermatinae in which it is nested (55%).

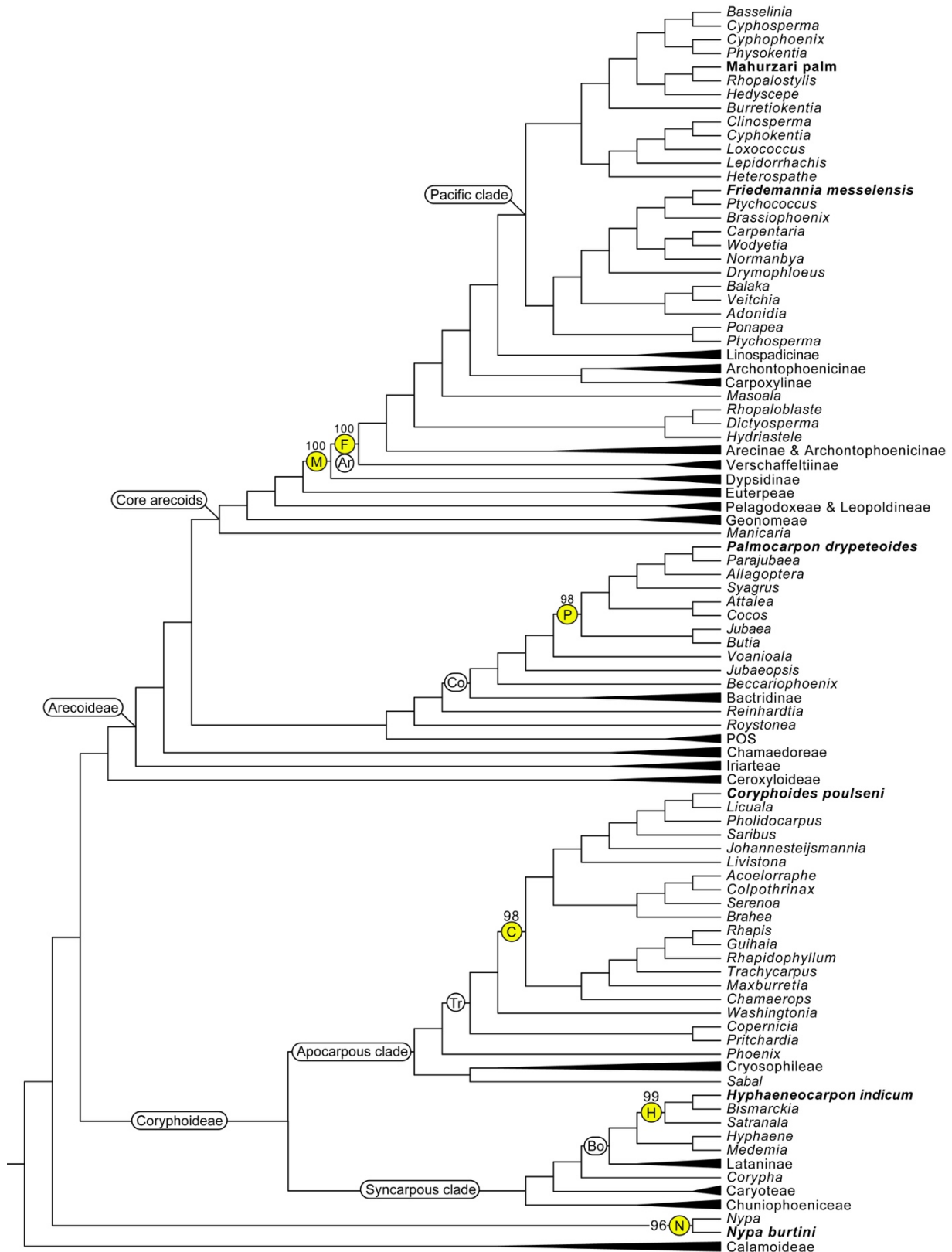


Figure 3.8 Phylogenetic relationships of six fossils from total-evidence maximum likelihood analysis. Note tree is drawn as a cladogram with uniform branch lengths for clarity. Subfamilies, tribes, or subtribes without fossils are collapsed (black triangles) for legibility. Fossil tips shown in bold text. Yellow circles indicate clades with which fossil affinities are well supported, with bootstrap values corresponding to those from constrained analyses. F = *Friedemannia messelensis*, M = Mahurzari palm, P = *Palmocarpon drypeteoides*, C = *Coryphoides poulseni*, H = *Hyphaeneocarpon indicum*, N = *Nypa burtini*. Tribes and other major clades indicated with bubbles: Ar = tribe Areceae, Co = tribe Cocoseae, Tr = tribe Trachycarpeae, Bo = tribe Borasseae. See Appendix D for all trees.

Discussion

Diversity of fruit structure and phylogenetic relationships of fossils

This survey reveals that despite the diversity in palm fruit structure and apparent convergent evolution of many traits, fruit characters carry strong taxonomic signal particularly below the subfamily level. Ordination plots based on principal coordinate analysis of fruit characters provide a useful means of visualizing the morphological data. Convex hulls around subfamilies show considerable overlap, but within subfamilies, most tribes occupy distinct regions of morphospace (Fig. 3.7). Tribes that overlap are often closely related to one another, such as Euterpeae and Areceae (Arecoideae), or Trachycarpeae and Cryosophileae (Coryphoideae). These patterns of morphospace occupation are congruent with my observation that circumscribing character suites for each subfamily, to the exclusion of others, is more difficult than it is for tribes and other major clades within subfamilies.

Phylogenetic analyses further demonstrate the utility of fruit characters for understanding systematic relationships of fossil species (Fig. 3.8). *Nypa burtini* is resolved as sister to extant *Nypa fruticans* using relatively few (17) characters. *Hyphaeneocarpon indicum* is positioned as a crown member of subtribe Hyphaeninae in tribe Borasseae (Coryphoideae), a relationship that makes sense given the unusual combination of characters seen in Hyphaeninae and *Hyphaeneocarpon*, such as apical embryos and germination pores, basal stigmatic remains, and aborted carpels in mature fruits. *Coryphoides poulseni* was placed in subtribe Livistoninae of

tribe Trachycarpeae (Coryphoideae) with high support. These affinities seem reasonable since the combination of a basal postament (intrusion of the seed coat) and lateral embryo are found only in subtribe Livistoninae. However, support for inclusion in Livistoninae appears somewhat sensitive to bootstrap resampling of characters, as bootstrap support varied between different iterations of the analyses, and recognition as a member of Trachycarpeae is therefore more conservative. *Palmocarpus drypeteoides* is recovered as a crown member of subtribe Attaleinae in tribe Cocoseae (Arecoideae), allied with the extant genera bearing subbasal germination pores and more than one seed. *Palmocarpus drypeteoides* was placed in subtribe Attaleinae by Manchester et al. (2016) based on those characters and other anatomical similarities with cocosoid palms.

The remaining two fossils, the Mahurzari palm and *Friedemannia messelensis*, are both nested within the core arecoid clade that includes tribes Manicarieae (*Manicaria*), Geonomeae, Pelagodoxeae, Leopoldinieae (*Leopoldinia*), Euterpeae, and Areceae. Tribe-level relationships within core arecoids are poorly resolved, due to both low node support in some regions and recovery of well-supported but conflicting topologies in independent analyses (Baker et al., 2009, 2011; Faurby et al., 2016). Because the backbone tree contained some poorly supported nodes, phylogenetic uncertainties must also be considered when evaluating the systematic relationships of the fossils. The Mahurzari palm receives strong support as a member of Areceae in both total-evidence and constrained analyses. However, some combinations of characters make me hesitant to place the Mahurzari palm in the Areceae crown group. First, the relative size and distribution of fibrovascular bundles in the pericarp is a more general feature that is found throughout core arecoids and is not restricted to Areceae. Other important characters of the Mahurzari palm include the presence of three low sessile stigmas, one of which is connected to a

single functional locule, and apical stigmatic remains in mature fruits. This combination of characters is distributed throughout tribes Areceae and Euterpeae, which are not recovered as sister lineages in every phylogenetic analysis. Therefore, the most conservative placement for the Mahurzari palm is as a crown member of the core arecoids in a clade that encompasses both Euterpeae and Areceae.

Friedemannia messelensis was scored for 12 characters, the fewest characters among the fossils analyzed. The phylogenetic analyses place *Friedemannia* within the western Pacific clade of tribe Areceae, although support for its nested position within the tribe is only strong when using a backbone constraint. Subtribe and genus level relationships within Areceae have low bootstrap values in the tree used as a backbone constraint and are similarly poorly resolved in other trees (Baker *et al.*, 2009, 2011; Faurby *et al.*, 2016), but a western Pacific clade has nevertheless been recovered repeatedly in other studies. Despite this, affinities with the western Pacific clade are not adequately justified by the morphology of *Friedemannia* as it is currently known. *Friedemannia* does exhibit characters found throughout the clade and more generally has the Areceae “gestalt” – oblong fruit with apical stigmatic remains forming a point or beak, persistent perianth at the base, and longitudinal bundles in the pericarp. It also has an apical hilum, indicating apical attachment of the seed within the fruit. Apical seed attachment is found in only six genera, all of which are in Areceae, but the character is not restricted to the western Pacific clade. Owing to these character distributions and the relatively limited amount of morphological data that can be gleaned from the fossil specimens, *Friedemannia* can still be confidently considered a member of Areceae but relationships with the western Pacific clade are equivocal.

Key fruit characters

Phylogenetic analyses of fossil palms revealed that certain characters are particularly useful for determining systematic placement, are often preserved in fossils, and should be investigated when describing new specimens. They include pericarp structure, endocarp anatomy, embryo attachment, seed attachment, position of stigmatic remains, seed coat structure, and any other structures that indicate carpel number such as vestigial locules. Key features of the pericarp include the organization and relative size of longitudinal fiber or fibrovascular bundles, and presence of other sclerenchyma within the pericarp such as radial fiber bundles. The μ CT survey focused on the general morphology of the pericarp and did not address anatomy in detail, owing in part to limits on the resolution of μ CT scans and prioritization of whole fruit scans. It is unclear whether other aspects of pericarp anatomy might provide useful characters, but it is likely that they would for at least some groups, and this would be a direction for future research. Endocarp morphology, anatomy, and developmental origin can also be very informative, although the latter may be impossible to document in fossils without multiple developmental stages preserved. Endocarp germination structures are found in several distantly related groups, but the number, form, and position usually have systematic value. For example, germination pores with opercula are found only in Arecoideae, and within core arecoids they are always basal. In Cocoseae, three germination pores are present on the surface of endocarps, and their position can be diagnostic for subtribes. Apical germination pores are found in Borasseae, while basal germination pores occur in *Nypa* and *Eugeissona* (Calamoideae). The position of stigmatic remains and embryo attachment tend to be conserved within clades, while seed attachment is more variable but can be useful in combination with other traits. For *Friedemannia*, seed

attachment proved an essential character because apical seed attachment is restricted to tribe Areceae.

The characters preserved in palm fruit fossils vary substantially among localities and mode of preservation, but all the key characters outlined above have been documented in fossils. Certain characters require exceptional preservation, such as embryo position, stigmatic remains, and vestigial carpels and are unlikely to be preserved in many fossils. Others, however, pertain to lignified and relatively degradation-resistant tissues of the fruit such as endocarp, sclerenchyma of the pericarp, and the seed coat. The fact that these tissues have relatively high preservation potential and can be systematically informative may have implications for taphonomic bias and our ability to detect certain clades in the fossil record. For instance, groups that tend to produce fruits with fibrous pericarp and thick endocarps (e.g. Cocoseae, Borasseae) may be more readily preserved and recognized in the fossil record, whereas those that produce fleshy fruits without extensively lignified tissues (e.g. Chamaedoreae, Chuniophoeniceae) are less likely to be both preserved and identified when their fossils are recovered. A corollary of this is that some groups are probably far more likely to be represented in the fossil record as seeds rather than whole fruits, such as many of the members of Coryphoideae that have fleshy pericarp and no endocarp at maturity. Most specimens of *Coryphoides poulseni* are seeds and there was only one complete specimen with intact pericarp. Similarly, numerous seeds resembling those of several genera of Coryphoideae have been described from the Eocene London Clay Formation, but very few whole fruits are known. Unfortunately, with this dataset seed characters by themselves are generally not very informative without knowing how they are oriented within the fruit. Characters could be recoded, however, to better accommodate these fossils.

The morphological dataset of fruit characters, assembled from my literature review and µCT survey, placed fossil fruits into several palm clades with high support. This demonstrates that phylogenetic analyses using fruit data can be highly informative and are an important step for understanding the affinities of fossil species. However, the results of these analyses should be evaluated critically, and the placement of fossils within the tree should make sense based on the characters scored, the distribution of those characters among palms, and other features of both the fossil and modern groups that are not included in the matrix. My dataset is an important and useful starting point, but it does not capture all the morphological variation in modern palms. Phylogenetic analyses using this dataset could, therefore, be vulnerable to spurious placement of fossil taxa, particularly when few characters are scored. For example, when including *Nypa* fossils in the phylogenetic analyses, the presence of the basal germination pore was extremely important. *Nypa burtini* from the London Clay was selected because it showed this and other characters very clearly. However, other *Nypa* fossils for which germination pores were not preserved were sometimes placed in Cocoseae, which also has thick endocarp and fibrous pericarp, despite lacking other diagnostic characters of the tribe. Additionally, I was cautious about accepting even well-supported sister relationships between fossils and extant genera (e.g. *Hyphaeneocarpon* and *Bismarckia*) because these relationships were based exclusively on analyses of fruit characters. There is little understanding of morphological evolution in palms and relative rates of change in vegetative and reproductive structures. Without whole-plant concepts for fossil species it is impossible to eliminate the possibility that different phylogenetic relationships would be obtained if the characters of other organs were included in the analysis.

Palm fruit fossil record

Numerous fossil palm fruits have been documented from Cretaceous and Paleogene localities worldwide. Many of these occurrences have been summarized by Harley (2006) so this discussion focuses on a few of the oldest records, as well as those not included in her review. The oldest putative palm fruits are those of *Hyphaeneocarpon aegyptiacum* Vaudois-Miéja & Lejal-Nicol from the Aptian (113–125 Ma) of Egypt (Vaudois-Miéja & Lejal-Nicol, 1987). However, the morphology of the specimens combined with its very early age make these specimens questionable as early palm fossils. The fossils are large, roughly pyriform in shape, and have an inner structure interpreted as the endocarp with a round germination pore. Unfortunately, no anatomy is preserved in the specimens. Although large, roughly pyriform fruits occur in some species of modern *Hyphaene*, few other characters are preserved that suggest affinities with palms. Additionally, *H. aegyptiacum* is Aptian and is thus as old as the oldest monocot fossils and significantly older than any other palms (Iles *et al.*, 2015). As one of the oldest reported palms, the burden of proof is high and the fossils should be re-examined before they can be accepted as palms.

Other occurrences that should be reinvestigated to confirm age and palm affinities include two fruits, *Cocoopsis* sp. Fliche and *Astrocaryopsis* sp. Fliche, described from Cenomanian strata near Sainte-Menehould, France (Fliche, 1894). In particular, *Cocoopsis* is described as having the characteristic endocarp pores of Cocoseae, but no figures of the specimens accompany the description. If the age of the fossils as Cenomanian and the presence of these pores could be confirmed, it would represent not only the oldest known member of the tribe but also the oldest palm.

Seeds of *Sabal bigbendense* and *Sabal bracknellense* originate from the Campanian Aguja Formation in Texas and were placed in the modern genus based on strong similarities in the overall morphology of the seeds (Manchester, Lehman, & Wheeler, 2010). µCT scans of *S. bigbendense* further reveal a thickened region of the seed coat along the hilum and a well-preserved embryo below the circular depression on the surface of the seed, positioned laterally–subapically within the seed relative to the hilum (Fig. 3.4H&I). The thickening of the seed coat near the hilum and lateral–subapical embryo position support relationships with *Sabal* and the “apocarpous” clade of Coryphoideae more generally (of which *Sabal* is the only syncarpous member). Unfortunately, the absence of whole fruits precludes inclusion of the fossils in these phylogenetic analyses and this was generally the case for most seed fossils. Many seed characters require knowledge of how the seed is oriented and attached within the fruit, as characters like embryo position are coded relative to the base of the fruit and not the base of the seed. The herbarium specimens I obtained infrequently contained fully mature seeds, which hindered coding of additional seed characters in this matrix. The lack of mature seeds in many specimens is due in part to the fact that endosperm often does not fully harden until the latest stages of fruit maturation; thus, the seeds of fruits collected in the field often shrink during the drying process unless they are very mature when collected (Bill Baker, pers. comm.). Future improvements of the matrix will be aimed at studying mature seeds to expand and recode seed characters to better facilitate inclusion of fossil palm seeds. Nevertheless, observations of the original specimens and modern palm fruits support the placement of the Aguja Formation palm seeds in *Sabal*.

Fossils of *Tripylocarpa aestuaria* Gandolfo & Futey originate from the Danian Salamanca Formation of Argentina (Futey *et al.*, 2012). Based on morphological comparisons

and phylogenetic analyses, the fossils were placed in subtribe Attaleinae of tribe Cocoseae. However, affinities with Cocoseae are equivocal because *Tripylocarpa* has a single apical germination pore rather than three pores, as is characteristic of tribe Cocoseae. Germination pores in subtribe Attaleinae, in which *Tripylocarpa* was placed, are either lateral or subbasal but never apical; subapical pores are found in Bactridinae. Among palms, fruits with a single apical germination pore occur only in Borasseae and consist of large holes or very thin portions of the endocarp. In contrast, the structure interpreted as a germination pore in *Tripylocarpa* is a narrow channel in the thick apical zone of the endocarp. While *Tripylocarpa* is intriguing, its relationships with Cocoseae or another group of palms remains equivocal until other details of its anatomy and morphology are documented.

Dispersed *Nypa* fruits are known from numerous localities starting in the Maastrichtian–Danian including from India, England, North America, Colombia, Spain, and Egypt (Reid & Chandler, 1933; Gee, 2001; Gomez-Navarro *et al.*, 2009; El-Soughier *et al.*, 2011; Moreno-Domínguez, Cascales-Miñana, & Diez, 2016). The distinctive morphology of *Nypa* fruits makes the genus relatively easy to recognize in the fossil record, but occurrences should be treated cautiously when preservation is incomplete, making external morphology and overall shape unclear, or when diagnostic characters such as the basal germination pore, internal endocarp ridge, and pericarp structure are not preserved. Compressions of palm fruits were recovered from the Danian Cerrejón Formation of Colombia (Gomez-Navarro *et al.*, 2009) and assigned to *Nypa* and *Cocos* based on the size and shape of the fruits, their fibrous appearance, and the presence of apparent longitudinal striations in the *Nypa* specimens.

These determinations from Cerrejón seem reasonable given the interpretation of the specimens and geographic distribution of modern taxa. However, the possibility that the

striations of the *Nypa* specimen result from taphonomic processes was not discussed and should be given some consideration, especially since it is the main feature that distinguishes it from the *Cocos* specimen. It is worth noting that the *Cocos*-like characters of the specimen (large size, ovate shape, apical stigmatic remains, longitudinal fibers and striations) are not restricted to cocosoid palms and are found also in Borasseae. These features alone, therefore, do not justify placement in *Cocos*, which also applies to other *Cocos* described from compressions or casts (e.g. Shukla, Mehrotra, & Guleria, 2012; Srivastava & Srivastava, 2014; Singh, Shukla, & Mehrotra, 2016). There is little doubt that both Cerrejón fruits are palms, but their precise taxonomic affinities are equivocal based on the characters described and figured images. The uncertain taxonomy of such fossils illustrates some of the challenges of ascertaining systematic relationships of palm fruits based on compression fossils or other modes of preservation lacking anatomy. Future morphological studies that quantify fruit and seed shape may provide a useful framework for evaluating systematic relationships of compression fossils and seeds.

Implications for palm macroevolution

This fruit morphology dataset enabled me to include six fossil palm fruits in genus-level phylogenetic analyses of Arecaceae, providing insights into the systematic relationships of these fossils and the age of major clades. Four represent new fossils suitable for node calibrations: *Coryphoides poulseni*, *Palmocarpon drypeteoides*, *Friedemannia messelensis*, and the Mahurzari palm. The age and phylogenetic relationships of these fossils indicate that several groups of palms have much earlier origins than estimated by molecular dating analyses (Table 3.1), suggesting diversification within subfamilies and tribes began during the Late Cretaceous, rather than the Cenozoic.

Refining age estimates for major clades of palms is important for understanding the contributions of climatic and biotic changes during the Cretaceous and Cenozoic to palm evolution. Late Cretaceous climate was warm and relatively dry in comparison to the wetter conditions of the late Paleocene and Eocene. Cooling and drying trends starting during the Eocene-Oligocene transition and continuing into the Neogene were accompanied by shifts in the composition of terrestrial biotas around the world and latitudinal range of tropical taxa like palms. Additionally, a major mass extinction and the Cretaceous-Paleogene boundary caused dramatic changes to Earth systems, particularly to terrestrial faunas. How palms responded to these changes at a macroevolutionary scale is currently not understood. These questions can be addressed and further explored using divergence time and diversification analyses, applying the fruit fossils investigated here as either node calibrations or tips in a total-evidence dating framework.

This study also provides important resources for studying the palm fossil record and investigating various aspects of macroevolution. The morphological matrix enables inclusion of fossils in phylogenetic and total-evidence dating analyses. Other fossil fruits can be scored in the matrix, facilitating the identification of new discoveries and re-examination of previously described occurrences. This dataset can further be augmented with other characters from the Baker *et al.* (2009) matrix to include fossils of other organs. Finally, all μ CT datasets, including raw data and products, are publicly archived and freely available for download through MorphoSource and can be used for a broad range of research and educational purposes.

Conclusions

I undertook a genus-level survey of palm fruit structure using µCT studies of over 200 species of extant palms and information from the literature. Data from the survey were used to develop a discrete character dataset on palm fruits, which was applied in phylogenetic and morphospace analyses. I observed substantial variation in fruit structure throughout the family and convergence of many traits, but also identified character suites that distinguish major groups of palms. Principal coordinate analyses similarly show that while subfamilies generally converge in morphospace, many tribes within subfamilies are non-overlapping, consistent with our ability to distinguish them using character suites. Phylogenetic analyses using the dataset successfully resolved tribe or subtribe relationships of six fossil palms, demonstrating the utility of fruit characters for evaluating the systematic relationships of fossils in a phylogenetic framework. Several of these fossils are suitable as calibrations on nodes for which empirical ages were previously lacking. Additionally, the age of some fossils indicate there was a more extensive Late Cretaceous diversification among subfamilies than was previously known. This study fills a substantial gap in our understanding of fruit morphology and the distribution of traits across Arecaceae, and lays a foundation for using the fossil record of fruits to better understand palm diversification and morphological evolution.

Table 3.1 Palm fruit fossils suitable as node calibrations. Groups with which relationships are strongly supported in phylogenetic analyses are indicated, as well as the estimated ages of those clades from Baker & Couvreur (2013) and the age of the fossils. Some key characters of the fossils that support their phylogenetic relationships are listed. Note that these relationships are based on multiple characters, which are discussed in the text.

Species	Group	Key characters	Fossil age	Estimated node age
			(million years)	(95% HPD Baker & Couvreur, 2013)
<i>Coryphoides poulseni</i>	Crown Trachycarpeae	Lateral embryo, basal postament	64–62	47.15–22.98
<i>Friedemannia messelensis</i>	Crown Areceae	Apical hilum/seed attachment	47	42.42–25.95
<i>Hyphaeneocarpion indicum</i>	Crown Hyphaeninae	Apical embryo & elongate germination pore	64–67	26.78–13.63
Mahurzari palm	Core arecoids (Areceae–Euterpeae)	Single functional locule	64–67	52.89–32.98 (Euterpeae stem)
<i>Palmocarpion drypeteoides</i>	Crown Attaleinae	Three subbasal germination pores	64–67	49.78–23.29

References

- Baker WJ & Couvreur TLP.** 2013. Global biogeography and diversification of palms sheds light on the evolution of tropical lineages. I. Historical biogeography. *Journal of Biogeography* **40**: 274–285.
- Baker WJ & Dransfield J.** 2016. Beyond Genera Palmarum: progress and prospects in palm systematics. *Botanical Journal of the Linnean Society* **182**: 207–233.
- Baker WJ, Norup M V., Clarkson JJ, et al.** 2011. Phylogenetic relationships among arecoid palms (Arecaceae: Arecoideae). *Annals of Botany* **108**: 1417–1432.
- Baker WJ, Savolainen V, Asmussen-Lange CB, et al.** 2009. Complete generic-level phylogenetic analyses of palms (Arecaceae) with comparisons of supertree and supermatrix approaches. *Systematic Biology* **58**: 240–256.
- Bobrov AVFC, Lorence DH, Romanov MS, et al.** 2012a. Fruit Development and Pericarp Structure in *Nypa fruticans* Wurmb (Arecaceae): A Comparison with Other Palms. *International Journal of Plant Sciences* **173**: 751–766.
- Bobrov A, Romanov MS & Romanova ES.** 2012b. Gynoecium and fruit histology and development in *Eugeissona* (Calamoideae: Arecaceae). *Botanical Journal of the Linnean Society* **168**: 377–394.
- Cailliez F.** 1983. The analytical solution of the additive constant problem. *Psychometrika* **48**: 305–308.
- Chapin MH, Essig FB & Pintaud JC.** 2001. The morphology and histology of the fruits of Pelagodoxa (Arecaceae): taxonomic and biogeographical Implications. *Systematic Botany* **26**: 779–785.
- Collinson ME, Manchester SR & Wilde V.** 2012. Fossil fruits and seeds of the Middle Eocene Messel biota, Germany. *Abh. Senckenberg Ges. Naturforsch.* **570**: 1–251.
- Dransfield J, Uhl NW, Asmussen CB, et al.** 2008. *Genera Palmarum: the evolution and classification of palms*. Richmond, Surrey, UK: Kew Publishing.
- El-Soughier MI, Mehrotra RC, Zhou ZY, et al.** 2011. *Nypa* fruits and seeds from the Maastrichtian-Danian sediments of Bir Abu Minqar, South Western Desert, Egypt. *Palaeoworld* **20**: 75–83.
- Eldrett JS, Greenwood DR, Harding IC, et al.** 2009. Increased seasonality through the Eocene to Oligocene transition in northern high latitudes. *Nature* **459**: 969–973.
- Essig FB.** 1977. A systematic histological study of palm fruits. I. The Ptychosperma alliance. *Systematic Botany* **2**: 151–168.
- Essig FB.** 2002. A systematic histological study of palm fruits. VI. Subtribe Linospadicinae

- (Arecaceae). *Brittonia* **54**: 196–201.
- Essig FB, Bussard L & Hernandez N. 2001.** A systematic histological study of palm fruits. IV. Subtribe Oncospermatinae (Arecaceae). *Brittonia* **53**: 466–471.
- Essig FB & Hernandez N. 2002.** A systematic histological study of palm fruits. V. Subtribe Archontophoenicinae (Arecaceae). *Brittonia* **54**: 65–71.
- Essig FB, Manka TJ & Bussard L. 1999.** A systematic histological study of palm fruits. III. Subtribe Iguanurinae (Arecaceae). *Brittonia* **51**: 307–325.
- Essig FB & Young BE. 1979.** A Systematic Histological Study of Palm Fruits . I . The Ptychosperma Alliance. *Systematic Botany* **4**: 16–28.
- Fadini RF, Fleury M, Donatti CI, et al. 2009.** Effects of frugivore impoverishment and seed predators on the recruitment of a keystone palm. *Acta Oecologica* **35**: 188–196.
- Faurby S, Eiserhardt WL, Baker WJ, et al. 2016.** An all-evidence species-level supertree for the palms (Arecaceae). *Molecular Phylogenetics and Evolution* **100**: 57–69.
- Fliche P. 1894.** Sur les fruits de palmiers trouvés dans le cénomanien environs de Sainte-Menehould. *Comptes rendus Hebdomadaires des Séances de l'Academie des Sciences* **118**: 889–890.
- Futey MK, Gandolfo MA, Zamaloa MC, et al. 2012.** Arecaceae Fossil Fruits from the Paleocene of Patagonia, Argentina. *Botanical Review* **78**: 205–234.
- Gee CT. 2001.** The mangrove palm *Nypa* in the geologic past of the new world. *Wetlands Ecology and Management* **9**: 181–194.
- Gomez-Navarro C, Jaramillo C, Herrera F, et al. 2009.** Palms (Arecaceae) from a Paleocene rainforest of northern Colombia. *American Journal of Botany* **96**: 1300–1312.
- Greenwood DR & West CK. 2017.** A fossil coryphoid palm from the Paleocene of western Canada. *Review of Palaeobotany and Palynology* **239**: 55–65.
- Harley MM. 2006.** A summary of fossil records for Arecaceae. *Botanical Journal of the Linnean Society* **151**: 39–67.
- Hopkins MJ & John KS. 2018.** A new family of dissimilarity metrics for discrete character matrices that include inapplicable characters and its importance for disparity studies. *Proceedings of the Royal Society B: Biological Sciences* **285**.
- Iles WJDD, Smith SY, Gandolfo MA, et al. 2015.** Monocot fossils suitable for molecular dating analyses. *Botanical Journal of the Linnean Society* **178**: 346–374.
- Katoh K & Standley DM. 2013.** MAFFT multiple sequence alignment software version 7: improvements in performance and usability. *Molecular biology and evolution* **30**: 772–80.

Koch BE. 1972. Coryphoid fruits and seeds from the Danian of Nûgssuaq, West Greenland. *The Geological Survey of Greenland* **99**: 1–37.

Lloyd GT. 2016. Estimating morphological diversity and tempo with discrete character-taxon matrices: Implementation, challenges, progress, and future directions. *Biological Journal of the Linnean Society* **118**: 131–151.

Löytynoja A. 2014. Phylogeny-aware alignment with PRANK BT - Multiple Sequence Alignment Methods. In: Russell DJ, ed. Totowa, NJ: Humana Press, 155–170.

Manchester SR, Bonde SD, Nipunage DS, et al. 2016. Trilocular Palm Fruits from the Deccan Intertrappean Beds of India. *International Journal of Plant Sciences* **177**: 633–641.

Manchester SR, Lehman TM & Wheeler EA. 2010. Fossil Palms (Arecaceae, Coryphoideae) Associated with Juvenile Herbivorous Dinosaurs in the Upper Cretaceous Aguja Formation, Big Bend National Park, Texas. *International Journal of Plant Sciences* **171**: 679–689.

Matsunaga KKS, Manchester SR, Srivastava R, et al. 2019. Fossil palm fruits from India indicate a Cretaceous origin of Arecaceae tribe Borasseae. *Botanical Journal of the Linnean Society* **190**: 260–280.

Moreno-Domínguez R, Cascales-Miñana B & Diez JB. 2016. First record of the mangrove palm *Nypa* from the northeastern Ebro Basin , Spain : With taphonomic criteria to ... *Geologica Acta* **14**: 1–11.

Murray SG. 1973. The formation of endocarp in palm fruits. *Principes* **17**: 91–102.

Paradis E & Schliep K. 2019. ape 5.0: an environment for modern phylogenetics and evolutionary analyses in R. *Bioinformatics* **35**: 526–528.

Pattengale ND, Alipour M, Bininda-Emonds ORPP, et al. 2009. How many bootstrap replicates are necessary? In: Batzoglou S, ed. *Research in Computational Molecular Biology*. Berlin, Heidelberg: Springer Berlin Heidelberg, 184–200.

Peters H a, Pauw A, Silman MR, et al. 2004. Falling palm fronds structure amazonian rainforest sapling communities. *Proceedings. Biological sciences / The Royal Society* **271**: S367–S369.

Pross J, Contreras L, Bijl PK, et al. 2012. Persistent near-tropical warmth on the Antarctic continent during the early Eocene epoch. *Nature* **488**: 73–7.

Read RW & Hickey LJ. 1972. A Revised Classification of Fossil Palm and Palm-like Leaves. *International Association for Plant Taxonomy* **21**: 129–137.

Reichgelt T, West CK & Greenwood DR. 2018. The relation between global palm distribution and climate. *Scientific Reports* **8**: 2–12.

Reid EM & Chandler MEJ. 1933. *The London Clay Flora*. London: British Museum (Natural

History).

Romanov MS, Bobrov AVFC, Wijesundara DSA, et al. 2011. Pericarp development and fruit structure in borassoid palms (Arecaceae-Coryphoideae-Borasseae). *Annals of Botany* **108**: 1489–1502.

Roncal J, Zona S & Lewis CE. 2008. Molecular phylogenetic studies of Caribbean palms (Arecaceae) and their relationships to biogeography and conservation. *Botanical Review* **74**: 78–102.

Shukla A, Mehrotra RC & Guleria JS. 2012. *Cocos sahnii* Kaul: A *Cocos nucifera* L.-like fruit from the Early Eocene rainforest of Rajasthan, western India. *Journal of Biosciences* **37**: 769–776.

Singh H, Shukla A & Mehrotra RC. 2016. A fossil coconut fruit from the early Eocene of Gujarat. *Journal of the Geological Society of India* **87**: 268–270.

Srivastava R & Srivastava G. 2014. Fossil fruit of *Cocos* L. (Arecaceae) from Maastrichtian-Danian sediments of central India and its phytogeographical significance. *Acta Palaeobotanica* **54**: 67–75.

Stamatakis A. 2014. RAxML version 8: A tool for phylogenetic analysis and post-analysis of large phylogenies. *Bioinformatics* **30**: 1312–1313.

Uhl NW & Moore HE. 1971. The palm gynoecium. *American Journal of Botany* **58**: 945–992.

Vaidya G, Lohman DJ & Meier R. 2011. SeqenceMatrix: Cladistics multi-gene datasets with character set and codon information. *Cladistics* **27**: 171–180.

Vaudois-Miéja N & Lejal-Nicol A. 1987. Paléocarpologie africaine: apparition dès l'Aptien en Égypte d'un palmier (*Hyphaeneocarpon aegyptiacum* n. sp.). *Comptes Rendus de l'Académie des Sciences Paris Série II* **304**: 233–238.

CHAPTER 4

New Insights into the Diversification of Palms (Arecaceae) from an Expanded Fossil Record of Fruits

Abstract

Arecaceae (palms) are widespread throughout modern tropical and subtropical environments. They have a rich fossil record extending into the Late Cretaceous, with numerous occurrences throughout the world during the Cenozoic, providing insights into their shifting geographic range over time. Less is known about the origin and diversification of major lineages of palms and how palm diversity has changed through time. Recent evidence from the fossil record of palm fruits provides important data for investigating evolutionary tempo and diversification history. Using these fossils as new calibrations, I performed molecular dating and diversification analyses to better understand the evolutionary history of Arecaceae. The results suggest that palms underwent an initial diversification during the Late Cretaceous that generated the stem lineages of modern tribes and coincided with their initial geographic expansion. Modern tribes diversified during the Paleogene, coeval with the origin and spread of angiosperm-dominated megathermal forests. Finally, a diversification rate shift associated with the largest palm tribe Areceae could be linked with geological changes and avian radiations in the Indo-Pacific. This study provides new insights into the evolution and diversification of palms and a framework for future macroevolutionary studies.

Introduction

Reconstructing the timing and rate of evolutionary events is essential for understanding the mechanisms that control biological diversity through time, and the contributions of biotic and abiotic processes to shaping evolutionary history. This can be accomplished by integrating data on modern and extinct species to infer phylogenetic relationships, clade age, and evolutionary rates, and examining the results in a broader geologic and environmental context.

The palm family (Arecaceae) is an ideal group for investigating how geologic and biological processes can shape evolutionary history. Palms have an extensive and well-sampled fossil record spanning all continents and the last ~90 million years of Earth history (Harley, 2006; Pan *et al.*, 2006; Dransfield *et al.*, 2008). Today palms are diverse and widespread throughout tropical and subtropical environments, comprising over 2500 species in five subfamilies and 29 tribes (Baker & Dransfield, 2016). Their geographic range is limited by anatomical and physiological constraints of their vascular system, which cannot withstand cavitation and embolism caused by freezing temperatures (Tomlinson, 1979, 2006). As a result, the diversity and distribution of palms on a global scale are strongly influenced by climate both today (Eiserhardt *et al.*, 2011; Reichgelt, West, & Greenwood, 2018) and in the geologic past, in which they serve as excellent indicators of frost-free environments (Morley, 2011; Greenwood & West, 2017). Palm fossils thus provide detailed information about past geographic distributions and response to climate, but less is known about when major lineages originated.

The fossil record provides some clues to their early diversification. Palms first appear in the Santonian of the Late Cretaceous in North America and Europe and subsequently underwent a major geographic expansion. Palms were widespread in terrestrial floras by the end of the Cretaceous, with pollen and macrofossils documented in the United States, Canada, Mexico,

Argentina, Cameroon, Somalia, India, Egypt, Austria, France, and Japan (Crié, 1892; Ôyama & Matsuo, 1964; Delevoryas, 1964; Jarzen, 1978; Schrank, 1994; Ancibor, 1995; Cevallos-Ferriz & Ricalde-Moreno, 1995; Harley, 2006; Ottone, 2007; Bonde, 2008; Dransfield *et al.*, 2008; Manchester, Lehman, & Wheeler, 2010; El-Soughier *et al.*, 2011; Estrada-Ruiz *et al.*, 2012).

Although many of these fossils are difficult to assign with confidence to major palm lineages, some specimens indicate that divergence of the five palm subfamilies probably occurred by the end of the Cretaceous. This is based on fossils belonging unequivocally to subfamilies Calamoideae (Schrank, 1994), Coryphoideae (Kvaček & Herman, 2004; Manchester *et al.*, 2010), Nypoideae (Gee, 2001), and Arecoideae (Manchester *et al.*, 2016).

Molecular dating analyses agree with the timeline implied by the fossil record. Using four calibration fossils, primarily leaves and pollen, node dating analyses have estimated a mid-Cretaceous origin of the family, divergence of subfamily stem lineages in the Late Cretaceous, and diversification within subfamilies and tribes in the Cenozoic, concentrated in the late Paleogene and Neogene (Couvreur, Forest, & Baker, 2011; Baker & Couvreur, 2013a,b). Together, molecular dating analyses and the fossil record suggest that palms underwent most of their taxonomic diversification during the Cenozoic, after an initial phase of geographic expansion in the Cretaceous.

However, my recent evidence from fossil fruits suggests palms underwent a more extensive diversification in the Late Cretaceous that coincided with their initial geographic expansion (Matsunaga *et al.*, 2019; Chapter 3). I recovered well-supported systematic relationships for six fruit fossils using a morphological dataset of fruit and gynoecial characters, demonstrating the utility of fruit characters for resolving the relationships of fossil palms (Chapter 3). These fossils are confidently assigned to several different clades within palms, but

their influence on age estimates for Arecaceae has not been investigated. In this study I test the hypothesis of a Cenozoic palm radiation and whether geographic expansion and taxonomic diversification were concomitant processes, using a new set of fossil calibrations based on a re-evaluation of the palm fossil record and phylogenetic relationships of fruit fossils. I employed several different calibration strategies to evaluate their influence on age estimates for palms. Using trees obtained from these analyses, I investigated diversification patterns and rate shifts within the family and discuss my results in the context of climatic, tectonic, and biotic changes that occurred during the Cretaceous and Cenozoic.

Methods

Calibration fossils

Eight fossils were selected to serve as calibrations for palms because they represent the oldest fossils of their respective groups (discussed below): *Sabalites carolinensis* Berry (Santonian, 86.3–83.6 Ma; Berry, 1914), *Mauritiidites crassibaculatus* Van Hoeken-Klinkenburg (Maastrichtian–Campanian, 72–66 Ma; Schrank, 1994; Harley, 2006), *Sabal bigbendense* Manchester, Wheeler, & Lehman (Campanian, 79.3–74.2 Ma; Befus *et al.*, 2008; Manchester, Lehman, & Wheeler, 2010), *Coryphoides poulseni* Koch (Danian, 64–62 Ma; Koch, 1972; Grímsson *et al.*, 2016), *Friedemannia messelensis* Collinson, Manchester, & Wilde (Eocene, ~47 Ma; Franzen, 2005; Collinson, Manchester, & Wilde, 2012), and three fossil from the Deccan intertrappean beds of India (Maastrichtian–Danian, ~64–67 Ma; Schoene *et al.*, 2015; Srivastava *et al.*, 2015). The Deccan fossils are *Hyphaeneocarpion indicum* Bande, Prakash & Ambwani, emend. Matsunaga, S.Y.Sm., Manch., Srivastava & Kapgate (Matsunaga *et al.*, 2019), *Palmocarpion drypeteoides* (Mehrotra, Prakash & Bande) Manchester, Bonde, Nipunage,

Srivastava, Mehrotra & Smith (Manchester *et al.*, 2016), and the “Mahurzari palm” (Matsunaga *et al.*, in prep).

Node calibrations

The calibration scheme used for Arecaceae (Fig. 4.1), detailed below, is different than previous studies and is based upon my review of the palm fossil record and phylogenetic analyses of several fossils (Chapter 3).

Root: *Liliacidites* Couper was used to calibrate the root node of the tree (*Liliacidites* sp. A; Aptian, 125–113 Ma; Doyle, 1973; Doyle & Hickey, 1976). Pollen grains of *Liliacidites* sp. A are considered the oldest unequivocal record of monocots (Iles *et al.*, 2015). By using it to calibrate the root node I assume that the divergence between Arecaceae and Dasypogonaceae is unlikely to be older than the oldest fossil monocot.

Arecaceae crown group: The oldest unequivocal palms include *Sabalites carolinensis*, *Sabalites magothiensis* Berry, and *Palmoxylon cliffwoodensis* Berry (Berry, 1905, 1914, 1916), all of which are Santonian in age (Christopher, 1979; Gohn *et al.*, 1992). *Sabalites carolinensis*, which consists primarily of lamina fragments, is usually used to calibrate the stem node of Coryphoideae because the leaves are palmate and described as *Sabal*-like, implying the presence of a costa (Berry, 1914). However, palmate and (weakly) costapalmate leaves also occur in Calamoideae (*Mauritia* L. and *Mauritiella* Burret), and currently no features of *Sabalites carolinensis* as documented in the literature explicitly rule out the possibility the fossils might belong to Calamoideae or a stem lineage nearer the base of the phylogeny. Based on these considerations I conservatively use *Sabalites carolinensis* to calibrate the crown node of Arecaceae rather than the stem node of Coryphoideae, until the original specimens can be re-

examined. To my knowledge the earliest unequivocal, strongly costapalmate leaves are those of *Sabalites longirhachis* Kvaček & Herman from the lower Campanian of Austria (Kvaček & Herman, 2004).

Calamoideae: I used *Mauritiidites crassibaculatus* pollen to calibrate the stem node of subtribe Mauritiinae in Calamoideae, as has been done in previous studied (Couvreur *et al.*, 2011). *Mauritiidites* has a distinct morphology characterized by clavate monosulcate grains with spines bearing swollen bases, which are rooted in depressions of the ectexine. These features are characteristic of *Mauritia* L.f. and other members of Mauritiinae, and thus *Mauritiidites* is accepted as a reliable pollen record for the subtribe (Harley, 2006).

Coryphoideae: Within Coryphoideae, I used *Hyphaeneocarpon indicum* for the Hyphaeninae crown node, *Coryphoides poulseni* for the Livistoninae stem node, and *Sabal bigendense* for the sister group to the syncarpous clade, which includes the modern lineages *Sabal*, Cryosophileae, Trachycarpeae, and *Phoenix*. *Hyphaeneocarpon indicum* has well-resolved relationships within the crown group of subtribe Hyphaeninae in tribe Borasseae. Phylogenetic analyses place it with very strong support as sister to either *Bismarckia* Hildebr. & H.Wendl., (Chapter 3) or *Satranala* Beentje & J.Dransf (Matsunaga *et al.*, 2019; Chapter 2), and so I use it for the Hyphaeninae crown node to accommodate this uncertainty. *Coryphoides poulseni* was placed in subtribe Livistoninae of tribe Trachycarpeae (Coryphoideae) with high support using a backbone constraint (Chapter 3). The morphology of *C. poulseni* is consistent with these relationships, as a basal postament (columnar intrusion of the seed coat) and lateral embryo are found only in some members of Livistoninae. However, owing to the overall low bootstrap support for Livistoninae in my backbone tree I use *C. poulseni* to calibrate the Livistoninae stem node (crown node Livistoninae+Rapidinae).

Sabal bigbendense was placed in a modern genus by Manchester *et al.* (2010) based on overall similarity to extant *Sabal* seeds, which have a unique shape. µCT scans of *S. bigbendense* further revealed a thickened zone of the seed coat at the hilum and a well-preserved embryo (Chapter 3). Unevenly thickened seed coats of the kind seen in *S. bigbendense* are found in several members of a clade comprising Trachycarpeae, Phoeniceae, Cryosophileae, and Sabaleae (hereafter “apocarpous clade”), and are absent in the syncarpous clade. Given the strong similarities between *S. bigbendense* and *Sabal*, based on extensive comparisons with extant species made by the original authors, I am comfortable using it as a crown node calibration for the apocarpous clade but am hesitant to use it for the stem node of Sabaleae until more characters are documented.

Arecoideae: *Palmocarpon drypeteoides* was assigned to subtribe Attaleinae in tribe Cocoseae based on the presence of three seeds and subbasal germination pores in mature fruits. Phylogenetic analyses placed it with high support within Attaleinae, nested with the genera characterized by subbasal germination pores (some Attaleinae genera have lateral pores; Dransfield *et al.*, 2008). I therefore use it as a calibration within the crown of subtribe Attaleinae. *Friedemannia messelensis* has seeds attached apically within fruits, an unusual character found only in some genera of tribe Arecaeae. Phylogenetic analyses using a backbone constraint place it with moderate to high support in the western Pacific clade of Areceae. However, support for this placement varies somewhat with the topology of the backbone constraint, and preservation of *F. messelensis* as lignitized compressions precludes observation of apomorphies or character combinations that might strongly indicate relationships with the Pacific clade. *Friedemannia messelensis* was therefore used conservatively as a calibration for the Areceae crown node.

Phylogenetic analyses placed the Mahurzari palm in tribe Areceae with high support, but affinities within the tribe are highly uncertain (Chapter 3). One set of morphological characters that indicates affinities with Areceae is a gynoecium containing three stigmatic surfaces but only one locule, which is connected to one of the stigmas by a narrow channel, suggesting the gynoecium was pseudomonomerous. Pseudomonomerous gynoecia are found in Areceae and Euterpeae, which are often resolved as sister to one another. Because no documented characters of the Mahurzari palm are apomorphies within Areceae, I used it to calibrate the node corresponding to the most recent common ancestor of Areceae and Euterpeae, which also accommodates the possibility that the two tribes are not monophyletic.

Divergence time analyses

The molecular dataset assembled for the analysis here contained 178 taxa, including 176 of the 181 valid palm genera, and *Dasypogon bromeliifolius* R.Br. and *Kingia australis* R.Br. (Dasypogonaceae) as the outgroup. Ten plastid and nuclear markers were sampled from GenBank: *18S*, *atpB*, *matK*, *ndhF*, *PRK*, *rbcL*, *RPB2*, *rps16*, *trnL-trnF* intragenic spacer, and *trnQ-rps16* intergenic spacer. Whenever possible I sampled each gene from the same species or individual (when whole plastid genomes were available), but some taxa in the dataset are represented by genes from different species (Appendix C). To reduce alignment computation time, sequences were aligned initially using MAFFT (Katoh & Standley, 2013) and then passed to PRANK (Löytynoja & Goldman, 2008) for the final alignment. PRANK alignments were left unmodified except to trim alignment edges. Aligned sequences were concatenated into a single matrix using SequenceMatrix (v.1.8; Vaidya, Lohman, & Meier, 2011). To assess optimal partitioning schemes and substitution models I used PartitionFinder2 (Lanfear *et al.*, 2017), with

the molecular dataset separated into 10 partitions, one for each gene. Codon partitioning was not tested to reduce the number of partitions in the downstream dating analyses, as a 10-partition model already requires significant computation time.

Divergence time analyses co-estimating topology and clade age were performed using a Bayesian Markov chain Monte Carlo (MCMC) approach implemented in BEAST 2 (v.2.5.1; Bouckaert *et al.*, 2014) on the CIPRES (Cyberinfrastructure for Phylogenetic Research) Science Gateway (v.3.3; Miller, Pfeiffer, & Schwartz, 2010), under an uncorrelated lognormal relaxed clock model and constant rate birth-death tree prior; both parameters were linked across gene partitions, which assumes all the genes evolve under the same clock model and tree generating process. Selection of a relaxed over a strict clock model was based on previous model testing of a similar dataset of palms that showed the sequence data are non-clock like (Couvreur *et al.*, 2011). There is evidence that a random local clock model has better fit to a monocot-wide dataset (Barrett *et al.*, 2016) but I did not implement this owing to computational limitations. Analyses of a dataset of this size using a random local clock model would require several months to complete owing to the large number of possible rate configurations (Ho *et al.*, 2005; Drummond & Suchard, 2010). Moreover, the impacts of rate heterogeneity are probably reduced by the use of a single family as the outgroup, Dasypogonaceae, which is now considered the sister group to Areceaceae (Givnish *et al.*, 2018). To speed up convergence and reduce overall computation time, I used chronograms constructed with penalized likelihood as starting trees. The chronograms were generated from maximum likelihood trees inferred in RAxML (Stamatakis, 2014) and the same set of fossil calibrations described above, using the ‘chronos’ function (Paradis, 2013) in the R package ‘ape’ (v.5.2; Paradis, Claude, & Strimmer, 2004). Chain length for MCMC runs was set to 100 million generations. I performed two independent

runs and checked for run convergence and effective sample size of all parameters with Tracer (v.1.6.0; Rambaut *et al.*, 2018).

Prior distributions on calibrated nodes

Both lognormal and uniform distributions were tested for all node age priors. The approach in setting the prior distributions was to accommodate uncertainty in the palm fossil record because the precise systematic affinities of many fossils are unclear.

Lognormal priors: I set the lognormal distributions such that the upper and lower tails of the distribution spanned the age of the calibration fossil and the age of the oldest fossil palm. By doing so I assumed that the time of origin for the calibrated node was likely to be close to but could be much older than the age of the fossils, and unlikely to exceed the age of the oldest fossil for Arecaceae. Lognormal distributions were initially set with the offset equal to the minimum age of the fossil and the 97.5% quantile of the distribution roughly equal to the oldest unequivocal palm fossil (83.6 Ma). However, this configuration of priors yielded some joint priors (i.e. marginal densities, effective priors) that were sometimes strongly bimodal or otherwise different than those that were specified (see Warnock *et al.*, 2015; Rannala, 2016; Brown & Smith, 2018), particularly for nodes for which monophyly was not enforced.

Ideally, the joint priors should reflect the user specified priors (Warnock *et al.*, 2015). To achieve this, I first applied monophyly constraints to all calibrated nodes except the Mahurzari palm, the taxon-set for which included Areceae and Euterpeae. Although the two tribes were resolved as monophyletic in my analyses, support was generally low; moreover, monophyly has not been recovered in all other studies. All the other calibrated nodes have been consistently recovered as monophyletic, so I was comfortable constraining them in the analyses. Monophyly

constraints yielded unimodal distributions for all priors, but a few of the joint priors were still significantly older than the specified distribution. To correct this I adjusted the distributions incrementally until the joint priors better reflected the initial user-specified priors, which were informed by paleontological evidence, as recommended by Warnock *et al.* (2015). A normal distribution was applied to the root node, with the upper and lower tails spanning the age of the oldest palms and the oldest monocot fossils

Uniform priors: Uniform priors were set with the lower bound equal to the age of the calibration fossil and the age of the earliest monocot fossils as the upper bound. *Liliacidites* is Aptian and therefore the maximum bound on its age is 125 Ma (Doyle & Hickey, 1976; Iles *et al.*, 2015).

No priors: To assess the impact of node calibrations within the Arecaceae crown group and to better understand the contribution of the molecular data to posterior estimates, I ran an analysis without node constraints. For this, I performed the same analysis as outlined for lognormal priors but removed the prior distributions on all calibrated nodes except the Arecaceae crown and stem node.

Monocot calibrations: A dataset that also included additional monocot outgroups and nine other monocot calibration was initially tested to determine impact of outgroup calibration on age estimates. However, these runs did not converge in the time frame of this study owing to computation challenges in estimating clock rate for such a large dataset (205 taxa), which probably contained significant rate heterogeneity (e.g. Barrett *et al.*, 2016). Preliminary results suggest relatively little impact on ages for palms, but this should be tested in the future.

Lineage-through-time and diversification analyses

Semilogarithmic lineage-through-time plots (LTT) were used to compare chronograms generated with different priors and sampling, and to visualize the diversification process inferred by my analyses. For comparison, I also plotted LTTs for 1000 randomly generated birth-death trees of comparable size. Because my trees were sampled at the genus level and thus extant taxon sampling is incomplete, a temporal cutoff was set for the simulated trees at approximately 27 million years before present; in other words, tree simulation was stopped in the mid-Oligocene rather than the present. This cutoff was based on time-dependent estimates of incomplete sampling from Couvreur *et al.* (2011), who used a similar taxon sampling strategy. The choice of 27 Ma was based on the stem age of *Calamus*, the most species-rich genus in the family, and dramatic increases in estimated numbers of unsampled species after this time (Couvreur *et al.*, 2011).

To investigate potential shifts in net diversification rate through time and to determine whether chronograms generated with this dataset recover the same rate shifts detected in previous studies, I examined lineage-specific diversification rates using maximum likelihood (MEDUSA; Alfaro *et al.*, 2009) and Bayesian approaches (BAMM; Rabosky, 2014). Both analyses can account for incomplete sampling at tips, but results are interpreted cautiously in light of the taxon sampling and concerns over the performance of these methods with empirical datasets (May & Moore, 2016; Moore *et al.*, 2016; Rabosky, Mitchell, & Chang, 2017; Meyer, Román-Palacios, & Wiens, 2018). MEDUSA (Modeling Evolutionary Diversification Using Step-wise AIC) uses step-wise AIC to find the optimal number of rate shifts on a tree. It works by first fitting a two-parameter, constant rate birth-death model to the tree, and then fits a five-parameter rate model to the tree based on the optimal location of a single rate shift. The corrected

Akaike information criterion (AICc) is then used to select between the two models using either a user-specified Δ AIC threshold (critical threshold, Δ AIC_{crit}), or one estimated by MEDUSA based on the number of terminal taxa (6 for a tree with 178 tips). MEDUSA iterates this process until no additional rate shifts are selected based on the critical threshold. To evaluate robustness of detected rate shifts, I tested models under birth-death and yule processes and increased the critical threshold until no rate shifts were selected by AICc.

In contrast to MEDUSA, which uses an AIC model selection framework, BAMM (Bayesian Analysis of Macroevolutionary Mixtures) uses reversible-jump MCMC to move between regions of model space with distinct configurations of rate shifts (Rabosky, 2014). I ran BAMM for 10 million generations using metropolis-coupled MCMC with three hot chains and one cold chain, which allows for more thorough exploration of parameter space than a standard MCMC search (Shi & Rabosky, 2015), and sampled from the posterior every 1000 generations. To account for incomplete sampling of palm diversity, I included in the analysis sampling percentages for each genus, based on species-richness estimates of Couvreur *et al.* (2011). To test for sensitivity to incomplete sampling, I ran an additional analysis with all of the sampling fractions halved, following Shi and Rabosky (2015). This simulates a situation in which the true species richness of Arecaceae is doubled and thus my taxon sampling is significantly more incomplete. To further check whether any detected rate shifts could be false positives resulting from poor taxon sampling, I also replicated the MEDUSA and BAMM analyses with the species-level supertree of Faurby *et al.* (2016), which has much younger ages than those estimated here but nearly complete species sampling of Arecaceae.

Results

Node dating analyses

I focus primarily on age estimates for subfamilies and tribes sensu Baker & Dransfield (2016), which are summarized in Table 4.1 (Fig. 4.1). Age estimates are similar but slightly older overall in the analysis using uniform node priors, especially for deeper nodes within the tree (Fig. 4.2A). Using both lognormal and uniform priors, the dating analyses indicate a mid-Cretaceous origin for the Arecaceae crown and the stem lineages of all subfamilies, and all tribes except Pelagodoxeae have mean stem ages in the Late Cretaceous (Fig. 4.1, Table 4.1; Appendix E). Four tribes have crown origins in the Late Cretaceous, while diversification of the remaining tribes is concentrated in the Paleogene. 95% highest posterior density (HPD) intervals, reflecting the distribution of ages sampled by the MCMC, are large for stem nodes of many genera, especially those nested in small clades sitting on long branches, indicating substantial age uncertainty (e.g. Chuniophoeniceae, Ceroxyloideae; Table 4.1). The taxon sampling in this study precludes recovery of crown ages for genera, since a single species was sampled from each genus, and this may exacerbate the uncertainty in some stem age estimates. Several tribes contain only a single genus (e.g. Sabaleae, Phoeniceae) but most of these are all sister to much larger clades and their stem ages tend to be well relatively constrained. The run without age constraints within the Arecaceae crown produced significantly younger ages throughout the tree, not just for deep nodes (Fig. 4.2).

“Diptych plots” (after Brown & Smith, 2018; Fig. 4.3) compare joint prior and posterior distributions on calibrated nodes, and are useful for gauging information content in the data and the sensitivity of results to the priors (Brown & Smith, 2018). For these analyses, the diptych plots indicate that posterior ages are not strongly influenced by the priors (Fig. 4.3). Arecaceae

crown and stem nodes have almost non-overlapping joint prior and posterior distributions, with the posterior ages substantially older. Some nodes have very similar prior and posterior distributions, but these appear to be driven by signal in the data more than the prior itself, since similar posteriors were obtained using lognormal and uniform priors, and the shape of the prior and posterior distributions differ. This was the case for lognormal priors on nodes calibrated by *Coryphoides poulseni*, the Mahurzari palm, and *Mauritiidites crassibaculites*. Many other calibrations within the Arecaceae crown group have posterior distributions that push as close to the younger age bound as possible, despite broader joint priors with older mean ages.

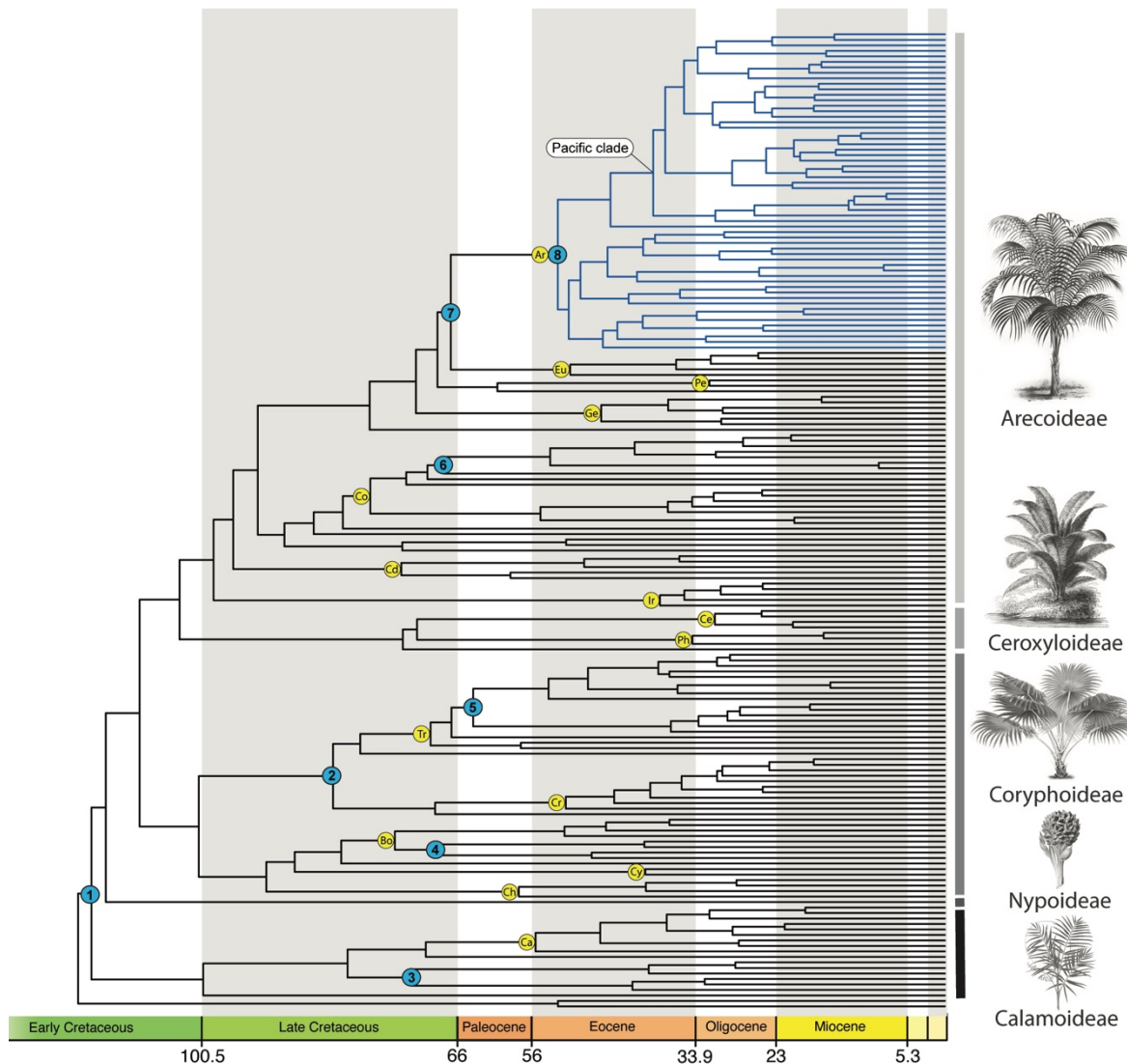


Figure 4.1 Chronogram based on node-dating analysis using lognormal priors. Subfamily delimitations indicated by gray bars at right with accompanying illustrations (all in the public domain). Crown nodes of non-monogeneric tribes indicated with yellow circle. See table 1 for abbreviations. Calibrated nodes marked with blue circles. 1=*Sabalites carolinensis*, 2=*Sabal bigbendense*, 3=*Mauritiidites crassibaculatus*, 4=*Hyphaeneocarpon indicum*, 5=*Coryphoides poulseni*, 6=*Palmocarpon drypeteoides*, 7=Mahurzari palm, 8=*Friedemannia messelensis*. Blue branches at tribe Areceae indicate diversification rate shift associated with the tribe. Note that the location of the rate shift varies between the stem branch, crown node, or stem node depending on method and dataset, and thus the location shown here is approximate. Illustrations: *Calamus mollis* and *Nypa fruticans* infructescence (Francisco Manuel Blanco, 1880–1883, from *Flora de Filipinas*), *Saribus rotundifolius* (Louis van Houtte, 1867–1868, *Flore des serres et des jardins de l'Europe XVII*), *Phytelephas macrocarpa* (from Meyers Konversations-Lexikon, 1888), *Geonoma cuneata* (Charles Antoine Lemaire, 1874, *L'Illustration horticole*).

Table 4.1 Stem and crown ages for subfamilies and tribes obtained using lognormal and uniform priors. Mean ages and 95% highest posterior density (HPD) intervals given, rounded up to the first decimal place. Crown ages for monogeneric tribes were not estimated and are indicated by dashes. Abbreviations next to some tribes correspond to those used in Fig. 4.1. Note Lepidocaryeae was paraphyletic and so was not included in table.

	Lognormal Priors		Uniform Priors	
	Stem age (Ma) [mean (95% HPD)]	Crown age (Ma) [mean (95% HPD)]	Stem age (Ma) [mean (95% HPD)]	Crown age (Ma) [mean (95% HPD)]
Arecaceae	117.1 (124.5–109.4)	115.3 (122.6–107.5)	123.9 (125.0–121.7)	122.5 (124.9–119.3)
Calamoideae	115.3 (122.6–107.5)	100.1 (110.5–90.2)	122.5 (124.9–119.3)	104.7 (116.4–93.6)
Calameae (Ca)	70.2 (83.4–56.3)	55.2 (70.2–41.0)	70.9 (84.9–55.7)	55.8 (70.8–40.9)
Eugeissoneae	70.2 (83.4–56.3)	—	70.9 (84.9–55.7)	—
Nypoideae	113.3 (120.9–105.8)	—	120.3 (124.1–115.7)	—
Coryphoideae	108.7 (116.2–101.5)	100.8 (109.0–92.6)	114.9 (120.3–109.2)	106.7 (114.2–98.7)
Sabaleae	69.3 (82.7–56.3)	—	80.7 (96.4–63.8)	—
Cryosophileae (Cr)	69.3 (82.7–56.3)	51.7 (64.9–38.4)	80.7 (96.4–63.8)	57.0 (74.1–41.0)
Phoeniceae	79.1 (87.8–71.5)	—	92.0 (103.4–79.9)	—
Trachycarpeae (Tr)	79.1 (87.8–71.5)	69.6 (75.1–64.9)	92.0 (103.4–79.9)	73.4 (82.8–65.5)
Chuniophoeniceae (Ch)	91.6 (99.3–84.3)	57.4 (78.9–35.5)	95 (103.8–85.9)	59.8 (81.7–37.5)
Caryoteae (Ct)	87.8 (95.1–80.7)	40.1 (60.7–19.1)	90.2 (99.3–81.3)	41.8 (20.8–65.5)
Corypheae	81.5 (88.0–75.5)	—	82.0 (74.1–90.9)	—
Borasseae (Bo)	81.5 (88.0–75.5)	74.3 (79.1–69.6)	82.0 (74.1–90.9)	72.5 (67.0–78.9)
Ceroxyloideae	103.4 (111.2–95.6)	73.1 (95.2–50.9)	108.2 (115.9–100.5)	75.9 (53.8–97.9)
Cyclospatheae	73.1 (95.2–50.9)	—	69.3 (46.2–91.4)	—
Ceroxyleae (Ce)	68.5 (89.4–45.3)	31.1 (47.8–16.4)	75.9 (53.8–97.9)	31.8 (48.6–15.7)
Phytelepheae (Ph)	68.5 (89.4–45.3)	33.9 (52.5–16.0)	69.3 (46.2–91.4)	35.4 (56.3–15.68)

Table 4.1 continued. Stem and crown ages for subfamily Arecoideae

	Lognormal Priors		Uniform Priors	
	Stem age (Ma) [mean (95% HPD)]	Crown age (Ma) [mean (95% HPD)]	Stem age (Ma) [mean (95% HPD)]	Crown age (Ma) [mean (95% HPD)]
Arecoideae	103.4 (111.2–95.6)	98.8 (106.6–91.1)	108.2 (115.9–100.5)	102.5 (110.6–94.7)
Iriarteae (Ir)	98.8 (106.6–91.1)	39.3 (59.5–22.1)	102.5 (110.6–94.7)	40.4 (60.3–22.4)
Chamaedoreae (Cd)	96.1 (103.9–88.5)	73.4 (89.1–56.8)	99.5 (107.4–91.2)	75.9 (92.2–58.8)
Podococceae	73.4 (91.1–53.0)	—	74.8 (92.3–52.9)	—
Oranieae	51.2 (75.8–27.5)	—	52.5 (76.6–28.3)	—
Sclerospermeae	51.2 (75.8–27.5)	—	52.5 (76.6–28.3)	—
Roystoneeae	85.4 (92.4–78.4)	—	86.4 (94.8–78.8)	—
Reinhardtiaeae	81.4 (88.2–75.1)	—	81.7 (89.3–74.6)	—
Cocoseae (Co)	81.4 (88.2–75.3)	77.7 (83.6–72.3)	81.7 (89.3–74.6)	77.1 (83.8–70.9)
Manicarieae	77.6 (87.2–69.3)	—	80.2 (91.0–69.5)	—
Euterpeae (Eu)	66.8 (69.1–65.0)	50.3 (65.6–31.5)	69.2 (77.0–64.0)	52.6 (70.8–33.5)
Geonomateae (Ge)	71.6 (78.7–65.6)	46.7 (62.5–30.9)	74.1 (83.7–65.3)	47.8 (64.3–31.1)
Leopoldinieae	60.5 (71.0–46.6)	—	63.2 (76.0–49.4)	—
Pelagodoxeae (Pe)	60.5 (71.0–46.6)	31.9 (49.0–16.3)	33.4 (51.4–16.7)	63.2 (76.0–49.4)
Areceae (Ar)	66.8 (69.1–65.0)	52.5 (57.0–48.4)	69.2 (77.0–64.0)	52.6 (59.3–47.0)

Diversification-rate analyses

LTT plots provide a way to visualize the diversification process and sensitivity of the node dating analyses to changes in priors (Fig. 4.2). In Fig. 4.2, these plots are overlain to allow comparison of overall shape between runs (Fig. 4.2A), as well as individually, with 95% HPD intervals for each node (Fig. 4.2B–D). HPD intervals are very similar between the analyses using uniform and lognormal priors. Age uncertainty is generally higher for more recent nodes in the analyses using crown calibrations. Differences in age estimates between runs using lognormal and uniform priors are larger deeper in time but become smaller toward the present; ages produced by the analyses converge around 70 Ma. The run using only a constraint on crown age produced significantly younger ages, which can be seen in the shape of its LTT plot (Fig. 4.2 A&D). For comparison, I traced the LTT plot of Couvreur *et al.* (2011) and overlaid LTT plots of simulated trees to show the shape distribution of diversification regimes generated with a random birth-death process. My analyses with lognormal and uniform priors plot along the upper edge of the distribution of simulated trees, indicating relatively early accumulation of lineages.

I also used diversification-rate analyses to investigate the locations of potential changes in net diversification rate within the tree (Appendix F). MEDUSA recovered variable numbers of rate shifts depending on model and critical threshold value. Using the $\Delta\text{AIC}_{\text{crit}}$ value of 6, which is default for a tree with 178 tips, MEDUSA estimated nine rate shifts under a birth-death model, 15 using a Yule model, and 11 when including both birth-death and Yule models. Most of these shifts were towards higher rates of net diversification but some indicated lower rates, such as on the branch leading to core arecoids (Appendix F). Two of these shifts were robust to substantial increases in the $\Delta\text{AIC}_{\text{crit}}$ and were selected using critical thresholds of up to 48 under a Yule model and 34 under a birth-death model. One of these shifts is associated with the stem of tribe

Areceae, while the other occurs on the branch leading to *Calamus*; both shifts correspond to higher net diversification rates.

In contrast, BAMM detected one significant rate shift towards higher net diversification rates on the Areceae stem, driven by higher speciation rates (posterior probability = 0.83; Appendix F). Three other shifts were sampled in the posterior distribution, but with low posterior probability, and the posterior probability of zero rate shifts was 0.009. Bayes factor strongly favors a scenario of a single rate shift over one with zero rate shifts (229.8), indicating strong support for a rate shift associated with tribe Areceae. I also ran a second BAMM analysis to test sensitivity of the result to incomplete taxon sampling. This analysis produced almost identical results, but with much lower support overall. Posterior probabilities were 0.65 for a single rate shift on the Areceae stem and 0.22 for zero rate shifts, with a much lower Bayes factor favoring a single rate shift model (5.8).

BAMM and MEDUSA analyses using the Faurby *et al.* (2016) species tree produced similar configurations of rate shifts, which were also similar those obtained using MEDUSA on the tree from this study using the default $\Delta\text{AIC}_{\text{crit}}$ value. Most of the rate shifts occur near the crown of highly species rich genera. Both methods also estimated a shift towards higher net diversification rates near the node subtending Areceae and Euterpeae. All rate shifts are towards higher rates of net diversification and appear to be driven by higher speciation rates (Appendix F). The rate shift associated with Areceae (Fig. 4.1), was the only one detected by both MEDUSA and BAMM, and is also present in the Faurby *et al.* (2016) species tree.

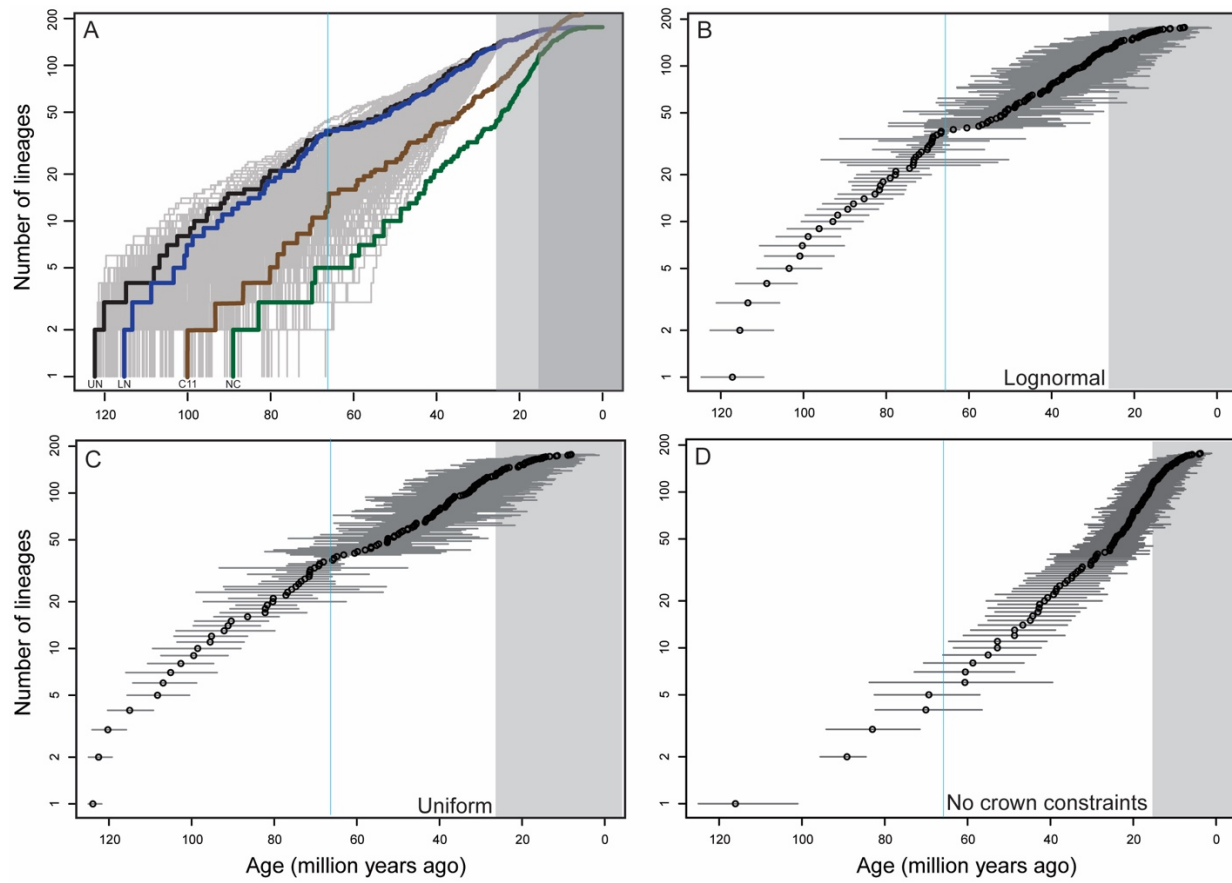


Figure 4.2 Lineage through time (LTT) plots based on trees generated using different priors and calibrations. Gray boxes indicate thresholds for LTT interpretation. Trees are sampled at the genus level and thus leveling of LTT plots towards the present is an artifact of taxon sampling. Thin blue lines correspond to the K-Pg boundary. (A) LTT plots generated from trees using lognormal priors (blue, “LN”), uniform priors (black, “UN”), and no crown calibrations (green, “NC”). The LTT plot from Couvreur *et al.*, (2011, Fig. 4.3) is shown for comparison (brown, “C11”), traced from the original figure. The first gray box indicates the threshold for LTT interpretation for trees calibrated with lognormal and uniform priors, while the second gray box is the threshold for the tree with no crown calibrations. Gray lines correspond to LTT plots of 1000 randomly generated birth-death trees. (B–D) LTT plots for chronograms using lognormal (B), uniform (C), and log crown priors (D). Gray bars are 95% HPD intervals on the age of each node.

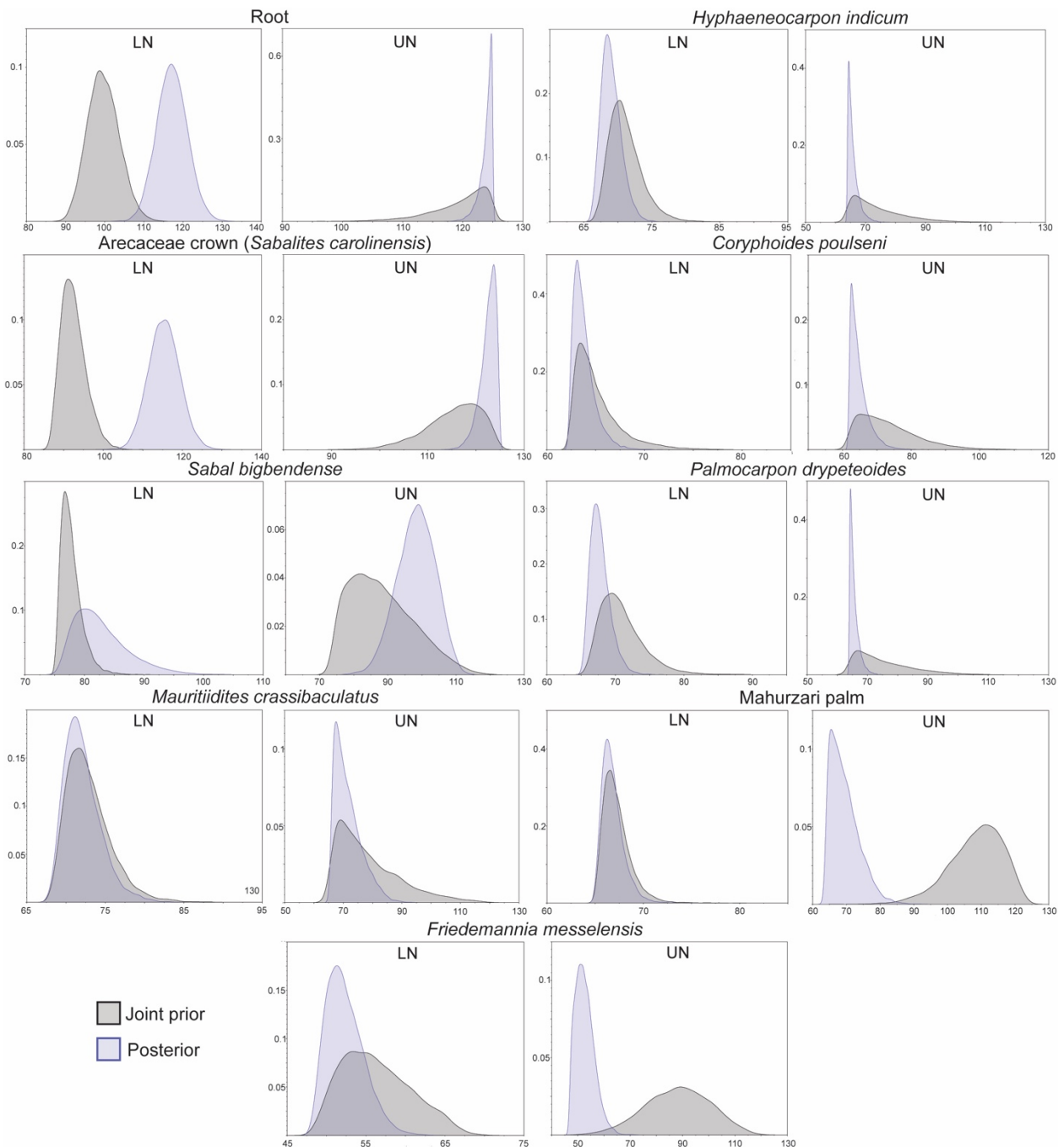


Figure 4.3 Diptych plots comparing distributions of joint priors and posteriors for each calibrated node in the tree. Time, in millions of years before present, is on the X axis and probability density is on the Y axis.

Discussion

Age estimates for Arecaceae

These results provide new insights into the evolutionary history of palms based on recent discoveries and syntheses of the fossil record. Node-dating analyses estimate the origin of Arecaceae and divergence of the subfamilies during the Aptian through the Cenomanian. Early diversification within subfamilies occurred during the Late Cretaceous, generating the stem lineages of most tribes. Several tribes appear to have crown origins before the end of the Cretaceous, but most show crown diversification in the Paleogene, establishing the stem lineages of modern genera primarily during the Eocene and Oligocene (Fig. 4.1, Table 4.1). Importantly, these conclusions appear robust to prior choice on node calibrations. Deep nodes are the most sensitive to these changes, and while differences in age estimates are small overall, some nodes have mean ages that differ by as much as 10 million years (e.g., stem node Trachycarpeae and Sabaleae).

When comparing prior and posterior distributions, I found that for some nodes the posterior distribution remained close to the minimum age bounds, despite having specified broader priors. This could imply that calibration nodes have been mis-specified; that is, the fossils in reality belong to another group and therefore should calibrate a different or deeper node in the tree (Brown & Smith, 2018). However, this is unlikely to be the case, since the placement of the fossils within clades was based on well-supported phylogenetic relationships, apomorphy criteria, and in most cases both. Moreover, many of the fossils were conservatively used as calibrations for deeper nodes than indicated by phylogenetic analyses. Instead, this behavior could be related to the low rates of molecular evolution in palms (Barrett *et al.*, 2016), which might preclude recovery of fossil ages without extensive calibration, at least using currently

available models. Without calibrations within the Arecaceae crown, age estimates are dramatically younger throughout the family, often by tens of millions of years (Fig. 4.2). The use of fewer and younger calibration fossils in other studies (e.g. Couvreur *et al.*, 2011; Baker & Couvreur, 2013a,b) probably also explains the much older ages estimated here. The difference in ages obtain in this versus previous studies highlights the need for reliable calibrations for recovering accurate age estimates in palms. Commonly used clock models appear unable to estimate ages close to those implied by fossils, in the absence of extensive calibration relying on the fossil record.

An interesting feature of the chronograms and LTT plots is the relatively few cladogenic events during the Paleocene. In the LTT plots, this manifests as a bump or a change in slope, around the K-Pg boundary (Fig. 4.2). This is possibly an artifact of the sampling of calibration fossils, most of which have ages near the K-Pg boundary, and thus adding more calibration fossils from the Paleogene could reduce this effect. Additionally, node ages are better interpreted as age distributions rather than point estimates, and so inferences based strictly on mean ages should be treated cautiously. However, it is still an intriguing pattern and if further testing indicates that it is a biological feature and not an artifact, then it has interesting implications for understanding how global changes at the K-Pg boundary affected palms. Impact winter and wildfires (Vellekoop *et al.*, 2014; Kaiho *et al.*, 2016) should at least have had transient effects on palms, since temperature seems to be a dominant driver of richness patterns and distributions in the modern day (Eiserhardt *et al.*, 2011; Rakotoarinivo *et al.*, 2013; Reichgelt *et al.*, 2018). If palms were significantly impacted by changes across the K-Pg boundary, it might explain my finding that most tribes have crown group origins during the Cenozoic.

Palm evolution during the Late Cretaceous and Cenozoic

Evidence from fossil fruits and node dating analyses together reveal that palms underwent an extensive taxonomic diversification during the Late Cretaceous that coincided with their initial geographic expansion. This Cretaceous phase was followed by diversification of tribes and origins of modern genera during the Paleogene, primarily in the Eocene and Oligocene. Age estimates from this study are older overall than those of previous analyses, which recovered crown origins of subfamilies around the Cretaceous–Paleogene boundary, diversification of tribes during the late Eocene through the Miocene, and increases in speciation rate among several groups starting around the early Oligocene (Baker *et al.*, 2011; Baker & Couvreur, 2013a,b). However, the timeline proposed here based on new fossil data makes more sense considering Cretaceous and Cenozoic climate and the ecological constraints of modern palms, approximately 90% of which are tropical rainforest species (Couvreur *et al.*, 2011).

The Late Cretaceous and much of the Paleogene was characterized by warm, wet (particularly Paleogene), and equable climatic conditions punctuated by intervals of warming during the late Paleocene and early Eocene (Zachos *et al.*, 2001). During this time palms greatly expanded their geographic range, extending into high-latitude regions of the northern and southern hemispheres (Eldrett *et al.*, 2009; Morley, 2011; Pross *et al.*, 2012; Reichgelt *et al.*, 2018). By contrast, Oligocene and Miocene climate are characterized by cooling and drying, expansion of polar ice sheets, and proliferation of grassland ecosystems (Zachos *et al.*, 2001; Morley, 2011; Strömborg, 2011). Megathermal forests retracted to lower latitudes in response to cooling climates across the Eocene-Oligocene transition (Morley, 2011).

My results suggest that the major cladogenic events generating much of the tribal and generic diversity in palms occurred in warmer climatic intervals, with tribal diversification

broadly coeval with wetter climates and the expansion of megathermal forests during the Paleocene and Eocene (Wolfe & Upchurch, 1987; Morley, 2000; Burnham & Johnson, 2004; Ellis & Johnson, 2013). Warming during the middle Miocene and geologic activity in South America and the Indo-Pacific region, causing mountain building and island formation, likely provided subsequent opportunities for range shifts and diversification in the Neogene, during which time many species-rich genera were radiating (Morley, 2011; Baker & Couvreur, 2013a; Sanín *et al.*, 2016).

Interestingly, fossil stem anatomy indicates that vascular functional traits indicative of rainforest biomes, such as vascular bundles with a single large-diameter vessel, do not appear in palms until the Cenozoic (Thomas & Boura, 2015). Cretaceous palms are characterized by dry-climate anatomy, consisting of multiple narrow-diameter vessels per vascular bundle, which was likely the ancestral condition (Thomas & Boura, 2015). This provides additional evidence that angiosperm-dominated megathermal rainforests did not gain a roothold until the Paleogene. In the context of my results, it also suggests that palms underwent their initial diversification in drier climates than those most species currently occupy, and refutes evidence from ancestral range reconstructions that the earliest palms were restricted to rainforest biomes (Couvreur *et al.*, 2011).

Diversification of Areceae: implications for understanding a rapid evolutionary radiation

Diversification analyses indicated a shift towards higher rates net diversification associated with tribe Areceae, which appear to be driven by higher speciation rates. This rate shift appears robust to taxon sampling, method, and age estimates, and has moreover been detected in previous studies (Baker & Couvreur, 2013a). Areceae are the largest palm tribe and

contains over 600 species in 61 genera distributed throughout the Indo-Pacific. The large number of species and problematic genus-level relationships are consistent with hypotheses of rapid radiations early in their evolutionary history (Hahn, 2002; Norup *et al.*, 2006). High diversification rates, driven by higher rates of speciation, could also be linked to their large geographic range spanning Pemba Island near East Africa all the way to Samoa, facilitated by relatively small fruit size and capacity for long distance dispersal (Baker & Couvreur, 2013a,b). My survey of fruit structure revealed that most members of Areceae have a thin but prominent endocarp with germination opercula (Chapter 3), which may facilitate ingestion and subsequent dispersal by frugivores and increase dispersal distance. Small fruit size, as seen in Areceae, is correlated with high speciation rates in palms, particularly among Old World species on small islands, and this pattern is moreover driven primarily by Southeast Asian palms (Onstein *et al.*, 2017). The combination of small fruit size and thin operculate endocarps may increase the chances of surviving rare (low probability) long-distance dispersal events, such as to distant oceanic islands. Such dispersal events could isolate successful colonizers from source populations and restrict gene flow, due to geographic distance and the low probability of successful dispersal events, increasing the probability of allopatric speciation. It therefore seems biologically plausible that a shift towards higher net diversification in Areceae was driven by higher speciation rates (rather than lower extinction rates) as the tribe spread throughout the Indo-Pacific, facilitated by the high dispersibility of fruits.

Node-dating analyses from this study indicate the crown group of Areceae originated around 52.5 Ma (59.3–47.6 Ma) and diversified during the Eocene through middle Miocene (Fig. 4.1, Table 4.1). Their origin and diversification thus coincide with evolutionary radiations of important avian dispersers, and geologic changes in the Indo-Australian archipelago. Large-

bodied avian frugivores are important dispersers of palm fruits (Zona & Henderson, 1989; Onstein *et al.*, 2017). Hornbills (Bucerotidae) and fruit pigeons (Columbidae) have relatively high species richness in the Indo-Pacific (Kissling, Böhning-Gaese, & Jetz, 2009). They are well documented dispersers of palm fruits, including those of Areceae (Zona & Henderson, 1989), and are capable of transporting fruits over long distances, including hundreds of kilometers over land and between islands (Steadman, 1997; Holbrook, Smith, & Hardesty, 2002; Bucher & Bocco, 2009; Onstein *et al.*, 2017). Pigeons in particular have colonized islands throughout the Pacific and are considered important seed dispersers within and between islands (Steadman, 1997). Bucerotidae are thought to have originated during the Eocene and are hypothesized as important dispersal agents of plant lineages between India and Southeast Asia during this time, as India approached and collided with Eurasia (Viseshakul *et al.*, 2011). Age estimates for Columbidae suggest they emerged during the Eocene, with diversification of the Indo-Pacific clade occurring later, around the Oligocene–Miocene transition (Soares *et al.*, 2016). Radiations within these lineages are therefore broadly coeval with the evolution and expansion of Areceae, particularly its Pacific clade. This indicates that at least some groups of important avian fruit dispersers may have been present in the Indo-Pacific when Areceae was radiating and could have contributed to the diversification of the tribe.

The Indo-Australian region was tectonically active during the Cenozoic. During the Eocene, the Indian subcontinent began its collision with Eurasia (Ali & Aitchison, 2008) and subduction of the Australian plate beneath Indonesia caused widespread volcanism, generating the Sunda island arc (Lohman *et al.*, 2011). This was followed by rotation of the Sunda region, the emergence of New Guinea, and mountain building throughout Borneo and Palawan during the Miocene (Lohman *et al.*, 2011). The dynamic geologic history of the Indo-Australian region

is linked with its high marine biodiversity and endemism (Renema *et al.*, 2008; Lohman *et al.*, 2011). More generally, landscape complexity and island colonization have demonstrated roles in promoting lineage diversification among both plants (including palms) and animals by creating more niche space and isolating populations (Parent & Crespi, 2006; Bentley, Verboom, & Bergh, 2014; Verboom *et al.*, 2015; Sanín *et al.*, 2016). It is therefore possible that the rapid radiation of Areceae, which is hypothesized to have occurred in Eurasia and the Indo-Pacific (Baker & Couvreur, 2013b), could have been facilitated by the dynamic Indo-Pacific landscape during the Cenozoic and contemporaneous diversification of avian dispersers. Several other species-rich genera (*Pinanga*, *Licuala*, and *Calamus*), also found throughout Indo-Australasia, suggest the region may have a more general role in evolutionary radiations in palms (Baker & Couvreur, 2013b).

Conclusions

I performed a series of node-dating and diversification analyses based on a new set of fossil calibrations informed by my study of the fossil record and phylogenetic relationships of fruit fossils. These analyses revealed palms underwent an extensive Late Cretaceous diversification that coincided with their initial geographic expansion, which was previously unknown from the fossil record or molecular dating analyses. A gap in lineage origination after the K-Pg boundary suggests possible impacts of the end-Cretaceous biodiversity crisis, which should be tested further. Tribe-level diversification within palms increased during the Paleogene as angiosperm-dominated megathermal forests were emerging and expanding in terrestrial environments. Finally, diversification-rate analyses indicate a shift towards higher speciation rates associated with the Indo-Pacific tribe Areceae, whose evolutionary radiation coincides with

those of important avian fruit dispersers and geologic activity in the Indo-Australian region. My results highlight the need for reliable calibration fossils and an important role of fruit fossils for estimating accurate ages of palm clades. Differences in age estimates between lognormal and uniform priors further indicate that prior choice can affect age estimates in palms by as much as 10 million years, particularly at deep nodes. More generally, these results provide new insights into the biotic, climatic, and geologic context of palm evolution and a temporal framework for future macroevolutionary studies.

References

- Alfaro ME, Santini F, Brock C, et al.** 2009. Nine exceptional radiations plus high turnover explain species diversity in jawed vertebrates. *Proceedings of the National Academy of Sciences* **106**: 13410–13414.
- Ali JR & Aitchison JC.** 2008. Gondwana to Asia: Plate tectonics, paleogeography and the biological connectivity of the Indian sub-continent from the Middle Jurassic through latest Eocene (166–35 Ma). *Earth-Science Reviews* **88**: 145–166.
- Ancibor E.** 1995. Palmeras fosiles del Cretacico Tardio de la Patagonia Argentina (Bajo de Santa Rosa, Rio Negro). *Ameghiniana* **32**: 287–299.
- Baker WJ & Couvreur TLP.** 2013a. Global biogeography and diversification of palms sheds light on the evolution of tropical lineages. II. Diversification history and origin of regional assemblages. *Journal of Biogeography* **40**: 286–298.
- Baker WJ & Couvreur TLP.** 2013b. Global biogeography and diversification of palms sheds light on the evolution of tropical lineages. I. Historical biogeography. *Journal of Biogeography* **40**: 274–285.
- Baker WJ & Dransfield J.** 2016. Beyond Genera Palmarum: progress and prospects in palm systematics. *Botanical Journal of the Linnean Society* **182**: 207–233.
- Baker WJ, Norup M V, Clarkson JJ, et al.** 2011. Phylogenetic relationships among arecoid palms (Arecaceae : Arecoideae) . : 1417–1432.
- Barrett CF, Baker WJ, Comer JR, et al.** 2016. Plastid genomes reveal support for deep phylogenetic relationships and extensive rate variation among palms and other commelinid monocots. *New Phytologist* **209**: 855–870.
- Befus KS, Hanson RE, Lehman TM, et al.** 2008. Cretaceous basaltic phreatomagmatic volcanism in West Texas: Maar complex at Peña Mountain, Big Bend National Park. *Journal of Volcanology and Geothermal Research* **173**: 245–264.
- Bentley J, Verboom GA & Bergh NG.** 2014. Erosive processes after tectonic uplift stimulate vicariant and adaptive speciation: Evolution in an Afrotropical-endemic paper daisy genus. *BMC Evolutionary Biology* **14**: 1–16.
- Berry EW.** 1905. A palm from the mid-Cretaceous. *Torreya* **5**: 30–33.
- Berry EW.** 1914. The Upper Cretaceous and Eocene floras of South Carolina and Georgia. *US Geological Survey, Professional Paper* **84**: 1–200.
- Berry EW.** 1916. A petrified palm from the Cretaceous of New Jersey. *American Journal of Science* **41**: 193–197.
- Bonde SD.** 2008. Indian fossil monocotyledons; current status, recent developments and future

- directions. *The Palaeobotanist* **57**: 141–164.
- Bouckaert R, Heled J, Kühnert D, et al.** 2014. BEAST 2: A Software Platform for Bayesian Evolutionary Analysis. *PLoS Computational Biology* **10**: 1–6.
- Brown JW & Smith SA.** 2018. The Past Sure is Tense: On Interpreting Phylogenetic Divergence Time Estimates. *Systematic Biology* **67**: 340–353.
- Bucher EH & Bocco PJ.** 2009. Reassessing the importance of granivorous pigeons as massive, long-distance seed dispersers. *Ecology* **90**: 2321–2327.
- Burnham RJ & Johnson KR.** 2004. South American palaeobotany and the origins of neotropical rainforests. *Philosophical Transactions of the Royal Society B: Biological Sciences* **359**: 1595–1610.
- Cevallos-Ferriz SRS & Ricalde-Moreno OS.** 1995. Palmeras fosiles del norte de mexico. *Anales Inst. Biol. Univ. Nac. Auton. Mexico* **66**: 37–106.
- Christopher RA.** 1979. Normapolles and triporate pollen assemblages from the Raritan and Magothy Formations (Upper Cretaceous) of New Jersey. *Palynology* **3**: 73–121.
- Collinson ME, Manchester SR & Wilde V.** 2012. Fossil fruits and seeds of the Middle Eocene Messel biota, Germany. *Abh. Senckenberg Ges. Naturforsch.* **570**: 1–251.
- Couvreur T, Forest F & Baker WJ.** 2011. Origin and global diversification patterns of tropical rain forests: inferences from a complete genus-level phylogeny of palms. *BMC Biology* **9**: 44.
- Crié L.** 1892. Recherches sur les Palmiers silicifiés des terrains Crétacés de l’Anjou. *Bulletin de la Société d’Études Sci-entifiques d’Angers* **21**: 97–103.
- Delevoryas T.** 1964. Two Petrified Angiosperms from the Upper Cretaceous of South Dakota. *Journal of Paleontology* **38**: 584–586.
- Doyle JA & Hickey LJ.** 1976. Pollen and leaves from the mid-Cretaceous Potomac Group and their bearing on early angiosperm evolution. In: Beck CB, ed. *Origin and early evolution of angiosperms*. New York: Columbia University Press, 139–206.
- Dransfield J, Uhl NW, Asmussen CB, et al.** 2008. *Genera Palmarum: the evolution and classification of palms*. Richmond, Surrey, UK: Kew Publishing.
- Drummond AJ & Suchard MA.** 2010. Bayesian random local clocks, or one rate to rule them all. *BMC Biology* **8**: 114.
- Eiserhardt WL, Svenning JC, Kissling WD, et al.** 2011. Geographical ecology of the palms (Arecaceae): Determinants of diversity and distributions across spatial scales. *Annals of Botany* **108**: 1391–1416.
- El-Soughier MI, Mehrotra RC, Zhou ZY, et al.** 2011. *Nypa* fruits and seeds from the

Maastrichtian-Danian sediments of Bir Abu Minqar, South Western Desert, Egypt. *Palaeoworld* **20**: 75–83.

Eldrett JS, Greenwood DR, Harding IC, et al. 2009. Increased seasonality through the Eocene to Oligocene transition in northern high latitudes. *Nature* **459**: 969–973.

Ellis B & Johnson KR. 2013. Comparison of Leaf Samples From Mapped Tropical and Temperate Forests: Implications for Interpretations of the Diversity of Fossil Assemblages. *Palaios* **28**: 163–177.

Estrada-Ruiz E, Upchurch GR, Wheeler EA, et al. 2012. Late Cretaceous Angiosperm Woods from the Crevasse Canyon and McRae Formations, South-Central New Mexico, USA: Part 1. *International Journal of Plant Sciences* **173**: 412–428.

Faurby S, Eiserhardt WL, Baker WJ, et al. 2016. Molecular Phylogenetics and Evolution An all-evidence species-level supertree for the palms (Arecaceae). *100*: 57–69.

Franzen JL. 2005. The implications of the numerical dating of the Messel fossil deposit (Eocene, Germany) for mammalian biochronology. *Annales de Paleontologie* **91**: 329–335.

Gee CT. 2001. The mangrove palm *Nypa* in the geologic past of the new world. *Wetlands Ecology and Management* **9**: 181–194.

Givnish TJ, Zuluaga A, Spalink D, et al. 2018. Monocot plastid phylogenomics, timeline, net rates of species diversification, the power of multi-gene analyses, and a functional model for the origin of monocots. *American Journal of Botany* **105**: 1888–1910.

Gohn GS, Dowsett HJ & Sohl NF. 1992. Biostratigraphy of the Middendorf Formation (Upper Cretaceous) in a Corehole at Myrtle Beach, South Carolina. *U.S. Geological Survey Bulletin* **2030**: 1–12.

Greenwood DR & West CK. 2017. A fossil coryphoid palm from the Paleocene of western Canada. *Review of Palaeobotany and Palynology* **239**: 55–65.

Grímsson F, Pedersen GK, Grimm GW, et al. 2016. A revised stratigraphy for the Palaeocene Agatdalen flora (Nuussuaq Peninsula, western Greenland): correlating fossiliferous outcrops, macrofossils, and palynological samples from phosphoritic nodules. *56*: 307–327.

Hahn WJ. 2002. A phylogenetic analysis of the Arecoideae based on plastid DNA sequence data. *Molecular Phylogenetics and Evolution* **23**: 189–204.

Harley MM. 2006. A summary of fossil records for Arecaceae. *Botanical Journal of the Linnean Society* **151**: 39–67.

Ho SYW, Phillips MJ, Drummond AJ, et al. 2005. Accuracy of rate estimation using relaxed-clock models with a critical focus on the early metazoan radiation. *Molecular Biology and Evolution* **22**: 1355–1363.

- Holbrook KM, Smith TB & Hardesty B.** 2002. Implications of Long-Distance Movements of Frugivorous Rain Forest Hornbills. *Ecography* **25**: 745–749.
- Iles WJDD, Smith SY, Gandolfo MA, et al.** 2015. Monocot fossils suitable for molecular dating analyses. *Botanical Journal of the Linnean Society* **178**: 346–374.
- Jarzen DM.** 1978. Some Maestrichtian Palynomorphs and Their Phytogeographical and Paleoecological Implications. *American Association of Stratigraphic Palynologists* **2**: 29–38.
- Kaiho K, Oshima N, Adachi K, et al.** 2016. Global climate change driven by soot at the K-Pg boundary as the cause of the mass extinction. *Scientific Reports* **6**: 1–13.
- Katoh K & Standley DM.** 2013. MAFFT multiple sequence alignment software version 7: improvements in performance and usability. *Molecular biology and evolution* **30**: 772–80.
- Kissling WD, Böhning-Gaese K & Jetz W.** 2009. The global distribution of frugivory in birds. *Global Ecology and Biogeography* **18**: 150–162.
- Koch BE.** 1972. Coryphoid fruits and seeds from the Danian of Nûgssuaq, West Greenland. *The Geological Survey of Greenland* **99**: 1–37.
- Kvaček J & Herman AB.** 2004. Monocotyledons from the Early Campanian (Cretaceous) of Grünbach, Lower Austria. *Review of Palaeobotany and Palynology* **128**: 323–353.
- Lanfear R, Frandsen PB, Wright AM, et al.** 2017. Partitionfinder 2: New methods for selecting partitioned models of evolution for molecular and morphological phylogenetic analyses. *Molecular Biology and Evolution* **34**: 772–773.
- Lohman DJ, de Bruyn M, Page T, et al.** 2011. Biogeography of the Indo-Australian Archipelago. *Annual Review of Ecology, Evolution, and Systematics* **42**: 205–226.
- Löytynoja A & Goldman N.** 2008. Phylogeny-aware gap placement prevents errors in sequence alignment and evolutionary analysis. *Science* **320**: 1632–1635.
- Manchester SR, Bonde SD, Nipunage DS, et al.** 2016. Trilocular Palm Fruits from the Deccan Intertrappean Beds of India. *International Journal of Plant Sciences* **177**: 633–641.
- Manchester SR, Lehman TM & Wheeler EA.** 2010. Fossil Palms (Arecaceae, Coryphoideae) Associated with Juvenile Herbivorous Dinosaurs in the Upper Cretaceous Aguja Formation, Big Bend National Park, Texas. *International Journal of Plant Sciences* **171**: 679–689.
- Matsunaga KKS, Manchester SR, Srivastava R, et al.** 2019. Fossil palm fruits from India indicate a Cretaceous origin of Arecaceae tribe Borasseae. *Botanical Journal of the Linnean Society* **190**: 260–280.
- May MR & Moore BR.** 2016. How Well Can We Detect Lineage-Specific Diversification-Rate Shifts? A Simulation Study of Sequential AIC Methods. *Systematic Biology* **65**: 1076–1084.

Meyer ALS, Román-Palacios C & Wiens JJ. 2018. BAMM gives misleading rate estimates in simulated and empirical datasets. *Evolution* **72**: 2257–2266.

Miller MA, Pfeiffer W & Schwartz T. 2010. Creating the CIPRES Science Gateway for inference of large phylogenetic trees. In: *2010 Gateway Computing Environments Workshop, GCE 2010.*, 7.

Moore BR, Höhna S, May MR, et al. 2016. Critically evaluating the theory and performance of Bayesian analysis of macroevolutionary mixtures. *Proceedings of the National Academy of Sciences* **113**: 9569–9574.

Morley RJ. 2000. *Origin and evolution of tropical rainforests*. Wiley.

Morley RJ. 2011. Cretaceous and Tertiary climate change and the past distribution of megathermal rainforests. *Tropical Rainforest Responses to Climatic Change*: 1–34.

Norup MV, Dransfield J, Chase MW, et al. 2006. Homoplasious character combinations and generic delimitation: A case study from the Indo-Pacific arecoid palms (Arecaceae: Areceae). *American Journal of Botany* **93**: 1065–1080.

Onstein RE, Baker WJ, Couvreur TLP, et al. 2017. Frugivory-related traits promote speciation of tropical palms. *Nature Ecology and Evolution* **1**: 1903–1911.

Ottone EG. 2007. A new palm trunk from the Upper Cretaceous of Argentina. *Ameghiniana* **44**: 719–725.

Ôyama T & Matsuo H. 1964. Notes on palmaean leaf from the Ôarai Flora (Upper Cretaceous), Ôarai Machi, Ibaraki Prefecture, Japan. *Transactions and Proceedings of the Paleontological Society of Japan* **55**: 241–246.

Pan AD, Pan AD, Jacobs BF, et al. 2006. The fossil history of palms (Arecaceae) in Africa and new records from the Late Oligocene (28–27 Mya) of north-western Ethiopia. *Botanical Journal of the Linnean Society* **151**: 69–81.

Paradis E. 2013. Molecular dating of phylogenies by likelihood methods: A comparison of models and a new information criterion. *Molecular Phylogenetics and Evolution* **67**: 436–444.

Paradis E, Claude J & Strimmer K. 2004. APE: Analyses of phylogenetics and evolution in R language. *Bioinformatics* **20**: 289–290.

Parent CE & Crespi BJ. 2006. Sequential Colonization and Diversification of Galápagos Endemic Land Snail Genus *Bulimulus* (Gastropoda, Stylommatophora). *Evolution* **60**: 2311.

Pross J, Contreras L, Bijl PK, et al. 2012. Persistent near-tropical warmth on the Antarctic continent during the early Eocene epoch. *Nature* **488**: 73–7.

Rabosky DL. 2014. Automatic detection of key innovations, rate shifts, and diversity-dependence on phylogenetic trees. *PLoS ONE* **9**.

- Rabosky DL, Mitchell JS & Chang J.** 2017. Is BAMM Flawed? Theoretical and Practical Concerns in the Analysis of Multi-Rate Diversification Models. *Systematic Biology* **66**: 477–498.
- Rakotoarinivo M, Blach-Overgaard A, Baker WJ, et al.** 2013. Palaeo-precipitation is a major determinant of palm species richness patterns across Madagascar: a tropical biodiversity hotspot. *Proceedings. Biological sciences / The Royal Society* **280**: 20123048.
- Rambaut A, Drummond AJ, Xie D, et al.** 2018. Posterior Summarization in Bayesian Phylogenetics Using Tracer 1.7. *Systematic biology* **67**: 901–904.
- Rannala B.** 2016. Conceptual issues in Bayesian divergence time estimation. *Philosophical Transactions of the Royal Society B: Biological Sciences* **371**: 20150134.
- Reichgelt T, West CK & Greenwood DR.** 2018. The relation between global palm distribution and climate. *Scientific Reports* **8**: 2–12.
- Renema W, Bellwood DR, Braga JC, et al.** 2008. Hopping Hotspots: Global Shifts in Marine Biodiversity. *Science* **321**: 654–657.
- Sanín MJ, Kissling WD, Bacon CD, et al.** 2016. The Neogene rise of the tropical Andes facilitated diversification of wax palms (Ceroxylon: Arecaceae) through geographical colonization and climatic niche separation. *Botanical Journal of the Linnean Society*: 303–317.
- Schrank E.** 1994. Palynology of the Yesomma Formation in Northern Somalia: a study of pollen, spores and associated phytoplankton from the Late Cretaceous Palmae Province. *Palaeontographica Abteilung B* **231**: 63–112.
- Shi JJ & Rabosky DL.** 2015. Speciation dynamics during the global radiation of extant bats. *Evolution* **69**: 1528–1545.
- Soares AER, Novak BJ, Haile J, et al.** 2016. Complete mitochondrial genomes of living and extinct pigeons revise the timing of the columbiform radiation. *BMC Evolutionary Biology* **16**: 1–9.
- Stamatakis A.** 2014. RAxML version 8: A tool for phylogenetic analysis and post-analysis of large phylogenies. *Bioinformatics* **30**: 1312–1313.
- Steadman DW.** 1997. The Historic Biogeography and Community Ecology of Polynesian Pigeons and Doves. *Journal of Biogeography* **24**: 737–753.
- Strömberg C a. E.** 2011. Evolution of Grasses and Grassland Ecosystems. *Annual Review of Earth and Planetary Sciences* **39**: 517–544.
- Thomas R & Boura A.** 2015. Palm stem anatomy: phylogenetic or climatic signal? *Botanical Journal of the Linnean Society* **178**: 467–488.
- Tomlinson PB.** 1979. Systematics and Ecology of the Palmae. *Annual Review of Ecology and Systematics* **10**: 85–107.

Tomlinson PB. 2006. The uniqueness of palms. *Botanical Journal of the Linnean Society* **151**: 5–14.

Vaidya G, Lohman DJ & Meier R. 2011. SeqenceMatrix: Cladistics multi-gene datasets with character set and codon information. *Cladistics* **27**: 171–180.

Vellekoop J, Sluijs A, Smit J, et al. 2014. Rapid short-term cooling following the Chicxulub impact at the Cretaceous-Paleogene boundary. *Proceedings of the National Academy of Sciences of the United States of America* **111**: 1–5.

Verboom GA, Bergh NG, Haiden SA, et al. 2015. Topography as a driver of diversification in the Cape Floristic Region of South Africa. *New Phytologist* **207**: 368–376.

Viseshakul N, Charoennitikul W, Kitamura S, et al. 2011. A phylogeny of frugivorous hornbills linked to the evolution of Indian plants within Asian rainforests. *Journal of Evolutionary Biology* **24**: 1533–1545.

Warnock RCM, Parham JF, Joyce WG, et al. 2015. Calibration uncertainty in molecular dating analyses: there is no substitute for the prior evaluation of time priors. *Proceedings of the Royal Society B: Biological Sciences* **282**: 20141013.

Wolfe JA & Upchurch GR. 1987. North American nonmarine climates and vegetation during the Late Cretaceous. *Palaeogeography, Palaeoclimatology, Palaeoecology* **61**: 33–77.

Zachos J, Pagani M, Sloan L, et al. 2001. Trends, Global Rhythms, Aberrations in Global Climate 65Ma to Present. *Science* **292**: 686–693.

Zona S & Henderson A. 1989. A review of animal-mediated seed dispersal of palms. *Selbyana* **11**: 6–21.

CHAPTER 5

Conclusions

Summary

In this dissertation I used the fossil record of fruits and the morphology of extant palms to understand the evolution and early diversification of Arecaceae. My work provides new data and resources for paleontologists and evolutionary biologists investigating the evolutionary history of Arecaceae, including a database of µCT scans of palm fruits from nearly every extant genus. Moreover, the results offer new insights into the timing, environmental context, and potential drivers of palm diversification.

In chapter 2 I presented the morphology of new palm fruit fossils from the Deccan Intertrappean Beds and compared them with other previously described specimens. These comparisons demonstrated that the new fossils and several previously described species were all the same species, *Hyphaeneocarpon indicum*, found in multiple localities throughout central India (Matsunaga *et al.*, 2019). X-ray µCT scans revealed several new, informative features of *Hyphaeneocarpon* that enabled comparisons with extant palms. Morphological similarities suggested relationships with subtribe Hyphaeninae of tribe Borasseae. These relationships were confirmed by including the fossil in a total-evidence phylogenetic analysis of palms, using a previously published morphological dataset. The results of this study indicated a much earlier origin of tribe Borasseae than was previously thought and pushed back the age of the group nearly 40 million years. It also demonstrated that fruit characters can be phylogenetically

informative, and further raised intriguing questions about the evolutionary history of palms. Are other groups of palms much older than molecular dating analyses suggest? If other fossil fruits from India and elsewhere could be included in phylogenetic analyses, would they change our understanding of palm evolution? These are some of the questions I tried to answer in chapters 3 and 4.

Chapter 3 focused on filling a gap in our knowledge of palm fruit morphology, which hindered our ability to use the fossil record of fruits to reconstruct palm evolution. This gap reflects a more general and pervasive problem in plant biology: the morphology and anatomy of many plant groups have still not been studied in detail or in a comparative framework. Palms present additional challenges for anatomical work. Whole plants and individual organs are large, difficult to collect, and often extremely fibrous, which makes standard histological procedures inefficient or impossible. Palms are also morphologically diverse and species rich, and thus comparative work at the level necessary for understanding systematic relationships of fossils requires time-consuming study of hundreds of specimens. However, the characteristics that make palms difficult to study using standard histological techniques, including large size and fibrous tissues, make them ideal for study with X-ray μ CT. Chapter 3 synthesized a large-scale μ CT survey of palm fruits to understand the diversity and distributions of morpho-anatomical characters across the family. I scanned at least one species of most palm genera, resulting in μ CT datasets for over 200 palm species. Using these scans, I developed a morphological matrix of fruit characters for phylogenetic analyses of fossils. To test the utility of fruit characters for understanding evolutionary relationships of fossils, I selected six fossil fruits and performed a series of phylogenetic analyses using both morphological and molecular data. These analyses recovered well-supported relationships for the fossils, many of which could be placed within

crown groups of major palm clades such as tribes and subtribes. This study not only demonstrated the systematic value of fruit characters in palm but also provided five new reliable calibration fossils for palms.

The age of the fruit fossils investigated in chapter 3, combined with their phylogenetic relationships, suggested the groups to which the fossils belong diverged earlier than was previously thought. However, without performing dating analyses it is difficult to predict the influence of the fossils on age estimates throughout the tree. This was the focus of chapter 4. Synthesizing and building on data from the previous two chapters, I performed a series of node-dating and diversification analyses using several different methods to visualize the diversification process and test for rate shifts. The dating analyses confirmed some of my predictions of older ages and revealed additional patterns. They estimated an origin of the Arecaceae crown group near the end of the Early Cretaceous and diversification in the Late Cretaceous, generating the crown groups of all subfamilies and stem lineages of modern tribes. The initial radiation of palms thus coincided with their geographic expansion during the Late Cretaceous into North and South America, Africa, India, and Eurasia. Origin and diversification of most modern tribes began during the warm, wet intervals of late Paleocene and Eocene and continued into the Oligocene through early Miocene. Diversification-rate analyses consistently recovered a shift in net diversification rate associated with the Indo-Pacific tribe Areceae, which is the largest palm tribe and often thought to represent a rapid radiation. Age estimates for Areceae, indicating diversification during the Eocene through Miocene, coincide broadly with radiations of avian fruit dispersers and geologic activity throughout the Indo-Pacific. Both factors may have had a role in generating the extraordinary diversity in the tribe, possibly by

promoting higher rates of speciation through long distance dispersal resulting in reproductively isolated populations, and stimulate questions for future study.

The work presented in this dissertation is an important contribution to our understanding of the evolutionary history of palms because it changes our view of the timing of their diversification and adds to our knowledge of extinct palm diversity. This is relevant to our more general knowledge of evolutionary tempo in monocots during the rise of flowering plants. Additionally, time-calibrated phylogenetic trees are required in numerous macroevolutionary methods, and this work thus provides a foundation for any future studies on palms that include a temporal component. It also contributes morphological data and resources essential for identifying new fossils. Insights from this work are moreover applicable beyond palm biology, from understanding evolutionary radiations during the Cretaceous to informing paleoenvironmental and climate reconstructions. It also raises numerous other questions, which I explore here. How can we better incorporate the rich fossil record of palms into dating analyses? What are the patterns of phenotypic evolution in palms? How has climate and environmental change over the Late Cretaceous and Cenozoic affected palm distributions and diversity? What do palms tell us about the origins of modern tropical rainforest ecosystems?

How can we better integrate the fossil record?

My work demonstrates that fossils are important for obtaining accurate age estimates, particularly within palms. I used eight calibration fossils in my analyses, but hundreds of other palm fossils have been documented or described (Chapter 1). These fossils represent a wealth of untapped data that can refine estimates of clade age and evolutionary tempo. The addition of more fossils data would help clarify some of the questions raised by my results, such as whether

palm diversity was affected by environmental changes at the K-Pg boundary, and potentially reduce age uncertainty in some groups. Many other fossils can be included in phylogenetic analyses, particularly if comparative work is done to expand existing morphological datasets to include characters of stems. Stems are very common throughout the palm fossil record and most are assigned to the form genus *Palmoxylon*. Palm stem anatomy is well documented in many groups (Tomlinson, Horn, & Fisher, 2011; Thomas & De Franceschi, 2013), and is systematically informative in some clades (Thomas & De Franceschi, 2012; Nour-El-Deen, Thomas, & El-Saadawi, 2017). Other sources of character data that should be explored are continuous (quantitative) characters, which can be highly informative and eliminate some of the subjectivity and replicability issues that plague discrete character datasets (Parins-Fukuchi, 2018).

Alternatively, other methods allow integration of DNA sequences, morphological data, and fossils in dating analyses, called “tip-dating” or “total-evidence dating” (Pyron, 2011; Ronquist *et al.*, 2012). In such analyses, fossils are included as tips and their phylogenetic positions are simultaneously inferred and used to date the tree. One of the advantages of total-evidence dating over node-dating is that it allows for inclusion of numerous fossils, not just the oldest representatives, and accommodates uncertainty in phylogenetic position when estimating ages. However, total-evidence dating requires that fossils are scored in morphological matrices. Many fossils contain apomorphies that unite them with clades but lack enough characters for placement in a phylogenetic framework. Node dating using the Fossilized Birth-Death (FBD) process provides an alternative to total-evidence and node dating by accommodating many fossils without requiring morphological data (Heath, Huelsenbeck, & Stadler, 2014). The two types of analyses, total-evidence dating and FBD, have now been integrated to accommodate

fossils with and without scorable morphological characters (Gavryushkina *et al.*, 2017).

Considering the apparent shortcomings in DNA sequence data alone for estimating ages for palms, FBD and total-evidence dating seem particularly promising for refining age estimates and incorporating fossil data. Neither type of analysis has so far been attempted, and thus represents a frontier in palm (and, more broadly, plant) biology.

Morphological evolution through time

This dissertation provides estimates of the timing of cladogenic events in palms, but broad patterns in palm macroevolution are not known, particularly with respect to phenotypic evolution and adaptive radiations. Were rates of phenotypic evolution high early on in their evolutionary history, possibly allowing palms to enter new environments, or did morphological diversity increase incrementally through time? Are evolutionary rates similar across all organs (e.g., leaves vs. fruits) or do some evolve more rapidly than others? Such macroevolutionary regimes have been observed in other organisms (e.g., Sallan & Friedman, 2012; Close *et al.*, 2015), but their prevalence among plants and their underlying causes are not well understood. Patterns of phenotypic evolution can be explored and tested using analyses that estimate rates of morphological evolution (Brusatte *et al.*, 2014; Lloyd, 2016; Wang *et al.*, 2016) or changes in disparity (morphological diversity) through time along a phylogeny (Guillerme & Cooper, 2018). Evidence from modern palms indicates that major phenotypic changes can occur on short time scales; rapid decreases in fruit size have been observed in response to local megafaunal extinctions in as little as ~100 years (Galetti *et al.*, 2013). Moreover, small fruit size appears to promote higher speciation rates throughout Arecaceae, through restricted gene flow between populations, which increases the probability of allopatric speciation (Onstein *et al.*, 2017).

Among Old World palms, low gene flow is probably caused by the establishment of isolated populations throughout island systems, facilitated by avian seed dispersers. In contrast, among Neotropical palms higher speciation rates are likely related to understory habit, caused by low gene flow among populations with small-bodied vertebrate dispersers with short dispersal distances (Onstein *et al.*, 2017). The impacts of extrinsic changes (e.g., extinctions) on palm morphology could, therefore, potentially affect diversity on macroevolutionary time scales.

Environmental change and the origins of tropical rainforest ecosystems

Palms have physiological constraints on their geographic distributions and are therefore an ideal group for investigating the interplay between climate and macroevolutionary patterns through time. Within a phylogenetic framework, insights into the diversification process outlined above can be examined in the context of environmental changes. Additionally, quantitative inferences of responses to local and global changes can be made using comprehensive datasets of fossil occurrences, documenting their presence in localities throughout the world. Dispersal rates for species between regions, as well as local extinctions, can be calculated to quantify range shifts through time, and also correlated with climatic variables to understand underlying causes (Silvestro *et al.*, 2016). These empirical approaches can be paired with more theoretical ones. Paleoecological niche modeling (Myers, Stigall, & Lieberman, 2015), for example, can reveal changes in available environmental niche space through time, providing insights into how global or regional climatic changes might have influenced geographic range and diversity (Chiarenza *et al.*, 2019).

Approximately 90% of extant palm species are restricted to tropical rainforest ecosystems, making palms an important system for understanding the origins of modern tropical rainforests (Couvreur, Forest, & Baker, 2011). Many functional traits in plants can serve as

proxies for environmental conditions, such as leaf morphology (aridity, temperature) and stomatal density (CO_2 ; Wolfe, 1993; McElwain & Chaloner, 1995; Wilf *et al.*, 1998; Royer, 2001; Hoganson *et al.*, 2011; Teodoridis *et al.*, 2011). Among palms, vessel size and number within vascular bundles are correlated with growth in wet (i.e. tropical rainforest [TRF]) versus dry (non-TRF) climates (Thomas & Boura, 2015). These traits are easily observed in fossil palm stems, and thus a broader survey of *Palmoxylon* anatomy could shed light on the distributions of rainforest ecosystems during the Cenozoic. Moreover, *Palmoxylon* records indicate that TRF traits appear in palms during the late Paleocene and Eocene (Thomas & Boura, 2015), around the same time that other lines of evidence from the paleobotanical record indicate an expansion of angiosperm-dominated megathermal rainforests (Greenwood, 1996; Morley, 2000, 2011; Burnham & Johnson, 2004; Herrera *et al.*, 2008; West, Greenwood, & Basinger, 2015). This also coincides with extensive diversification within modern palm tribes, and possibly a shift towards higher diversification rates in Areceae (Chapter 4). This raises questions on the impact of emerging tropical rainforest ecosystems on macroevolutionary patterns in palms. Did the origin and expansion of megathermal rainforest environments during the Eocene promote diversification in palms? One way this could be tested is using trait-dependent diversification models that investigate correlations between TRF traits and speciation rates. This is an intriguing subject for future studies, with broad relevance to plant macroevolution.

Conclusions

The work presented in this dissertation is an important step forward in understanding the fossil record and evolutionary history of palms and provides resources for future progress. The discussions above, outlining exciting avenues of future research, help illustrate the broader

relevance of studying palm evolution. Palms have an extensive fossil record, well understood climatic and ecological constraints, and broad geographic distributions through time. This makes them exceptionally well suited for elucidating biotic responses to mass extinctions, drivers of organismal diversity and distributions through time, floral response to climatic and environmental change, and the origins of tropical ecosystems, which are centers of biodiversity today. Such topics are the focus of research programs throughout biology and the Earth sciences. Future work in these directions will thus provide insights into not only the evolution of a diverse and highly charismatic plant lineage, but also fundamental aspects of the history of life.

References

- Brusatte SL, Lloyd GT, Wang SC, et al.** 2014. Gradual assembly of avian body plan culminated in rapid rates of evolution across the dinosaur-bird transition. *Current Biology* **24**: 2386–2392.
- Burnham RJ & Johnson KR.** 2004. South American palaeobotany and the origins of neotropical rainforests. *Philosophical Transactions of the Royal Society B: Biological Sciences* **359**: 1595–1610.
- Chiarenza AA, Mannion PD, Lunt DJ, et al.** 2019. Ecological niche modelling does not support climatically-driven dinosaur diversity decline before the Cretaceous/Paleogene mass extinction. *Nature Communications* **10**.
- Close RA, Friedman M, Lloyd GT, et al.** 2015. Evidence for a mid-Jurassic adaptive radiation in mammals. *Current Biology* **25**: 2137–2142.
- Couvreur T, Forest F & Baker WJ.** 2011. Origin and global diversification patterns of tropical rain forests: inferences from a complete genus-level phylogeny of palms. *BMC Biology* **9**: 44.
- Galetti M, Guevara R, Côrtes MC, et al.** 2013. Functional Extinction of Birds Drives Rapid Evolutionary Changes in Seed Size. *Science* **340**: 1086–1091.
- Gavryushkina A, Heath TA, Ksepka DT, et al.** 2017. Bayesian Total-Evidence Dating Reveals the Recent Crown Radiation of Penguins. *Systematic Biology* **66**: 1–17.
- Greenwood DR.** 1996. Eocene Monsoon Forests in Central Australia? *Australian Systematic Botany* **9**: 95–112.
- Guillerme T & Cooper N.** 2018. Time for a rethink: time sub-sampling methods in disparity-through-time analyses. *Palaeontology* **61**: 481–493.
- Heath T a, Huelsenbeck JP & Stadler T.** 2014. The fossilized birth–death process for coherent calibration of divergence-time estimates. *Proceedings of the National Academy of Sciences* **111**: E2957–E2966.
- Herrera FA, Jaramillo CA, Dilcher DL, et al.** 2008. Fossil Araceae from a Paleocene neotropical rainforest in Colombia. *American Journal of Botany* **95**: 1569–1583.
- Hoganson JW, Wing SL, Lusk CH, et al.** 2011. Sensitivity of leaf size and shape to climate: global patterns and paleoclimatic applications. *New Phytologist* **190**: 724–739.
- Lloyd GT.** 2016. Estimating morphological diversity and tempo with discrete character-taxon matrices: Implementation, challenges, progress, and future directions. *Biological Journal of the Linnean Society* **118**: 131–151.

Matsunaga KKS, Manchester SR, Srivastava R, et al. 2019. Fossil palm fruits from India indicate a Cretaceous origin of Arecaceae tribe Borasseae. *Botanical Journal of the Linnean Society* **190**: 260–280.

McElwain JC & Chaloner WG. 1995. Stomatal density and index of fossil plants track atmospheric carbon dioxide in the Palaeozoic. *Annals of Botany* **76**: 389–395.

Morley RJ. 2000. *Origin and evolution of tropical rainforests*. Wiley.

Morley RJ. 2011. Cretaceous and Tertiary climate change and the past distribution of megathermal rainforests. *Tropical Rainforest Responses to Climatic Change*: 1–34.

Myers CE, Stigall AL & Lieberman BS. 2015. PaleoENM: applying ecological niche modeling to the fossil record. *Paleobiology* **41**: 226–244.

Nour-El-Deen S, Thomas R & El-Saadawi W. 2017. First record of fossil Trachycarpeae in Africa: three new species of *Palmoxylon* from the Oligocene (Rupelian) Gebel Qatrani Formation, Fayum, Egypt. *Journal of Systematic Palaeontology* **16**: 741–766.

Onstein RE, Baker WJ, Couvreur TLP, et al. 2017. Frugivory-related traits promote speciation of tropical palms. *Nature Ecology and Evolution* **1**: 1903–1911.

Parins-Fukuchi C. 2018. Use of Continuous Traits Can Improve Morphological Phylogenetics. *Systematic Biology* **67**: 328–339.

Pyron RA. 2011. Divergence time estimation using fossils as terminal taxa and the origins of lissamphibia. *Systematic Biology* **60**: 466–481.

Ronquist F, Klopstein S, Vilhelmsen L, et al. 2012. A total-evidence approach to dating with fossils, applied to the early radiation of the hymenoptera. *Systematic Biology* **61**: 973–999.

Royer DL. 2001. Stomatal density and stomatal index as indicators of paleoatmospheric CO₂ concentration. *Review of Palaeobotany and Palynology* **114**: 1–28.

Sallan LC & Friedman M. 2012. Heads or tails: Staged diversification in vertebrate evolutionary radiations. *Proceedings of the Royal Society B: Biological Sciences* **279**: 2025–2032.

Silvestro D, Zizka A, Bacon CD, et al. 2016. Fossil biogeography: a new model to infer dispersal, extinction and sampling from palaeontological data. *Philosophical Transactions of the Royal Society B: Biological Sciences* **371**: 20150225.

Teodoridis V, Mazouch P, Spicer RA, et al. 2011. Refining CLAMP - Investigations towards improving the Climate Leaf Analysis Multivariate Program. *Palaeogeography, Palaeoclimatology, Palaeoecology* **299**: 39–48.

Thomas R & Boura A. 2015. Palm stem anatomy: phylogenetic or climatic signal? *Botanical Journal of the Linnean Society* **178**: 467–488.

Thomas R & De Franceschi D. 2012. First evidence of fossil Cryosophileae (Arecaceae) outside the Americas (early Oligocene and late Miocene of France): Anatomy, palaeobiogeography and evolutionary implications. *Review of Palaeobotany and Palynology* **171**: 27–39.

Thomas R & De Franceschi D. 2013. Palm stem anatomy and computer-aided identification: The Coryphoideae (Arecaceae). *American Journal of Botany* **100**: 289–313.

Tomlinson PB, Horn JW & Fisher JB. 2011. *The Anatomy of Palms: Arecaceae - Palmae*. OUP Oxford.

Wang M, Lloyd GT, Wang M, et al. 2016. Rates of morphological evolution are heterogeneous in Early Cretaceous birds Rates of morphological evolution are heterogeneous in Early Cretaceous birds. : 17–20.

West CK, Greenwood DR & Basinger JF. 2015. Was the Arctic Eocene ‘rainforest’ monsoonal? Estimates of seasonal precipitation from early Eocene megafloras from Ellesmere Island, Nunavut. *Earth and Planetary Science Letters* **427**: 18–30.

Wilf P, Wing SL, Greenwood DR, et al. 1998. Using fossil leaves as paleoprecipitation indicators: an Eocene example. *Geology* **26**: 203–206.

Wolfe JA. 1993. A method of obtaining climatic parameters from leaf assemblages. *US Geological Survey Bulletin* **2040**: 1–71.

APPENDIX A

GenBank accession numbers and taxon sampling from Chapter 2

18S

GenBank Accession	Genus	Species
NC_029973.1:c6020-4865	Acoelorraphe	wrightii
KT312939.1:c6074-4926	Arenga	caudata
JX088664.1:c6189-5073	Bismarckia	nobilis
NC_029969.1:c5968-4847	Borassodendron	machadonis
KP901247.1:c5965-4849	Borassus	flabellifer
AM116783.1	Brahea	berlandieri
JX088663.1:c5949-4804	Calamus	caryotoides
AJ242161.1	Calospatha	scortechinii
NC_029948.1:c5983-4869	Caryota	mitis
AJ242162.1	Ceratolobus	concolor
NC_029967.1:c6026-4891	Chamaerops	humilis
AJ240845.1	Chelyocarpus	ulei
NC_029966.1:c6109-4987	Chuniophoenix	nana
AJ240848.1	Coccothrinax	argentata
AM116784.1	Colpothrinax	wrightii
AM116785.1	Copernicia	prunifera
AJ240858.1	Corypha	umbraculifera
AJ240846.1	Cryosophila	sp.
AJ242164.1	Daemonorops	fissa
AJ242179.1	Eleiodoxa	conferta
AJ240868.1	Eremospatha	wendlandiana
NC_029963.1:c6067-4949	Eugeissona	tristis
AJ240852.1	Guishaia	argyrata
AM116772.1	Hemithrinax	compacta
AJ240865.1	Hyphaene	thebaica
AJ404923.1	Itaya	amicorum
AJ240855.1	Johannesteijsmannia	altifrons
AJ240861.1	Kerriodoxa	elegans
AJ242175.1	Korthalsia	cheb
AJ240867.1	Lacosperma	acutiflorum

AJ242182.1	Lepidocaryum	tenue
NC_029961.1:c5992-4876	Leucothrinax	morrisii
AJ240856.1	Licuala	kunstleri
AJ240854.1	Livistona	chinensis
NC_029960.1:c5906-4798	Lodoicea	maldivica
NC_029947.1:c6053-4920	Mauritia	flexuosa
AJ242183.1	Mauritiella	armata
AM116779.1	Maxburretia	rupicola
AM116791.1	Medemia	argun
AM116769.1	Metroxylon	salomonense
AJ242169.1	Myrialepis	paradoxa
AJ240859.1	Nannorrhops	ritchiana
NC_029958.1:c6112-4970	Nypa	fruticans
AJ240871.1	Oncocalamus	mannii
AM116775.1	Phoenix	canariensis
AM116780.1	Pholidocarpus	macrocarpus
NC_029956.1:c5915-4776	Pigafetta	elata
AJ242168.1	Plectocomia	mulleri
AJ242170.1	Plectocomiopsis	geminiflora
AJ242163.1	Pogonotium	ursinum
AM116786.1	Pritchardia	arecina
AM116781.1	Pritchardiopsis	(Saribus)
AJ242184.1	Raphia	farinifera
AJ242166.1	Retispathe	dumetosa
AM116778.1	Rhipidophyllum	hystrix
AJ240853.1	Rhapis	excelsa
AM116770.1	Sabal	minor
NC_029954.1:c6093-4969	Salacca	ramosiana
NC_029953.1:c6006-4871	Serenoa	repens
AM116774.1	Thrinax	radiata
AJ404925.1	Trachycarpus	fortunei
AJ240844.1	Trithrinax	campestris
AJ240884.1	Wallichia	disticha
NC_029974.1:c5993-4849	Washingtonia	robusta
AM116771.1	Zombia	antillarum
JX088662.1:c5955-4831	Pseudophoenix	vinifera
AJ240875.1	Ceroxylon	quindiuense
AJ240908.1	Phytelephas	aequatorialis
AJ240885.1	Iriartea	deltoidea
AJ240881.1	Chamaedorea	microspadix
AJ404936.1	Roystonea	oleracea
HQ265710.1	Reinhardtia	simplex
HG969823.1	Cocos	nucifera

AJ240886.1	Podococcus	barteri
AJ404948.1	Sclerosperma	mannii
AJ240887.1	Orania	lauterbachiana
AJ404932.1	Leopoldinia	pulchra
AJ240888.1	Manicaria	saccifera
AJ240906.1	Geonoma	congesta
AM116812.1	Pelagodoxa	henryana
AJ240899.1	Areca	triandra
JX088665.1:c5972-4879	Dasypogon	bromeliifolius
JX051651.1:c5907-4857	Kingia	australis
AJ240889.1	Euterpe	oleracea
NC_029952.1:c5908-4793	Tahina	spectabilis

ndhF

GenBank Accession	Genus	Species
NC_029973.1:c115569-113365	Acoelorraphe	wrightii
KT312939.1:c116913-114676	Arenga	caudata
JX088664.1:c115819-113582	Bismarckia	nobilis
NC_029969.1:c115624-113387	Borassodendron	machadonis
KP901247.1:c116883-114646	Borassus	flabellifer
KT312936.1:c115943-113706	Brahea	brandegeei
DQ273115.1	Calamus	aruensis
NC_029948.1:c116975-114738	Caryota	mitis
NC_029967.1:c115651-113414	Chamaerops	humilis
NC_029966.1:c112571-110334	Chuniophoenix	nana
HQ720608.1	Colpothrinax	wrightii
HQ720620.1	Copernicia	prunifera
HQ720624.1	Corypha	umbraculifera
HQ720625.1	Cryosophila	stauracantha
EU186189.1	Daemonorops	fissa
EU186180.1	Eremospatha	wendlandiana
EU186181.1	Eugeissona	utilis
HQ720626.1	Guishaia	argyrata
HQ720630.1	Johannesteijsmannia	altifrons
EU186211.1	Kerriodoxa	elegans
EU186184.1	Korthalsia	cheb
EU186178.1	Laccosperma	acutiflorum
NC_029961.1:c116009-113772	Leucothrinax	morrissii
HQ720655.1	Licuala	kunstleri
HQ720673.1	Livistona	chinensis
NC_029960.1:c116033-113826	Lodoicea	maldivica
NC_029947.1:c114177-112189	Mauritia	flexuosa
HQ720690.1	Maxburretia	rupicola

EU186183.1	Metroxylon	salomonense
EU186201.1	Myrialepis	paradoxa
NC_029958.1:c115856-113619	Nypa	fruticans
EU186208.1	Oncocalamus	tuleyi
HQ720691.1	Phoenix	roebelenii
HQ720694.1	Pholidocarpus	macrocarpus
NC_029956.1:c115069-112832	Pigafetta	elata
EU186204.1	Plectocomia	mulleri
EU186198.1	Pogonotium	ursinum
JF905124.1	Pritchardia	arecina
HQ720714.1	Saribus	jeanneneyi
EU186207.1	Raphia	farinifera
EU186200.1	Retispatha	dumetosa
HQ720702.1	Rhipidophyllum	hystrix
HQ720704.1	Rhapis	excelsa
HQ720713.1	Sabal	palmetto
NC_029954.1:c114469-112232	Salacca	ramosiana
NC_029954.1:c114469-112232	Salacca	ramosiana
AY044526.1	Thrinax	radiata
HQ720721.1	Trachycarpus	fortunei
KT312918.1:c115953-113716	Trithrinax	brasiliensis
KT312916.1:c116760-114517	Wallichia	densiflora
NC_029974.1:c115175-112938	Washingtonia	robusta
JX088662.1:c115171-112934	Pseudophoenix	vinifera
EU186212.1	Ceroxylon	quindiuense
AY044533.1	Phytelephas	aequatorialis
AY044545.1	Iriartea	deltoidea
DQ273098.1	Chamaedorea	microspadix
AY044554.1	Roystonea	oleracea
AY044551.1	Reinhardtia	simplex
AY044566.1	Cocos	nucifera
AY044550.1	Podococcus	barteri
EU004898.1	Sclerosperma	mannii
EU004897.1	Orania	lauterbachiana
AY044547.1	Leopoldinia	pulchra
AY044548.1	Manicaria	saccifera
EF128266.1	Geonomia	congesta
EU004902.1	Pelagodoxa	henryana
AY044535.1	Areca	vestiaria
JX051651.1:c116493-114274	Kingia	australis
JX088665.1:c114687-112456	Dasypogon	bromeliifolius
NC_029952.1:c85838-83613	Tahina	spectabilis

PRK

GenBank Accession	Genus	Species
EU215477.1	Acoelorraphe	wrightii
AM900724.1	Arenga	hookeriana
AM900729.1	Bismarckia	nobilis
AM900737.1	Borassodendron	machadonis
AM900744.1	Borassus	flabellifer
AM900751.1	Calamus	aruensis
AF453338.1	Caryota	mitis
AF453339.1	Chamaerops	humilis
EU215461.1	Chelyocarpus	ulei
AM900721.1	Chuniophoenix	nana
AM900718.1	Coccothrinax	argentata
EU215482.1	Copernicia	prunifera
AM900727.1	Corypha	umbraculifera
KY020693.1	Cryosophila	warscewiczii
FR729730.1	Eremospatha	wendlandiana
EU215468.1	Hemithrinax	compacta
AM900733.1	Hyphaene	thebaica
EU215456.1	Itaya	amicorum
KF991781.1	Johannesteijsmannia	altifrons
AJ831355.1	Kerriodoxa	elegans
AM900750.1	Latania	verschaffeltii
KY020717.1	Leucothrinax	morrissii
KY020697.1	Licuala	peltata
AF453357.1	Lodoicea	maldivica
AM900734.1	Medemia	argun
AM900722.1	Nannorrhops	ritchiana
AJ831357.1	Nypa	fruticans
AM900719.1	Phoenix	reclinata
EU215458.1	Rhipidophyllum	hystrix
KY020734.1	Sabal	minor
AM900735.1	Satranala	decussilvae
KY020705.1	Schippia	concolor
EU215464.1	Serenoa	repens
KY020707.1	Thrinax	radiata
KY020725.1	Trithrinax	campestris
AM900726.1	Wallichia	densiflora
EU215484.1	Zombia	antillarum
AJ831363.1	Pseudophoenix	vinifera
AJ831349.1	Ceroxylon	quindiuense
AJ831361.1	Phytelephas	aequatorialis

EF491109.1	Iriartea	deltoidea
AJ831352.1	Chamaedorea	microspadix
AJ831372.1	Roystonea	oleracea
AJ831371.1	Reinhardtia	simplex
AY601232.1	Cocos	nucifera
AF453370.1	Podococcus	barteri
AF453377.1	Sclerosperma	mannii
AF453365.1	Orania	lauterbachiana
AF453355.1	Leopoldinia	pulchra
AF453358.1	Manicaria	saccifera
AY772745.1	Geonoma	congesta
AF453347.1	Euterpe	precatoria
AJ831321.1	Pelagodoxa	henryana
AY772776.1	Areca	triandra
AM900723.1	Tahina	spectabilis

rbcL

GenBank Accession	Genus	Species
NC_029973.1:57072-58514	Acoelorraphe	wrightii
AJ404819.1	Areca	triandra
KT312939.1:57917-59350	Arenga	caudata
JX088664.1:57164-58627	Bismarckia	nobilis
NC_029969.1:56672-58135	Borassodendron	machadonis
KP901247.1:57901-59364	Borassus	flabellifer
AM110198.1	Brahea	berlandieri
JX088663.1:56032-57495	Calamus	caryotoides
AJ829855.1	Calospatha	scortechnii
NC_029948.1:58040-59494	Caryota	mitis
AJ829860.1	Ceratolobus	pseudoconcolor
AJ404781.1	Ceroxylon	quindiuense
NC_029967.1:57067-58509	Chamaerops	humilis
AJ404746.1	Chelyocarpus	ulei
NC_029966.1:54898-56361	Chuniophoenix	nana
AJ404751.1	Coccothrinax	argentata
AM110211.1	Cocos	nucifera
AJ829862.1	Colpothrinax	wrightii
AM110199.1	Copernicia	prunifera
AJ404761.1	Corypha	umbraculifera

JQ590460.1	Cryosophila	warszewiczii
AJ829866.1	Daemonorops	acamptostachys
AJ829868.1	Eleiodoxa	conferta
AM117812.1	Eremospatha	wendlandiana
NC_029963.1:56437-57879	Eugeissona	tristis
AJ404755.1	Guishaia	argyrata
AJ829869.1	Hemithrinax	compacta
AJ404770.1	Hyphaene	thebaica
AJ404748.1	Itaya	amicorum
AJ404758.1	Johannesteijsmannia	altifrons
AJ404765.1	Kerriodoxa	elegans
AM110188.1	Korthalsia	cheb
AJ404772.1	Laccosperma	acutiflorum
AJ829878.1	Latania	verschaffeltii
AJ829880.1	Lepidocaryum	tenue
NC_029961.1:57563-59005	Leucothrinax	morrisii
AJ404759.1	Licuala	kunstleri
AJ404757.1	Livistona	chinensis
NC_029960.1:57263-58705	Lodoicea	maldivica
NC_029947.1:56039-57502	Mauritia	flexuosa
AJ829883.1	Mauritiella	aculeata
AJ829884.1	Maxburretia	rupicola
AJ829885.1	Medemia	argun
AM110190.1	Metroxylon	salomonense
AJ829887.1	Myrialepis	paradoxa
AJ404763.1	Nannorrhops	ritchiana
NC_029958.1:57503-58966	Nypa	fruticans
AJ404776.1	Oncocalamus	mannii
AM110194.1	Phoenix	canariensis
AJ829894.1	Pholidocarpus	macrocarpus
NC_029956.1:56161-57624	Pigafetta	elata
AJ829899.1	Plectocomia	mulleri
AJ829900.1	Plectocomiopsis	geminiflora
AJ829901.1	Pogonotium	ursinum
AJ829905.1	Pritchardia	arecina
AM110196.1	Pritchardiopsis	(Saribus)
AJ829907.1	Raphia	farinifera
AJ829908.1	Retispatha	dumetosa

AJ404753.1	Rhipidophyllum	hystrix
AJ404756.1	Rhapis	excelsa
AM110191.1	Sabal	minor
NC_029954.1:55705-57168	Salacca	ramosiana
AJ404771.1	Satranala	decussilvae
AJ404749.1	Schippia	concolor
NC_029953.1:57091-58545	Serenoa	repens
AJ404750.1	Thrinax	radiata
AJ404752.1	Trachycarpus	fortunei
AJ404745.1	Trithrinax	campestris
AJ404792.1	Wallichia	disticha
NC_029974.1:56567-58030	Washingtonia	robusta
AM110192.1	Zombia	antillarum
JX088662.1:56497-57951	Pseudophoenix	vinifera
AJ404835.1	Phytelephas	aequatorialis
AJ404793.1	Iriartea	deltoidea
AJ404787.1	Chamaedorea	microspadix
AJ404805.1	Roystonea	oleracea
AJ404799.1	Reinhardtia	simplex
AM110207.1	Podococcus	barteri
AJ404823.1	Sclerosperma	mannii
AJ404796.1	Orania	lauterbachiana
AJ404798.1	Leopoldinia	pulchra
AJ404797.1	Manicaria	saccifera
AM110219.1	Geonomia	congesta
AJ404802.1	Euterpe	oleracea
AJ829892.1	Pelagodoxa	henryana
JX088665.1:57260-58714	Dasypogon	bromeliifolius
JX051651.1:57450-58910	Kingia	australis
NC_029952.1:54303-55745	Tahina	spectabilis

RPB2

GenBank

Accession

EU215508.1

AM903114.1

AM903123.1

AM903131.1

FJ200374.1

HQ720490.1

Genus

Acoelorraphe

Arenga

Bismarckia

Borassodendron

Borassus

Brahea

Species

wrightii

hookeriana

nobilis

machadonis

flabellifer

brandegeei

AM903105.1	Calamus	aruensis
GU584941.1	Caryota	mitis
AY543097.1	Chamaerops	humilis
EU215491.1	Chelyocarpus	ulei
AM903111.1	Chuniophoenix	nana
KY020455.1	Coccothrinax	argentata
EU215499.1	Colpothrinax	wrightii
EU215513.1	Copernicia	prunifera
GU929696.1	Corypha	umbraculifera
KY020470.1	Cryosophila	warscewiczii
KJ501067.1	Daemonorops	rarispinosa
FR729729.1	Eremospatha	wendlandiana
KX346441.1	Eugeissona	tristis
EU215498.1	Hemithrinax	compacta
GU936620.1	Hyphaene	thebaica
EU215485.1	Itaya	amicorum
HQ720517.1	Johannesteijsmannia	altifrons
HQ720523.1	Kerriodoxa	elegans
KJ501075.1	Korthalsia	laciniosa
KX346461.1	Laccosperma	acutiflorum
AM903144.1	Latania	verschaffeltii
KX346446.1	Lepidocaryum	tenue
EU215514.1	Thrinax	morrisii
HQ720530.1	Licuala	kunstleri
HQ720541.1	Livistona	chinensis
AJ830171.1	Lodoicea	maldivica
KX346444.1	Mauritia	flexuosa
HQ720558.1	Maxburretia	rupicola
AM903128.1	Medemia	argun
KX346442.1	Metroxylon	salomonense
AM903112.1	Nannorrhops	ritchiana
GU584942.1	Nypa	fruticans
KX346451.1	Oncocalamus	tuleyi
HQ720559.1	Phoenix	roebelenii
HQ720561.1	Pholidocarpus	macrocarpus
KJ501081.1	Plectocomia	himalayana
JF905199.1	Pritchardia	arecina
HQ720580.1	Saribus	jeanneneyi
GU936624.1	Raphia	hookeri
HQ720571.1	Rapidophyllum	hystrix
HQ720573.1	Rhapis	excelsa
KY020492.1	Sabal	minor
AM903129.1	Satranala	decussilvae

EU215486.1	Schippia	concolor
HQ720586.1	Serenoa	repens
EU215495.1	Thrinax	radiata
HQ720588.1	Trachycarpus	fortunei
KY020505.1	Triithrinax	campestris
AM903119.1	Wallichia	disticha
HQ720593.1	Washingtonia	robusta
EU215515.1	Zombia	antillarum
FJ200370.1	Areca	triandra
AJ830162.1	Ceroxylon	quindiuense
AJ830178.1	Phytelephas	aequatorialis
KF775758.1	Iriartea	deltoidea
AJ830166.1	Chamaedorea	microspadix
AJ830184.1	Roystonea	oleracea
HQ265665.1	Reinhardtia	simplex
EF491150.1	Cocos	nucifera
AJ830180.1	Podococcus	barteri
AJ830190.1	Sclerosperma	mannii
AY779373.1	Orania	lauterbachiana
AY543102.1	Leopoldinia	pulchra
AY543103.1	Manicaria	saccifera
HM140604.1	Geonomia	congesta
AJ830135.1	Pelagodoxa	henryana
AJ830181.1	Pseudophoenix	vinifera
AM903113.1	Tahina	spectabilis

rps16

GenBank Accession	Genus	Species
NC_029973.1:c6020-4865	Acoelorraphe	wrightii
KT312939.1:c6074-4926	Arenga	caudata
JX088664.1:c6189-5073	Bismarckia	nobilis
NC_029969.1:c5968-4847	Borassodendron	machadonis
KP901247.1:c5965-4849	Borassus	flabellifer
AM116783.1	Brahea	berlandieri
JX088663.1:c5949-4804	Calamus	caryotoides
AJ242161.1	Calospatha	scortechinii
NC_029948.1:c5983-4869	Caryota	mitis
AJ242162.1	Ceratolobus	concolor
NC_029967.1:c6026-4891	Chamaerops	humilis
AJ240845.1	Chelyocarpus	ulei
NC_029966.1:c6109-4987	Chuniophoenix	nana
AJ240848.1	Coccothrinax	argentata
AM116784.1	Colpothrinax	wrightii

AM116785.1	Copernicia	prunifera
AJ240858.1	Corypha	umbraculifera
AJ240846.1	Cryosophila	sp.
AJ242164.1	Daemonorops	fissa
AJ242179.1	Eleiodoxa	conferta
AJ240868.1	Eremospatha	wendlandiana
NC_029963.1:c6067-4949	Eugeissona	tristis
AJ240852.1	Guihaia	argyrata
AM116772.1	Hemithrinax	compacta
AJ240865.1	Hyphaene	thebaica
AJ404923.1	Itaya	amicorum
AJ240855.1	Johannesteijsmannia	altifrons
AJ240861.1	Kerriodoxa	elegans
AJ242175.1	Korthalsia	cheb
AJ240867.1	Laccosperma	acutiflorum
AJ242182.1	Lepidocaryum	tenue
NC_029961.1:c5992-4876	Leucothrinax	morrissii
AJ240856.1	Licuala	kunstleri
AJ240854.1	Livistona	chinensis
NC_029960.1:c5906-4798	Lodoicea	maldivica
NC_029947.1:c6053-4920	Mauritia	flexuosa
AJ242183.1	Mauritiella	armata
AM116779.1	Maxburretia	rupicola
AM116791.1	Medemia	argun
AM116769.1	Metroxylon	salomonense
AJ242169.1	Myrialepis	paradoxa
AJ240859.1	Nannorrhops	ritchiana
NC_029958.1:c6112-4970	Nypa	fruticans
AJ240871.1	Oncocalamus	mannii
AM116775.1	Phoenix	canariensis
AM116780.1	Pholidocarpus	macrocarpus
NC_029956.1:c5915-4776	Pigafetta	elata
AJ242168.1	Plectocomia	mulleri
AJ242170.1	Plectocomiopsis	geminiflora
AJ242163.1	Pogonotium	ursinum
AM116786.1	Pritchardia	arecina
AM116781.1	Pritchardiopsis	(Saribus)
AJ242184.1	Raphia	farinifera
AJ242166.1	Retispathe	dumetosa
AM116778.1	Rhipidophyllum	hystrix
AJ240853.1	Rhapis	excelsa
AM116770.1	Sabal	minor
NC_029954.1:c6093-4969	Salacca	ramosiana

NC_029953.1:c6006-4871	Serenoa	repens
AM116774.1	Thrinax	radiata
AJ404925.1	Trachycarpus	fortunei
AJ240844.1	Trithrinax	campestris
AJ240884.1	Wallichia	disticha
NC_029974.1:c5993-4849	Washingtonia	robusta
AM116771.1	Zombia	antillarum
JX088662.1:c5955-4831	Pseudophoenix	vinifera
AJ240875.1	Ceroxylon	quindiuense
AJ240908.1	Phytelephas	aequatorialis
AJ240885.1	Iriartea	deltoidea
AJ240881.1	Chamaedorea	microspadix
AJ404936.1	Roystonea	oleracea
HQ265710.1	Reinhardtia	simplex
HG969823.1	Cocos	nucifera
AJ240886.1	Podococcus	barteri
AJ404948.1	Sclerosperma	mannii
AJ240887.1	Orania	lauterbachiana
AJ404932.1	Leopoldinia	pulchra
AJ240888.1	Manicaria	saccifera
AJ240906.1	Geonoma	congesta
AM116812.1	Pelagodoxa	henryana
AJ240899.1	Areca	triandra
JX088665.1:c5972-4879	Dasypogon	bromeliifolius
JX051651.1:c5907-4857	Kingia	australis
AJ240889.1	Euterpe	oleracea
NC_029952.1:c5908-4793	Tahina	spectabilis

trnL-trnF

GenBank Accession	Genus	Species
NC_029973.1:c3283-1736	Acoelorraphe	wrightii
KT312939.1:c3268-1715	Arenga	caudata
JX088664.1:c3404-1854	Bismarckia	nobilis
NC_029969.1:c3276-1726	Borassodendron	machadonis
KP901247.1:c3294-1744	Borassus	flabellifer
AM113628.1	Brahea	berlandieri
JX088663.1:47650-48427	Calamus	caryotoides
NC_029948.1:c3250-1697	Caryota	mitis
NC_029967.1:c3261-1717	Chamaerops	humilis
AJ241254.1	Chelyocarpus	ulei
NC_029966.1:c3378-1810	Chuniophoenix	nana
AJ241257.1	Coccothrinax	argentata
AM113629.1	Colpothrinax	wrightii

AM113630.1	Copernicia	prunifera
AJ241267.1	Corypha	umbraculifera
AJ241255.1	Cryosophila	sp.
AJ241277.1	Eremospatha	wendlandiana
NC_029963.1:c3370-1829	Eugeissona	tristis
AJ241261.1	Guihaia	argyrata
AM113620.1	Hemithrinax	compacta
AJ241274.1	Hyphaene	thebaica
AJ404890.1	Itaya	amicorum
AJ241264.1	Johannesteijsmannia	altifrons
AJ241270.1	Kerriodoxa	elegans
AM113613.1	Korthalsia	cheb
AJ241276.1	Laccosperma	acutiflorum
AM113636.1	Latania	verschaffeltii
NC_029961.1:c3285-1732	Leucothrinax	morrissii
AJ241265.1	Licuala	kunstleri
AJ241263.1	Livistona	chinensis
NC_029960.1:c3279-1723	Lodoicea	maldivica
NC_029947.1:c3262-1721	Mauritia	flexuosa
AM113624.1	Maxburretia	rupicola
AM113635.1	Medemia	argun
AM113615.1	Metroxylon	salomonense
AJ241268.1	Nannorrhops	ritchiana
NC_029958.1:c3369-1822	Nypa	fruticans
AJ241376.1	Oncocalamus	mannii
AM113622.1	Phoenix	canariensis
AM113625.1	Pholidocarpus	macrocarpus
NC_029956.1:c3273-1726	Pigafetta	elata
AM113617.1	Plectocomia	mulleri
AM113631.1	Pritchardia	arecina
AM113626.1	Pritchardiopsis	(Saribus)
AM113612.1	Raphia	farinifera
AJ241259.1	Rhipidophyllum	hystrix
AJ241262.1	Rhapis	excelsa
AM113618.1	Sabal	minor
NC_029954.1:c3444-1891	Salacca	ramosiana
AJ241275.1	Satranala	decussilvae
AJ404891.1	Schippia	concolor
NC_029953.1:c3276-1732	Serenoa	repens
AM779617.1	Tahina	spectabilis
AJ241256.1	Thrinax	radiata
AJ404892.1	Trachycarpus	fortunei
AJ241253.1	Triithrinax	campestris

AJ241293.1	Wallichia	disticha
NC_029974.1:c3268-1724	Washingtonia	robusta
AM113619.1	Zombia	antillarum
AJ241283.1	Pseudophoenix	sargentii
AJ241284.1	Ceroxylon	quindiuense
AJ241317.1	Phytelephas	aequatorialis
AJ241294.1	Iriartea	deltoidea
AJ241290.1	Chamaedorea	microspadix
HQ265805.1	Reinhardtia	simplex
HG969955.1	Cocos	nucifera
AJ241295.1	Podococcus	barteri
AJ241296.1	Orania	lauterbachiana
AJ241297.1	Manicaria	saccifera
AM113656.1	Pelagodoxa	henryana
AJ241308.1	Areca	triandra
AJ241298.1	Euterpe	oleracea
AJ241315.1	Geonoma	congesta
AM779617.1	Tahina	spectabilis

APPENDIX B

Character definitions, morphological matrix, PCoA scree plot, and list of eigenvalues from chapter 3

Character definitions

1. Carpel number

0 = one, 1 = three, 2 = more than three

2. Carpel fusion

0 = distinct (unfused), 1 = connate basally, 2 = connate throughout, 3 = connate by styles only

3. Carpels pseudomonomerous (one functional carpel at anthesis)

0 = not pseudomonomerous, 1 = pseudomonomerous

4. Ovule attachment within locule

0 = basal, 1 = lateral, 2 = pendulous

5. Pericarp scales

0 = lacking scales, 1 = with scales

6. Pericarp forming corky warts

0 = absent, 1 = present

7. Position of stigmatic remains in mature fruit

0 = apical or subapical, 1 = lateral or basal

8. Seed attachment within fruit

0 = basally, 1 = laterally, 2 = apical

9. Endosperm structure

0 = homogeneous, 1 = ruminate

10. Embryo position within seed (relative to base of fruit)

0 = basal to subbasal, 1 = lateral, 2 = apical to subapical

11. Number of seeds per fruit

0 = always one, 1 = up to 3, 2 = more than three

12. Structure of multi-seeded fruits

0 = not lobed/fruits multilocular, 1 = multi-seeded fruits deeply lobed (resembling fused fruits)

13. Endocarp prominent at maturity

0 = absent, 1 = present

14. Endocarp with external sculpturing

0 = absent, 1 = present

15. Endocarp with internal ridges intruding into seed

0 = absent, 1 = present

16. Endocarp with intruding into seed basally, forming depression

0 = absent, 1 = present

17. Endocarp forming basal button (circular appendage seen on surface; from Baker et al., 2009)

0 = absent, 1 = present

18. Endocarp forming pyrenes around seeds

0 = absent, 1 = present

19. Developmental origin of endocarp within pericarp

0 = innermost zone, 1 = middle zone (immature fruits with parenchyma to inside)

20. Endocarp anatomy: single palisade layer from locular epidermis

0 = absent, 1 = present

21. Endocarp anatomy: fiber bundles and/or sclereids

0 = absent, 1 = present

22. Endocarp with hilar seam (endocarp interrupted where seed attaches to fruit)

0 = absent, 1 = present

23. Endocarp with a germination structure (i.e. pore, operculum)

0 = absent, 1 = present

24. Position of germination structure

0 = basal, 1 = lateral, 2 = apical, 3 = subbasal, 4 = subapical

25. Germination structure type

0 = pore (endocarp thins or with aperture), 1 = operculum

26. Germination structure shape

0 = circular, 1 = elongate

27. Postament (deep columnar or irregular intrusion of the seed coat into endosperm)

0 = absent, 1 = present

28. Postament position (origin of intrusion relative to base of fruit)
0 = basal or subbasal, 1 = lateral, 2 = apical subapical

29. Seed coat unevenly thickened (e.g. thickened along one side, or along raphe)
0 = absent, 1 = present

30. Seed with fleshy, thickened sarcotesta
0 = absent, 1 = present

31. Longitudinal vascular or fiber bundles in pericarp
0 = absent, 1 = present

32. Size of longitudinal vascular or fiber bundles in pericarp (when seen in transverse section)
0 = uniform (mostly the same size), 1 = non-uniform (markedly different sizes)

33. Size distribution of longitudinal vascular or fiber bundles in pericarp (when seen in transverse section)
0 = forming size gradient (continuous variation in bundle size), 1 = discrete bundle sizes (e.g. very large bundles intermixed with small ones)

34. Spatial distribution of longitudinal vascular or fiber bundles in pericarp (when seen in transverse section)
0 = forming a single layer or ring in pericarp, 1 = forming multiple layers in pericarp, 2 = embedded in endocarp

35. Prominent anastomosis of longitudinal fiber or fibrovascular bundles
0 = absent or very rare, 1 = present

36. Cross sectional shape of longitudinal vascular bundles
0 = not flattened (e.g. mostly circular), 1 = flattened

37. Presence of radially oriented fiber bundles in pericarp
0 = absent, 1 = present

38. Position of radial fiber bundles (if present) RFB position
0 = in outermost zone of pericarp only, 1 = throughout pericarp (e.g. traversing pericarp from endocarp)

39. Stigma and pericarp form prominent beak when seen in longitudinal section
0 = absent, 1 = present

40. Traces of abortive carpel in fruit (e.g. vestigial locules)
0 = absent, 1 = present

41. Abortive carpel type

0 = basal remains, 1 = vestigial locules (e.g. within endocarp, as in Cocoseae)

42. Locule number in gynoecium (not in fruit). Characters scored from *Genera palmarum*.

0 = one, 1 = three, 2 = more than three

43. Stigma shape

0 = low, not prominent, 1 = trifid, 2 = capitate or entire, 3 = 3-angled or lobed, 4 = tubular or funnel-shaped, 5 = recurved and follicular, 6 = highly elongated

44. Gynoecium style

0 = absent, 1 = present

45. Seed with prominent raphe

0 = absent, 1 = present

Morphological Matrix

Acanthophoenix	12120001000-10000001011-100-101111110-00-0000
Acoelorraphe	13000000010-100000?0100---0-101100110-010-211
Acrocomia	12010000010-100000001011100-000----0-0111100
Actinokentia	12120001000-10000001010---0-001101101010-0101
Actinorhytis	12110001100-100000010110100-001111110-10-0101
Adonidia	121?0001100-10000001110000-001111100-10-0101
Aiphanes	12010000010-10000001011000-0010-???0-0111100
Allagoptera	12010000000-1000000?1013100-0010-1?00-1111101
Ammandra	220001000020100?110???0-?????0----110??2611
Aphandra	2200010000201000110??00---0-000----11111261?
Archontophoenix	12110000100-100000010110000-001111111000-0101
Areca	12100000100-100-000100---0-001111000-10-0101
Arenga	1201000001100-----000----0-00-1100
Asterogyne	12020010000-1000000?00---0-001111000-10-1111
Astrocaryum	120100000210100000001014000-001101000-1111100
Attalea	120000001010110000011013100-001101000-1111111
Bactris	12010000010-100000010141-0-0010-1000-0111000
Balaka	12120001000-1000000??10---????1111101010-0001
Barcella	120100000110100000001011100-001101000-1110100
Basselinia	12120010000-100000010?10110-??10-0?11100-1110
Beccariophoenix	120?0000110-100000---011-00-001101000-10-1100
Bentinckia	12120010000-100000010010100-000----0-00-0101
Bismarckia	12000010020-101101101012010-0010-210110101100
Borassodendron	120000000210101001101012000-0010-???110111300
Borassus	120000000211101001101012000-0010-100110111200
Brahea	13000000010-100000?0100---11001101000-010-311
Brassiophoenix	12120001000-1100000110100?0-001112000-10-0101
Burretokentia	12120001000-1100000101101-0-0010-1000-10-0101
Butia	1201000001101000000110131-0-0010-??00-0111101
Calamus	120010000?0-0-----0-010----0-00-1110
Calyptroclyx	12110001000-0-----0-001111000-10?0101
Calyptogyne	12000010000-10000001000---0-101110100-00-1111
Calyptronoma	12020010000-10000001000---0-001110100-00-1111
Carpentaria	12110001000-1000000??0---0-001111110-1?0100
Carpoxylon	1211000?0?0-1000000101?????0-??1111100-10?000?
Caryota	12010000111010000001000---0-000----0-0111100
Ceroxylon	12020010010-10000001000---0-000----0-00-1101
Chamaedorea	120100100?0-10000001000---0-000----0-00-1100
Chamaerops	10-000001111100000101----11000----0-010-500
Chambeyronia	12110001000-10000001010---0-00111111010-0101
Chelyocarpus	10-00100010-1000000??100---0-000----0-00--211
Chuniophoenix	11000000000-0-----0-000----0-00-1111
Clinosperma	12120010000-100000010?101-0-00??????00-0000
Clinostigma	121?0010000-1000000101101-0-001111101000-0101

Coccothrinax	0--00000120-0-----0-000----0-00-0410
Cocos	12010000000-100000001013100-001101000-111100?
Colpothrinax	13000000010-100000??00---0-101??1100-00--211
Copernicia	13000000100-10000010100---0-100----0-010-211
Corypha	11000010020-100000??00---0-000----0-0101110
Cryosophila	10-00000010-0-----0-000----0-00--211
Cyphokentia	121?0010000-100000010010100-0010-0010-00-0100
Cyphophoenix	12120002000-100000010110100-000----1010-0101
Cyphosperma	12120001000-110000010110100-000----1100-0101
Cyrtostachys	12120002010-100000010?????0-?01??1??0-1??0100
Deckenia	12110010000-100000010?10100-0011-0??0-00-0100
Desmoncus	12010000010-100000001011000-001100110-0111100
Dictyocaryum	12000010000-0-----0-000----0-00-1101
Dictyosperma	12110001100-100000010110100-001100110-10-0001
Dransfieldia	121?0001100-1000000?00---0-001101000-10?000?
Drymophloeus	121?0002000-1000000101?????0-001101000-10?0101
Dypsis	12110010010-1000000?000---0-001100110-00?0101
Elaeis	12010000020-1000000?1014100-001101000-1111100
Eleiodoxa	12001000000-0-----11010----0-00-1100
Eremospatha	1200100001100-----0-100----0-011131?
Eugeissona	12001000000-101000??010000-001101000-1??1300
Euterpe	12110011100-100000--?0---0-0010-110110100101
Gaussia	12010010010-100000????0---0-?00----0-0??1100
Geonoma	12100010000-100000010010100-0010-0111100-0111
Guishaia	10-00001010-0-----11100----0-0??-?11
Hedyscepe	12100001000-10000001010---0-001111000-10-0101
Hemithrinax	0--00000020-0-----10000---0-00?0411
Heterospathe	12120001100-10000001011-100-0010-0110-10-0101
Howea	12110001000-100000010010100-001101000-10-0101
Hydriastele	12110001100-10000001010---0-001101000-10-0101
Hyophorbe	12010010010-1000000100---0-?010-0110-0101100
Hyospathe	12110010000-0-----0-0010-1100-00-0100
Hyphaene	120000100211100001101012000-000----110101100
Iguanura	12110011100-10000001001-100-?010-0110-00-0100
Iriartea	12000000010-100000-0000---0-000----0-00-1001
Iriartella	120?0010020-100000??00---0-000----0-00-1101
Itaya	0-00000000-0-----?-?00----0-00-051?
Johannesteijsmannia	130001000111100000?0?00---10000----0-00-210
Juania	12020000010-100000---00---0-000----0-00-1101
Jubaea	12010000010-1000000?1011100-001101000-0111?00
Jubaeopsis	12010000010-100000001011100-001101000-0111101
Kentiopsis	12120001000-10000001010---0-001111001010-0101
Kerriodoxa	11010010100?0-----0-000----0-0101501
Korthalsia	12001000110-0-----0-000----0-10-1311
Laccospadix	12110001100?????????????????????????????0001
Lacosperma	12001000010-0-----0-100----0-10-1311

Latania	120000000210110001101?12010-0010-210110111300
Lemurophoenix	1210011?1?0-100010???00---0-000----0-00-000?
Leopoldinia	120?0011000-100000???00---0-001101100-00-1100
Lepidocaryum	12001000010-0-----0-1010-01?0-011131?
Lepidorrhachis	12120002000-100000010110100-0010-0111000-0001
Leucothrinax	0--00000020-100000??100---10000----0-00-0411
Licuala	13000000010-10000010100---10000----0-010-211
Linospadix	12110001000-0-----0-?00----1110-0101
Livistona	13000000010-10000010100---11000----0-00--111
Lodoicea	120000000210100001101012000-001101000-0??1300
Loxococcus	12110001100-0-----0-0010-0010-00-0101
Manicaria	120001100011100011010110100-?00----110101310
Marojejya	12120012010-100000-0000---0-0010-1010-00-0100
Masoala	121?000?0?0-?????????????0-001??0????1??010?
Mauritia	12001000000-0-----0-000----0-00-1311
Mauritiella	12001000000-0-----0-000----0-00-1111
Maxburretia	10-00000010-0-----0-100----0-0??-510
Medemia	120000101211100001101012010-000----110101100
Metroxylon	12001000010-0-----0-000----0-00-1310
Myrialepis	12001000000-0-----120010-1100-00-1100
Nannorrhops	11000010000-0-----0-000----0-0??1111
Nenga	12110001100-0-----0-001101100-10-0101
Neonicholsonia	12100000100-100-00-0000---0-001101111010-0101
Neoveitchia	12110001000-100000010110100-?0111110-10-0001
Nephrosperma	12110010000-100000010110100-0010-1010-00-0001
Normanbya	12120001100-0-----0-001101000-10-0101
Nypa	10-00000000-101000101010000-001101001100--401
Oenocarpus	12100000100-0-----0-001101011000-0101
Oncocalamus	12001000010-0-----11000----0-00-121?
Oncosperma	121?0001100-100000011110100-001??2101000-0001
Orania	12020010011110001101000---0-0010-011110101100
Oraniopsis	12010010010-0-----000----0-0101100
Parajubaea	120100010010110000?01013000-?010-1?0??111130?
Pelagodoxa	12110110000-10000001000---0-000----1100-1100
Phoenicophorium	12110010100-10000001010-100-001111100-00-0000
Phoenix	10-00000010-100000-0000---11?00----0-00--511
Pholidocarpus	13000101010-100000-??00---11000----1100--211
Pholidostachys	12010010000-100000010010100-001111100-00-1611
Physokentia	12110001?00-110000010110100-000----1010-0101
Phytelephas	22000100002110001101000---0-000----110??2610
Pigafetta	12001000010-0-----0-010----0-00-010?
Pinanga	12100000100-100000-0000---0-001101000-10-0200
Plectocomia	1200100000100-----0-010----0-00-1100
Plectocomiopsis	1200100000100-----0-0110-1000-00-1100
Podococcus	1202001001110-----0-001100100-0101100
Ponapea	12110001000-110?00011?????????01101000-10-010?

Prestoea	12100011100-100000??00---0-0010-0?10-00-0101
Pritchardia	13000000000-10000010100---11000----0-00--311
Pseudophoenix	12010010001110000001010---0-000----0-0101301
Ptychococcus	12120002100-11000001110000-001101000-10-0301
Ptychosperma	12120001000-110000010110100-001101000-10-0101
Raphia	12001000110-0-----0-010----0-00-1311
Ravenea	12020000000-100-0001000---0-000----0-00-1101
Reinhardtia	12000000000-100000-0000---0-001101000-10-1111
Rhipidophyllum	10-00001011110000010100---0-100----0-010-511
Rhapis	10-00001010-10000010100---110010-1100-00--411
Rhopaloblaste	12120001100-10000001000---0-001101000-10-0101
Rhopalostylis	12110001000-10000001000---0-001101000-00-0101
Roscheria	12110010100-100000010010100-000----0-00-0100
Roystonea	12110011000-100-0001010---0-1010-0110-00-0100
Sabal	12000010010-10000010100---0-10?----0-0101211
Salacca	1200100000100-----0-010----0-0111100
Saribus	13000000020?????????????10?0?????????????-111
Satakentia	12120001000-100000010110100-101111010-10-0101
Satranala	120?00101211110101101012010-?010-2000-010????
Schippia	0--00000020-0-----0-000----0-00-0410
Sclerosperma	12120001000-1000000??00---0-0010-0?00-00-0301
Serenoa	13000000010-100000??00---0-1010-0010-010-211
Socratea	12000000020-100000??00---0-000----100111100
Sommieria	121?0110000-10000001000---0-000----110100101
Syagrus	120100001010100000011013100-00110100010111101
Synechanthus	12010010110-100000-?200---0-000----0-00-1101
Tahina	120?0000100-100000-0000---0-000----0-00-131?
Tectiphiala	12120001000-100?00010??-?????0????????????0001
Thrinax	0--00000010-100000-??00---11000----0-00-0411
Trachycarpus	10-00001010-100-001010---11000----0-010-501
Trithrinax	10-00000010-100000--?0---111010-01?0-010-211
Veitchia	12110001000-10000001000---0-001101000-10-0101
Verschaffeltia	12110010100-110000010110100-000----0-00-0101
Voanioala	120?000?1?0-110000001010100-001101000-011110?
Washingtonia	130000000000-10000010100---0-100----0-00--211
Welfia	12010011000-100000-??00---0-?01101000-00-1111
Wendlandiella	12020010010-??????????-?????0?????????????1101
Wettinia	12?00010000-100000-??00---0-100----11010-601
Wodyetia	121?0001000-100000011010000-001111101010-0310
Zombia	0--00000020-100000-??00---0-0010-0100-00-0410
Hyphaeneocarbon	12000010020-100101101012010-0010-200110101???
Mahurzari_palm	121?000?000-10000?0?0?0---0-001101000-00-000?
Palmocarbon_drypeteoides	1?0?00??0010100000011013000-0010-1?00-?111???
Friedemannia_messelensis	????0002??0-?????????????????01??1????10????1
Coryphoides_poulseni	????00?0010-100?0???10????1000?????????????1
Nypa_burtini	????000???0-10100??0101000??01??1????0???????

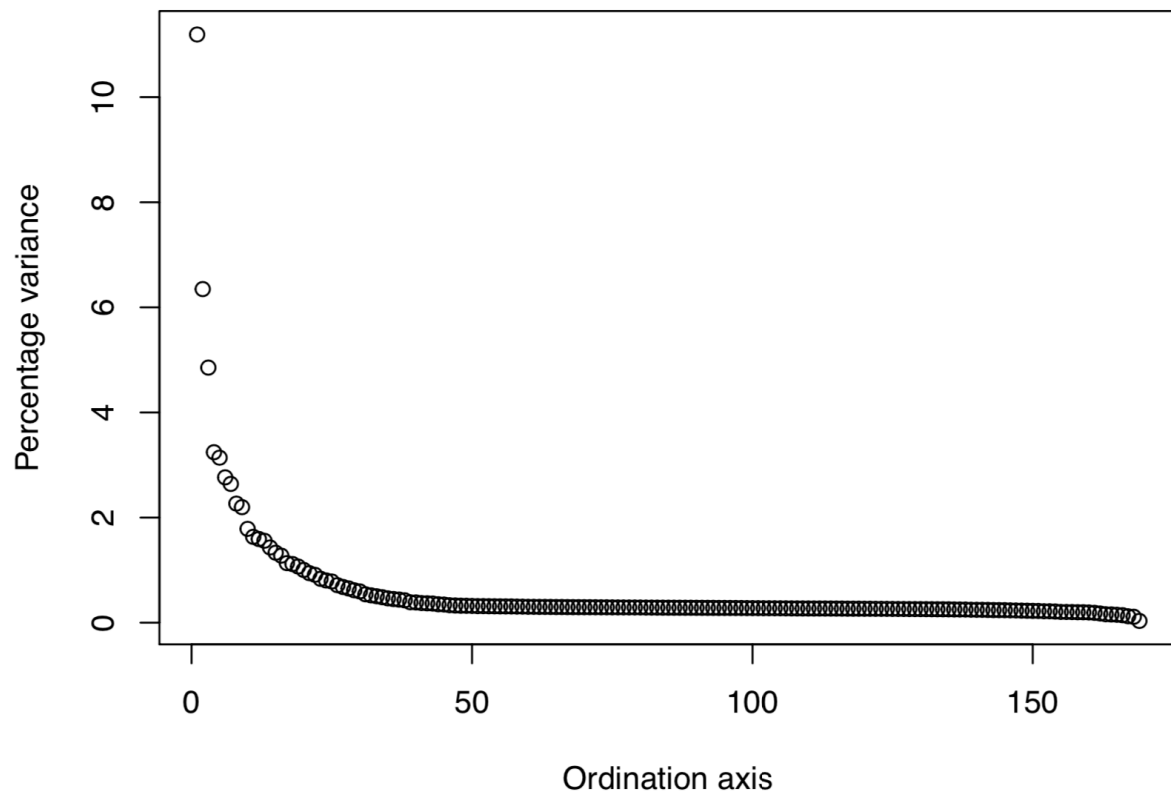


Figure B.1. Scree plot of percent variance along ordination axes from principal coordinate analysis.

List of eigenvalues from principal coordinate ordination

Ordination Axis	Eigenvalues	Corrected eigenvalue (Cailleze)
1	9.49686778	24.4633409
2	5.19468283	13.8739636
3	3.81285732	10.6077673
4	2.57091709	7.08884416
5	2.36757804	6.86236062
6	2.08456258	6.04375253
7	2.01105927	5.77127094
8	1.63029296	4.95196966
9	1.56515789	4.80474952
10	1.20674519	3.90186964
11	1.08955701	3.57029879
12	1.0570104	3.47975595
13	1.00775886	3.4065748
14	0.89349025	3.12865997
15	0.8137438	2.90944453
16	0.76866282	2.78832436
17	0.65934123	2.477025
18	0.63945692	2.43897017
19	0.63101477	2.33578643
20	0.55880317	2.19254826
21	0.48285836	2.0606729
22	0.45548242	1.99105082
23	0.38202726	1.82494447
24	0.37851147	1.75565357
25	0.35095126	1.7137278
26	0.2979607	1.55918532
27	0.26972591	1.48462744
28	0.24243025	1.42470023
29	0.21584115	1.34766238
30	0.20483198	1.2999945
31	0.17333884	1.18104607
32	0.13761322	1.13635243
33	0.12441311	1.09905128
34	0.11625416	1.05989359
35	0.09789147	1.01073768
36	0.09117186	0.98301952

37	0.08035543	0.96058221
38	0.06743971	0.93012008
39	0.05172102	0.84931057
40	0.04216583	0.84289782
41	0.03575471	0.81660184
42	0.02666909	0.80671424
43	0.01395925	0.79482473
44	0.00920177	0.76607977
45	0.00554751	0.75592011
46	0.00493791	0.7262278
47	0.00377488	0.71555449
48	0.00329728	0.70488196
49	0.00270995	0.70186366
50	0.00157012	0.69684999
51	0.0014418	0.68920058
52	0.00050024	0.68854811
53	0.00025583	0.68404564
54	0.00011539	0.68116639
55	0	0.67768092
56	-0.0001283	0.67549872
57	-0.0007058	0.67490219
58	-0.0008889	0.66953265
59	-0.0011551	0.66743857
60	-0.0017736	0.66170058
61	-0.0021262	0.66087861
62	-0.0022655	0.65749321
63	-0.0024201	0.65663298
64	-0.0027544	0.65451128
65	-0.0031191	0.65207031
66	-0.0033893	0.65119904
67	-0.0034955	0.64799324
68	-0.0038134	0.64656685
69	-0.0041947	0.64528505
70	-0.0049718	0.64433928
71	-0.0052219	0.64243509
72	-0.005492	0.64148754
73	-0.0058863	0.639878
74	-0.006283	0.63981102
75	-0.0066195	0.63755832
76	-0.0069001	0.63653869

77	-0.0074292	0.63530117
78	-0.0075618	0.63421289
79	-0.0078473	0.63362433
80	-0.0081223	0.63260366
81	-0.008592	0.63020416
82	-0.0092228	0.62831587
83	-0.0094632	0.62795903
84	-0.0099035	0.62558526
85	-0.0102461	0.62400881
86	-0.0110217	0.62331195
87	-0.0111706	0.62191077
88	-0.0116975	0.62122357
89	-0.0122436	0.62054729
90	-0.0128735	0.61884472
91	-0.0134646	0.61722767
92	-0.0139419	0.61604994
93	-0.0141593	0.61544229
94	-0.0150841	0.61254347
95	-0.0158456	0.61172208
96	-0.0161983	0.61106497
97	-0.0166265	0.61017225
98	-0.0170154	0.60885664
99	-0.018154	0.60673871
100	-0.0187354	0.60560751
101	-0.0194634	0.6048663
102	-0.0198734	0.60186714
103	-0.0210614	0.60122034
104	-0.0219209	0.59966992
105	-0.0223556	0.59858374
106	-0.0232807	0.59643089
107	-0.0240374	0.59417451
108	-0.0254688	0.59322592
109	-0.0257073	0.59296838
110	-0.0261271	0.59159053
111	-0.027437	0.59050091
112	-0.0281247	0.59006585
113	-0.0292226	0.5891324
114	-0.0295804	0.58850644
115	-0.0301733	0.58692404
116	-0.0313059	0.58553426

117	-0.0317231	0.58279257
118	-0.0343065	0.58182186
119	-0.0349628	0.58128771
120	-0.0364662	0.57941728
121	-0.037495	0.57877036
122	-0.0386256	0.57711626
123	-0.039468	0.57598673
124	-0.0415163	0.575003
125	-0.043036	0.57264912
126	-0.0436541	0.57040031
127	-0.0451319	0.56927013
128	-0.0452461	0.56744383
129	-0.0470803	0.565724
130	-0.0502749	0.56487139
131	-0.0511304	0.56306941
132	-0.0529056	0.5603505
133	-0.056465	0.55866645
134	-0.0577794	0.55694016
135	-0.0608457	0.55479401
136	-0.0617901	0.54981457
137	-0.0624109	0.54754906
138	-0.0646801	0.54675927
139	-0.0676081	0.53864425
140	-0.0682304	0.5367848
141	-0.0719411	0.53546499
142	-0.0743169	0.53083685
143	-0.0758858	0.52482989
144	-0.0811854	0.52255582
145	-0.0830454	0.51998702
146	-0.0879082	0.51303652
147	-0.0893748	0.5086741
148	-0.0916233	0.50261159
149	-0.0948646	0.49654478
150	-0.0973739	0.49092239
151	-0.1027677	0.48668979
152	-0.108221	0.47575024
153	-0.111666	0.47536948
154	-0.1161015	0.46469156
155	-0.1218646	0.44806304
156	-0.13102	0.44521601

157	-0.1334935	0.4424431
158	-0.1402044	0.43556096
159	-0.1523231	0.43348993
160	-0.15284	0.42527
161	-0.1616279	0.41050137
162	-0.1669518	0.38358239
163	-0.1780596	0.35178355
164	-0.1961427	0.34277973
165	-0.215328	0.32889155
166	-0.2219334	0.31039071
167	-0.236469	0.26639069
168	-0.2592409	0.2458127
169	-0.2774095	0.07378734
170	-0.3509758	0
171	-0.4829907	0

APPENDIX C

GenBank Accessions and taxon sampling for chapters 3 and 4

18S

GenBank Accession	Genus	Species
AF406632.1	Aphandra	natalia
AY952409.1	Areca	triandra
AY012379.1	Balaka	seemannii
AY012392.1	Beccariophoenix	madagascariensis
AY012385.1	Bentinckia	nicobarica
AY012355.1	Borassus	flabellifer
AY012386.1	Burretiokentia	hapala
AF168828.1	Calamus	caesius
AY012387.1	Calyptrocalyx	stenocrista
AF406630.1	Calyptronoma	occidentalis
AF168831.1	Caryota	mitis
AY012342.1	Chamaerops	humilis
AY012375.1	Chambeyronia	macrocarpa
AY012343.1	Chelyocarpus	repens
AY012393.1	Cocos	nucifera
AY012352.1	Corypha	utan
AY012388.1	Cyphophoenix	nucelle
AY012377.1	Cyrtostachys	renda
AY012365.1	Dictyocaryum	lamarckianum
AY012389.1	Dictyosperma	album
AY012380.1	Drymophloeus	beguinii
AY012372.1	Dypsis	lastelliana
AY012395.1	Elaeis	oleifera
KY860917.1	Euterpe	oleracea
GQ325591.1	Gaussia	princeps
AF406631.1	Geonomia	oxycarpa
AY012378.1	Howea	belmoreana
AY012390.1	Hydriastele	wendlandiana
AY012362.1	Hyophorbe	lagenicaulis

AY012356.1	Hyphaene	coriacea
AF168854.1	Iriartea	deltoidea
AY012376.1	Kentiopsis	oliviformis
AY012370.1	Leopoldinia	pulchra
AY012348.1	Licuala	grandis
AY952394.1	Livistona	chinensis
AY012369.1	Manicaria	saccifera
AY012359.1	Mauritia	flexuosa
AY012357.1	Nypa	fruticans
AY012391.1	Oncosperma	tigillarum
AY012368.1	Orania	trispatha
AF206991.1	Phoenix	canariensis
AY012398.1	Phytelephas	aequatorialis
AF168870.1	Podococcus	barteri
AY012373.1	Prestoea	acuminata
AY012350.1	Saribus	jeanneneyi
AY012360.1	Pseudophoenix	vinifera
AY012381.1	Ptychosperma	burretianum
AY012361.1	Ravenea	hildebrandti
AY012371.1	Reinhardtia	simplex
AY012344.1	Rhapis	subtilis
AY012374.1	Roystonea	regia
AH001752.2	Sabal	minor
AY012358.1	Salacca	zalacca
AY012366.1	Socratea	exorrhiza
AY012345.1	Thrinax	radiata
AY012346.1	Trachycarpus	fortunei
AY012347.1	Trithrinax	campestris
AY012382.1	Veitchia	sessilifolia
AY012351.1	Washingtonia	filifera
AY012363.1	Wendlandiella	polyclada
AY012367.1	Wettinia	hirsuta

atpB

GenBank Accession	Genus	Species
NC_029973.1:c56284-54788	Acoelorraphe	wrightii
NC_037084.1:c54791-53295	Acrocomia	aculeata
AY044463.1	Aiphanes	aculeata
AY044468.1	Allagoptera	arenaria
AY044458.1	Aphandra	natalia
AF449170.1	Archontophoenix	alexandrae
JX903939.1	Areca	triandra
NC_029971.1:c57099-55603	Arenga	caudata
JX903941.1	(Astrocaryum)	mexicanum
AY012451.1	Attalea	speciosa
AY044464.1	Bactris	humilis
AY012436.1	Balaka	seemannii
AY044467.1	Barcella	odora
AY012449.1	Beccariophoenix	madagascariensis
AY012442.1	Bentinckia	nicobarica
JX088664.1:c56391-54895	Bismarckia	nobilis
NC_029969.1:c55904-54408	Borassodendron	machadonis
NC_029968.1:c56318-54822	Brahea	brandegeei
AY012443.1	Burretokentia	hapala
JX903942.1	Butia	capitata
JX088663.1:c55262-53766	Calamus	caryotoides
AY012444.1	Calyptrocalyx	stenocrista
AY044459.1	Calytronoma	occidentalis
KT312915.1:c57259-55763	Caryota	mitis
AF233083.1	Chamaedorea	seifrizii
AF233083.1	Chamaedorea	seifrizii
AY012432.1	Chambeyronia	macrocarpa
AY012400.1	Chelyocarpus	repens
NC_029966.1:c54077-52581	Chuniophoenix	nana
AF449171.1	Clinostigma	savoryanum
KX028884.1:100838-102334	Cocos	nucifera
NC_028026.1:c56282-54786	Colpothrinax	cookii
NC_029965.1:c52868-51372	Corypha	lecomtei
AY012445.1	Cyphophoenix	nucelle
AY012434.1	Cyrtostachys	renda
AY044465.1	Desmoncus	orthacanthos
AY012422.1	Dictyocaryum	lamarckianum

AY012446.1	Dictyosperma	album
AY012437.1	Drymophloeus	beguinii
AY012429.1	Dypsis	lastelliana
NC_017602.1:c55736-54240	Elaeis	guineensis
NC_029964.1:c53868-52372	Eremospatha	macrocarpa
NC_029963.1:c55646-54150	Eugeissona	tristis
AY044460.1	Geonoma	oxycarpa
KP221707.1:c55805-54300	Heterospathe	cagayanensis
AY012435.1	Howea	belmoreana
KP221708.1:c55735-54230	Hydriastele	microspadix
AY012419.1	Hyophorbe	lagenicaulis
AY012413.1	Hyphaene	coriacea
AF233084.1	Iriartea	deltoidea
AY012433.1	Kenttiopsis	oliviformis
AY012427.1	Leopoldinia	pulchra
NC_029961.1:c56772-55276	Leucothrinax	morrisii
KT312928.1:c56661-55165	Licuala	paludosa
AF449172.1	Linospadix	longicurvis
AY012406.1	Livistona	speciosa
NC_029960.1:c56474-54978	Lodoicea	maldivica
AY012426.1	Manicaria	saccifera
NC_029947.1:c55271-53775	Mauritia	flexuosa
AF233087.1	Metroxylon	vitiense
AY012414.1	Nypa	fruticans
AY044461.1	Oenocarpus	bataua
AY012448.1	Oncosperma	tigillarium
AY012425.1	Orania	trispatha
KP221687.1:c55462-53957	Pelagodoxa	henryana
AF209652.1	Phoenix	canariensis
NC_029957.1:c56867-55371	Phytelephas	aequatorialis
NC_029956.1:c55392-53896	Pigafetta	elata
AF233086.1	Podococcus	barteri
AY012430.1	Prestoea	acuminata
KT312922.1:c56291-54795	Pritchardia	thurstonii
AY012407.1	Saribus	jeanneneyi
JX088662.1:c55723-54227	Pseudophoenix	vinifera
AY012438.1	Ptychosperma	burretianum
AY012418.1	Ravenea	hildebrandti
AY012428.1	Reinhardtia	simplex
AY012401.1	Rhapis	subtilis

AY012431.1	Roystonea	regia
AY012410.1	Sabal	domingensis
NC_029954.1:c54929-53433	Salacca	ramosiana
KP221695.1:c56587-55082	Satakentia	liukiuensis
KP221696.1:c56157-54661	Sclerosperma	profizianum
AJ621817.1	Serenoa	repens
AY012423.1	Socratea	exorrhiza
AY044471.1	Syagrus	glaucescens
AY012402.1	Thrinax	radiata
AY012403.1	Trachycarpus	fortunei
AY012404.1	Trithrinax	campestris
NC_029950.1:c55479-53983	Veitchia	arecina
AY044472.1	Voanioala	gerardii
NC_029974.1:c55799-54303	Washingtonia	robusta
AY012420.1	Wendlandiella	polyclada
AY012424.1	Wettinia	hirsuta

matK

GenBank Accession	Genus	Species
AM114691.1	Acanthophoenix	rubra
AM114579.1	Acoelorraphe	wrightii
AM114639.1	Acrocomia	aculeata
AM114661.1	Actinokentia	divaricata
AM114659.1	Actinorhytis	calapparia
AM114641.1	Aiphanes	aculeata
AM114635.1	Allagoptera	arenaria
KJ598371.1	Adonidia	merrillii
AM114611.1	Ammandra	decasperma
AM114612.1	Aphandra	natalia
AM114660.1	Archontophoenix	purpurea
AM114664.1	Areca	triandra
AM114592.1	Arenga	hookeriana
AM114654.1	Asterogyne	martiana
EU004872.1	Astrocaryum	mexicanum
AM114636.1	Attalea	allenii
AM114642.1	Bactris	gasipaes
AM114695.1	Balaka	seemannii
HQ265562.1	Barcella	odora
AM114667.1	Basselinia	velutina

AM114632.1	Beccariophoenix	madagascariensis
AM114705.1	Bentinckia	nicobarica
AM114597.1	Bismarckia	nobilis
AM114603.1	Borassodendron	machadonis
AM114604.1	Borassus	flabellifer
AM114580.1	Brahea	berlandieri
AM114699.1	Brassiophoenix	schumannii
FR832736.1	Burretokentia	grandiflora
EU004870.1	Butia	capitata
AM114551.1	Calamus	aruensis
AM114687.1	Calyptrocalyx	albertianus
AM114652.1	Calyptrogyne	ghiesbrechtiana
AM114653.1	Calyptronoma	occidentalis
AM114697.1	Carpentaria	acuminata
AM114673.1	Carpoxylon	macrospermum
AM114590.1	Caryota	mitis
AM114607.1	Ceroxylon	quindiuense
AM114623.1	Chamaedorea	microspadix
AM114568.1	Chamaerops	humilis
AM114662.1	Chambevronia	macrocarpa
AM114562.1	Chelyocarpus	ulei
AM114587.1	Chuniophoenix	nana
AM114680.1	Clinosperma	bracteale
AM114706.1	Clinostigma	savoryanum
AM114558.1	Coccothrinax	argentata
AM114637.1	Cocos	nucifera
AM114581.1	Colpothrinax	wrightii
AM114582.1	Copernicia	prunifera
AM114595.1	Corypha	umbraculifera
AM114563.1	Cryosophila	warscewiczii
AM114676.1	Cyphokentia	macrostachya
AM114669.1	Cyphophoenix	nucelle
AM114670.1	Cyphosperma	balansae
AM114707.1	Cyrtostachys	renda
AM114643.1	Desmoncus	orthacanthos
AM114616.1	Dictyocaryum	lamarckianum
AM114708.1	Dictyosperma	album
AM114709.1	Dransfieldia	micrantha
KJ598356.1	Drymophloeus	litigiosus
AM114681.1	Dypsis	lutescens

AM114644.1	Elaeis	guineensis
AM114542.1	Eremospatha	wendlandiana
AM114540.1	Eugeissona	tristis
AM114647.1	Euterpe	oleracea
AM114624.1	Gaussia	maya
AM114655.1	Geonomia	congesta
AM114569.1	Guishaia	argyrata
AM114702.1	Hedyscepe	canterburyana
AM114559.1	Hemithrinax	compacta
AM114710.1	Heterospathe	elata
GQ248137.2	Howea	forsteriana
AM114712.1	Hydriastele	microspadix
AM114620.1	Hyophorbe	lagenicaulis
AM114646.1	Hyospathe	macrorhachis
AM114599.1	Hyphaene	thebaica
AM114714.1	Iguanura	wallichiana
AM114617.1	Iriartea	deltoidea
AM114615.1	Iriartella	stenocarpa
AM114564.1	Itaya	amicorum
AM114576.1	Johannesteijsmannia	altifrons
AM114608.1	Juania	australis
EU004869.1	Jubaea	chilensis
AM114633.1	Jubaeopsis	caffra
AM114663.1	Kentiopsis	oliviformis
AM114588.1	Kerriodoxa	elegans
AM114546.1	Korthalsia	cheb
AM114689.1	Laccospadix	australasica
AM114543.1	Laccosperma	acutiflorum
AM114601.1	Latania	verschaffeltii
AM114682.1	Lemurophoenix	halleuxii
AM114656.1	Leopoldinia	pulchra
AM114715.1	Lepidorrhachis	mooreana
AM114560.1	Thrinax	morrisii
AM114575.1	Licuala	kunstleri
AM114688.1	Linospadix	monostachya
AM114574.1	Livistona	chinensis
AM114602.1	Lodoicea	maldivica
AM114716.1	Loxococcus	rupicola
AM114645.1	Manicaria	saccifera
AM114684.1	Marojejya	insignis

AM114685.1	Masoala	madagascariensis
AM114545.1	Mauritia	flexuosa
FR832790.1	Mauritiella	aculeata
AM114572.1	Maxburretia	rupicola
AM114600.1	Medemia	argun
AM114548.1	Metroxylon	salomonense
AM114589.1	Nannorrhops	ritchiana
AM114665.1	Nenga	pumila
AM114649.1	Neonicholsonia	watsonii
AM114675.1	Neoveitchia	storckii
KJ598368.1	Normanbya	normanbyi
AM114552.1	Nypa	fruticans
JQ626533.1	Oenocarpus	bataua
AM114541.1	Oncocalamus	tuleyi
AM114690.1	Oncosperma	tigillarium
AM114627.1	Orania	lauterbachiana
AM114609.1	Oraniopsis	appendiculata
AM114657.1	Pelagodoxa	henryana
AM114703.1	Phoenicophorium	borsigianum
AM114566.1	Phoenix	canariensis
AM114577.1	Pholidocarpus	macrocarpus
AM114651.1	Pholidostachys	pulchra
AM114671.1	Physokentia	rosea
AM114613.1	Phytelephas	aequatorialis
AM114549.1	Pigafetta	elata
AM114550.1	Plectocomia	mulleri
AM114625.1	Podococcus	barteri
AM114694.1	Ponapea	ledermanniana
AM114648.1	Prestoea	pubens
AM114583.1	Pritchardia	arecina
AM114578.1	Pritchardiopsis	(Saribus)
AM114606.1	Pseudophoenix	vinifera
AM114700.1	Ptychosoccus	paradoxus
AM114693.1	Ptychosperma	macarthurii
AM114544.1	Raphia	farinifera
AM114610.1	Ravenea	louvelii
AM114631.1	Reinhardtia	simplex
AM114571.1	Rhipidophyllum	hystrix
AM114573.1	Rhipis	excelsa
AM114717.1	Rhopaloblaste	augusta

AM114701.1	Rhopalostylis	baueri
AM114704.1	Roscheria	melanochaetes
AM114630.1	Roystonea	oleracea
KY020656.1	Sabal	minor
AM114547.1	Salacca	ramosiana
AM114674.1	Satakentia	liukiuensis
AM114598.1	Satranala	decussilvae
AM114555.1	Schippia	concolor
AM114629.1	Sclerosperma	mannii
AM114585.1	Serenoa	repens
AM114618.1	Socratea	exorrhiza
AM114658.1	Sommieria	leucophylla
AM114638.1	Syagrus	smithii
AM114622.1	Synechanthus	warscewiczianus
KT312919.1:c3405-1837	Tahina	spectabilis
AM114561.1	Thrinax	radiata
AM114570.1	Trachycarpus	fortunei
AM114556.1	Trithrinax	campestris
AM114696.1	Veitchia	arecina
AM114634.1	Voanioala	gerardii
AM114586.1	Washingtonia	robusta
AM114650.1	Welfia	regia
AM114621.1	Wendlandiella	gracilis
AM114619.1	Wettinia	hirsuta
AM114698.1	Wodyetia	bifurcata
AM114557.1	Zombia	antillarum
AM114719.1	Dasypogon	bromeliifolius
AM114718.1	Kingia	australis

ndhF

GenBank Accession	Genus	Species
NC_029973.1:c115569-113365	Acoelorraphe	wrightii
AY044535.1	Areca	vestiaria
KT312939.1:c116913-114676	Arenga	caudata
JX088664.1:c115819-113582	Bismarckia	nobilis
NC_029969.1:c115624-113387	Borassodendron	machadonis
KP901247.1:c116883-114646	Borassus	flabellifer
KT312936.1:c115943-113706	Brahea	brandegeei
DQ273115.1	Calamus	aruensis

NC_029948.1:c116975-114738	Caryota	mitis
EU186212.1	Ceroxylon	quindiuense
DQ273098.1	Chamaedorea	microspadix
NC_029967.1:c115651-113414	Chamaerops	humilis
NC_029966.1:c112571-110334	Chuniophoenix	nana
AY044566.1	Cocos	nucifera
HQ720608.1	Colpothrinax	wrightii
HQ720620.1	Copernicia	prunifera
HQ720624.1	Corypha	umbraculifera
HQ720625.1	Cryosophila	stauracantha
JX088665.1:c114687-112456	Dasypogon	bromeliifolius
KP221703.1	Dictyosperma	album
EU186180.1	Eremospatha	wendlandiana
EU186181.1	Eugeissona	utilis
EF128266.1	Geonoma	congesta
HQ720626.1	Guishaia	argyrata
AF453473.1	Hydriastele	wendlandiana
AY044545.1	Iriartea	deltoidea
HQ720630.1	Johannesteijsmannia	altifrons
EU186211.1	Kerriodoxa	elegans
JX051651.1:c116493-114274	Kingia	australis
EU186184.1	Korthalsia	cheb
EU186178.1	Laccosperma	acutiflorum
AY044547.1	Leopoldinia	pulchra
NC_029961.1:c116009-113772	Leucothrinax	morrissii
HQ720655.1	Licuala	kunstleri
HQ720673.1	Livistona	chinensis
NC_029960.1:c116033-113826	Lodoicea	maldivica
AY044548.1	Manicaria	saccifera
NC_029947.1:c114177-112189	Mauritia	flexuosa
HQ720690.1	Maxburretia	rupicola
EU186183.1	Metroxylon	salomonense
EU186201.1	Myrialepis	paradoxa
EU186201.1	Myrialepis	paradoxa
NC_029958.1:c115856-113619	Nypa	fruticans
EU186208.1	Oncocalamus	tuleyi
EU004897.1	Orania	lauterbachiana
EU004902.1	Pelagodoxa	henryana
HQ720691.1	Phoenix	roebelenii
HQ720694.1	Pholidocarpus	macrocarpus

AY044533.1	Phytelephas	aequatorialis
NC_029956.1:c115069-112832	Pigafetta	elata
EU186204.1	Plectocomia	mulleri
AY044550.1	Podococcus	barteri
JF905124.1	Pritchardia	arecina
JX088662.1:c115171-112934	Pseudophoenix	vinifera
EU186207.1	Raphia	farinifera
AY044551.1	Reinhardtia	simplex
HQ720702.1	Rhipidophyllum	hystrix
HQ720704.1	Rhapis	excelsa
AY044554.1	Roystonea	oleracea
HQ720713.1	Sabal	palmetto
NC_029954.1:c114469-112232	Salacca	ramosiana
NC_029954.1:c114469-112232	Salacca	ramosiana
HQ720714.1	Saribus	jeanneneyi
KP221695.1	Satakentia	liukiuensis
EU004898.1	Sclerosperma	mannii
NC_029952.1:c85838-83613	Tahina	spectabilis
AY044526.1	Thrinax	radiata
HQ720721.1	Trachycarpus	fortunei
KT312918.1:c115953-113716	Trithrinax	brasiliensis
NC_029974.1:c115175-112938	Washingtonia	robusta

PRK

GenBank Accession	Genus	Species
AF453329.1	Acanthophoenix	rubra
EU215477.1	Acoelorraphe	wrightii
AJ831344.1	Acrocomia	aculeata
AJ831221.1	Actinokentia	divaricata
AF453330.1	Actinorhytis	calapparia
AJ831224.1	Adonidia	merrillii
AY601207.1	Aiphanes	aculeata
AF453331.1	Allagoptera	arenaria
AF453332.1	Ammandra	decasperma
AJ831345.1	Aphandra	natalia
AJ831227.1	Archontophoenix	purpurea
AY772776.1	Areca	triandra
AM900724.1	Arenga	hookeriana
AF453334.1	Asterogyne	martiana

JQ821945.1	Astrocaryum	alatum
AJ831346.1	Attalea	allenii
KP218842.1	Bactris	gasipaes
JF833372.1	Balaka	seemannii
EF491112.1	Barcella	odora
AJ831233.1	Basselinia	velutina
AF453335.1	Beccariophoenix	madagascariensis
AJ831234.1	Bentinckia	nicobarica
AM900729.1	Bismarckia	nobilis
AM900737.1	Borassodendron	machadonis
AM900744.1	Borassus	flabellifer
KJ598275.1	Brassiophoenix	schumannii
AJ831242.1	Burretokentia	grandiflora
AY601251.1	Butia	capitata
AM900751.1	Calamus	aruensis
AJ831244.1	Calyptrocalyx	albertisanus
AY772764.1	Calyptrogyne	ghiesbreghtiana
AY772765.1	Calyptronoma	occidentalis
AJ831259.1	Carpentaria	acuminata
AF453337.1	Carpoxylon	macropermum
AF453338.1	Caryota	mitis
AJ831349.1	Ceroxylon	quindiuense
AJ831352.1	Chamaedorea	microspadix
AF453339.1	Chamaerops	humilis
AJ831260.1	Chambeyronia	macrocarpa
EU215461.1	Chelyocarpus	ulei
AM900721.1	Chuniophoenix	nana
AJ831261.1	Clinosperma	bracteale
AJ831263.1	Clinostigma	savoryanum
AM900718.1	Coccothrinax	argentata
AY601232.1	Cocos	nucifera
EU215482.1	Copernicia	prunifera
AM900727.1	Corypha	umbraculifera
KY020693.1	Cryosophila	warscewiczii
AJ831264.1	Cyphokentia	macrostachya
AJ831266.1	Cyphophoenix	nucifera
AF453340.1	Cyphosperma	balansae
AF453341.1	Cyrtostachys	renda
AF453342.1	Deckenia	nobilis
AY601212.1	Desmoncus	chinantlensis

KF775845.1	Dictyocaryum	lamarckianum
AF453343.1	Dictyosperma	album
AJ831326.1	Dransfieldia	(Ptychosperma)
AJ831267.1	Drymophloeus	litigiosus
AF453346.1	Dypsis	lutescens
AY601219.1	Elaeis	guineensis
AF453347.1	Euterpe	precatoria
AF453348.1	Gaussia	maya
AY772745.1:1-60,464-649	Geonoma	congesta
AJ971822.1	Hedyscepe	canterburyana
EU215468.1	Hemithrinax	compacta
AJ831279.1	Heterospathe	elata
AJ831294.1	Howea	belmoreana
AY348932.1	Hydriastele	microspadix
AM900733.1	Hyphaene	thebaica
AF453351.1	Hyophorbe	lagenicaulis
AF453352.1	Iguanura	wallichiana
EF491109.1	Iriartea	deltoidea
KF775849.1	Iriartella	stenocarpa
EU215456.1	Itaya	amicorum
KF991781.1	Johannesteijsmannia	altifrons
EF128383.1	Juania	australis
AY601255.1	Jubaea	chilensis
AY601272.1	Jubaeopsis	caffra
AF453353.1	Kentiopsis	oliviformis
AJ831355.1	Kerriodoxa	elegans
AJ831300.1	Laccospadix	australasica
AM900750.1	Latania	verschaffeltii
AF453354.1	Lemurophyoenix	halleuxii
AF453355.1	Leopoldinia	pulchra
AJ831303.1	Lepidorrhachis	mooreana
KY020717.1	Leucothrinax	morrisii
KY020697.1	Licuala	peltata
AJ831305.1	Linospadix	albertisiana
AF453357.1	Lodoicea	maldivica
AY348942.1	Loxococcus	rupicola
AF453358.1	Manicaria	saccifera
AF453359.1	Marojejya	darianii
AF453360.1	Masoala	madagascariensis

AM900722.1	Nannorrhops	ritchiana
AM900722.1	Nannorrhops	ritchiana
AY348914.1	Nenga	pumila
AJ831356.1	Neonicholsonia	watsonii
AJ831319.1	Neoveitchia	storckii
AF453362.1	Nephrosperma	vanhoutteanum
AF453363.1	Normanbya	normanbyi
AJ831357.1	Nypa	fruticans
AF453364.1	Oncosperma	tigillarum
AF453365.1	Orania	lauterbachiana
AJ831359.1	Oraniopsis	appendiculata
AY601264.1	Parajubaea	torallyi
AJ831321.1	Pelagodoxa	henryana
AF453368.1	Phoenicophorium	borsigianum
AJ831360.1	Pholidostachys	pulchra
AJ831322.1	Physokentia	rosea
AJ831361.1	Phytelephas	aequatorialis
AY348944.1	Pinanga	coronata
AF453370.1	Podococcus	barteri
AJ831328.1	Ponapea	palauensis
AJ831363.1	Pseudophoenix	vinifera
AJ831324.1	Ptychosoccus	paradoxus
AJ831325.1	Ptychosperma	macarthurii
AJ831371.1	Reinhardtia	simplex
EU215458.1	Rapidophyllum	hystrix
AJ831332.1	Rhopaloblaste	ledermanniana
AJ831333.1	Rhopalostylis	baueri
AF453374.1	Roscheria	melanochaetes
AJ831372.1	Roystonea	oleracea
KY020734.1	Sabal	minor
AM900720.1	Livistona	(Saribus)
AF453376.1	Satakentia	liukiuensis
AF453377.1	Sclerosperma	mannii
AF453378.1	Socratea	exorrhiza
AJ831334.1	Solfia	samoensis
AJ831335.1	Sommieria	leucophylla
AY601259.1	Syagrus	amara
AM900723.1	(Tahina	spectabilis)
AJ831342.1	Veitchia	spiralis
AF453381.1	Verschaffeltia	splendida

AY601266.1	Voanioala	gerardii
AY772771.1	Welfia	regia
AJ831353.1	Wendlandiella	gracilis
AJ831373.1	Wettinia	hirsuta
AJ831343.1	Wodyetia	bifurcata
KX346544.1	Oncocalamus	tuleyi
KX346551.1	Laccosperma	acutiflorum
KX346540.1	Raphia	palma-pinus
KX346538.1	Mauritiella	armata
KX346537.1	Mauritia	flexuosa
KX346536.1	Metroxylon	salomonense
KX346535.1	Eugeissona	tristis
KX346557.1	Eremospatha	laurentii

rbcL

GenBank Accession	Genus	Species
AM110234.1	Acanthophoenix	rubra
AM110197.1	Acoelorraphe	wrightii
AM110212.1	Acrocomia	aculeata
AM110221.1	Actinokentia	divaricata
AJ829847.1	Actinorhytis	calapparia
AJ829848.1	Adonidia	merrillii
AJ404831.1	Aiphanes	aculeata
AJ404828.1	Allagoptera	arenaria
AJ404838.1	Ammandra	decasperma
AJ404837.1	Aphandra	natalia
AJ404806.1	Archontophoenix	purpurea
AJ404819.1	Areca	triandra
AJ404788.1	Arenga	hookeriana
AJ404833.1	Asterogyne	martiana
AY012510.1	Astrocaryum	alatum
AJ404829.1	Attalea	allenii
AM110214.1	Bactris	gasipaes
AJ404814.1	Balaka	seemannii
AY044630.1	Barcella	odora
AM110223.1	Basselinia	velutina
AJ404826.1	Beccariophoenix	madagascariensis
AM110239.1	Bentinckia	nicobarica
AJ829852.1	Bismarckia	nobilis

AJ404768.1	Borassodendron	machadonis
AM110202.1	Borassus	flabellifer
AM110198.1	Brahea	berlandieri
AJ404815.1	Brassiophoenix	schumannii
AY012500.1	Burretokentia	hapala
JX903252.1	Butia	capitata
AJ404775.1	Calamus	hollrungii
AM110232.1	Calyptrocalyx	albertisianus
AM110218.1	Calyptrogyne	ghiesbreghtiana
AJ404832.1	Calyptronoma	occidentalis
AJ829858.1	Carpentaria	acuminata
AJ829859.1	Carpoxylon	macrospermum
AJ404790.1	Caryota	mitis
AJ404781.1	Ceroxylon	quindiuense
AJ404787.1	Chamaedorea	microspadix
AJ404754.1	Chamaerops	humilis
AM110222.1	Chambeyronia	macrocarpa
AJ404746.1	Chelyocarpus	ulei
AJ404764.1	Chuniophoenix	nana
AJ829861.1	Clinosperma	bracteale
AM110240.1	Clinostigma	savoryanum
AJ404751.1	Coccothrinax	argentata
AM110211.1	Cocos	nucifera
AJ829862.1	Colpothrinax	wrightii
AM110199.1	Copernicia	prunifera
AJ404761.1	Corypha	umbraculifera
JQ590460.1	Cryosophila	warscewiczii
AJ829864.1	Cyphokentia	macrostachya
AJ404821.1	Cyphophoenix	nucelle
AM110225.1	Cyphosperma	balansae
AJ404810.1	Cyrtostachys	renda
AJ829867.1	Deckenia	nobilis
AM110215.1	Desmoncus	orthacanthos
AM110204.1	Dictyocaryum	lamarckianum
AM110241.1	Dictyosperma	album
AM110242.1	Dransfieldia	micrantha
AY012494.1	Drymophloeus	beguinii
AJ404800.1	Dypsis	lutescens
AJ404830.1	Elaeis	guineensis
AJ829868.1	Eleiodoxa	conferta

AM117812.1	Eremospatha	wendlandiana
AJ404774.1	Eugeissona	tristis
AJ404802.1	Euterpe	oleracea
AJ404784.1	Gaussia	maya
AM110219.1	Geonomia	congesta
AJ404755.1	Guihaia	argyrata
AJ404807.1	Hedyscepe	canterburyana
AJ829869.1	Hemithrinax	compacta
AM110243.1	Heterospathe	elata
AY012492.1	Howea	belmoreana
AJ404817.1	Hydriastele	microspadix
AJ404785.1	Hyophorbe	lagenicaulis
AJ404804.1	Hyospathe	macrorhachis
AJ404770.1	Hyphaene	thebaica
AJ404820.1	Iguanura	wallichiana
AJ404793.1	Iriartea	deltoidea
AM110203.1	Iriartella	stenocarpa
AJ404748.1	Itaya	amicorum
AJ404758.1	Johannesteijsmannia	altifrons
AJ829874.1	Juania	australis
AJ829875.1	Jubaea	chilensis
AJ829876.1	Jubaeopsis	caffra
AJ404809.1	Kentiopsis	oliviformis
AJ404765.1	Kerriodoxa	elegans
AM110188.1	Korthalsia	cheb
AJ404812.1	Laccospadix	australasica
AJ404772.1	Laccosperma	acutiflorum
AJ829878.1	Latania	verschaffeltii
AM110229.1	Lemuropheonix	halleuxii
AJ404798.1	Leopoldinia	pulchra
AJ829880.1	Lepidocaryum	tenue
AJ829881.1	Lepidorrhachis	mooreana
AM110193.1	(Leucothrinax)	morrisii
AJ404759.1	Licuala	kunstleri
AJ404811.1	Linospadix	monostachya
AJ404757.1	Livistona	chinensis
AJ404769.1	Lodoicea	maldivica
AJ829882.1	Loxococcus	rupicola
AJ404797.1	Manicaria	saccifera
AM110230.1	Marojejya	insignis

AJ404824.1	Masoala	madagascariensis
AJ404777.1	Mauritia	flexuosa
AJ829883.1	Mauritiella	aculeata
AJ829884.1	Maxburretia	rupicola
AJ829885.1	Medemia	argun
AM110190.1	Metroxylon	salomonense
AJ829887.1	Myrialepis	paradoxa
AJ404763.1	Nannorrhops	ritchiana
AJ404818.1	Nenga	pumila
AJ404803.1	Neonicholsonia	watsonii
AJ829888.1	Neoveitchia	storckii
AJ829889.1	Nephrosperma	vanhoutteanum
AJ829890.1	Normanbya	normanbyi
AJ404778.1	Nypa	fruticans
AY044624.1	Oenocarpus	bataua
AJ404776.1	Oncocalamus	mannii
AM110233.1	Oncosperma	tigillarium
AJ404796.1	Orania	lauterbachiana
AJ404782.1	Oraniopsis	appendiculata
AJ829891.1	Parajubaea	torallyi
AJ829892.1	Pelagodoxa	henryana
AM110237.1	Phoenicophorium	borsigianum
AJ829894.1	Pholidocarpus	macrocarpus
AM110217.1	Pholidostachys	pulchra
AJ829896.1	Physokentia	rosea
AJ404835.1	Phytelephas	aequatorialis
AM110194.1	Phoenix	canariensis
AJ829894.1	Pholidocarpus	macrocarpus
AJ829897.1	Pigafetta	elata
AJ829898.1	Pinanga	simplicifrons
AJ829899.1	Plectocomia	mulleri
AJ829900.1	Plectocomiopsis	geminiflora
AM110207.1	Podococcus	barteri
AJ829903.1	Ponapea	ledermanniana
AM110216.1	Prestoea	pubens
AJ829905.1	Pritchardia	arecina
AM110196.1	Pritchardiopsis	(Saribus)
AJ404780.1	Pseudophoenix	vinifera
AJ829906.1	Ptychococcus	paradoxus
AM110235.1	Ptychosperma	macarthuri

AJ829907.1	Raphia	farinifera
AJ404783.1	Ravenea	louvelii
AJ404799.1	Reinhardtia	simplex
AJ404753.1	Rhipidophyllum	hystrix
AJ404756.1	Rhapis	excelsa
AM110244.1	Rhopaloblaste	augusta
AJ404808.1	Rhopalostylis	baueri
AM110238.1	Roscheria	melanochaetes
AJ404805.1	Roystonea	oleracea
AM110191.1	Sabal	minor
AM110189.1	Salacca	ramosiana
AM110227.1	Satakentia	liukiuensis
AJ404771.1	Satranala	decussilvae
AJ404749.1	Schippia	concolor
AJ404823.1	Sclerosperma	mannii
AJ404760.1	Serenoa	repens
AM110205.1	Socratea	exorrhiza
AM110220.1	Sommieria	leucophylla
AJ404827.1	Syagrus	smithii
AJ404786.1	Synechanthus	warscewiczianus
KT312919.1:54303-55745	Tahina	spectabilis
AJ404750.1	Thrinax	radiata
AJ404752.1	Trachycarpus	fortunei
AJ404745.1	Trithrinax	campestris
AJ404813.1	Veitchia	arecina
AJ829916.1	Verschaffeltia	splendida
AM110210.1	Voanioala	gerardii
AM110201.1	Washingtonia	robusta
AJ829917.1	Welfia	regia
AM110206.1	Wendlandiella	gracilis
AJ404794.1	Wettinia	hirsuta
AM110236.1	Wodyetia	bifurcata
AM110192.1	Zombia	antillarum
AM110246.1	Dasypogon	bromeliifolius
AM110245.1	Kingia	australis

RPB2

GenBank Accession	Genus	Species
AJ830020.1	Acanthophoenix	rubra

EU215508.1	Acoelorraphe	wrightii
AJ830151.1	Acrocomia	aculeata
AJ830023.1	Actinokentia	huerlimannii
AJ830024.1	Actinorhytis	calapparia
AJ830193.1	Adonidia	merrillii
AJ830152.1	Allagoptera	arenaria
AY543096.1	Ammandra	decasperma
AJ830153.1	Aphandra	natalia
AJ830028.1	Archontophoenix	purpurea
FJ200370.1	Areca	triandra
AM903114.1	Arenga	hookeriana
AJ830154.1	Asterogyne	martiana
AJ830207.1	Attalea	allenii
AJ830194.1	Balaka	burretiana
AJ830030.1	Basselinia	humboldtiana
AJ830155.1	Beccariophoenix	madagascariensis
AJ830032.1	Bentinckia	condapanna
AM903123.1	Bismarckia	nobilis
AM903131.1	Borassodendron	machadonis
FJ200374.1	Borassus	flabellifer
HQ720490.1	Brahea	brandegeei
AJ830195.1	Brassiophoenix	drymophloeoides
AJ830033.1	Brongniartikentia	lanuginosa
AJ830037.1	Burretiokentia	grandiflora
AM903105.1	Calamus	aruensis
AJ830040.1	Calyptrocalyx	albertisianus
AJ830208.1	Calyptrogyne	costatifrons
AY779367.1	Calyptronoma	plumeriana
AJ830054.1	Campecarpus	fulcitus
AJ830196.1	Carpentaria	acuminata
AJ830055.1	Carpoxylon	macrospermum
GU584941.1	Caryota	mitis
AJ830157.1	Ceroxylon	quindiuense
AJ830166.1	Chamaedorea	microspadix
AY543097.1	Chamaerops	humilis
AJ830056.1	Chambeyronia	macrocarpa
EU215491.1	Chelyocarpus	ulei
AM903113.1	Chuniophoeniceae	sp.
AM903111.1	Chuniophoenix	nana
AJ830057.1	Clinosperma	bracteale

AJ830059.1	Clinostigma	savoryanum
KY020455.1	Coccothrinax	argentata
EF491150.1	Cocos	nucifera
EU215499.1	Colpothrinax	wrightii
EU215513.1	Copernicia	prunifera
GU929696.1	Corypha	umbraculifera
KY020470.1	Cryosophila	warscewiczii
AJ830060.1	Cyphokentia	macrostachya
AJ830061.1	Cyphophoenix	nucelle
AY543098.1	Cyphosperma	balansae
AJ830062.1	Cyrtostachys	renda
KJ501067.1	Daemonorops	rarispinosa
AJ830063.1	Deckenia	nobilis
AJ830064.1	Dictyosperma	album
AJ830197.1	Drymophloeus	litigiosus
AJ830078.1	Dypsis	lutescens
AJ830163.1	Elaeis	oleifera
AJ830164.1	Eremospatha	laurentii
KX346441.1	Eugeissona	tristis
AJ830165.1	Gaussia	maya
HM140604.1	Geonoma	congesta
AJ971833.1	Hedyscepe	canterburyana
EU215498.1	Hemithrinax	compacta
AJ830084.1	Heterospathe	elata
AJ830098.1	Howea	belmoreana
AY543136.1	Hydriastele	microspadix
AJ830168.1	Hyophorbe	lagenicaulis
GU936620.1	Hyphaene	thebaica
AY543099.1	Iguanura	wallichiana
KF775758.1	Iriartea	deltoidea
EU215485.1	Itaya	amicorum
HQ720517.1	Johannesteijsmannia	altifrons
AY543100.1	Kentiopsis	oliviformis
HQ720523.1	Kerriodoxa	elegans
AJ830108.1	Laccospadix	australasica
KX346461.1	Laccosperma	acutiflorum
AM903144.1	Latania	verschaffeltii
AJ830110.1	Lavoixia	macrocarpa
AJ830112.1	Lemurophoenix	halleuxii
AY543102.1	Leopoldinia	pulchra

KX346446.1	Lepidocaryum	tenue
AJ830117.1	Lepidorrhachis	mooreana
HQ720530.1	Licuala	kunstleri
AJ830119.1	Linospadix	albertisiana
HQ720541.1	Livistona	chinensis
AJ830171.1	Lodoicea	maldivica
AY543151.1	Loxococcus	rupicola
AJ830173.1	Manicaria	saccifera
AJ830121.1	Marojejya	darianii
AJ830128.1	Masoala	madagascariensis
KX346444.1	Mauritia	flexuosa
HQ720558.1	Maxburretia	rupicola
AM903128.1	Medemia	argun
KX346442.1	Metroxylon	salomonense
AJ830129.1	Moratia	cerifera
AM903112.1	Nannorrhops	ritchiana
AY543154.1	Nenga	gajah
AJ830172.1	Neonicholsonia	watsonii
AJ830130.1	Neoveitchia	storckii
AJ830131.1	Nephrosperma	vanhoutteanum
AJ830132.1	Normanbya	normanbyi
GU584942.1	Nypa	fruticans
KX346451.1	Oncocalamus	tuleyi
AJ830175.1	Orania	lauterbachiana
AJ830177.1	Oraniopsis	appendiculata
AJ830135.1	Pelagodoxa	henryana
AJ830136.1	Phoenicophorium	borsigianum
HQ720559.1	Phoenix	roebelenii
HQ720561.1	Pholidocarpus	macrocarpus
AJ830211.1	Pholidostachys	pulchra
AJ830138.1	Physokentia	rosea
AJ830178.1	Phytelephas	aequatorialis
AY543156.1	Pinanga	coronata
KJ501081.1	Plectocomia	himalayana
AJ830180.1	Podococcus	barteri
AJ830203.1	Ponapea	palauensis
JF905199.1	Pritchardia	arecina
AJ830181.1	Pseudophoenix	vinifera
AJ830200.1	Ptychococcus	paradoxus
AJ830201.1	Ptychosperma	macarthurii

GU936624.1	Raphia	hookeri
HQ265665.1	Reinhardtia	simplex
HQ720571.1	Rapidophyllum	hystrix
HQ720573.1	Rhapis	excelsa
AJ830143.1	Rhopaloblaste	ledermanniana
AJ830145.1	Rhopalostylis	baueri
AJ830140.1	Roscheria	melanochaetes
AJ830184.1	Roystonea	oleracea
KY020492.1	Sabal	minor
HQ720580.1	Saribus	jeanneneyi
AJ830146.1	Satakentia	liukiuensis
AM903129.1	Satranala	decussilvae
EU215486.1	Schippia	concolor
AJ830190.1	Sclerosperma	mannii
HQ720586.1	Serenoa	repens
AY543108.1	Socratea	exorrhiza
AJ830147.1	Sommieria	leucophylla
AJ830148.1	Tectiphiala	ferox
EU215514.1	Thrinax	morrisii
HQ720588.1	Trachycarpus	fortunei
KY020505.1	Triithrinax	campestris
AJ830149.1	Veillonia	alba
AJ830205.1	Veitchia	spiralis
AJ830150.1	Verschaffeltia	splendida
HQ720593.1	Washingtonia	robusta
AY779371.1	Welfia	regia
AJ830167.1	Wendlandiella	gracilis
AJ830191.1	Wettinia	hirsuta
AJ830206.1	Wodyetia	bifurcata
EU215515.1	Zombia	antillarum

rps16

GenBank Accession	Genus	Species
AM116836.1	Acanthophoenix	rubra
AM116782.1	Acoelorraphe	wrightii
AM116804.1	Acrocomia	aculeata
AM116815.1	Actinokentia	divaricata
AM116814.1	Actinorhytis	calapparia
AJ404953.1	Aiphanes	aculeata

AJ240902.1	Allagoptera	arenaria
AJ404955.1	Ammandra	decasperma
AJ404954.1	Aphandra	natalia
AJ404937.1	Archontophoenix	purpurea
AJ404945.1	Areca	triandra
AJ240882.1	Arenga	hookeriana
AJ240905.1	Asteroxyne	martiana
HQ265675.1	Astrocaryum	alatum
AJ240903.1	Attalea	allenii
AM116806.1	Bactris	gasipaes
AJ240896.1	Balaka	seemannii
HQ265702.1	Barcella	odora
AM116818.1	Basselinia	velutina
AJ404951.1	Beccariophoenix	madagascariensis
AM116844.1	Bentinckia	nicobarica
AM116790.1	Bismarckia	nobilis
AJ404927.1	Borassodendron	machadonis
AM116793.1	Borassus	flabellifer
AM116783.1	Brahea	berlandieri
AJ240897.1	Brassiophoenix	schumannii
EU004908.1	Butia	capitata
AJ240870.1	Calamus	hollrungii
AM116834.1	Calyptrocalyx	albertisanus
AM116811.1	Calyptrogyne	ghiesbreghtiana
AJ240904.1	Calyptronoma	occidentalis
AM116840.1	Carpentaria	acuminata
AM116824.1	Carpoxylon	macrospermum
AJ240883.1	Caryota	mitis
AJ240875.1	Ceroxylon	quindiuense
AJ240881.1	Chamaedorea	microspadix
AM116777.1	Chamaerops	humilis
AM116816.1	Chambevonia	macrocarpa
AJ240845.1	Chelyocarpus	ulei
AJ240860.1	Chuniophoenix	nana
AM116831.1	Clinosperma	bracteale
AM116845.1	Clinostigma	savoryanum
AJ240848.1	Coccothrinax	argentata
AM116803.1	Cocos	nucifera
AM116784.1	Colpothrinax	wrightii
AM116785.1	Copernicia	prunifera

AJ240858.1	Corypha	umbraculifera
AY656160.1	Costus	pulverulentus
AJ240846.1	Cryosophila	sp.
AM116827.1	Cyphokentia	macrostachya
AM116820.1	Cyphophoenix	nucelle
AM116821.1	Cyphosperma	balansae
AJ404940.1	Cyrtostachys	renda
AM116854.1	Dasypogon	bromeliifolius
AM116807.1	Desmoncus	orthacanthos
AM116796.1	Dictyocaryum	lamarckianum
AM116846.1	Dictyosperma	album
AM116847.1	Dransfieldia	micrantha
AJ404934.1	Dypsis	lutescens
AJ404952.1	Elaeis	guineensis
AJ242179.1	Eleiodoxa	conferta
AJ240868.1	Eremospatha	wendlandiana
AJ240869.1	Eugeissona	tristis
AJ240889.1	Euterpe	oleracea
AJ240878.1	Gaussia	maya
AJ240906.1	Geonomia	congesta
AJ240852.1	Guiaia	argyrata
AJ404938.1	Hedyscepe	canterburyana
AM116772.1	Hemithrinax	compacta
AM116848.1	Heterospathe	elata
AJ404943.1	Hydriastele	microspadix
AJ240879.1	Hyophorbe	lagenicaulis
AJ240891.1	Hyospathe	macrorachis
AJ240865.1	Hyphaene	thebaica
AJ404946.1	Iguanura	wallichiana
AJ240885.1	Iriartea	deltoidea
AM116795.1	Iriartella	stenocarpa
AJ404923.1	Itaya	amicorum
AJ240855.1	Johannesteijsmannia	altifrons
AM116794.1	Juania	australis
EU004907.1	Jubaea	chilensis
AM116801.1	Jubaeopsis	caffra
AJ240892.1	Kentiopsis	oliviformis
AJ240861.1	Kerriodoxa	elegans
AM116853.1	Kingia	australis
AJ242175.1	Korthalsia	cheb

AJ240895.1	Laccospadix	australasica
AJ240867.1	Laccosperma	acutiflorum
AM116792.1	Latania	verschaffeltii
AJ404935.1	Lemurophoenix	halleuxii
AJ404932.1	Leopoldinia	pulchra
AJ242182.1	Lepidocaryum	tenue
AM116850.1	Lepidorrhachis	mooreana
AJ240856.1	Licuala	kunstleri
AJ404941.1	Linospadix	monostachya
AJ240854.1	Livistona	chinensis
AJ240864.1	Lodoicea	maldivica
AM116851.1	Loxococcus	rupicola
AJ240888.1	Manicaria	saccifera
AM116832.1	Marojejya	insignis
AJ404949.1	Masoala	madagascariensis
AJ240872.1	Mauritia	flexuosa
AJ242183.1	Mauritiella	armata
AM116779.1	Maxburretia	rupicola
AM116791.1	Medemia	argun
AM116769.1	Metroxylon	salomonense
AJ242169.1	Myrialepis	paradoxa
AJ240859.1	Nannorrhops	ritchiana
AJ404944.1	Nenga	pumila
AJ240890.1	Neonicholsonia	watsonii
AM116826.1	Neoveitchia	storckii
AJ240873.1	Nypa	fruticans
AJ240871.1	Oncocalamus	mannii
AM116835.1	Oncosperma	tigillarium
AJ240887.1	Orania	lauterbachiana
AJ240876.1	Oraniopsis	appendiculata
AM116812.1	Pelagodoxa	henryana
AM116843.1	Phenicophorium	borsigianum
AM116775.1	Phoenix	canariensis
AM116780.1	Pholidocarpus	macrocarpus
AM116810.1	Pholidostachys	pulchra
AM116822.1	Physokentia	rosea
AJ240908.1	Phytelephas	aequatorialis
AJ242171.1	Pigafetta	elata
AJ242168.1	Plectocomia	mulleri
AJ242170.1	Plectocomiopsis	geminiflora

AJ240886.1	<i>Podococcus</i>	<i>barteri</i>
AM116839.1	<i>Ponapea</i>	<i>ledermanniana</i>
AM116808.1	<i>Prestoea</i>	<i>pubens</i>
AM116786.1	<i>Pritchardia</i>	<i>arecina</i>
AM116781.1	(<i>Saribus</i>)	<i>jeanneneyi</i>
AJ404928.1	<i>Pseudophoenix</i>	<i>vinifera</i>
AM116842.1	<i>Ptychococcus</i>	<i>paradoxus</i>
AM116838.1	<i>Ptychosperma</i>	<i>macarthurii</i>
AJ242184.1	<i>Raphia</i>	<i>farinifera</i>
AJ240877.1	<i>Ravenea</i>	<i>louvelii</i>
AJ404933.1	<i>Reinhardtia</i>	<i>simplex</i>
AJ242166.1	<i>Retispathe</i>	<i>dumetosa</i>
AM116778.1	<i>Rhipidophyllum</i>	<i>hystrix</i>
AJ240853.1	<i>Rhapis</i>	<i>excelsa</i>
AM116852.1	<i>Rhopaloblaste</i>	<i>augusta</i>
AJ404939.1	<i>Rhopalostylis</i>	<i>baueri</i>
AJ404947.1	<i>Roscheria</i>	<i>melanochaetes</i>
AJ404936.1	<i>Roystonea</i>	<i>oleracea</i>
AM116770.1	<i>Sabal</i>	<i>minor</i>
AJ242176.1	<i>Salacca</i>	<i>ramosiana</i>
AM116825.1	<i>Satakentia</i>	<i>liukiuensis</i>
AM116813.1	<i>Sommieria</i>	<i>leucophylla</i>
AJ240901.1	<i>Syagrus</i>	<i>smithii</i>
AJ240880.1	<i>Synechanthus</i>	<i>warscewiczianus</i>
NC_029952.1:c5908-4793	<i>Tahina</i>	<i>spectabilis</i>
AM116773.1	(<i>Leucothrinax</i>)	<i>morrисii</i>
AM116774.1	<i>Thrinax</i>	<i>radiata</i>
AJ404925.1	<i>Trachycarpus</i>	<i>fortunei</i>
AJ240844.1	<i>Trithrinax</i>	<i>campestris</i>
AJ404942.1	<i>Veitchia</i>	<i>arecina</i>
AM116802.1	<i>Voanioala</i>	<i>gerardii</i>
AM116789.1	<i>Washingtonia</i>	<i>robusta</i>
AM116809.1	<i>Welfia</i>	<i>regia</i>
AM116798.1	<i>Wendlandiella</i>	<i>gracilis</i>
AJ404931.1	<i>Wettinia</i>	<i>hirsuta</i>
AM116841.1	<i>Wodyetia</i>	<i>bifurcata</i>
AM116771.1	<i>Zombia</i>	<i>antillarum</i>

trnL-trnF

GenBank Accession	Genus	Species
AM113679.1	Acanthophoenix	rubra
AM113627.1	Acoelorraphe	wrightii
AM113648.1	Acrocomia	aculeata
AM113659.1	Actinokentia	divaricata
AM113658.1	Actinorhytis	calapparia
AJ404920.1	Aiphanes	aculeata
AJ241311.1	Allagoptera	arenaria
AM113661.1	Alloschmidia	glabrata
AJ404922.1	Ammandra	decasperma
AJ404921.1	Aphandra	natalia
AJ404904.1	Archontophoenix	purpurea
AJ404912.1	Areca	triandra
AJ241291.1	Arenga	hookeriana
AJ241314.1	Asteroxyne	martiana
AJ241312.1	Attalea	allenii
AM113650.1	Bactris	gasipaes
AJ241305.1	Balaka	seemannii
AM113662.1	Basselinia	velutina
AJ404918.1	Beccariophoenix	madagascariensis
AM113687.1	Bentinckia	nicobarica
AM113634.1	Bismarckia	nobilis
AJ404894.1	Borassodendron	machadonis
AM113637.1	Borassus	flabellifer
AM113628.1	Brahea	berlandieri
AJ241306.1	Brassiophoenix	schumannii
AJ241279.1	Calamus	hollrungii
AM113677.1	Calyptrocalyx	albertisanus
AM113655.1	Calyptrogyne	ghiesbreghtiana
AJ241313.1	Calyptronoma	occidentalis
AM113683.1	Carpentaria	acuminata
AM113667.1	Carpoxylon	macrospermum
AJ241292.1	Caryota	mitis
AJ241284.1	Ceroxylon	quindiuense
AJ241290.1	Chamaedorea	microspadix
AJ241260.1	Chamaerops	humilis
AM113660.1	Chambevonia	macrocarpa
AJ241254.1	Chelyocarpus	ulei

AJ241269.1	Chuniophoenix	nana
AM113674.1	Clinosperma	bracteale
AM113688.1	Clinostigma	savoryanum
AJ241257.1	Coccothrinax	argentata
AM113647.1	Cocos	nucifera
AM113629.1	Colpothrinax	wrightii
AM113630.1	Copernicia	prunifera
AJ241267.1	Corypha	umbraculifera
AJ241255.1	Cryosophila	sp.
AM113670.1	Cyphokentia	macrostachya
AJ241309.1	Cyphophoenix	nucele
AM113664.1	Cyphosperma	balansae
AJ404907.1	Cyrtostachys	renda
AM113651.1	Desmoncus	orthacanthos
AM113640.1	Dictyocaryum	lamarckianum
AM113689.1	Dictyosperma	album
AM113690.1	Dransfieldia	micrantha
AJ404901.1	Dypsis	lutescens
AJ404919.1	Elaeis	guineensis
AJ241277.1	Eremospatha	wendlandiana
AJ241278.1	Eugeissona	tristis
AJ241298.1	Euterpe	oleracea
AJ241287.1	Gaussia	maya
AJ241315.1	Geonoma	congesta
AJ241261.1	Guihaia	argyrata
AJ404905.1	Hedyscepe	canterburyana
AM113620.1	Hemithrinax	compacta
AM113691.1	Heterospathe	elata
AJ404910.1	Hydriastele	microspadix
AJ241288.1	Hyophorbe	lagenicaulis
AJ241300.1	Hyospathe	macrorachis
AJ241274.1	Hyphaene	thebaica
AJ404913.1	Iguanura	wallichiana
AJ241294.1	Iriartea	deltoidea
AM113639.1	Iriartella	stenocarpa
AJ404890.1	Itaya	amicorum
AJ241264.1	Johannesteijsmannia	altifrons
AM113638.1	Juania	australis
AM113645.1	Jubaeopsis	caffra
AJ241788.1	Kentiopsis	oliviformis

AJ241270.1	Kerriodoxa	elegans
AM113613.1	Korthalsia	cheb
AJ241304.1	Laccospadix	australasica
AJ241276.1	Laccosperma	acutiflorum
AM113636.1	Latania	verschaffeltii
AJ404902.1	Lemurophoenix	halleuxii
AJ404899.1	Leopoldinia	pulchra
AM113693.1	Lepidorrhachis	mooreana
AJ241265.1	Licuala	kunstleri
AJ404908.1	Linospadix	monostachya
AJ241263.1	Livistona	chinensis
AJ241273.1	Lodoicea	maldivica
AM113694.1	Loxococcus	rupicola
AJ241297.1	Manicaria	saccifera
AM113675.1	Marojejya	insignis
AJ404916.1	Masoala	madagascariensis
AJ241281.1	Mauritia	flexuosa
AM113624.1	Maxburretia	rupicola
AM113635.1	Medemia	argun
AM113615.1	Metroxylon	salomonense
AJ241268.1	Nannorrhops	ritchiana
AJ404911.1	Nenga	pumila
AJ241299.1	Neonicholsonia	watsonii
AM113669.1	Neoveitchia	storckii
AJ241282.1	Nypa	fruticans
AJ241376.1	Oncocalamus	mannii
AM113678.1	Oncosperma	tigillarium
AJ241296.1	Orania	lauterbachiana
AJ241285.1	Oraniopsis	appendiculata
AM113622.1	Phoenix	canariensis
AM113625.1	Pholidocarpus	macrocarpus
AM113617.1	Plectocomia	mulleri
AJ241295.1	Podococcus	barteri
AM113682.1	Ponapea	ledermanniana
AM113652.1	Prestoea	pubens
AM113631.1	Pritchardia	arecina
AM113626.1	Pritchardiopsis	jeanneneyi
AJ404895.1	Pseudophoenix	vinifera
AM113685.1	Ptychosperma	paradoxus
AM113681.1	Ptychosperma	macarthurii

AM113612.1	Raphia	farinifera
AJ241286.1	Ravenea	louvelii
AJ404900.1	Reinhardtia	simplex
AJ241259.1	Rhipidophyllum	hystrix
AJ241262.1	Rhapis	excelsa
AM113695.1	Rhopaloblaste	augusta
AJ404906.1	Rhopalostylis	baueri
AJ404914.1	Roscheria	melanochaetes
AM113618.1	Sabal	minor
AM113614.1	Salacca	ramosiana
AJ241275.1	Satranala	decussilvae
AJ404891.1	Schippia	concolor
AJ404915.1	Sclerosperma	mannii
AJ241266.1	Serenoa	repens
AM113641.1	Socratea	exorrhiza
AM113657.1	Sommieria	leucophylla
AJ241310.1	Syagrus	smithii
AJ241787.1	Synechanthus	warscewiczianus
AM779617.1	Tahina	spectabilis
AM113680.1	Tectiphiala	ferox
AJ241256.1	Thrinax	radiata
AJ404892.1	Trachycarpus	fortunei
AJ241253.1	Trithrinax	campestris
AJ404909.1	Veitchia	arecina
AM113646.1	Voanioala	gerardii
AM113633.1	Washingtonia	robusta
AM113653.1	Welfia	regia
AM113642.1	Wendlandiella	gracilis
AJ404898.1	Wettinia	hirsuta
AM113684.1	Wodyetia	bifurcata
AM113619.1	Zombia	antillarum
AM113697.1	Dasypogon	bromeliifolius
AM113696.1	Kingia	australis

trnQ-rps16

GenBank Accession	Genus	Species
AY044602.1	Acrocomia	aculeata
HG969892.1	Actinokentia	divaricata

HG969912.1	Actinorhytis	calapparia
AY044603.1	Aiphanes	aculeata
AY044611.1	Allagoptera	arenaria
AY044581.1	Aphandra	natalia
AF449145.1	Archontophoenix	alexandrae
AY044584.1	Areca	vestiaria
AY044604.1	Astrocaryum	alatum
AY044617.1	Attalea	speciosa
AY044605.1	Bactris	humilis
EF605576.1	Basselinia	deplanchei
AY044608.1	Barcella	odora
AY044610.1	Beccariophoenix	madagascariensis
AF449146.1	Bentinckia	nicobarica
AY044579.1	Borassus	flabellifer
AF449147.1	Burretokentia	hapala
AY044612.1	Butia	eriospatha
AY044572.1	Calamus	caesius
HG969913.1	Calyptrocalyx	albertisianus
AY044587.1	Calyptronoma	occidentalis
HG969917.1	Carpentaria	acuminata
EF605581.1	Carpoxylon	macrospermum
AY044580.1	Caryota	mitis
KM597766.1	Ceroxylon	quindiuense
AY044585.1	Chambeyronia	macrocarpa
AF449148.1	Clinostigma	savoryanum
AY044613.1	Cocos	nucifera
EF605582.1	Cyphokentia	macrostachya
HG969921.1	Cyphosperma	balansae
AF449149.1	Cyrtostachys	renda
AY044606.1	Desmoncus	orthacanthos
AY044586.1	Drymophloeus	beguinii
AY044583.1	Dypsis	lastelliana
AY044609.1	Elaeis	oleifera
EF605566.1	Euterpe	oleracea
AY044588.1	Geonoma	oxycarpa
EF605590.1	Heterospathe	elata
AF449151.1	Howea	belmoreana
AF449152.1	Hydriastele	wendlandiana
AY044589.1	Hyophorbe	lagenicaulis
EF605568.1	Hyospathe	macrorhachis

AY044592.1	Iriartea	deltoides
KM597759.1	Juania	australis
EF605534.1	Jubaeopsis	caffra
HG969904.1	Kenttiopsis	pyriformis
AY044594.1	Leopoldinia	pulchra
AF449153.1	Linospadix	longicurvis
AY044577.1	Livistona	speciosa
AY044595.1	Manicaria	saccifera
AY044573.1	Mauritia	flexuosa
EF605570.1	Neonicholsonia	watsonii
AY044574.1	Nypa	fruticans
AY044599.1	Oenocarpus	bataua
AF449154.1	Oncosperma	tigillarum
AY044596.1	Orania	trispatha
EF605573.1	Pelagodoxa	henryana
HG969919.1	Phoenicophorium	borsigianum
EF605521.1	Phoenix	canariensis
AY044601.1	Roystonea	oleracea
AY044582.1	Phytelephas	aequatorialis
AY044597.1	Podococcus	barteri
AY044600.1	Prestoea	acuminata
AY044590.1	Pseudophoenix	vinifera
AF449155.1	Ptychosperma	burretianum
AY044591.1	Ravenea	hildebrandti
AY044598.1	Reinhardtia	simplex
HG969918.1	Rhopalostylis	baueri
HG969925.1	Sabal	bermudana
EF605580.1	Satakentia	liukiuensis
AY044615.1	Syagrus	glaucescens
AY044575.1	Thrinax	radiata
EF605588.1	Verschaffeltia	splendida
AY044616.1	Voanioala	gerardii
AY044576.1	Washingtonia	filifera
AY044593.1	Wettinia	hirsuta

APPENDIX D

RAxML trees from chapter 3

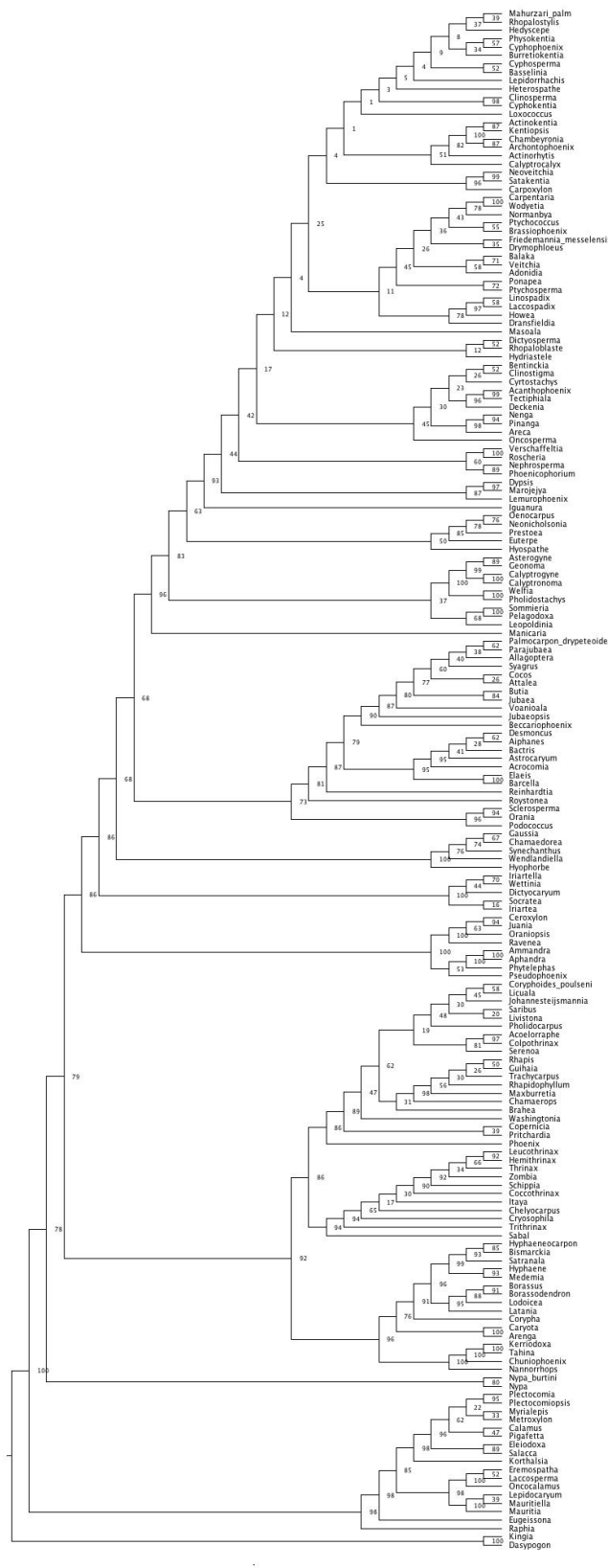


Figure D.1. Maximum likelihood total evidence tree with all six fossils. Node labels are bootstrap values.

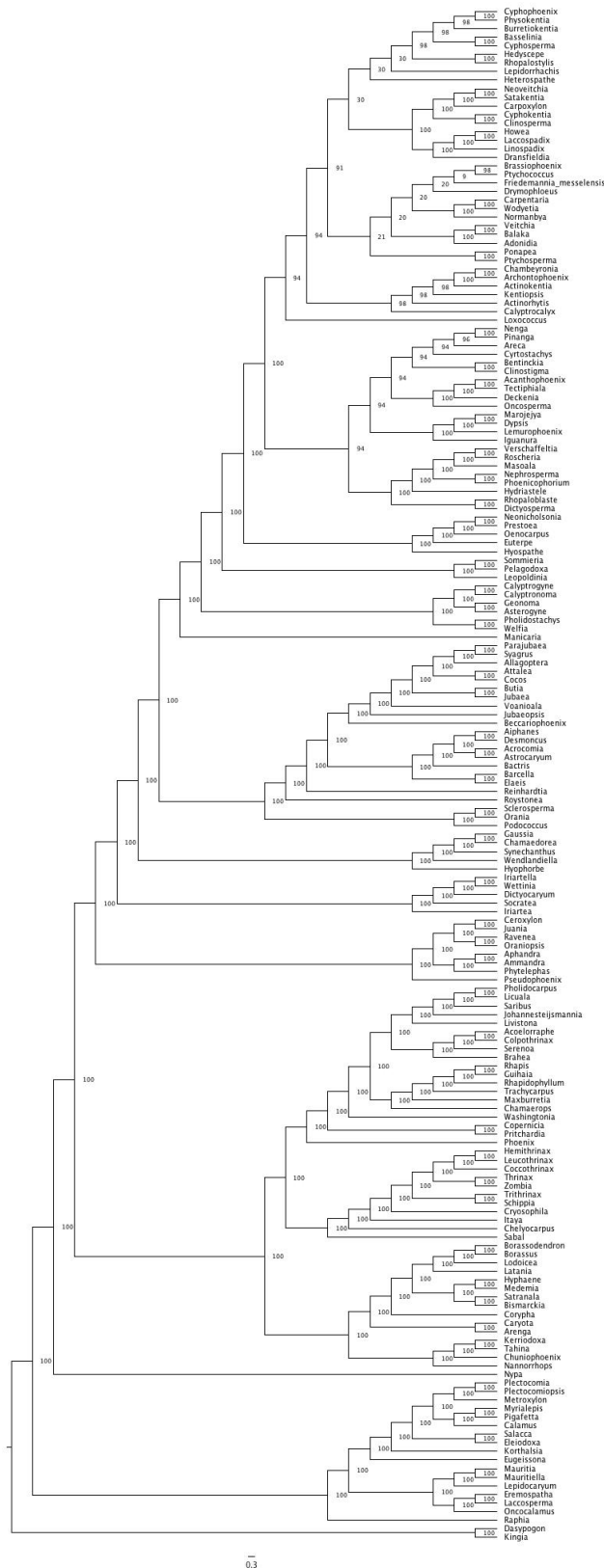


Figure D.2. Constrained analysis with all fossils except the Mahurzari palm. Node labels are bootstrap values.

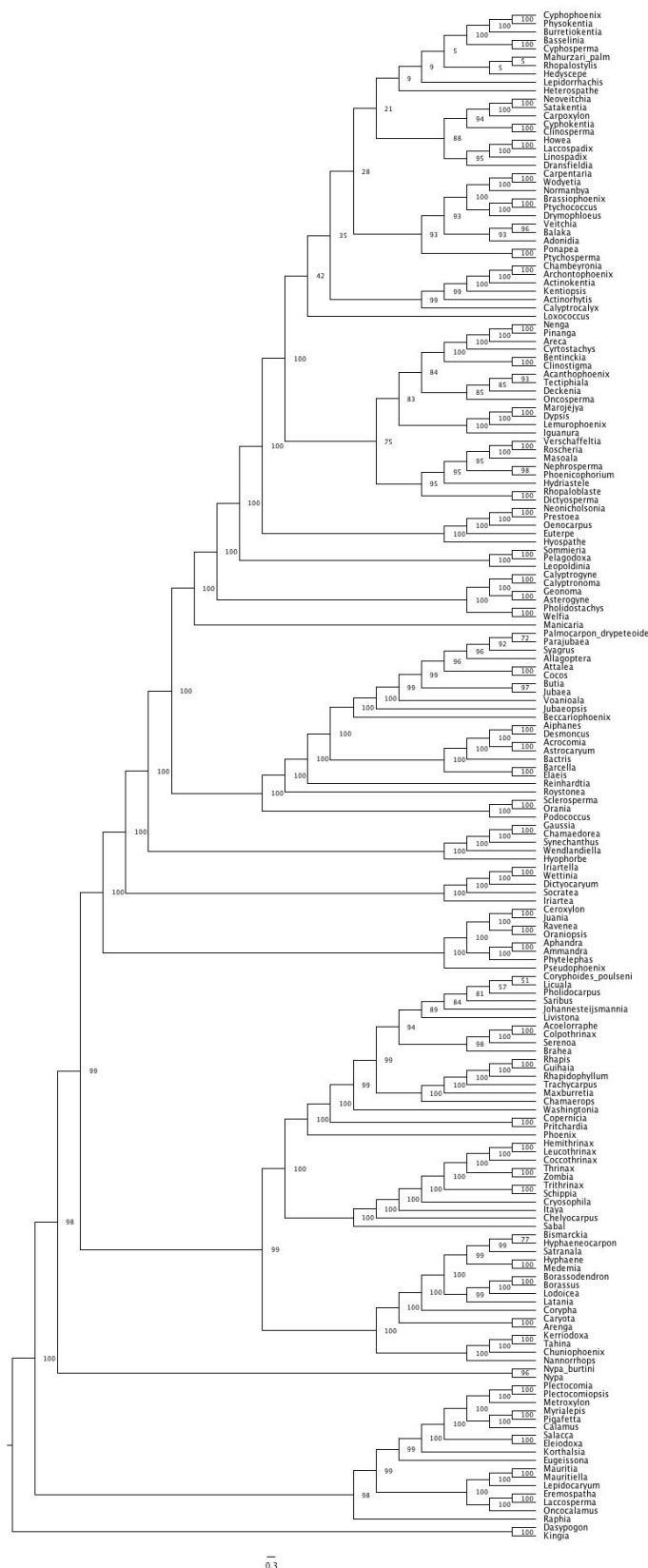


Figure D.3. Constrained analysis with all fossils except *Friedemannia messelensis*. Node labels are bootstrap values.

APPENDIX E

BEAST2 trees from chapter 4

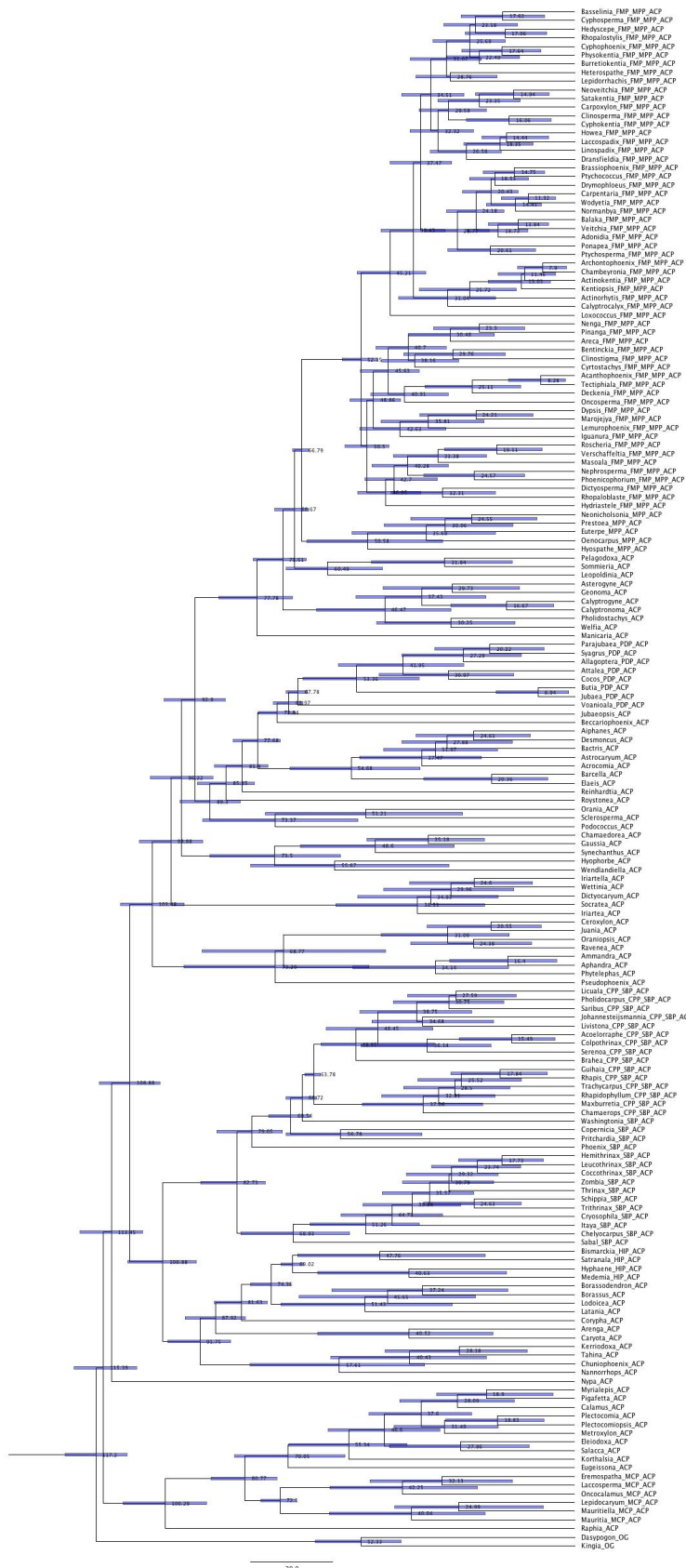


Figure E.1. Chronogram from node-dating analysis using lognormal priors.

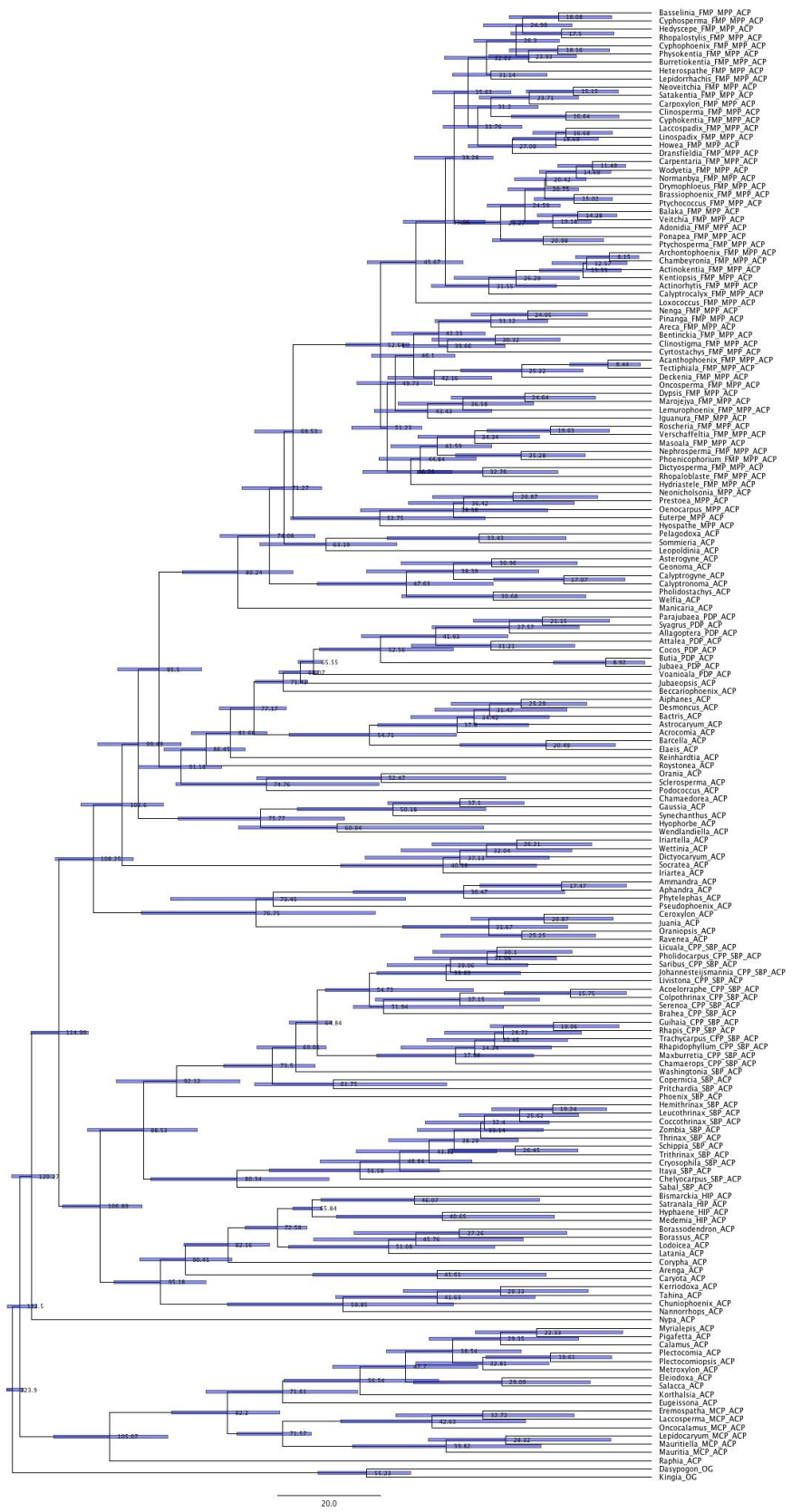


Figure E.2. Chronogram from node-dating analysis using uniform priors.

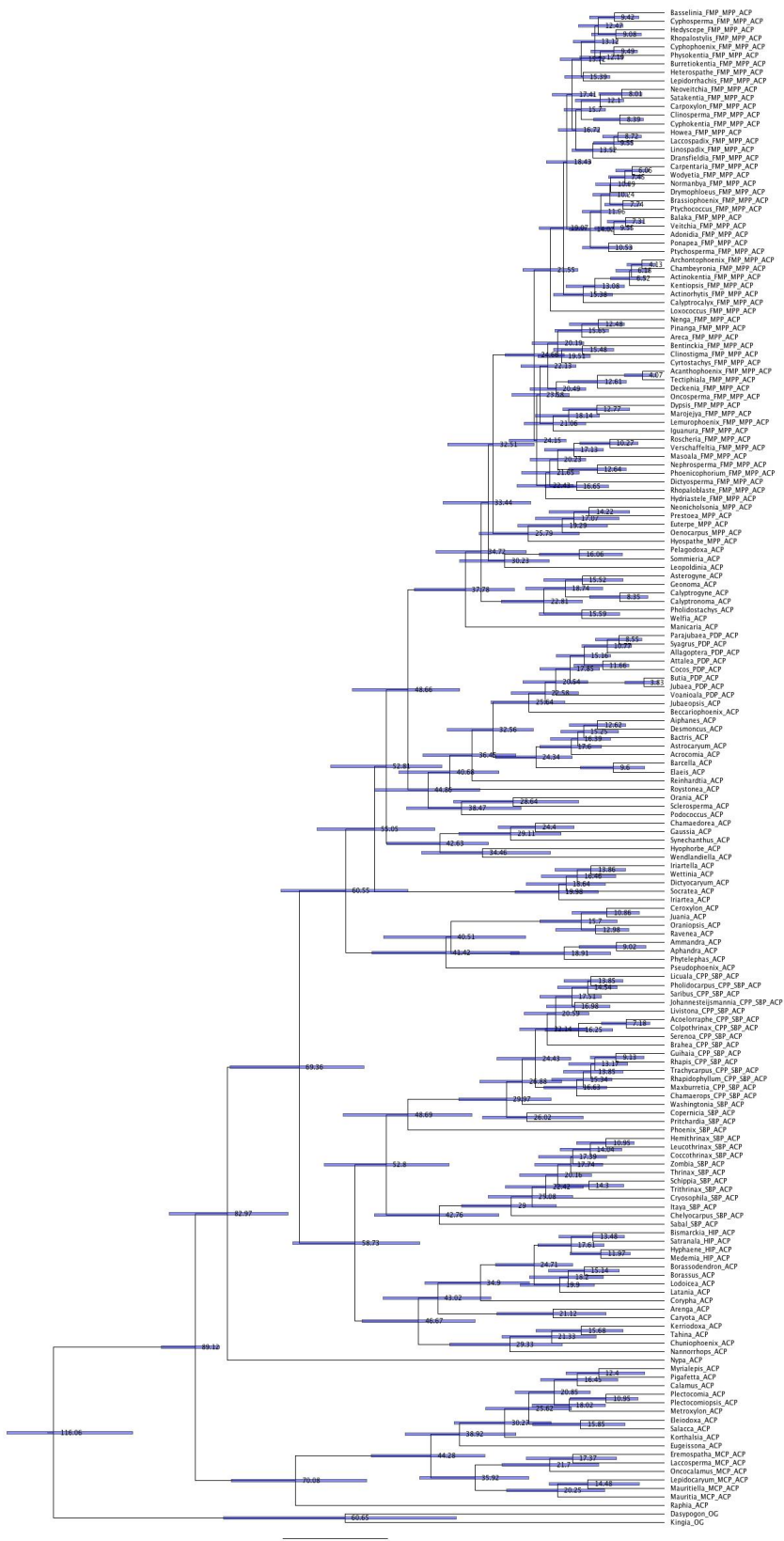


Figure E.3. Chronogram from node-dating analysis using calibrations on only the Arecaceae crown and stem nodes.

APPENDIX F
MEDUSA and BAMM results from chapter 4

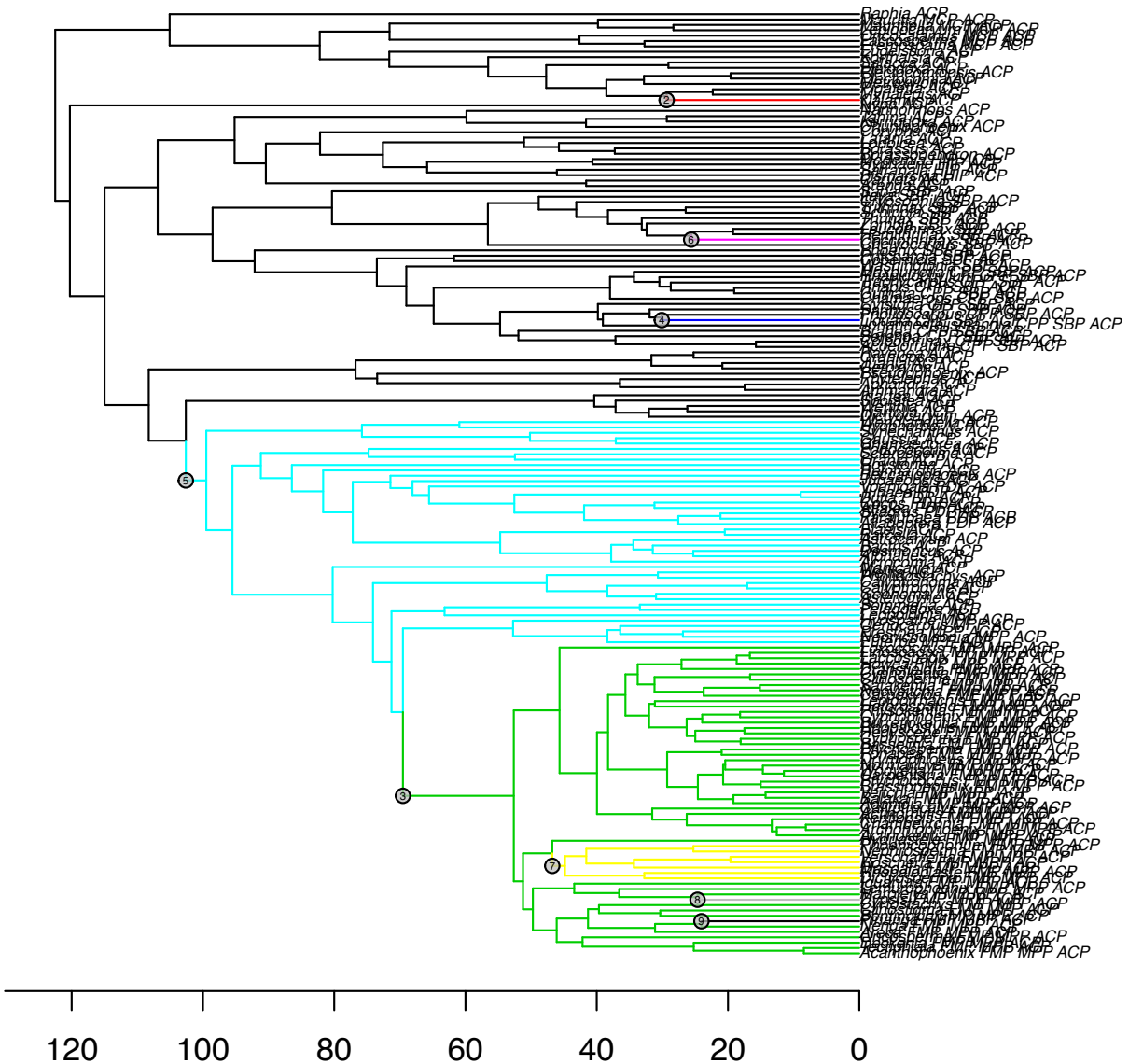


Figure F.1. MEDUSA output using birth-death model and critical threshold value of 6. Numbers correspond to the Model.ID number in table F1 below.

Table F.1. MEDUSA summary for analysis shown in Fig. F1. Note low and high values represent 95% confidence intervals on r (net-diversification rate) and epsilon (relative extinction rate).

Model.ID	Shift.Node	Cut.At	Model	Ln.Lik.part	r	epsilon	r.low	r.high	eps.low	eps.high
2	30	stem	bd	-7.252867	0.185983	0.54964	0.1358477	0.28339	0	0.974285
3	188	stem	bd	-285.1802	0.0907343	3.70E-06	0.0797554	0.1030833	0	0.2277414
4	97	stem	bd	-5.894099	0.114586	0.771073	0.0683768	0.2088264	0	1
5	182	stem	bd	-316.6963	0.0343893	0.844014	0.0287201	0.0410886	0.7884157	1
6	45	stem	bd	-4.901956	0.107172	0.702693	0.0560049	0.2168675	0	1
7	204	stem	bd	-30.9497	0.0369518	6.85E-07	0.0195282	0.0632615	0	0.5219764
8	61	stem	bd	-5.938062	0.129196	0.8335	0.0740093	0.2438922	0.2581168	1
9	132	stem	bd	-5.871371	0.150948	0.71737	0.0924661	0.2690637	0	1

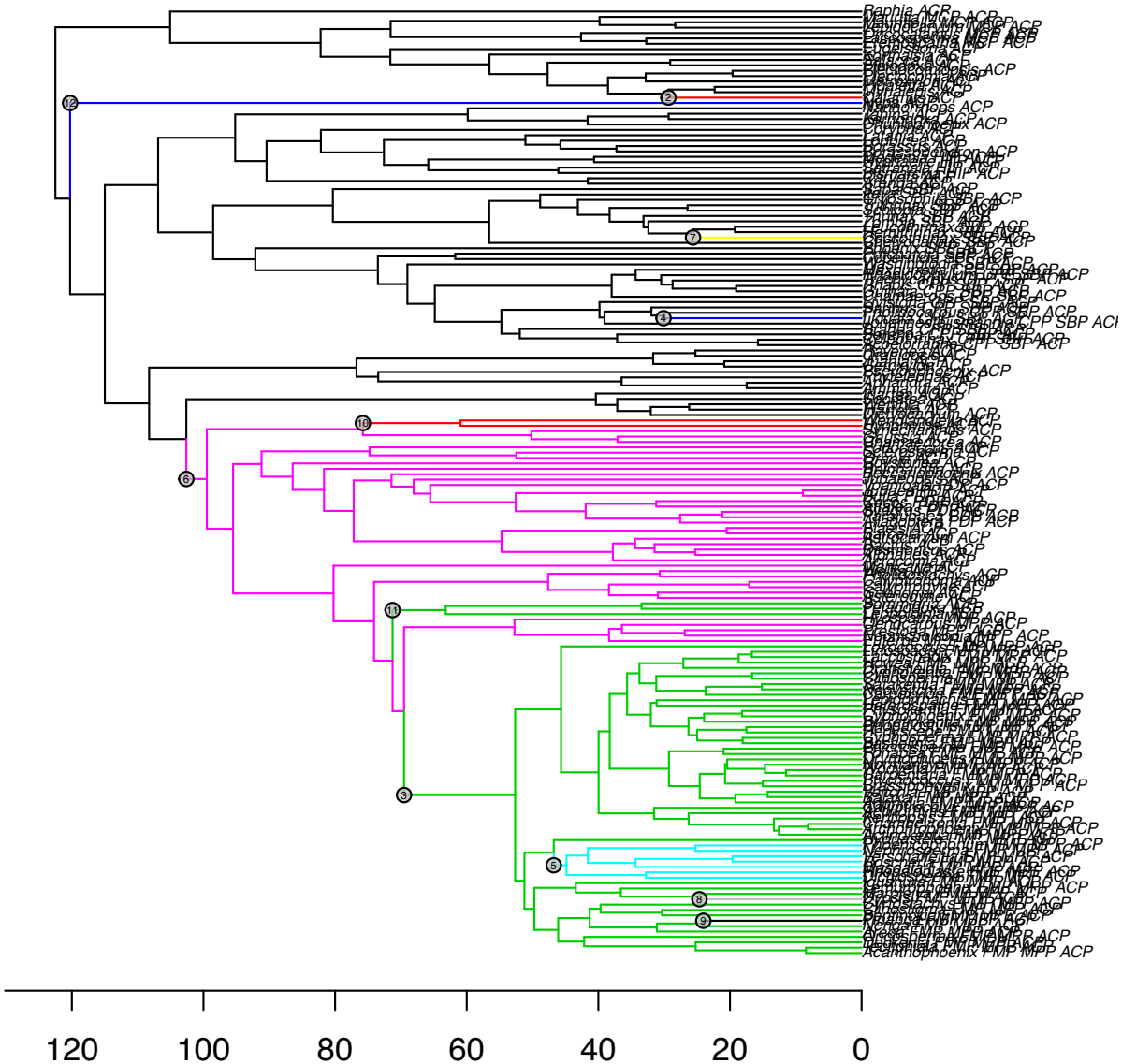


Figure F.2. MEDUSA output using both birth-death and Yule models, with critical threshold value of 6.

Table F.2. MEDUSA summary for analysis shown in Fig. F2. Note low and high values (e.g., r.low, r.high) represent 95% confidence intervals on r (net-diversification rate) and epsilon (relative extinction rate).

Model.ID	Shift.Node	Cut.At	Model	Ln.Lik.part	r	epsilon	r.low	r.high	eps.low	eps.high
2	30	stem	yule	-7.252867	0.213057	NA	0.1626913	0.3105352	NA	NA
3	188	stem	yule	-285.1801	0.0907252	NA	0.0797555	0.1030834	NA	NA
4	97	stem	yule	-5.894099	0.162744	NA	0.1139355	0.2577555	NA	NA
5	204	stem	yule	-30.94969	0.0369678	NA	0.0195281	0.0632615	NA	NA
6	182	stem	bd	-287.5504	0.0382623	0.837077	0.0318797	0.045803	0.7749652	1
7	45	stem	yule	-4.901956	0.152721	NA	0.0962094	0.2641198	NA	NA
8	61	stem	yule	-5.938062	0.200521	NA	0.1409018	0.3165548	NA	NA
9	132	stem	yule	-5.871371	0.020269	NA	0.1416273	0.3215675	NA	NA
10	280	stem	yule	-5.917847	0.00731487	NA	0	0.0322271	NA	NA
11	249	stem	yule	-11.82968	0.0182486	NA	0	0.0439031	NA	NA
12	117	stem	yule	0	0	NA	0	0.0159642	NA	NA

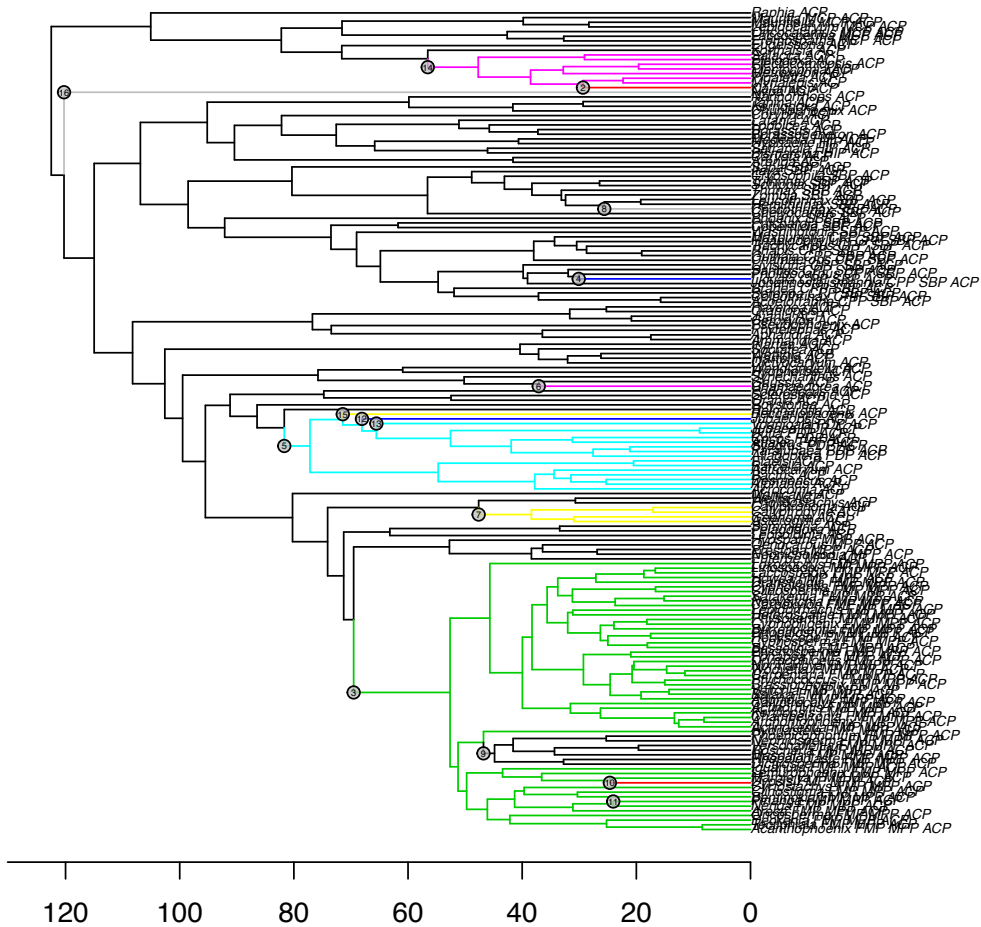


Figure F.3. MEDUSA output using Yule model and critical threshold value of 6.

Table F.3. MEDUSA summary for analysis shown in Fig. F3. Note low and high values (e.g., r.low, r.high) represent 95% confidence intervals on r (net-diversification rate) and epsilon (relative extinction rate).

Model.ID	Shift.Node	Cut.At	Model	Ln.Lik.part	r	epsilon	r.low	r.high
2	30	stem	yule	-7.252867	0.213057	NA	0.1626913	0.3105352
3	188	stem	yule	-285.1801	0.0907252	NA	0.0797555	0.1030834
4	97	stem	yule	-5.894099	0.162744	NA	0.1139355	0.2577555
5	259	stem	yule	-109.2361	0.103264	NA	0.0870786	0.1225316
6	38	stem	yule	-5.695921	0.1267	NA	0.0871686	0.2037544
7	252	stem	yule	-25.42194	0.109837	NA	0.0808331	0.1506836
8	45	stem	yule	-4.901956	0.152721	NA	0.0962094	0.2641198
9	204	stem	yule	-30.94969	0.0369678	NA	0.0195281	0.0632615
10	61	stem	yule	-5.938062	0.200521	NA	0.1409018	0.3165548
11	132	stem	yule	-5.871371	0.20269	NA	0.1416273	0.3215675
12	85	stem	yule	0	0	NA	0	0.0282054
13	170	stem	yule	0	0	NA	0	0.0292915
14	340	stem	yule	-44.40442	0.0831932	NA	0.0601245	0.1134114
15	21	stem	yule	-1.386294	0.00970374	NA	0	0.0457429
16	117	stem	yule	0	0	NA	0	0.0159642

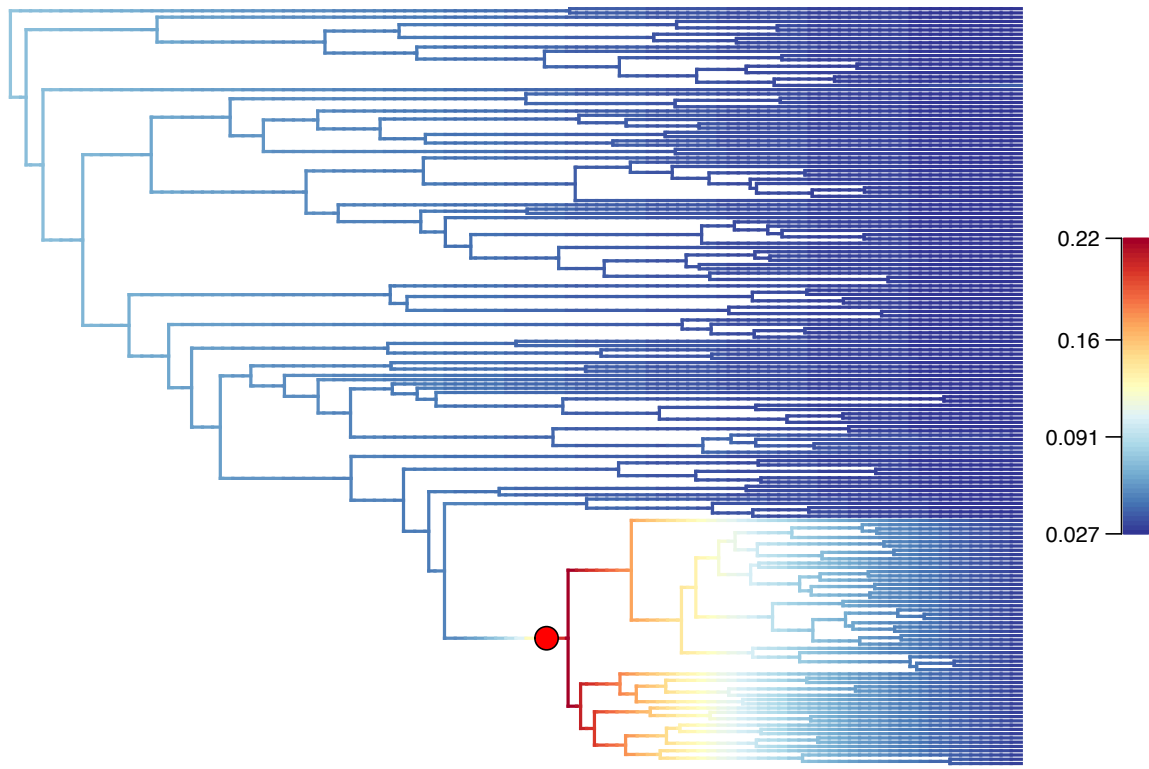


Figure F.4. Net diversification rates from BAMM mapped on chronogram. Note shift towards higher rates along the Areceae stem (red dot).

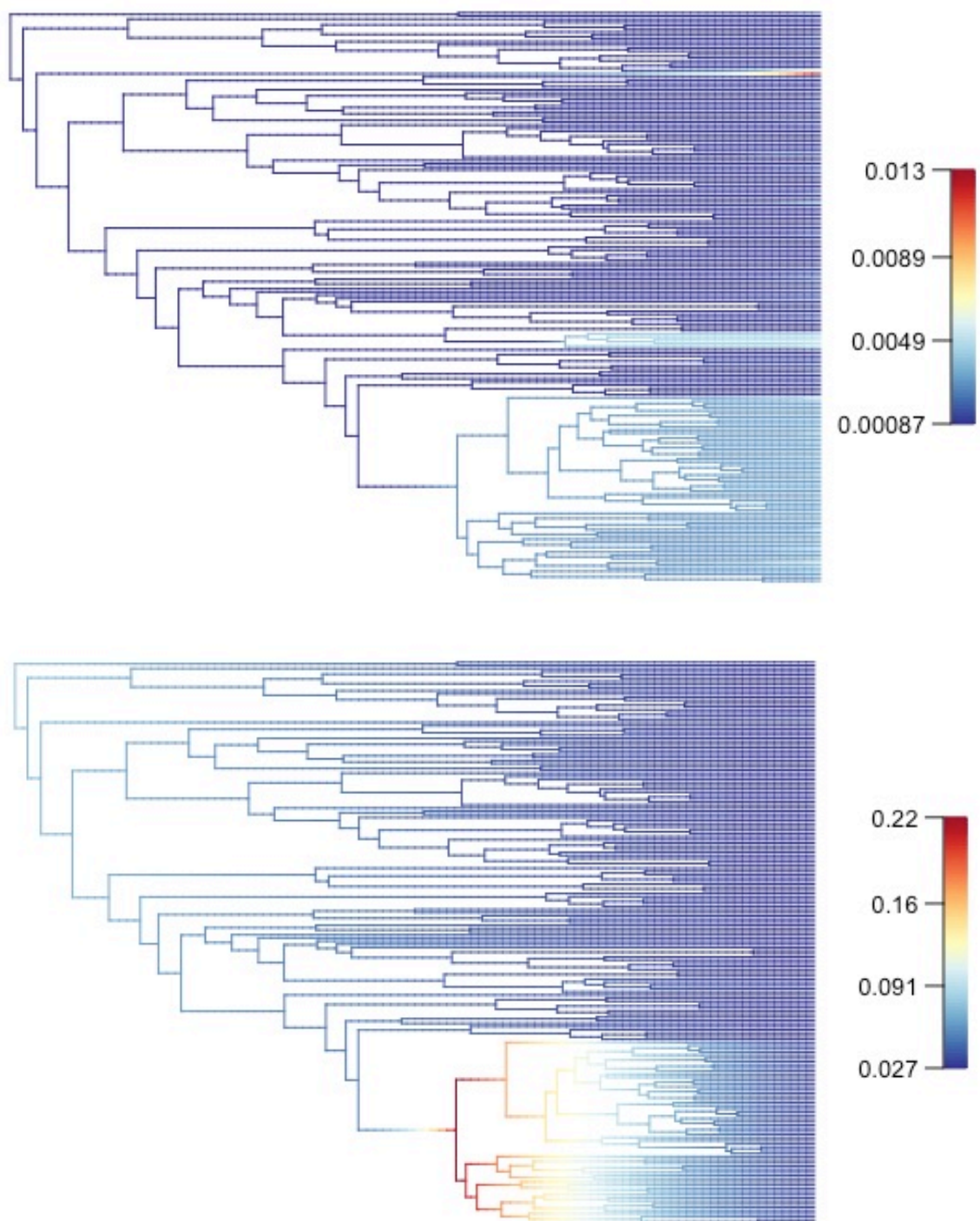


Figure F.5. Rates of extinction (top) and speciation (bottom) from BAMM, mapped onto chronogram.

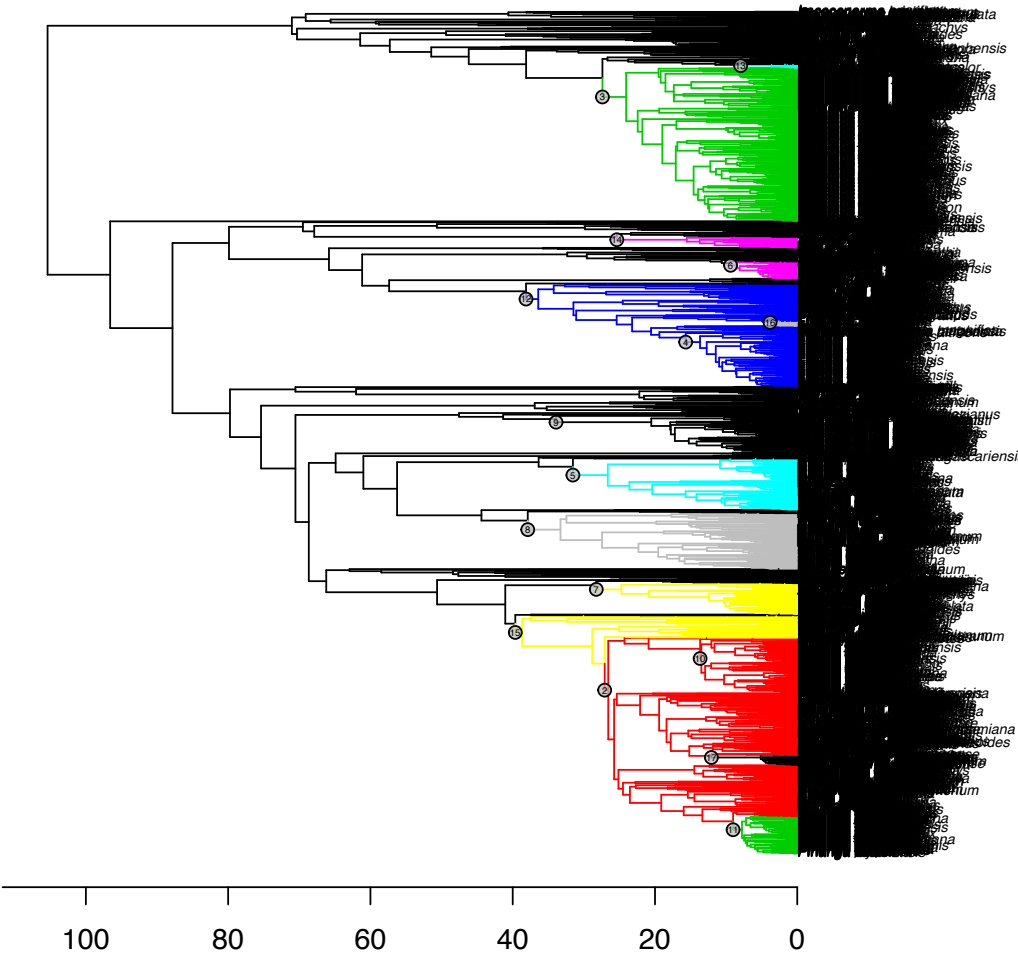


Figure F.6. MEDUSA output using both birth-death and Yule models and species-level tree of Faurby et al. 2016.

Table F.4. MEDUSA summary for analysis shown in Fig. F6. Note low and high values (e.g., $r.\text{low}$, $r.\text{high}$) represent 95% confidence intervals on r (net-diversification rate) and epsilon (relative extinction rate).

Model.ID	Shift.Node	Cut.At	Model	Ln.Lik.part	r	epsilon	r.low	r.high	eps.low	eps.high
2	3145	stem	yule	-1000.521	0.154614	NA	0.1389373	0.1714001	NA	NA
3	4482	stem	bd	-1130.632	0.201377	0.247896	0.1823572	0.2217555	0.1201743	0.3573757
4	2732	stem	yule	-350.972	0.303133	NA	0.2585656	0.3525732	NA	NA
5	4115	stem	yule	-382.8971	0.22255	NA	0.1891301	0.2596934	NA	NA
6	2981	stem	yule	-108.3509	0.311294	NA	0.2327931	0.4057089	NA	NA
7	3832	stem	yule	-246.084	0.18734	NA	0.151607	0.2282521	NA	NA
8	3947	stem	yule	-486.7196	0.14485	NA	0.1239221	0.1680245	NA	NA
9	4291	stem	yule	-306.6022	0.146602	NA	0.1203109	0.1764372	NA	NA
10	3633	stem	yule	-341.6945	0.325522	NA	0.2778011	0.3784373	NA	NA
11	3173	stem	yule	-224.8387	0.358591	NA	0.2959631	0.4294909	NA	NA
12	2640	stem	yule	-431.8044	0.110965	NA	0.0932859	0.1307698	NA	NA
13	4954	stem	yule	-18.25015	0.43823	NA	0.2196199	0.768551	NA	NA
14	2547	stem	yule	-87.84368	0.159826	NA	0.109963	0.2228755	NA	NA
15	3111	stem	bd	-214.1895	0.0729607	0.539559	0.0540078	0.0963564	0.2927201	0.700871
16	2693	stem	yule	-26.32126	0.414746	NA	0.2336828	0.67142	NA	NA
17	3469	stem	yule	-58.35957	0.363346	NA	0.2466562	0.51208	NA	NA

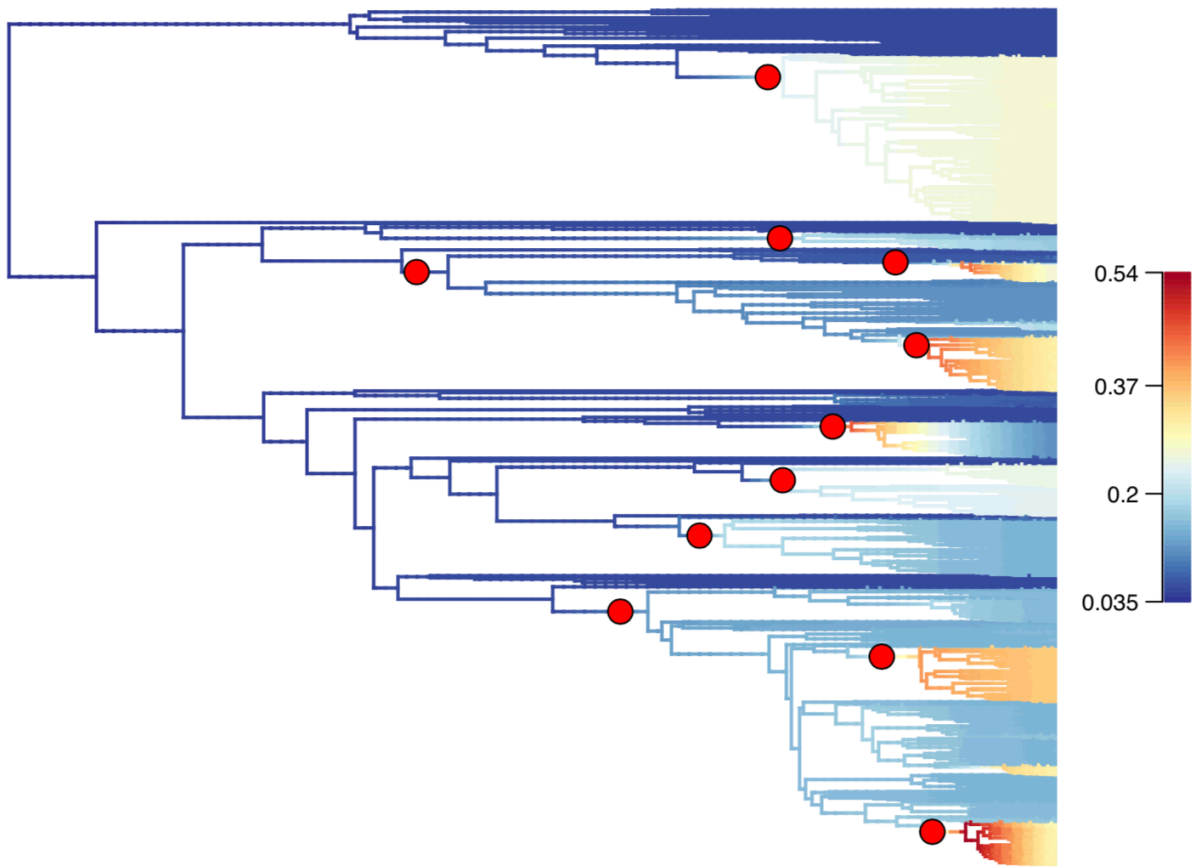


Figure F.7. Rates of net diversification from BAMM mapped onto species-level tree of Faurby et al. 2016. Estimated positions of rate shifts indicated by red dots.

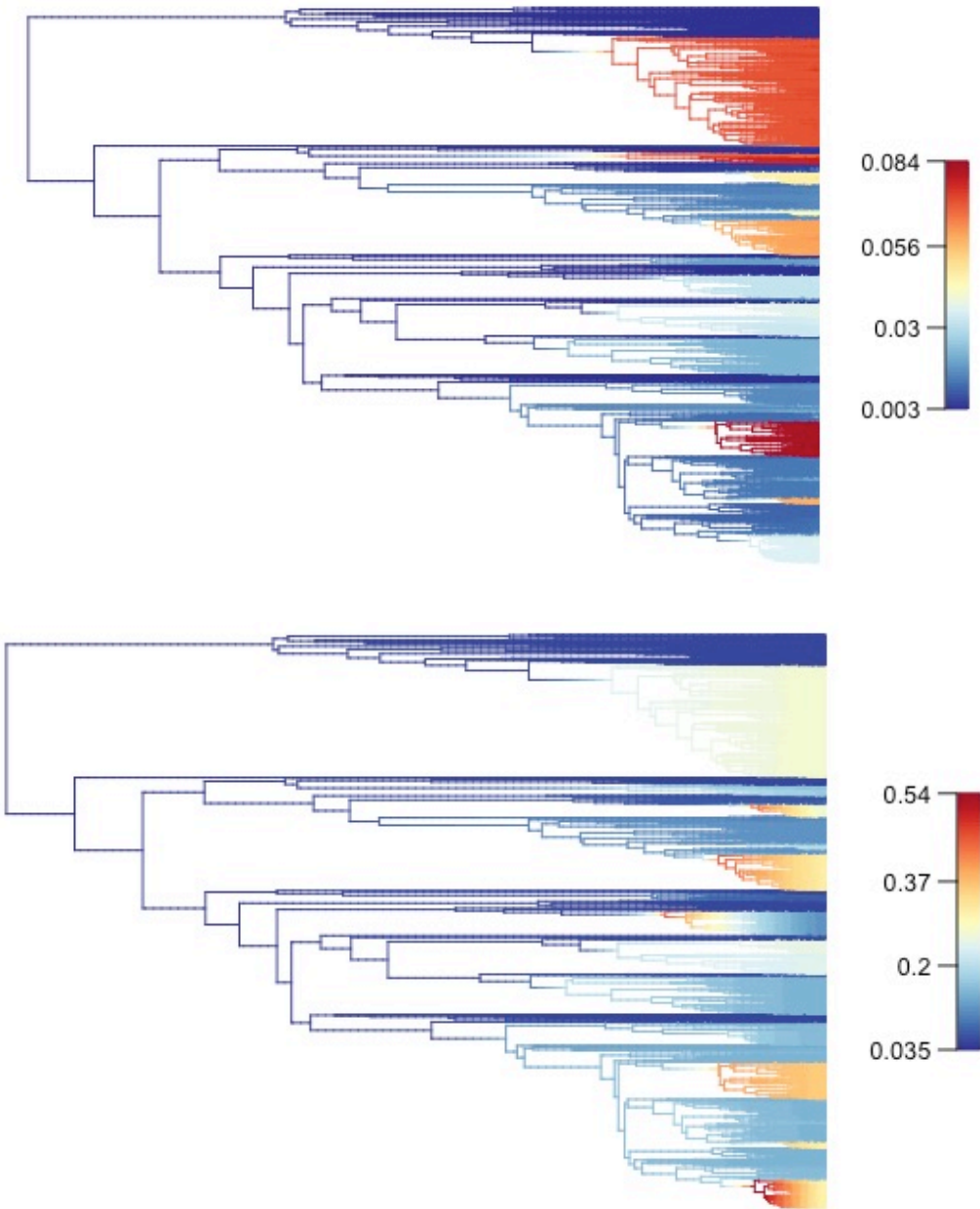


Figure F.8. Rates of extinction (top) and speciation (bottom) from BAMM, mapped onto species-level tree of Faurby et al. 2016.